`

Keele University

Investigation of cellular and scaffold strategies for engineering articular cartilage

Hamza Abu Owida

School of Postgraduate Medicine

Institute for Science and Technology in Medicine

Submitted for the degree of Doctor of Philosophy

Keele University

October 2018

`

Abstract

Articular cartilage is a thin hydrated tissue, which covers articulating surfaces. In the native articular cartilage tissue, the extracellular matrix (ECM) is a fibrillar mesh of interacting proteoglycans, collagens, and other non-collagenous proteins residing in a highly aqueous environment. Chondrocytes are surrounded by a pericellular matrix (PCM) forming chondrons. The PCM, exclusively rich in collagen VI, is more easily destroyed during their extraction and subsequent in vitro culture than ECM. The retention of the PCM has a significant influence on the metabolic activity of the chondrocytes in addition to the mechanical signalling from and to the ECM via cell-matrix interactions. The ECM and the residing chondrocytes are organised into three distinct zones: superficial, middle and deep. The complex and organised structure of cartilage allows it to resist the tensile stress 'superficial zone', sheer stress 'middle zone', and compressive stress 'middle and deep zones' imposed by articulation.

This study initially focused on the morphology and chondrogenic capacity of chondrocytes, chondrons (bovine) and mesenchymal stromal cells (MSCs, rat) alone in monolayer cultures to establish a baseline of PCM preservation and regeneration approaches. Co-culture monolayer models of cartilage cells with MSCs (20%, 50% and 80%) was established to assess the effect of MSC on PCM maintenance and ECM production by biochemical assays, immunofluorescence and histological staining. Co-culture of MSCs with chondrons enhanced ECM production, as compared to chondrocyte or chondron monocultures. The co-culture of MSCs with chondrons appeared to decelerate the loss of the PCM as determined by collagen VI expression, whilst the expression of a high temperature requirement family of serine proteases, HtrA1, demonstrated an inverse relationship to that of the collagen VI. The 50:50 ratio of MSCs: chondrons in co-culture presented the highest potential for better cartilage regeneration. For the first time, it is confirmed that MSCs directly or indirectly inhibited HtrA1 activity in the co-culture, which played a role in enhancement of ECM synthesis and the preservation of the PCM. However, PCM could not be fully preserved or

`

regenerated in 2D culture up to 7 day culture even starting from chondron, and co-culture with MSCs.

Next 3D model systems using hydrogels to improve PCM formation and maintenance were developed. Four culture conditions were compared; hyaluronic acid (HA) versus agarose hydrogel; basal medium versus chondrogenic medium; chondron or chondrocytes versus co-culture with 50% MSC. Up to 21 day culture, chondron samples in both mono- and co-culture maintained PCM at all culture conditions. The quantity and quality of regenerated PCM in chondrocyte samples were culture condition dependent. HA in combination with chondrogenic media and co-culture with MSC was the best support for PCM generation and ECM deposition. Basal and chondrogenic culture mediums influenced the expression of cartilage-specific ECM markers but did not affect collagen VI synthesis. Synchrotron microFTIR measurements assisting with PCA analysis of spectra in fingerprint and lipid regions on the 3D cultured samples have cross-validated that culturing chondrocytes in HA hydrogel up to 21 days might generate chondron-like cell morphology and composition because day 14 and day 21 samples clustered to chondron spectra, whilst day 7 samples to chondrocyte spectra.

Zonal-specific 3D hybrid scaffolds have been fabricated using a combination of polylactic acid and HA to induce the generation of near-native cartilage. For the superficial and middle zones, specifically orientated or randomly arranged polylactic acid nanofibre meshes were embedded in HA. For the deep zone, vertical channels in HA were created. The aligned nanofiber mesh used in the superficial zone induced an elongated cell morphology, lower GAG and collagen II production, than the middle zone scaffold. Within the middle zone scaffold, which comprised of a randomly orientated nanofiber mesh, the cells were clustered and expressed more collagen II. The deep zone scaffold induced the highest GAG production, the lowest cell proliferation and the lowest collagen I expression of the three zones. Overall a convenient and reproducible model system which mimics the zonal organisation of articular cartilage has been developed.

`

Table of contents

`

`

`

`

`

`

List of figures

`

`

`

`

`

List of tables

`

List of abbreviations

Abbreviation	Meaning
α-MEM	Modified Eagle's medium
3D	Three dimensional
2D	Two dimensional
µm	Micrometre
nm	Nanometre
A+A	Antibiotics and Antimycotic
ACI	Autologous Chondrocyte Implantation
ag	Agarose
ANOVA	Analysis of variance
Bas	Basal media
BMP	Bone morphogenetic protein
BSA	Bovine serum albumin
Ch	Chondrogenic media
CO_2	Carbon dioxide
Col I	Collagen I (protein)
Col II	Collagen II (protein)
CN	Chondron
CY	Chondrocytes
DAPI	4′,6-diamidino-2-phenylindole, dihydrochloride
dH_2O	Distilled water
DMEM	Dulbecco's Modified Eagle Medium
DMMB	1,9-DiMethylMethylene Blue

`

DMSO	Dimethyl sulfoxide
DNA	Deoxyribonucleic acid
ECM	Extracellular matrix
EDTA	Ethylenediaminetetraacetic acid
FCS	Fetal Calf serum
FITC	Fluorescein isothiocyanate
GAG	Glycosaminoglycans
HA	Hyaluronic acid
HEPES	(4-(2-hydroxyethyl)-1-piperazineethanesulfonic acid)
HTRA1	High-Temperature Requirement A1
IGF	Insulin-like growth factor
IMS	Industrial Methylated Spirit
IM	Interterritorial matrix
OCT	Optimal cutting temperature medium
MSCs	Mesenchymal Stem Cells
NaCl	Sodium chloride
P0/P1/P2	Passage 0/1/2
PBS	Phosphate-Buffered Saline
PCA	Principle component analysis
PCM	Pericellular matrix
PFA	Paraformaldehyde
PI	Propidium iodide
PLA	Poly-L,D-lactic acid
RIPA	Radioimmunoprecipitation

`

Rpm	Revolutions per minute
TM	Territorial matrix
TGF- β	Transforming growth factor type β
TRITC	Tetramethylrhodamin
PTFE	Polytetrafluoro ethylene
UV	Ultra violet
w/v	Weight to volume

`

Acknowledgements

I would like to thank my supervisor Prof. Ying Yang, for her tireless help and support throughout my PhD and for her advice, patient, motivation, which allow me to grow as a research scientist. As my PhD has come to an end, I would like to thank her for being a wonderful supervisor and also a wonderful Mom.

Also, my deep thanks go to my co-supervisor Dr Nicola Kuiper for making my PhD full of knowledge and for her help and guidance. I would also like to thank my advisor Prof. Nick Forsyth for his supportive comments.

I would like to thank the British Council Newton Fund: PhD Placement grant for the opportunity to work in East China University of Technology. Also I am also grateful to Prof. Lian Cen for her help and guidance from the first day I arrived china.

I am also grateful to the Diamond Light Source MIRIAM B22 beamline staff; Dr Gianfelice Cinque, Dr Katia Wehbe and Dr Que Nguyen for their collaboration and support.

I would like to extend my gratitude to the many people I have worked with at the ISTM, who created a wonderful working environment. Also I must express my very profound gratitude to my colleagues, I spent the best moments in my life with you and I am lucky to have great friends like you.

Most of all, I would like to give a big thank to my mum, dad and aunt as well as my brother and sister for their help and love in my academic pursuits, without whom I would not have achieved any of them.

`

List of publications

A- Publications

- Owida H, Ruiz, T De Las Heras, Dhillon A, Yang Y, Kuiper N. Histochemistry and cell biology, 148(6), pp.625-638.
- Yang, Y., Owida, H. and Kuiper, N., Novel 3D nano-fabricated zonal scaffolds for articular cartilage regeneration. Frontiers in Bioengineering and Biotechnology. Conference Abstract: 10th World Biomaterials Congress (2016).
- Owida, H.A., Yang, R., Cen, L., Kuiper, N.J. and Yang, Y., 2018. Induction of zonal-specific cellular morphology and matrix synthesis for biomimetic cartilage regeneration using hybrid scaffolds. Journal of The Royal Society Interface, 15(143), p.20180310.
- Owida H, Rutter A, Nnguyen Q, Cinque G, Kuiper N, Sule-Suso, Yang Y. Assessment of cellular evolution of tissue engineered cartilage by SR-FTIR, Analytics, under review.
- Owida H, Gater R, Njoroge W, Yang Y. Scaffolds mimicking the native structure of tissues. Handbook of Tissue Engineering Scaffolds. Editors: Mozafari M, Sefat F and Atala A, Elsevier, 2018, under review.

B- Presentations

- Owida, H., Yang, Y., and Kuiper, N., Novel 3D nano-fabricated zonal scaffolds for articular cartilage regeneration. World Biomaterials Congress (WBC) 2016, Montreal, Canada, May 2016. (Oral presentation).
- Owida, H., Yang, Y., and Kuiper, N., Exploration of Novel 3D Nanofabricated Zonal Scaffold for Articular Cartilage Regeneration. Future Investigators of Regenerative Medicine Symposium (FIRM) 2016, Gerona, Spain, September 2016. (Oral presentation).

`

- Owida H, Yang Y, Yang R, Cen L, Kuiper N., A new 3D hybrid zonal scaffold for articular cartilage tissue engineering. TERMIS European Chapter Meeting 2017 (TERMIS-EU), Davos, Switzerland, June 2017. (Poster presentation).
- Owida H, Yang Y, Yang R, Cen L, Kuiper N., Exploration of anisotropic scaffolds for articular cartilage regeneration. Tissue and Cell Engineering Society Annual Conference (TCES) 2017, Manchester, UK, July 2017. (Poster presentation).
- Owida H, Rutter A, Nnguyen Q, Cinque G, Kuiper N, Sule-Suso, Yang Y Assessment of cellular evolution of tissue engineered cartilage by SR-FTIR. The International Conference on Clinical Vibrational Spectroscopy (SPEC) 2018, Glasgow, UK, June 2018. (Poster presentation).

C- <u>Funds</u>

- British Council Newton Fund: PhD Placement grant. East China University of Technology, Shanghai, China, March 2016.
- Diamond Light Source Fund: Assessment of preservation and production of pericellular matrix in tissue engineered cartilage by SR-microFTIR molecular microanalysis. Oxford, UK, November 2017.

`

Chapter 1 : Introduction and literature review

`

1.1 Introduction

Cartilage tissue is a soft connective tissue that is found in different parts of the human body such as the pinna of the ear, intervertebral discs, nose, and the knee. It has elastic, flexible and semi-transparent properties, and can be classified into; elastic cartilage, fibrocartilage and hyaline cartilage based on its location, structure, and relative contribution as well as distribution of extracellular matrix (ECM) composition (Stockwell, 1979; Huber et al., 2000).

The most common type of cartilage is hyaline cartilage which is found in the articular surfaces of joints. Proteoglycans (mainly aggrecan), collagen II and water are the key ECM components in hyaline cartilage. Fibrocartilage is often found at the ends of tendons and ligaments in bone attachment. The main ECM components of fibrocartilage include collagen I with smaller amounts of collagen II and aggrecan. The ear and nose are the places where elastic cartilage is found. This cartilage type is characterized by the presence of elastin (elastic fibres) in the ECM (Stockwell, 1979; Nigg et al., 1999).

Articular cartilage is a thin hydrated tissue that has a thickness approximately 1.5–3 mm in the adult knee (Zhang et al., 2009). It has a complex framework that provides the mechanical properties required to perform its functions (Huber et al., 2000). The major functions of articular cartilage include providing a smooth and stable movement of the joints, reducing the friction between the bones as well as providing resistance to shear and compressional force (Nigg et al., 1999).

Nevertheless, the ability of articular cartilage to repair itself is very low, since is lacks both blood vessels and nerves. Hence, both the cartilage and the joint are unable to function when the cartilage is damaged. Damage and subsequent degeneration can progress to a medical condition known as osteoarthritis (OA) (Hoemann, 2004).

`

OA is characterized by a gradual loss of cartilage which is accompanied by abnormal changes in the subchondral bone and synovium. Pain in the joints and restriction in joint movement resulting in disability can lead to a poor quality of life among patients (Loeser et al., 2012). According to Arthritis Research UK, 33% of people who are 45 years old and above have sought treatment for OA of the hip and knee (Arthritis Research UK, 2013).

1.2 Composition and structure of articular cartilage

Articular cartilage is a unique type of connective tissue that covers the ends of the long bones in synovial joints such as the knee. It is solely composed of a particular type of cell known as chondrocyte which greatly varies in density and phenotype with increasing depth from the articular surface (Huber et al., 2000). Chondrocytes are encapsulated within dense ECM (Stockwell, 1979) which is depicted in Figure 1.1.

`

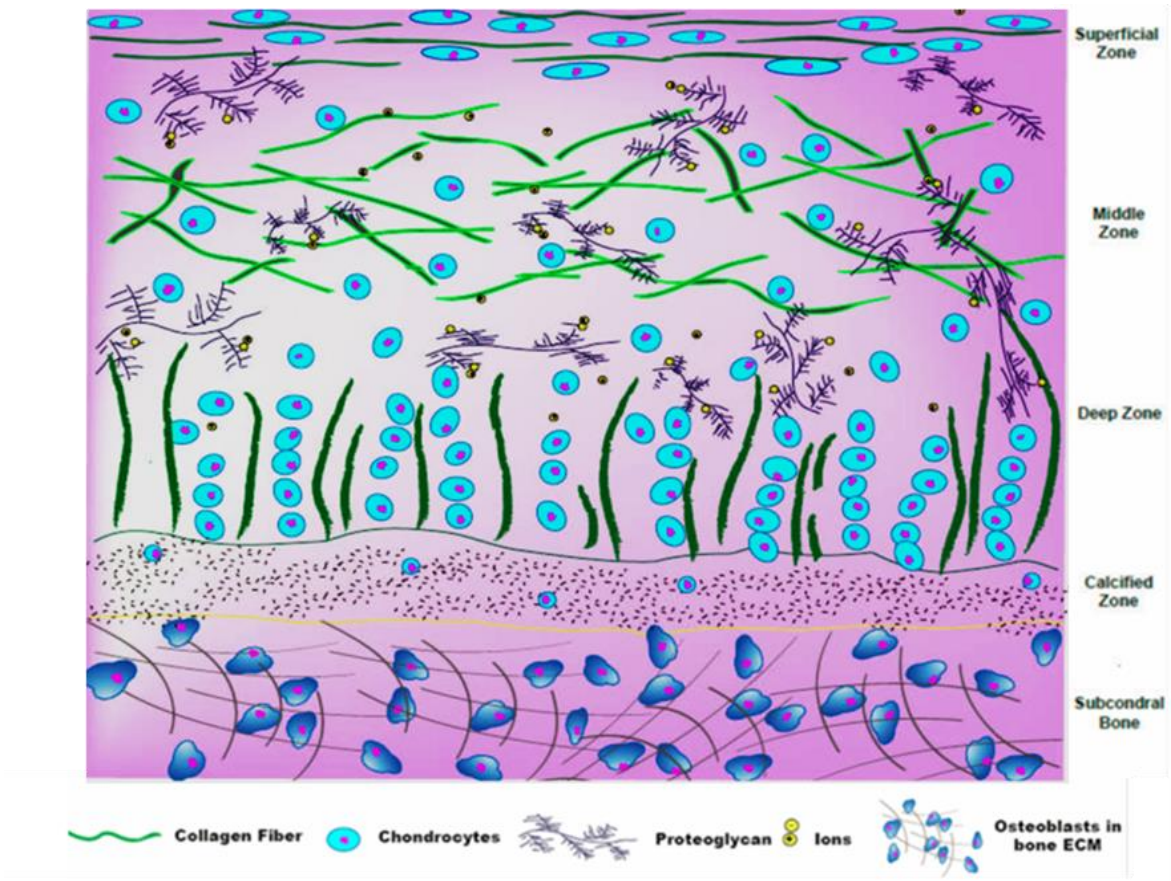

Figure 1.1: Composition and structure of articular cartilage (Taken from Zhang et al., 2009).

1.2.1 Chondrocytes

About 1-5% of the total volume of cartilage tissue is occupied by chondrocytes and this is low compared to other tissue types such as skin or liver. In general, chondrocytes have a diameter approximately 13 μm (Hunziker, 2002). Chondrocytes vary in size and morphology across different regions of articular cartilage as they change from being spherical to being flat though they generally have an ovoid shape (Hunziker et al., 2002).

In ECM, chondrocytes are responsible for the anabolic and catabolic activities to maintain the function and integrity of tissue (Archer and Francis-West, 2003). The correct size and mechanical properties of cartilage are maintained by chondrocytes actively replacing degraded matrix molecules to maintain homeostasis. Furthermore, the net synthesis and degradation of matrix

`

components (matrix turnover) must be maintained in order to guarantee consistent functioning of tissues. In fact, in the event that homeostasis becomes unbalanced then it will greatly affect the mechanical properties (Melero-Martin et al., 2007).

1.2.2 Cartilage extracellular matrix (ECM)

A hydrated ECM forms a major part of articular cartilage which contains a substantial amount of fluid (mainly water and also dissolved ions, gases and metabolites) corresponding to 60-80% of the total wet weight of the tissue (Mankin and Thrasher, 1975; Hoemann, 2004). The remaining 20-40% of the total weight of the tissue consists of a variety of ECM molecules which are mainly collagens (50-70%, dry weight), proteoglycans (15- 30%, dry weight), and other non-collagenous proteins (15-20%, dry weight) (Buckwalter et al., 2005). The major components of articular cartilage are shown in Figure 1.2.

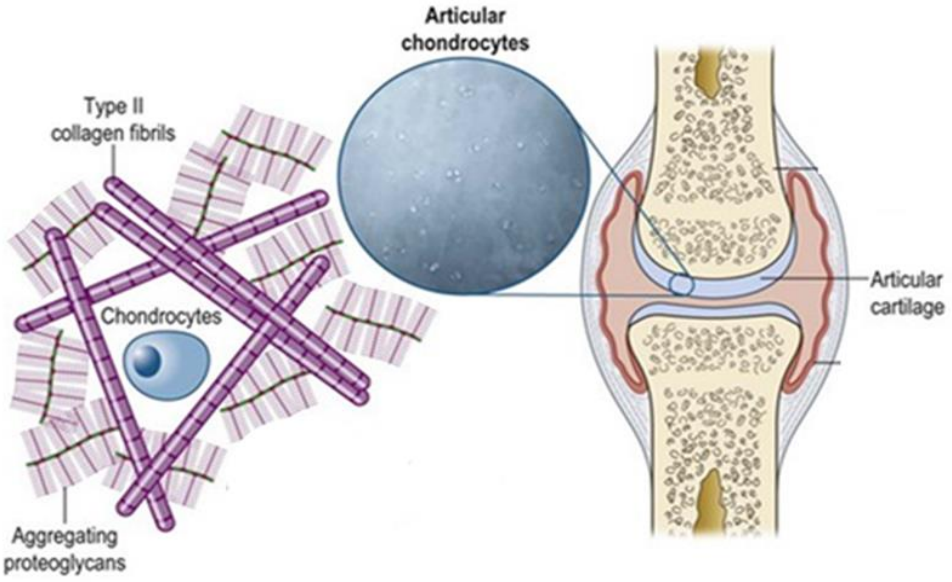

Figure 1.2: A schematic drawing showing the major components of articular cartilage including chondrocytes, collagen II fibrils and aggregating proteoglycans (aggrecans) (Taken from https://veteriankey.com/oral-joint-supplements-in-the-management-of-osteoarthritis/).

`

1.2.2.1 Collagens of articular cartilage

In most tissues, the major insoluble fibrous proteins of the ECM are collagens. Structurally, collagen comprises 3 polypeptide chains connected together by hydrogen bond to form a triple helical structure (Eyre, 2004). Each collagen chain has a sequence of amino acid with a unique pattern of repeating glycine in every third unit. Amino acids, proline and hydroxyproline make up about 20 % of the amino acids in collagen (Brodsky and Shah, 1995).

The ECM contains at least 20 different types of collagen, and the predominant type varies based on the tissue. Although collagen II is the most abundant and characteristic collagen of articular cartilage, other types such as collagens I, V, VI, IX, X and XI are also found in smaller amounts (Mayne, 1989). Large fibrils are formed through the combination of types II, IX and XI, which then join together to give a mesh-like network. This mesh is responsible for the strength and tensile properties of articular cartilage (Cohen et al., 1998). Collagen VI is considered the main part of pericellular matrix (PCM) immediately surrounding the chondrocyte. Collagen VI supports the linking of chondrocytes to the ECM but its precise role is still under investigation (Poole, 1997). Collagen X contributes to the mineralization of cartilage and produces strength in the tissue. It only exists in cartilage-bone interface area (osteochondral region) (Schmid and Linsenmayer, 1985). The main collagens types found in articular cartilage are summarized in Table 1.1.

`

Table 1-1: Collagens found in cartilage and their roles within articular cartilage (Adapted from Mayne, 1989)

Collagen type	Description
Type II	Makes up 80-95% of total collagen; forms the collagen fibrils
Type IX	Present on the surface of fibrils of collagen II; links fibrils to other components or to each other
Type XI	Present on the surface of fibrils collagen II; role in determining fibril diameter
Type X	Present in cartilage – bone interference area; contributes to cartilage mineralization and provide tissue integrity
Type VI	Present in the PCM surrounding the chondrocytes; supports chondrocytes linking to the ECM

1.2.2.2 Proteoglycans of Articular Cartilage

Proteoglycans are large hydrophilic molecules composed of approximately 95% polysaccharide and 5% protein (Bayliss et al., 1983; Mankin et al., 2000). The proteoglycan distension mechanism enables the collagen fibres to contribute to cartilage compressive resistance (Huber et al., 2000).

One of the main constituent of proteoglycan is the glycosaminoglycan (GAG). GAGs are long unbranched polysaccharides containing repeating disaccharides together with an amino sugar. GAGs are divided into 3 major groups based on their sugars, which include hyaluronan, chondroitin sulfate and keratan sulfate (Temenoff and Mikos, 2000). Table 1.2 demonstrates the major glycosaminoglycan found in cartilage.

`

Table 1-2: Major glycosaminoglycan found in cartilage and their roles within articular cartilage (Adapted from Muir, 1978)

Glycosaminoglycan (GAG) type	**Description**
Hyaluronan	An anionic and non-sulfated disaccharide unit. It attachs to aggrecan to form huge supramolecular proteoglycan aggregates, which bind to collagen fibrillar network for load bearing
Chondroitin sulfate	It is a disaccharide unit with highly sulfate modified. It represents up to 90% of the total GAG, providing a viscous phase to reduce friction and compressive load
Keratan sulfate	A highly sulfated disaccharide unit. It helps to maintain the charge density of the aggrecan molecules to provide essential osmotic pressure

The major type of proteoglycan found in articular cartilage is aggrecan (Hardingham et al., 1994). Its structure is made up of a polypeptide core protein to which are attached GAG side chains; chondroitin sulphate and keratan sulphate polysaccharides. Link protein connects the long polysaccharide chain of hyaluronan to aggrecan molecules. About 100 aggrecan molecules can align and interact with a single hyaluronan fibre giving rise to huge supramolecular proteoglycan aggregates which are trapped within a dense collagen II fibre network (Hardingham and Muir, 1972; Huber et al., 2000; Milner et al., 2012).

The main functions of articular cartilage include minimizing joint friction, distributing loads and resisting shear and compressive forces (Nigg et al., 1999; Ateshian et al., 2003).

Cartilage has viscoelastic properties because contains solid and liquid phases and the interactions between these two phases characterise the viscoelastic properties of this tissue (Zhang et al., 2009). Articular cartilage encounters numerous mechanical stimuli such as compressive stress, shear stress and tensile stress under normal physiological conditions (Nigg et al., 1999). The biochemical composition of articular cartilage is affected by these mechanical stimuli. For instance, the ECM content of a cartilage in high-loading areas is more than that of a cartilage in low-loading areas (Treppo et al., 2000). Collagen fibrils are the main contributors to the tensile properties of articular

`

cartilage. Since different zones have different collagen organization, the tensile properties vary significantly among zones (Klein et al., 2009).

The negative charge density increases as a result of the presence of proteoglycans with highly negatively charged GAGs in the ECM, and this helps to attract free cations in the fluid into the tissue (Bayliss et al., 1983; Zhang et al., 2009). An osmotic pressure known as the 'Donnan osmotic pressure' is formed due to the resultant high density of ions within the tissue. The water is expelled over the cartilage pores when the tissue is compressed. However, some residual water remains inside the tissue due to the Donnan osmotic pressure. This residual water experiences the compressive force in the cartilage and endows the cartilage with its viscoelastic properties (Ateshian et al., 2003; Zhang et al., 2009). This allows for a better load distribution and helps in lubrication of joint throughout loading (Stockwell, 1979; Nigg et al., 1999).

The proteoglycan aggregate (aggrecan) found in the ECM of articular cartilage is shown in Figure 1.3.

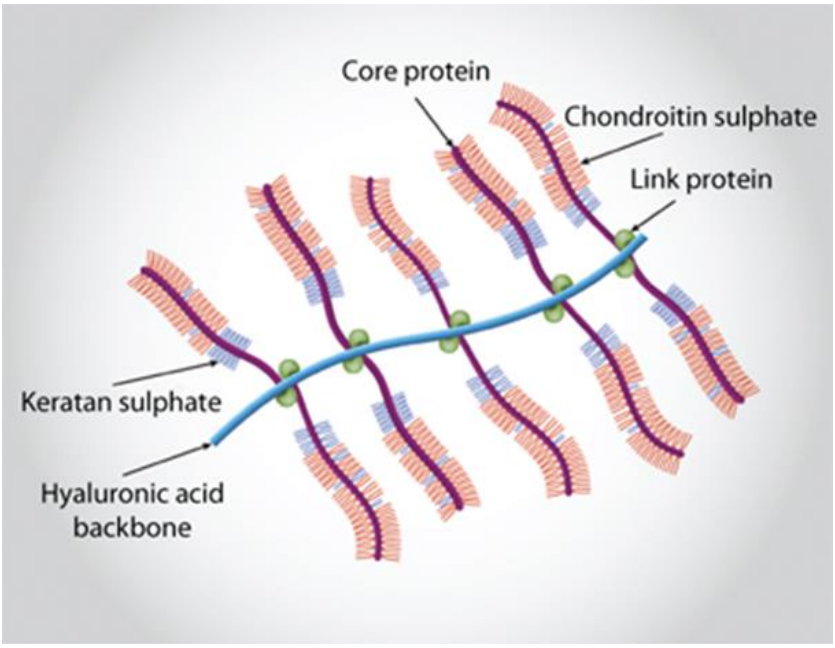

Figure 1.3 : A proteoglycan aggregate present in articular cartilage ECM (Taken from King, 2014. Integrative Medical Biochemistry and Board Review. www.accesspharmacy.com)

`

Aside from large proteoglycan (aggrecan), smaller proteoglycans like decorin, biglycan and fibromodulin also found articular cartilage and they constitute approximately 3% of total proteoglycan mass (Huber et al., 2000). They have shorter protein cores and fewer GAG chains than their aggrecan. Unlike aggrecan, these molecules do not affect physical properties of the tissue, but are thought to play a role in cell function and organization of the collagen matrix (Temenoff and Mikos, 2000). Decorin and fibromodulin are binding to collagen II and help to organise and stabilise the collagen II mesh. Biglycan is concentrated in PCM region and bind to collagen VI and contribute in organise and stabilise the collagen VI meshwork (Chu et al., 2017).

1.2.2.3 Non-collagenous proteins and glycoproteins

The roles played by the non-collagenous proteins in ECM assembly include interactions with major macromolecules and chondrocytes, cell attachment and matrix maintenance as well as regulation of matrix metabolism (Roughley, 2001). These proteins have interrelated functions, which may increase the response of chondrocytes to environmental changes (Zhang et al., 2005).

Polysaccharide and protein are the major components of glycoprotein just like proteoglycan, but the difference is that it contains more protein. The glycoproteins that are usually found in the ECM of cartilage as well as in the PCM of various tissues are fibronectin (Temenoff and Mikos, 2000). Fibronectin is rich in Arginyl-glycyl-aspartic acid (RGD) subunit and plays a vital role as a cell attachment molecule (Enomoto et al., 1993). In addition, it can attach to many substances such as collagen and fibrin. Lubricin is a large water-soluble glycoprotein that is found in the superficial zone and synovial fluid. Lubricating the joint surface as well as preventing the movement of large molecules into articular cartilage or synovial fluid is the main function of lubricin (Jones et al., 2007).

1.2.3 Cartilage tissue fluid

The avascular cartilage gets sufficient nutrients and oxygen from the fluid through an exchange process with the synovial fluid (Maroudas et al., 1968). The fluid also helps in tissue compression

`

resistance and restoring the original dimension after load evanescence (Temenoff and Mikos, 2000).

1.2.4 ECM organization

ECM is secreted by chondrocytes around which it forms a framework. Depending on the distance from the cell, the secreted ECM can be divided into three different regions, namely; pericellular matrix (PCM), territorial matrix (TM) and interterritorial matrix (IM) (Zhang et al., 2009). The PCM is regarded as the closest matrix to the chondrocyte, and it contains a lot of collagen VI and smaller amounts of collagen II, IX, XI as well as proteoglycans and other non-collagenous proteins (Poole et al., 1984).

The TM lies between the regions of the other two matrices and has the largest organized collagen fibre in comparison with the other two matrices. The IM has the greatest distance from the cells and contains collagen fibres which are the least organized when compared to the other two matrix regions (Buckwalter et al., 2005). Figure 1.4 illustrates the ECM regions in articular cartilage.

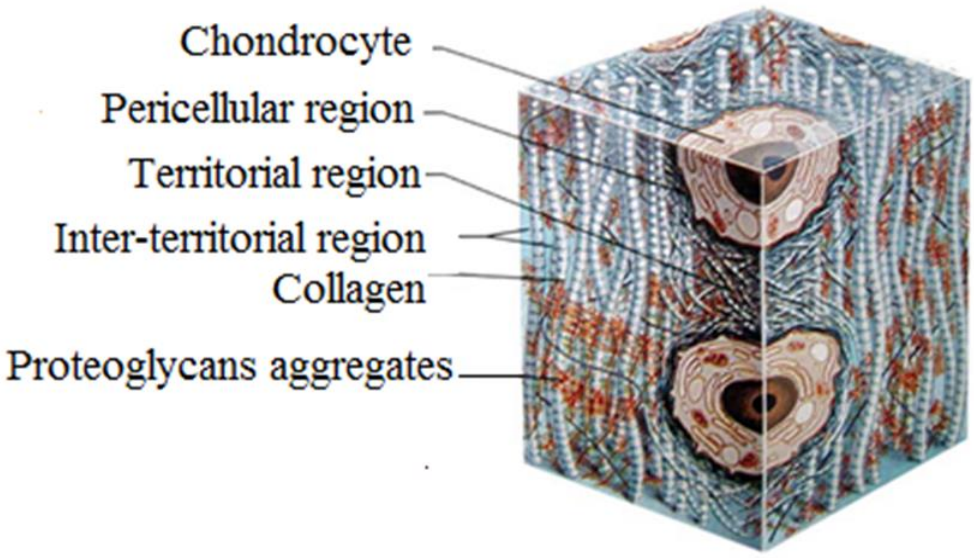

Figure 1.4: Illustration of the ECM regions of articular cartilage, comprising pericellular matrix, territorial matrix and interterritorial matrix (Taken from Landínez et al., 2012)

`

1.2.5 Articular cartilage zonal structure

Articular cartilage has an anisotropic, zone-specific structure that extends from the articular surface to the subchondral bone with different composition and functions. It is made up of the superficial zone, the transitional or middle zone, the radial or deep zone and the calcified zone (Figure 1.5). There is a unique composition and arrangement of chondrocytes and ECM within each zone (Hunziker et al., 2002).

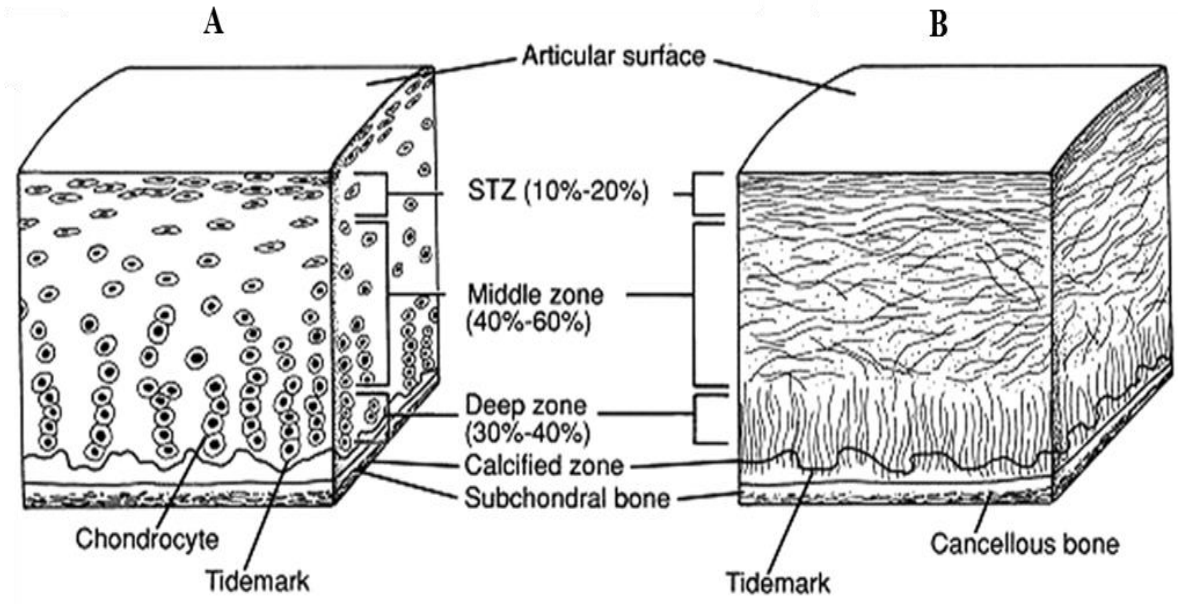

Figure 1.5: Schematic drawing showing articular cartilage zones; A. Cellular shape in each zone. B. Collagens fibers orientation in each zone (Taken Sophia et al., 2009)

- **The superficial zone**

It constitutes 10% of whole cartilage thickness (Weiss et al., 1968; Camarero-Espinosa et al., 2016). This zone has the least thickness and comprises flattened chondrocytes interspersed between parallel collagen fibres (Camarero-Espinosa et al., 2016). It has the lowest proteoglycans concentration of than that in middle and deep zones (Crockett et al., 2007). The superficial zone structure and composition produces shear resistance and tensile strength (Guilak et al., 1994).

`

- **The middle zone**

Within the middle zone which constitutes 60% thickness of articular cartilage, chondrocytes have a round shape with a random distribution (Camarero-Espinosa et al., 2016). An abundant amount of proteoglycan is found in the middle zone. In order to support resistance to the multidirectional compressive force and aid the retention of proteoglycan, the collagen fibres are oriented in random direction (Stockwell, 1979).

- **The deep zone**

In the deep zone chondrocytes are stacked like coins into vertical columns. This zone zones forms 30% of the thickness of articular cartilage and it is rich in proteoglycans, (Klein et al., 2009). The deep zone also orientates thick collagen fibres in radial direction in order to help generate strength between cartilage and bone (Poole et al., 2001).

- **The calcified zone**

This zone is characterized by the presence of collagen X and absence of proteoglycan (Zhang et al., 2009). It consists of collagen X fibres arching from cartilage into the bone to help attach cartilage to bone. This zone helps to transmit force and the limit diffusion from bone to deep zone (Cohen et al., 1998).

1.2.6 The pericellular matrix and chondron

Pericellular matrix is a specialized, thin layer of the ECM which immediately surrounds chondrocytes in cartilage (Poole et al., 1987). A chondron is a chondrocyte surrounded by its PCM. The PCM comprises different collagen II, VI, IX and XI, as well as proteoglycans and hyaluronan (Poole et al., 1997). Figure 1.6 illustrated the chondrons consist of chondrocytes surrounded by PCM.

`

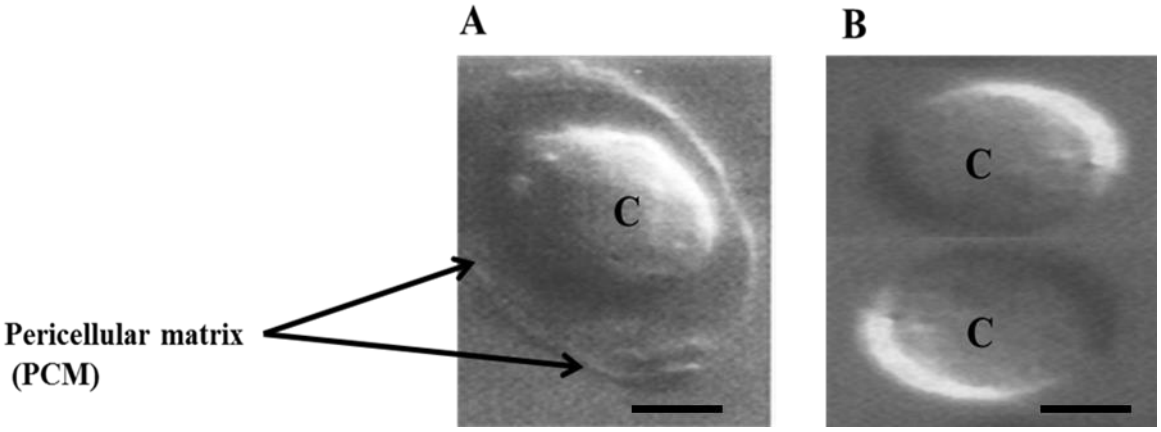

Figure 1.6: Chondron morphology. A) an isolated chondron consists of a chondrocyte (C) surrounded by its pericellular matrix (PCM). B) Two isolated chondrocytes (C) without a PCM (Taken from Lee al., 1997).Scale bar =10 μm

Although the PCM contains many of the same molecular constituents as the ECM, there are some distinct differences between the structure and composition of these regions. This region has been shown to contain a lot of proteoglycans (e.g., aggrecan, hyaluronan, and biglycan), and collagens (II and VI), but is primarily defined by the presence of VI collagen as compared to the ECM (Poole et al., 1997). Collagen VI is generally regarded as a basic component in PCM, and it is segmented into fibrils which form a fibrillar basket around the cell by intersecting at different angles. A mechanical protection against loading and deformation of cartilage is provided by this multi-angled configuration for chondrocytes (Chang and Poole, 1997). This significantly affects the stress-strain produced on the cartilage as well as the control of fluid flow of chondrocytes (Alexopoulos et al., 2005).

The interactions between the ECM and the chondrocyte play an important role in regulating the development and maintenance of cartilage. For example, the gene expression, proteoglycan metabolism and the response to growth factors are significantly affected by the interactions between the cell surface and ECM components (Adams and Watt, 1993). PCM likely influences the signals (both biochemical and biophysical) perceived by the chondrocyte since it is completely surrounded by the PCM (Poole et al., 1997). Thus, direct interactions are likely to occur between

`

cell surface receptors like integrins and the tissue matrix at the PCM level (Bidanset et al., 1992; Salter et al., 1992).

The metabolic activity of chondrocytes has been shown to be altered by the retention of the native PCM (Larson et al., 2002, Vonk et al., 2010), which suggests that the PCM may affect the biochemical and biophysical factors of the cell, and as such, play a biological role in controlling cell biosynthesis.

In addition to the fact that the PCM has a biological function, the chondron has also biomechanical function in nature. It performs a micro-mechanical function because it has the capacity to absorb the mechanical load by undergoing deformation and completely recovering when the load is removed (Szirmai, 1974). This potentially provides a protective role for the chondrocytes during loading through an "adaptive water loss from PCM proteoglycans" (Poole et al., 1988). According to a number of previous studies, the chondron serves as a filter or transducer of mechanical signals (Poole et al., 1992; Poole et al. 1997) particularly through the interaction of VI collagen with cell surface integrins or hyaluronan (McDevitt et al., 1991).

The notion that the chondron represents a compression resistant, which absorbs mechanical load and provides hydrodynamic protection for the chondrocyte) was first considered by Benninghoff (1925) (Poole et al. 1997). This was later confirmed by Szirmai (1974) who concluded that physically robust chondrons could be considered as mechanical units of cartilage.

A key marker of the PCM microenvironment is collagen VI (Poole et al., 1987), which is known to interact with various matrix macromolecules such as collagen II and decorin (Bidanset et al., 1992), proteoglycan and hyaluronan (Kielty et al., 1992). In addition, collagen VI has been shown in previous studies to interact with the integrin receptors of chondrocytes (Salter et al., 1992; Loeser, 2014). This implies that collagen VI plays a dual role, one of which is creating macromolecular interactions to ensure the structural and functional integrity of the chondron, the other is to mediate

`

cell surface anchorage and signalling potential between the chondrocyte and its pericellular microenvironment (Cesconet al., 2015).

Collagen VI in PCM, however, is a somewhat unique collagen in that it is not degraded by matrix metalloproteinases or by collagenase but is digested by some serine proteases (Lee et al., 1997). Previous studies suggest that a secretory enzyme and a member of the high temperature requirement family of serine proteases (HtrA1) is capable of degrading molecules in the pericellular matrix (Polur et al., 2010; Hou et al., 2013). HtrA1, a member of the mammalian HtrA serine protease family, has a highly conserved protease domain. In cartilage chondrocytes and synovial fibroblasts identified as major sources of secreted HtrA1which plays important regulatory roles. Substrates of HtrA1 have been identified, including aggrecan, decorin, biglycan, fibromodulin and fibronectin (Tsuchiya et al., 2005). It is also stated that collagen VI was not existent in chondrocytes synthesis HtrA1 in mouse OA joints, which is revealing of the disruption of the PCM of chondrocytes (Polur et al., 2010). HtrA1 has been implicated in rheumatoid arthritis (RA) and OA. Expression of HtrA1 is up-regulated in synovial fluids obtained from human RA and OA joints (Hu et al., 1998) and HtrA1 is the most abundant protease in human OA cartilages.

1.3 Articular cartilage repair and current treatments

Sport accident, trauma and irregular compression of cartilage can result in the damage of articular cartilage, are thought to lead to a loss of cartilage tissue, and without treatment, the injury can progress to OA (Hoemann, 2004). However, articular cartilage has poor repair capacity due to lack of blood supply and limited chondrocyte proliferation. The entrapment of chondrocyte in the dense ECM is thought to reduce chondrocyte proliferation (Huber et al., 2000).

Cartilage injuries are grouped into three main types. The first type is the matrix disruption, caused by blunt force trauma to the tissue which results to damage to the ECM (Zhang et al., 2009). The presence of viable chondrocytes after the damage usually facilitates the recovery of this type of

`

injury. Their ECM turnover compensates for the change in durability of the cartilage which effectively increases their synthetic activity to recover the damaged ECM (Temenoff and Mikos, 2000). The second type is the partial thickness defect which only affects the articular cartilage zones and does not permeate to subchondral bone. This defect frequently fails to repair as it does not allow the release of stem cells. Although chondrocytes are present in the cartilage tissue, they fail to move into the defect and proliferate to regenerate the injured region because they are embedded within the ECM (Fuller and Ghadially, 1972; Laurencin et al., 1999). The third type of cartilage injury is the full thickness defect which penetrates through all zones of articular cartilage down to the subchondral bone. This defect allows the release of stem cells such as mesenchymal stem cells (MSC) 'undifferentiated cells able to differentiate into different cell types' from the bone marrow into the damaged region and formation of fibrocartilage. Fibrocartilage has mechanical properties that are not the same as articular cartilage (Caplan et al., 1999; Hunziker et al., 1999).

It has indeed become necessary to intervene in the repair process due to the low capacity of self-healing or regeneration in damaged articular cartilage. Several surgical methods such as debridement, microfracture, autografts and cell therapy approaches like autologous chondrocyte implantation (ACI) have been employed to provide pain relief and improve joint function (Schurman et al., 2000).

- **Debridement**

Debridement involves removing the roughness of the cartilage surface by cleaning and smoothing the defect area in the knee joint. While this technique is easy to perform, the result is still questionable as only temporary improvements are usually experienced among patients with advanced stages of degeneration (Jackson et al., 2003).

`

- **Microfracture**

Microfracture is a commonly employed method for repairing articular cartilage of patients having lesions less than 2 cm in diameter (Zhang et al., 2009). It is a less invasive process with short surgery and recovery time compared to other treatments (Clair et al., 2009). Microfracture involves boring a hole through articular cartilage and the subchondral bone to release bone marrow stem cells to the damaged site (Redman et al., 2005). Instead of the fibrin clot, the MSC which are gradually fill the lesion site and then totally fill the injured site after one week (Hunziker et al., 1999). Over time, most of these MSCs can differentiate to chondrocytes, which then secrete articular cartilage proteins into ECM and repair the damaged articular cartilage site (Redman et al., 2005). The main disadvantage of this method is the production of fibrocartilage with weaker mechanical properties that are not suitable for articular cartilage, which is linked with increased failure rate (Laurencin et al., 1999; Zhang et al., 2009).

- **Autograft transplantation**

In this technique, a full depth plug of tissue is collected from non-weight bearing area in the joint of the patient, followed by an implantation process into damage region of joint in order to obtain healthy tissue graft (Clair et al., 2009). In spite of the excellent medical outcomes using this autografting method, there are some shortcomings which include inadequate donor tissues both in terms of capacity and quality, donor area morbidity (Laurencin et al., 1999). Also, stability of the graft tissue at high weight-bearing region over time as a result of the graft tissue being extracted from a non-weight bearing area (Malloy et al., 2002).

- **Total and partial joint replacement**

When other methods fail to repair the cartilage damage or when the articular cartilage has severe damage and advanced joint disease, then either total or partial joint replacement are employed. This

`

method is done to restore typical function by removing the injured joint and implanting artificial shell (such as alloys and titanium), a polymer surface (such as polyethylene) as well as a metal stem. However, it comes with its own limitations including loosening of the artificial implant, wearing off and short life-span of implant (maximum of 15 years) and increasing pain of the patient (Zhang et al., 2009).

- **Autologous chondrocyte implantation**

Autologous Chondrocyte Implantation (ACI) is a process in which cells are harvested from the donor site within the injured joint, expanded *in vitro* and re-injected into the defect site under a natural or synthetic patch (Brittberg et al., 1994). ACI has evolved over the last 20 years and as result of its 80% clinical success rate (Mistry et al., 2017). This method is the first cartilage tissue engineering approach to be applied clinically, and cartilage tissue engineering is presently aimed at improving the method and outcomes using different cells, materials, and culture environments (Brittberg et al., 1994).

Brittberg et al (1994) were the pioneers of the Autologous Chondrocyte Implantation (ACI) for cartilage. The ACI technique has been applied by different generations for several years (Marlovits et al., 2006). The first generation of ACI is the Brittberg's technique which is based on two surgical processes. The first process involves the removal of a small piece of undamaged articular cartilage tissue, isolation of chondrocytes and their expansion in vitro to the required number of cells. In the second process, the cells are injected into the damaged region of articular cartilage and sutured by periosteal patch as a cover to ensure chondrocytes are within the defected area (Brittberg et al., 1994). In the second generation of ACI, the cells are placed on a collagen matrix instead of the periosteal patch after being expanded in a monolayer. A collagen matrix is sutured over the cartilage lesion and the cell suspension is injected beneath (Haddo et al., 2004). In the third generation of ACI, the chondrocytes are spread homogeneously into the defect by placing their

`

suspension on a 3D biomaterial scaffold, and grafting is done using fibrin glue (Marlovits et al., 2006). The whole surgical morbidity is minimized in the second and third generation of ACI as they facilitate the surgical process as well as reduce the surgical time and number of injury cases (Marlovits et al., 2006). In spite of the favourable outcomes recorded, this technique has a number of limitations such as the possibility of producing fibrocartilage, which has a different mechanical property from hyaline cartilage and requires multiple invasive surgeries. Also, it reduces the long term stability (Zhang et al., 2009).

1.4 Cartilage tissue engineering

Tissue engineering has witnessed a lot of growth over the last 30 years, and this has given rise to many innovative treatment sessions seeking to optimise the traditional treatment methods for damaged living tissue (Ikada, 2006). It is known to be an effective approach for repairing damaged living tissue through the application of some basic engineering, material science and biology concepts (Lanza et al., 2011). It has rapidly developed to include a variety of cell types (such as stem cell and chondrocytes), scaffolds (such as biodegradable and natural or synthetic materials), growth factors and mechanical stimuli (Melero-Martin et al., 2007).

The ability of articular cartilage to repair itself is low, and the present treatments for cartilage damage are faced with some challenges. There is a continuous development in the field of tissue engineering, and a promising approach for articular cartilage regeneration is articular cartilage engineering. The production of tissue with similar structure, biochemical and biomechanical properties to native articular cartilage tissue is one of the objectives of cartilage tissue engineering (Solchaga et al., 2001).

The cell source, biomaterial scaffolds, and stimulatory factors to mimic the natural articular cartilage environment are crucial factors that determine the successful repair and regeneration of cartilage (Ikada 2006).

`

Various cell sources such as chondrocytes and mesenchymal stem cells from various tissues have been investigated for potential use in cartilage tissue engineering (Muschler et al., 2011). The ability of numerous natural and synthetic materials to support cartilage engineering *in vitro* and/or *in vivo* have been evaluated (Hutmacher, 2000). Furthermore, important stimulatory factors like mechanical stress and biochemical stimuli have been introduced during culturing of cartilage constructs (Zhang et al., 2009).

1.4.1 Cell sources for cartilage tissue engineering

Finding the ideal and optimal cell source is the main challenge facing cartilage tissue engineering (Liu et al., 2017). An ideal cell source for cartilage tissue engineering should have little or no immunogenicity, be easy to access, as well as have the ability to expand and maintain /differentiate to form functional cartilage tissue (Zhang et al., 2009). The main cells that have been used in cartilage tissue engineering are chondrocytes and stem cells (Vinatier et al., 2009).

1.4.1.1 The chondrocyte, chondron and PCM

Autologous chondrocytes have been extensively used in articular cartilage repair and regeneration; however, there are some limitations using this cell source (Ikada, 2006; Liu et al., 2017).

Some of these challenges include limited availability of autologous chondrocytes and the invasiveness of chondrocytes harvest process as well as the fact that it causes donor-site morbidity (Kock et al., 2012). The monolayer culture methods that are used to gather plentiful cell numbers cause chondrocytes to dedifferentiate towards fibroblastic with different properties for articular cartilage (Bonaventure et al., 1994; Goessler et al., 2004).

De-differentiation decreases the expression of collagen II, aggrecan, and other proteins related with articular cartilage as well as an increased expression of collagen I, which is the main limitation of monolayer culture of chondrocytes (Bonaventure et al., 1994; Stewart et al., 2000; Goessler et al., 2004).

`

In articular cartilage, each chondrocyte is surrounded by a 2-4 μm thick collagen VI-rich PCM forming a chondron (Poole, 1997). Freshly extracted chondrons form a more cartilage-like ECM than chondrocytes (Larson et al., 2002; Vonk et al., 2014) and their surrounding PCM is thought to maintain chondrocyte phenotype. Chang and Poole (Chang and Poole, 1997) cultured chondrocytes for 24 h producing aggrecan, decorin, and fibronectin. A week later, the chondrocytes were surrounded by a ring of PCM containing collagen VI. Vonk et al., (2010) compared chondron with chondrocytes culture. They found that in the chondrons, the type VI collagen was traced around the cells along culture duration. Some type VI collagens were found around the chondrocytes after 25 days of culture in alginate beads, but chondrocytes had a smaller amount of type VI collagen than that found around the chondrons and it has been demonstrated that maintaining the native chondrocyte's PCM enhanced the cartilage markers (collagen type II and GAG) production. Shafaei et al., (2017) showed that float chondrons maintain their round morphology and PCM at day 7 and the gene expression showed that attached chondrons has low gene expression of collagen II and aggrecan with high collagen I versus floating cells. Also, they have been reported using unattached form of chondron in cartilage tissue engenering could be a promising method to solve dedifferentiation problem of chondrocyte.

Through a combination of nanomanipulation, single cell RT-PCR and single cell immunolocalisation (Wang et al., 2008; Nguyen et al., 2010) determined that the presence of the PCM and its associated collagen VI makes the chondron stiffer than the chondrocyte and enhances ECM gene expression. Chondrons have a promising potential for the recovery of damaged articular cartilage. The use of chondrocytes together with chondrons has been predicted to have a better chance of self-healing compared to using only isolated chondrocytes.

1.4.1.2 Stem cells

Much effort is currently being put in place to explore better alternative cell sources as a result of the several aforementioned limitations associated with chondrocyte sources. Accessibility,

`

availability, and chondrogenic capacity are some of the desirable features for such sources (Saha et al., 2011). Stem cells are defined as undifferentiated cells with a capacity to self-renew and ability to differentiate into different types of specialized cells as chondrocytes, osteocytes and adipocytes. Therefore, stem cells such as adult MSCs have emerged as possible cell sources for articular cartilage tissue engineering (Mauck et al., 2003; Song et al., 2004; Boeuf and Richter, 2010; Liu et al., 2017).

Friedenstein was the first person to provide details about MSCs in 1974, and since then there has a rapid increase in the interest of using them as potential source for cell therapy and regenerative medicine because of their capacity to proliferate and differentiate into different cell types of the mesodermal origin (Van Pham et al., 20016).

MSCs can be extracted from bone, muscle, adipose tissue, synovial fluid (Johnstone et al., 2013). These stem cells have a relatively high capability to produce a sufficient amount of cells without altering their respective phenotypes, and also without causing any immune reactions. The minimally invasive isolation method can be used to separate MSCs from several mesenchymal tissues such as the skin and adipose. In comparison to other cell sources, this is most likely to reduce donor site morbidity as well as any form of harm to patients (Vinatier et al., 2009).

Bone marrow-derived MSCs are considered to be vital source of adult cells and as optimal substitute for chondrocytes in cartilage tissue engineering experiments due to their availability and easy access, capacity for differentiation, and lack of minimal immunogenic effect (Wakitani et al., 1994; Saha et al., 2011).

1.4.1.3 Co-culture in cartilage tissue engineering

In the UK, the standard treatments for small to medium sized cartilage defects in people of an age where they cannot have a joint replacement are either microfracture (Vijayan et al., 2010) or ACI (Richardson et al., 1999; Van Osch et al., 2009). Both procedures have their limitations and are not ideal to tackle large or full depth defects.

`

One favourable alternative could be using MSCs in cell therapy (Saha et al., 2011). Co-culture, a promising cell culture technology, enables delivery of the physical, chemical, and biological signals required by cells (Zhang et al., 2017). Co-culture systems have achieved tremendous success achieving a more realistic microenvironment of in vivo metabolism than monoculture system in the past several decades (Kook et al., 2017). There is some evidence that MSC co-culture with chondrocytes (Qing et al., 2011; Wu et al., 2011; Leijten et al., 2012) has the potential to enhance ECM production. While it is assumed that MSCs repair damaged tissues by differentiating them into specific cells to replace the lost cells (Bruder et al., 1994), but they produce cartilage tissues with inferior properties compared to chondrocytes because of the subsequent hypertrophy and mineralization of these cells after extended culture in chondrogenic conditions (Leijten et al., 2012; Kock et al., 2012).

The co-culture of articular chondrocytes and bone marrow mesenchymal stem cells has been reported to enhance matrix deposition (Tsuchiya et al., 2004). The differentiation of MSCs into chondrocytes has been suggested to be largely responsible for the beneficial effects of co-culturing chondrocytes with MSCs. Chondrogenesis has been shown to be supported by the release of soluble factors from chondrocytes in an indirect co-culture model of bone marrow MSCs and chondrocytes through the significant enhancement of proteoglycans and collagen II production (Qing et al., 2011; Wu et al., 2011; Levorson et al., 2014).

For example, studies by Wu et al., (2012) and Qing et al., (2011) demonstrated that co-cultures of human MSCs and chondrocytes resulted in enhanced ECM (collagen II and aggrecan) production. The resultant phenotypic changes are considered to be the result of signalling via direct cell–cell contacts, in addition to other parameters generated by the cell types. Other studies have provided evidence in support of co-cultures (Levorson et al., 2014). Levorson et al., (2014) confirmed the cartilaginous ECM-like (collagen II and GAGs) production was prompted in a xenogeneic co-culture model using rabbit MSCs and bovine chondrocytes within a nonwoven fibrous substrate.

`

Previous studies have stated that enhancement in ECM production by chondron and human MSCs in co-cultures for 4 weeks of pellet culture (Bekkers et al., 2013). Nikpou et al., (2016) used indirect human chondrons co-culture with human adipose-derived stem cells and used a nanofiber scaffold. In addition, Nikpou et al., (2016) used chondrons from osteoarthritis patients and reprted that chondrons obtained from osteoarthritic articular cartilage did not stimulate chondrogenic differentiation of adipose-derived stem cells in co-culture.

1.4.2 Scaffolds for articular cartilage tissue engineering

Biomaterial scaffolds are considered to be an essential aspect in tissue engineering because of their ability to provide structural and mechanical support as well as to promote cell attachment, proliferation and differentiation in three-dimensional (3D) environment (Hubbell, 1995; Frenkel and Di Cesare, 2004). Scaffolds should promote cell adherence and migration as well as be biocompatible, and biodegradable with suitable mechanical properties (Ahmed and Hincke, 2010; Mujeeb and Ge, 2014).

Several investigations have been carried out on biomaterial scaffolds for tissue engineering, which covers a wide range of scaffold materials including natural materials obtained from living organisms as well as synthetic materials produced from various chemical processes (Hubbell, 1995).

1.4.2.1 Synthetic scaffolds

Poly-α-hydroxy esters polymers such as poly (lactic acid) (PLA) and poly (lactic-co-glycolic acid) (PLGA) are the most popular synthetic polymers for cartilage tissue engineering scaffolds (Woodruff and Hutmacher, 2010). Through electrospinning, 3D printing, and gas foaming particulate leaching, these FDA approved biodegradable synthetic polymers can be fabricated into 3D matrices (Zhang et al., 2009). The fabricated polymer scaffolds have a controllable porosity and a suitable surface structure for cell attachment, proliferation, and differentiation (Hutmacher,

`

2000). Furthermore, their structure, degradation features, and mechanical properties can be adjusted by modifying these materials (Nuernberger et al., 2011)

However, there are some disadvantages associated with using synthetic polymers in cartilage engineering applications. For example, scaffolds used for cartilage tissue engineering lack signalling molecules for cell attachment, and their degradation products may give rise to a host response including inflammation which might lead to failure of the implant *in vivo* (Zhang et al., 2009).

1.4.2.2 Natural scaffolds

The biocompatibility of several natural biomaterials for cell attachment and differentiation has led to their development for cartilage repair and regeneration (Hubbell, 1995). Hyaluronic acid (Burdick et al., 2011), agarose (Rahfoth et al., 1998) and alginate (Fragonas et al., 2000) and protein-based collagen (Nehrer et al., 1998) are some natural scaffolds used in articular cartilage tissue engineering.

Collagens make up essential protein content in articular cartilage ECM, and they play a major role in cell adhesion, proliferation and differentiation. Thus, it is regarded as one of the promisng materials for constructing cartilage tissue engineering scaffolds. Yuan et al., (2016) have combined type I and type II collagens to construct a favorable injectable hydrogel whose compressive modulus can be regulated by changing the type I collagen content in the hydrogel. The chondrocytes embedded in the hydrogel maintain their natural morphology and secrete cartilage-specific ECM. Funayamaet al., (2008) have developed an injectable type II collagen hydrogel scaffold and have embedded chondrocytes in the collagen-based hydrogel and injected it into the damaged rabbit cartilage without a periosteal graft. At 8 weeks after the injection, favorable hyaline cartilage regeneration with good chondrocyte morphology was observed, and significant differences between the transplanted and control groups were observed after 24 weeks. Hyaluronic acid cell carriers or scaffolds have bioactive properties as well as the ability to interact with

`

chondrocytes. Although the chondrocyte synthesis (such as collagen type II and GAG) in ECM in vitro and in *vivo* is enhanced by hyaluronan based matrices, but their mechanical properties cannot satisfy the cartilage tissue (Solchaga et al., 1999). Kontturi et al., (2014) have developed an injectable, in *situ* forming type II collagen/hyaluronic acid hydrogel for cartilage tissue engineering. After encapsulation of chondrocytes and chondrogenic growth factor transforming growth factor-β1 into the hydrogel, the cell viability and proliferation, morphology, glycosaminoglycan production, and gene expression have been investigated. This hydrogel is able to maintain chondrocyte viability and characteristics, and it maybe a potential injectable scaffold for cartilage tissue engineering. Yu et al., (2014) have fabricated an injectable hyaluronic acid/ polyethylene glycol hydrogel with excellent mechanical properties for cartilage tissue engineering. Han et al., (2018) have been provided a biocompatible cross-linkable hyaluronic acid hydrogel and have been demonstrated that the encapsulation of chondrocytes within the hydrogel matrix in *vitro* and in *vivo* supported cell survival, and the cells regenerated cartilaginous tissue.

Cells encapsulated in the hydrogel in *situ* demonstrate high metabolic viability and proliferation. Typical example of polysaccharide biocompatible 3D scaffolds is agarose which is usually extracted from seaweed and are used to encapsulate cells for cartilage tissue engineering (Zarrintaj et al., 2018).

Dimicco et al., (2007) have been reported that the structure of collagen VI around chondrocytes embedded withn agarose is different than that in native structure that found in native articular cartilage. Garcia et al., (2017) have been facilated apromising method to encapsulate humanchondrocytes into thin biodegradable and natural fibrin-agarose hydrogels by using nanostructuration techniques with cartilaginous ECM production (collagen II and proteoglycan).

`

1.4.3 Hydrogels for cartilage tissue engineering

Hydrogels are 3D hydrated networks made of hydrophilic polymers that are linked together either through covalent bonds or physical intramolecular and intermolecular attractions (Vega et al., 2017). The use of hydrogel for scaffold construction in tissue engineering has generated a lot of interest for many years because of its flexibility and ability to be moulded into any shape, which is a required attribute for clinical applications (Grieshaber et al., 2011; Liu et al., 2017). In addition, insoluble hydrated polymers can take the shape of natural ECM both macroscopically and microscopically (Varghese and Elisseeff, 2006). Other benefits of hydrogels include the ability to act as a 3D structure to maintain cell shape and structure but unfortunately, this flexible nature decreases the mechanical strength of the hydrogel (Vega et al., 2017).

Taking Hyaluronic acid (HA) hydrogel into view, HA, a naturally occurring polysaccharide composed of N-acetyl-d-glucosamine and d-glucuronic acid, is a major component of the ECM in connective tissues and is particularly abundant in vitreous and synovial fluids (Garg and Hales, 2004). There are many advantages in using HA as a tissue scaffold. Some of these advantages include;

(1) Biodegradability, biocompatibity and bioresorbability (Drury and Mooney, 2003),

(2) it plays an important role in lubrication, cell differentiation and cell growth in ECM and these functions can be transferred to the scaffold (Balazs and Denlinger, 1989),

(3) its functional groups (carboxylic acids and alcohols) enable crosslinking (Garg and Hales, 2004),

(4) its exogenous form can promote healing (Balazs and Denlinger, 1989),

(5) it has the ability to maintain a hydrated environment, and

`

(6) it can be used to create a scaffold that is bioactive both in its intact structure and in the degraded form (Collins and Birkinshaw, 2013).

While the application of HA as a tissue scaffold material is hindered by its short residence time and lack of mechanical integrity in an aqueous environment, these drawbacks can be addressed through chemical modification and crosslinking (Collins and Birkinshaw, 2013).

Agarose is another hydrogel used in cartilage tissue engineering. It is a hydrophilic linear polymer extracted from “Gelidium gracilaria” and is composed of repeated units of disaccharide, 3, 6-anhydro-L-galactose and D galactose (Kuhtreiber et al., 1999). Agarose can vary in its mechanical stiffness since hydrogel contains flexible molecules. In addition, its low melting point makes it useful in facilitating the cell encapsulation before the gel setting (Zarrintaj et al., 2018). Furthermore, agarose hydrogel lack of cell adhesion or biomolecule interaction, and there is no integrin binding between cells and agarose. Thus, the use of agarose encapsulated chondrocytes helps to maintain the round shape of chondrocytes. In comparison to chondrocytes being seeded in monolayer, the preservation of the round cell shape and lack of cell attachments enhances chondrogenesis (Steward et al., 2011). As a result, agarose hydrogel has been used for a long time to encapsulate chondrocytes in cartilage tissue engineering because it provides a hydrated environment to native cartilage as well as preserves chondrogenic phenotype (Kuhtreiber et al., 1999).

Although there are many benefits of using agarose hydrogels as scaffolds in cartilage tissue engineering, there are some limitations which cannot be ignored such as their weak mechanical properties (Steward et al., 2011). Another major weakness is that the zonal organisation in native cartilage tissue can't be replicated by encapsulating chondrocytes with agarose hydrogel.

`

1.5 Nanofibers for cartilage tissue engineering

In articular cartilage tissue, the ECM is composed of a collagen network, essentially nano-scale collagen II fibres organized in different directions, which acts as a natural scaffold to provide mechanical and structural support as well as promote cell attachment and proliferation (Camarero-Espinosa et al., 2016). Nano-fabricated techniques make it possible to create nanofibers which closely mimic the nanofibrous collagen matrices that are found in articular cartilage ECM (Smith and Ma, 2004).

In the field of tissue engineering, the term "nanofiber" is usually used to describe fibers whose diameters are between 1 and 1000 nanometres (Kumbar et al., 2008). These fabricated nanofibers possess the structural and mechanical properties of ECM, which promote the formation of 3D tissue structures (Jayakumar and Nair, 2012). Typically, nanofibres have large surface area per unit volume (Kumbar et al., 2008), which supports cell adhesion and proliferation (Dalby et al., 2002; Glass-Brudzinski et al., 2008). Nanofibers have been observed to have higher rates of protein absorption than macro-scale surfaces, which are a key mediator in cell attachment to a biomaterial surface (Baharvand, 2014). Furthermore, the nanofibrous constructs have been found to selectively enhance the absorption of specific proteins such as fibronectin and vitronectin, (Woo et al., 2007) which is significant as fibronectin is a protein known to enhance cell adhesion and bind many growth factors.

1.5.1 Production methods

There are different methods to fabricate polymeric nanofibers, fore example; electrospinning, phase separation, drawing, and template synthesis (Barnes et al., 2007). Electrospinning is a highly efficient method of producing nanofiber, and as such, it is used in this project (Dahlin et al., 2006).

`

- **Phase Separation**

Phase separation is a technique that has long been used to create porous polymer membranes and scaffolds (Van de Witte, 1996, Mikos, 2000). To produce a porous nanofiber structure, a polymer is dissolved in a proper solvent and rapidly cooled to induce phase separation. Then, the solvent is later exchanged with water, and the construct is freeze-dried (Van de Witte, 1996). Nanofibers can be obtained by selecting the appropriate gelling temperature. Higher gelling temperatures have been shown to produce microfiber formation while lower gelling temperatures reduce the diameter to nanofiber dimensions (Zhao et al., 2011).

The advantages of this method include the fact that it does not require specialized equipment. In addition, constructs can be produced in a mould to achieve a specific geometry. However, this process can only be carried out with a limited number of polymers and would be difficult to scale-up to a commercial setting (Barnes et al., 2007).

- **Drawing**

In this technique, the fibres are obtained when the polymer droplet on the flat surface comes in contact with a micropipette. The pipette is withdrawn from the surface of the droplet, and a fine fibre is pulled from the bulk (Ondarcuhu and Joachim, 1998). Unfortunately, the fibre formation appears inconsistent because the surface tension at the bulk material surface during drawing increases due to the evaporation of the solvent over time. However, this method is considered to be a time consuming and discontinuous technique though it is simple and requires minimum equipment (Ramakrishna et al., 2005).

- **Template Synthesis**

This technique is generally considered to be simple as it basically involves forcing the polymer solution through the specified dimensions and shape pores, and as a result, fibres having dimensions of the pores of the template are generated. The major drawback of this method is that it is limited to only a few number polymers .i.e conductive polymers like poly (p-phenylene

`

vinylene), polyphenylenes and poly (acetylene), and as such, it fabricates on a small scale (Ramakrishna et al., 2005).

- **Electrospinning**

Electrospinning is a time and cost-efficient technique for producing polymer fibres and is the most commonly used method for producing fibre meshes in tissue engineering. It has the capacity of producing long, continuous fibres ranging from 3 nm to 10 μm in diameter (Pham et al., 2006). Moreover, a 3D architecture for cell culture and tissue construction is provided by nanofibrous scaffolds which in turn promote 3D tissue formation (Barnes et al., 2007).

1.5.2 Principles of electrospinning

There are basically three essential components involved in the electrospinning technique; a syringe pump, a high voltage generator and a collector. As shown in Figure 1.7, an electrical field has been generated between the collector and needle on the syringe pump due to the potential difference between them. There are two basic forces that affect the solution drop in the fabrication of electrospun fibres, and these are the surface tension force and the applied electric field. The strength of the electric field causes the solution to drop from the needle in a conical shape manner known as Taylor Cone. If the surface tension of the polymer solution is overcome by the electrical force, the charged droplet forms a jet that arises from the tip of the Taylor Cone. As the jet extends, it is drawn into a thin fibre which undergoes a whipping motion as it travels towards the collector. The jet splits into smaller fibers due to the instability and repulsive forces created within it. During this process, the solvent gradually evaporates into the traveling space between the needle and the collector, which eventually leads to the formation of continuous and thin fibres on the collector (Teo and Ramakrishna, 2006).

`

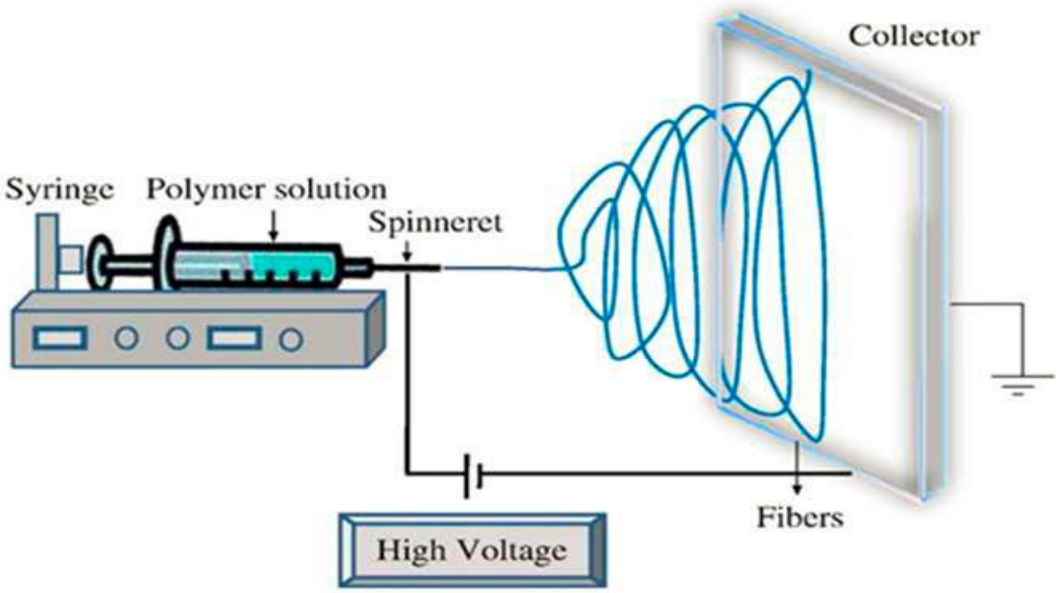

Figure 1.7: The principles of electrospinning (Taken from Zhu et al., 2013).

1.5.3 Electrospinning nanofibers for cartilage tissue engineering

In the field of tissue engineering, electrospinning is considered as a favourable technique for fabricating 3D scaffolds. Electrospun scaffolds are very effective in facilitating cartilage repair in articular cartilage tissue engineering simply because electrospun fibres are very similar in size to collagen fibres in native articular cartilage tissue (Braghirolli et al., 2014). As a result, the influence of nanofibers in cartilage tissue engineering has been investigated by many researchers (Yang et al., 2011).

It has been observed that electrospun scaffolds fabricated from PCL have the ability to proliferate and preserve the phenotypic characteristics of chondrocytes. Moreover, combining of nanofiber scaffolds with growth factors, human mesenchymal stem cells could be effectively differentiated into chondrocyte phenotype (Li et al., 2003).

Sonomoto et al., (2016) demonstrated that PLGA electrospun scaffold induce MSCs derived from healthy donors and patients with OA to differentiate into chondrocytes with chondrogenic markers

`

(production of proteoglycan and collagen II). Other study reported that PCL /gelatin scaffolds fabricated using electrospinning processes were biocompatible with articular cartilage. In addition, the scaffold enhanced the chondrogenesis of MSCs and showed evidence of rabbit articular cartilage defect repair, resulting in an enhanced gross appearance cartilage-specific gene expression, suggesting a possible application in the treatment of articular cartilage defects (Liu et al., 2014). The behaviour of chondrocytes was investigated by Wimpenny et al., (2012) with the use of nanofiber composites (poly (L, Dlactide) (PLDLA) nanofibre coatings on PLDLA film). Electrospun nanofibers were found to enhance chondrocyte attachment as well as maintain the rounded phenotypic nature of chondrocytes.

Steele et al., (2014) created a multi-zone cartilage construct by using electrospun polycaprolactone nanofibers. Analysis of the multi-zone scaffolds demonstrated region-specific variations in chondrocyte number, ECM composition, and chondrogenic gene expression.

Mirzaei et al., (2017) have been provided a nanofibrous glucosamine - poly(L-lactide) acid / polyethylene glycol scaffolds which enhanced the biological properties such as cell adhesion, proliferation and protein absorption rate, and induction of chondrogenesis (collagen II and prtoglycan production).

1.6 Aim and objectives of the project

The overall aim of the thesis was to investigate new cellular and scaffold strategies for better engineering articular cartilage, particularly to assess the effect of MSCs' role and other factors in 2D and 3D culture environments on the maintenance and regeneration of PCM and ECM, and to assess whether the zonally-organised hybrid scaffolds can separately and synergistically replicate the three zonal structures of articular cartilage.

The objectives of the thesis were:

`

1. To study 2D MSC co-culture with chondron and chondrocytes to determine whether there were any beneficial effects imparted by the direct cell-cell contact with MSCs on the process of chondrogenesis. The experimental approaches allowed the characterisation of maintenance and regeneration of PCM (collagen VI), the expression of HtrA1 and its relationship with the collagen VI expression (Chapter 3);
2. To define the key factors in 3D culture environment that facilitated PCM maintenance and regeneration alongside ECM production by both chondrocytes and chondron monoculture and co-culture with MSCs (Chapter 4);
3. To investigate whether FTIR microspectroscopy can reveal the impact of culture environments on chondrocyte's phenotype change and ECM production (Chapter 4);
4. To design hybrid zonal-specific 3D scaffolds in order to induce the formation of biomimetic zonal organisation and composition of ECM as in native articular cartilage tissue (Chapter 5).

`

Chapter 2 : Materials and methods

`

I: Materials: All used materials are listed in Table 2.1.

Table: 2-1 List of materials, catalogue number and supplier

Name	**Catalogue number**	**Supplier**
α-minimal essential medium (α-MEM)	BE12-169F	Lonza, UK
β-Glycerophosphate	G9422	Sigma-Aldrich, UK
β-mercaptoethanol	M6250	Sigma-Aldrich, UK
3-Isobutyl-1-methylxanthin	I7018	Sigma-Aldrich, UK
1,4-Butanediol diglycidyl ether	220892	Sigma-Aldrich, UK
1,9-dimethylmethylene blue (DMMB)	341088	Sigma-Aldrich, UK
4′,6-Diamidino-2-phenylindole (DAPI)	D9542	Sigma-Aldrich, UK
4-20% Protein Gels, 10 wells x 50 μL	NH21-420	Novex Life Technologies, UK
Acetic Acid	537020	Sigma-Aldrich, UK
Acetone, for analysis	A/0600/PC21	Fisher Chemical, UK
Alcian blue	A5268	Sigma-Aldrich, UK
Agarose	A9045	Sigma-Aldrich, UK
Alizarin Red	TMS-008-C	Sigma-Aldrich, UK

`

Amersham Hybond P 0.45 PVDF	10600029	GE Healthcare Life Science, UK
Anti-aggrecan antibody (rabbit monoclonal IgG)	ab36861	Abcam
Anti-Collagen I antibody (rabbit monoclonal IgG)	ab138492	Abcam
Anti-Collagen II antibody (mouse monoclonal IgG)	ab185430	Abcam
Anti- Collagen VI (rabbit monoclonal IgG)	ab182744	Abcam
Anti-GAPDH antibody	ab8245	Abcam
Anti-goat IgG, HRP-linked Antibody	7078P2	Cell Signaling Technology, UK
Anti-HtrA1 antibody (rabbit polyclonal IgG)	ab38611	Abcam
Anti-mouse IgG, HRP-linked Antibody	7076P2	Cell Signaling Technology, UK
Anti-rabbit IgG, HRP-linked Antibody	7074P2	Cell Signaling Technology, UK
Ascorbic acid	A8960	Sigma-Aldrich, UK
Bicinchoninic acid assay Kit	23225	Thermo- Fisher Scientific, UK
Bovine serum albumin (BSA)	A2153-50G	Sigma-Aldrich, UK
Bovine tracheal chondroitin sulphate	C9819	Sigma-Aldrich, UK
BupH™ Tris-HEPES-SDS Running Buffer	28398	Thermo- Fisher Scientific, UK
Chloroform	288306	Sigma-Aldrich, UK

`

Chondroitinase ABC	C3667	Sigma-Aldrich, UK
Collagenase IA	C9891	Sigma-Aldrich, UK
Collagenase II	C234155	Sigma-Aldrich, UK
cysteine-HCL	C7477	Sigma-Aldrich, UK
Dexamethasone	D4902	Sigma-Aldrich, UK
Dimethyl sulfoxide (DMSO)	D2650	Sigma-Aldrich, UK
Dispase II	D4693	Sigma-Aldrich, UK
Dulbecco's Modified Eagle's Medium (DMEM)	BE12-707F	Lonza, UK
Donkey anti-rabbit polyclonal antibody	SC-2089	Santa Cruz Biotechnology
Ethylenediaminetetraacetic acid (EDTA)	E6758	Sigma-Aldrich, UK
Ethanol (absolute)	E0650/17	Thermo-Fisher Scientific, UK
Falcon cell strainer	08-771-2	Thermo-Fisher Scientific, UK
FCS (fetal calf serum)	DE14-801F	Biosera labtech,UK
Filter card	5991040	Shandon, UK
Fluorescein isothiocyanate isomer I	F7250-250MG	Sigma-Aldrich, UK
Formaldehyde solution	F8775	Sigma-Aldrich, UK

`

Glycine	G8898	Sigma-Aldrich, UK
Goat anti-mouse monoclonal antibody	SC-16516	Santa Cruz Biotechnology, UK
Goat anti-mouse IgG	sc-2010	Santa Cruz Biotechnology, UK
Goat anti-Mouse IgG (H+L) Poly-HRP Secondary Antibody, HRP	32230	Thermo- Fisher Scientific, UK
Goat anti-Rabbit IgG (H+L) Secondary Antibody, Alexa Fluor® 594 conjugate	A-11037	Thermo-Fisher Scientific, UK
Halt™ Protease Inhibitor Cocktail (100X)	78429	Thermo- Fisher Scientific, UK
Hank Buffer saline solution (HBSS)	H9394-500ML	Sigma-Aldrich, UK
Hyaluronic acid (HA) sodium salt powder	HA-T	Shangdong Freda Biopharm, China
Hyaluronidase	H3506	Sigma-Aldrich, UK
Hydrochloric acid (HCL)	H1758	Sigma-Aldrich, UK
L-Proline	P0380	Sigma-Aldrich, UK
L-glutamine	17-605E	Lonza, UK
Live/Dead Assay Kit	L3224	Thermo- Fisher Scientific, UK
Indomethacin	I7378	Sigma-Aldrich, UK
Industrial Methylated Spirit (IMS)	I99050	Genta medical, UK
Insulin	I9278	Sigma-Aldrich, UK

`

Insulin-Transferrin (ITS)	T5240 6559	Sigma-Aldrich, UK
Isopropyl alcohol	I0398	Sigma-Aldrich, UK
Methanol	322415	Sigma-Aldrich, UK
Rabbit anti- mouse IgG-B	ab8517	Abcam
N,N-Dimethylformamide	227056	Sigma-Aldrich, UK
NOVEX Sharp pre-stained protein ladder	LC5800	Thermo- Fisher Scientific, UK
Novex® Tris-Glycine SDS Running Buffer (10X)	LC2675	Thermo- Fisher Scientific, UK
NuPAGE 4 -20 % Bis-Tris gel	NH21-420	Generon, UK
NuPAGE® MES SDS Running Buffer (20X)	NP0002	Thermo- Fisher Scientific, UK
Optimal Cutting Temperature (OCT) compound	AGR1180	Agar scientific , UK
Oil Red O	O0625	Sigma-Aldrich, UK
Page Ruler™ Unstained Low Range Protein Ladder	4360954	Invitrogen , UK
Papain	P4762	Sigma-Aldrich, UK
Paraformaldehyde	158127	Sigma-Aldrich, UK
Penicillin, streptomycin,	17-602E	Lonza, UK
Phosphate buffered saline (PBS)	BE17-516F	Lonza, UK

`

Pierce BCA protein assay kit	23221	Thermo Fisher Scientific, UK
Pierce™ 20X TBS Tween™ 20 Buffer	28360	Thermo Fisher Scientific, UK
Pierce™ ECL Western Blotting Substrate	32109	Thermo Fisher Scientific, UK
Poly-l,d-lactic acid (PLA)	96% l/4% d	Purac BV, the Netherlands
Poly-L-lysine coated slides	P0425	Sigma-Aldrich, UK
Proteinase K	P2308	Sigma-Aldrich, UK
Quant-iTTM Picogreen® dsDNA assay kit	P7589	Invitrogen, UK
Radioimmunoprecipitation assay buffer (RIPA)	89900	Thermo- Fisher Scientific, UK
Silica gel grains	10087	Sigma-Aldrich, UK
Sodium acetate	S2889	Sigma-Aldrich, UK
Sodium chloride (NaCL)	433209	Sigma-Aldrich, UK
Sodium phosphate	342483	Sigma-Aldrich, UK
Sodium pyruvate	P2256	Sigma-Aldrich, UK
Toluidine blue	T3260	Sigma-Aldrich, UK
Tris base	741883	Sigma-Aldrich, UK
Tris Buffered Saline with Tween® 20 (TBST-10X)	80-INSRT-E0l-ALP	Stratech Scientific Ltd

`

Trizma hydrochloride	T3253	Sigma-Aldrich, UK
Transforming Growth Factor- beta 3 (β3)	T5425	Sigma-Aldrich, UK
Trypsin/EDTA10X	89900	Lonza, UK

II: Methods

2.1 Cell isolation and expansion

2.1.1 Chondrocyte extraction and culture

Bovine knee joints were collected from a local slaughter house and washed with 70% industrial methylated spirit (IMS). Cartilage tissue was extracted from the joints using a scalpel (Figure 2.1) and cut pieces were washed in sterile phosphate-buffered saline (PBS) supplemented with 2% (w/v) penicillin-streptomycin. The washed cartilage was finely chopped. The enzymatic chondrocytes isolation employed was based on published protocol (Wang et al., 2008) with minor modification. Cartilage pieces were digested with 0.1% (w/v) proteinase K at 37˚C for one hour. The proteinase solution was discarded and then the cartilage was further digested with 0.3% collagenase IA at 37˚C and 5% CO_2 for 3 hours. The suspension was filtered using a 70 μm nylon mesh. The filtrate was centrifuged for 4 minutes at 750 g. The cell pellet was resuspended in Dulbecco's Modified Eagle's Medium (DMEM) supplemented with 10% fetal calf serum (FCS) and 1% L-glutamine and 1% penicillin-streptomycin (basal media). Cell passaging or splitting is a technique that enables an individual to keep cells alive and growing under cultured conditions for extended periods of time. When cells reached confluence i.e. 80% cell coverage, they were released from tissue culture flasks by trypsinisation process through washing twice with PBS and incubating with 0.25% trypsin in 1 mM ethylenediamine tetraacetic acid (EDTA) for 5 minutes at 37 °C. The DMEM medium with 10% FCS was used in inhibit the trypsinisation. The cell suspension was

`

collected and centrifuged for 3 minutes to get the cell pellet. The chondrocytes were cultured on T75 tissue culture plastic flasks at 3 x 10^3 cells/cm^2 cell density. The passage number of a cell culture is a record of the number of times the culture has been subcultured, i.e. harvested and reseeded into multiple 'daughter' cell culture flasks. In this study passage 0 (P0) refered to fresh isolated cells from tissues without culture and passage 1 (P1) cells refered to the first subcultured cells. Cells up to passage 1 were used for experiments.

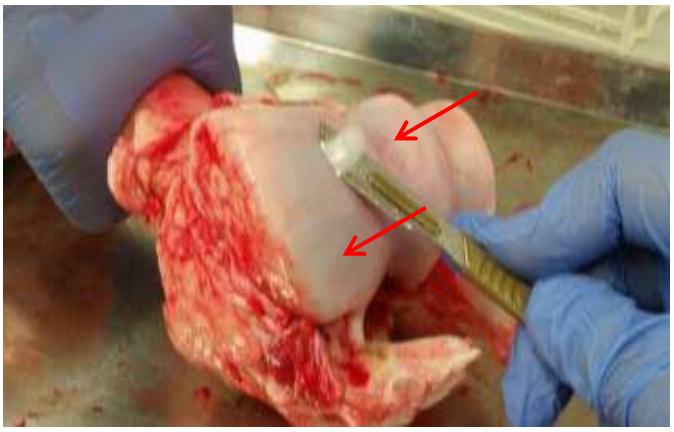

Figure 2.1: Cartilage tissues isolated from a bovine knee joint with scalpel. The arrows indicate the cartilage tissue.

2.1.2 Chondron isolation and culture

The enzymatic chondron isolation was based on established protocol (Wang et al., 2008) with minor modification. The chopped cartilage was digested with mixture of 0.3% (w/v) dispase II and 0.2% (w/v) collagenase II dissolved in PBS for 5 h in an incubator at 37˚C and the suspension was filtered through 70 μm nylon mesh. The filtrate was centrifuged for 4 minutes at 750g. The cell pellet was resuspended in supplemented DMEM mentioned previously. For passage 1 experiments, chondron were seeded on T75 tissue culture plastic flasks at a density of 3 x 10^3 cells/cm^2 with expansion medium as described above.

`

2.1.3 Rat mesenchymal stromal cells isolation and culture

MSCs were extracted according to Mao et al., 2005 and in strict accordance with the Animal (Scientific Procedures) Act 1986. The femurs and tibias from 28 days old Sprague–Dawley rats were dissected (Figure 2.2). After cutting both ends of the bones along the epiphysis, the bone marrow was driven out using 10 mL of α-minimal essential medium (α-MEM) supplemented with 10% FCS and 1% L-glutamine and 1% penicillin-streptomycin. Bone marrow cells were cultured in a T25 flask and incubated at 37°C with 5% CO_2. Non-attached cells were discarded, and culture medium was changed every 3 days. In this study P1 and P2 MSCs were used. Rat MSCs differentiation potential was assessed by the conventional tri-lineage differentiation assays according to the protocols (Carvalho et al., 2013).

Histological staining studied the MSCs capacity to adhere to the tissue culture plastic and undergo differentiation into chondrocytes, osteocytes and adipocytes for Chondrogenic (Toluidine Blue), Osteogenic (Alizarin Red) and Adipogenic (Oil Red O) lineages. Cells were seeded at a density of 2 x 10^4 cells/cm^2 (n=3) and cultured in the relevant differentiation media:

- **Chondrogenic differentiation medium**

Chondrogenic differentiation media was comprised of supplementing DMEM with; 1% penicillin-streptomycin, 1% L-glutamine, 1% FCS, insulin-transferrin-selenium (1% v/v), dexamethasone (0.1 μM), ascorbic acid (50 μM), l-proline (40 μg/ml), sodium pyruvate (1% v/v) and transforming growth factor (Mackay et al., 1998).

- **Osteogenic differentiation medium**

Osteogenic differentiation media consisted of: DMEM with; 1% penicillin-streptomycin,1% L-glutamine, 1% FCS, dexamethasone (10 nM), ascorbic acid (50 μg/ml) and β-glycerophosphate (10 mM) (Jaiswal et al., 1997).

`

- **Adipogenic differentiation medium**

Adipogenic differentiation media was composed of DMEM with; 1% penicillin-streptomycin, 1% L-glutamine, 1% FCS, dexamethasone (0.5 μM), 3-isobutyl-1-methylxanthine (IBMX) (0.5 mM), insulin (10 μg/ml) and indomethacin (100 μM) (Pittenger et al., 1999).

The cells that were cultured in proliferation media acted as the experimental controls, and all cells were cultured for 21 days with the media being changed every three days. Cells were fixed by formalin after 21 days culture for histological analysis.

Figure 2.2: Dissected rat femur for extraction of rat MSCs

2.2 Hydrogels scaffolds fabrication

2.2.1 Agarose hydrogel preparation

Agarose (2%) with a low gelation temperature ~ 26˚C was used. The agarose powder was mixed in distilled water (dH_2O) and dissolved into viscous solution by using a microwave. Prior to use, agarose solution was sterilised three times under ultraviolet light for 90 seconds.

`

2.2.2 Cross-linked hyaluronic acid gel

Hyaluronic acid (HA) sodium salt powder with an average molecular weight of 1.5 x 10^6 Da was supplied by Shangdong Freda Biopharm Co., Ltd. China. The crosslinked HA hydrogel was formed following established protocol (Yang et al., 2016). The HA powder was dissolved in 1% sodium hydroxide (NaOH) at a concentration of 10% in a glass beaker. The solution was mixed by the mixer (MESE, United Kingdom) with the rate of 100 rpm for overnight at ambient temperature and the beaker was covered with Parafilm to avoid evaporation (Figure 2.3.A). 1,4-Butanediol diglycidyl ether (BDDE) was later added to the HA solution to a final concentration of 0.4 % (v/v) at a mixing speed of 200 rpm for 30 minutes. The reaction between HA and BDDE was performed in strong alkaline conditions to form a stable covalent ether bond. At a very high pH range, the epoxide groups of BDDE preferentially react with the hydroxyl groups of HA. In theory, six sites in every HA–disaccharide unit are available for the reaction with BDDE. The deprotonated hydroxyls are much stronger nucleophiles than both the anionic carboxylic group and the amide. Hence the hydroxyl groups are the most likely reaction sites, forming stable ether bonds with the BDDE.

The solution was transferred to a petri dish and was allowed to crosslink at an operating condition of 40°C and 0.6 bar in a vacuumed oven for 5 hours, after that dried at room temperature for 3 days using a desiccator filled with silica gel grains (Figure 2.3.B). The dried hydrogel was swollen by adding 300 ml of dH_2O until the pH value reaches almost 7 by using pH stripper measurement. PBS was then added to the crosslinked HA for rehydration (Figure 2.3.C). The swollen HA was dialyzed against deionized water and then PBS to remove any residual BDDE.

The above HA gel was directly used to generate deep zone or the base for individual zone. Metal puncher was used to produce a 1 cm^2 HA hydrogel pieces (Figure 2.3.D). The HA gel was further processed to allow the reconstruction into gels and was used for experiments. Briefly, the crosslinked HA gel was pulverised with a homogenizer (the mixer equipped with a metal drill bit)

`

(Figure 2.3.E) to obtain mini gel particles of 0-400 µm (Figure 2.3.F). The mixture of homogenised crosslinked HA gels and 2% (w/v) agarose in a ratio of 9:1 was used to enable the gel to be reconstructed with the required shape and thickness.

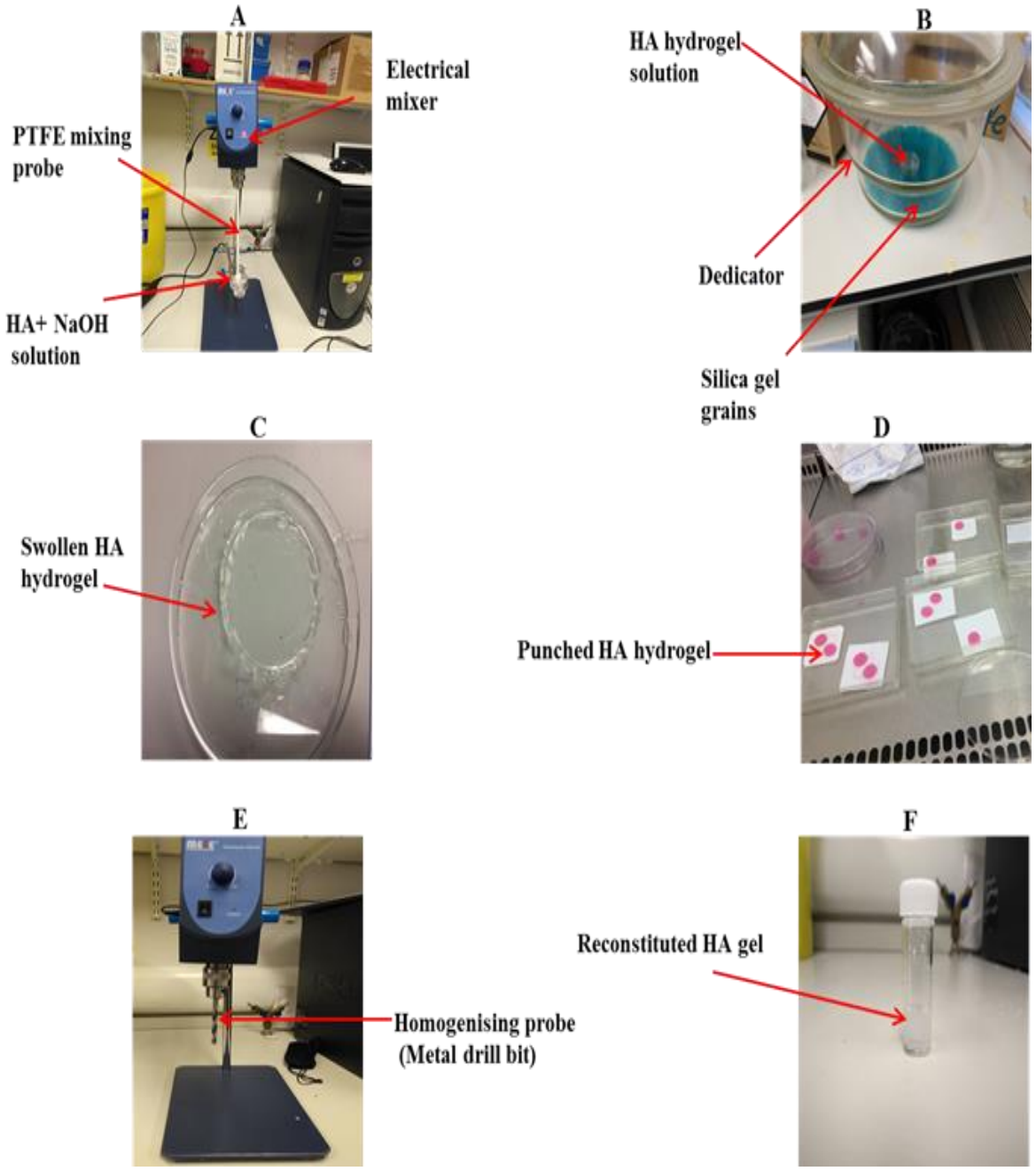

Figure 2.3: HA hydrogel fabrication process. A) Hydrogel solution mixing process. B) Drying process. C) Swollen HA hydrogel. D) Punched HA hydrogel blocks. E) Homogenising process F) Reconstituted HA hydrogel after Homogenising process

`

2.3 Electrospinning of polylactic acid nanofibers

2.3.1 General set-up of electrospinning system

The electrospinning technique is used to fabricate different organised nanofibers to construct zonal-specific scaffolds. The established protocol in the lab (Yang et al., 2011) was adopted to fabricate organised nanofibers. 2% poly-l,d-lactic acid (PLA) solution was prepared by dissolving PLA granules in a mixture of chloroform plus N,N-Dimethylformamide (solvents in a (7:3) ratio to produce nanofibers. The resulting 0.2 ml PLA solution was delivered at a 0.025 mL/ minute flow rate by a syringe pump through an 18G needle attached to the positive electrode. The distance between the positive and the collector (the negative electrode) was fixed to 15 cm. The needle and the collector were connected to a power supply charged at ±6 kV (Spellman HV, Pulborough, United Kingdom) as shown in Figure 2.4. The nanofibers formed were collected and glued to cellulose acetate frames of 16 cm^2 in which the adhesive glue has been deposited to stabilize their orientation. Before use, these nanofibers were sterilised three times under ultraviolet light for 90 seconds.

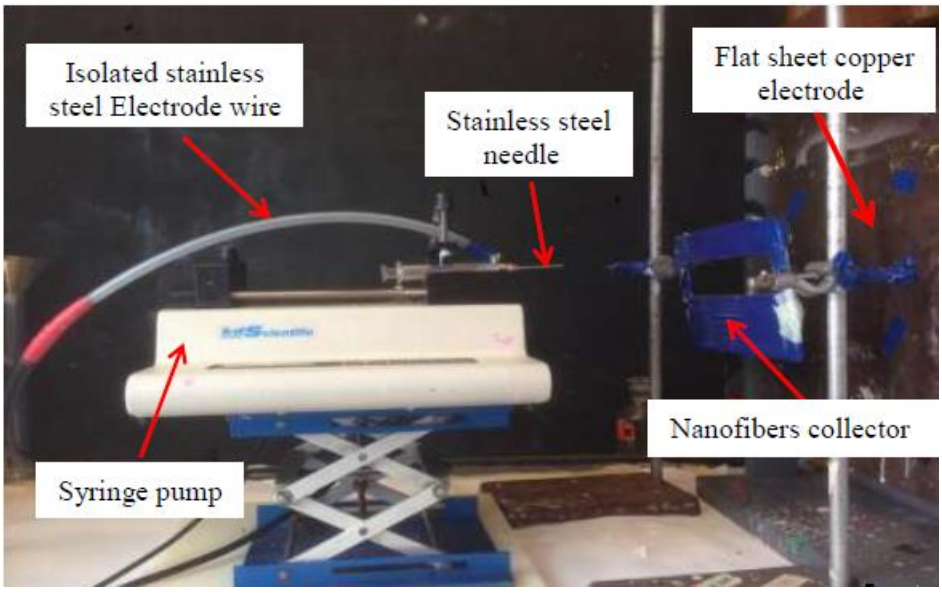

Figure 2.4: The main parts of electrospinning set-up

`

2.3.2 New collector design for zonal specific nanofiber meshes

A rectangular portable collector made up of a non-conductive material frame with conductive wires attached to the negative electrode (Figure 2.5) was used to produce highly aligned nanofibers meshes with low line density to replicate the matrix in superficial zone of articular cartilage (Yang et al., 2011).

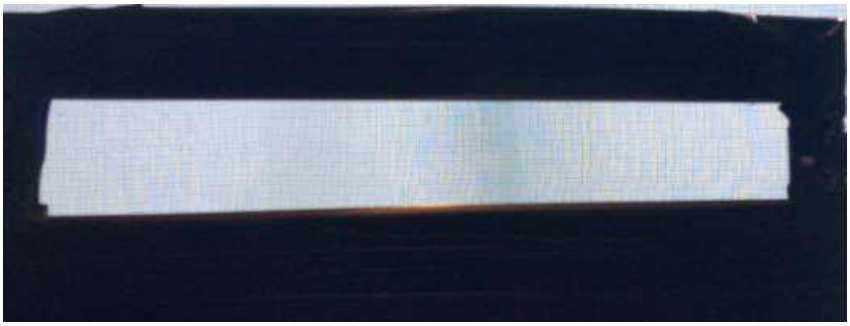

Figure 2.5: The rectangular collector for aligned nanofibers

A metal ring collector (Figure 2.6) was used to collect random nanofibers to replicate the matrix in middle zone of articular cartilage.

Figure 2.6: The ring collector for random nanofibers

`

2.4 Papain digestion for biochemical analysis

The digestion solution was made at a pH of 6.5 by dissolving 125 μg/mL of papain in 0.1 M sodium phosphate, 5 mM EDTA, and 5 mM cysteine-HCl. At the end of the culture time point, the experimental samples were separately digested with 300 μL papain solution per sample for 8 hours at 60°C. The digested solutions were stored at -20°C for further analysis (DNA and GAG analysis).

2.5 Cell viability and DNA assessment

2.5.1 PicoGreen DNA assay

PicoGreen DNA assay was used in quantifying the cell number. The Quant-iTTM Picogreen® dsDNA assay kit was used by the manufacturer's instructions. Serial dilutions of DNA standard (0–1 μg/mL) were used to construct a calibration curve. The PicoGreen solution was prepared as a 1:200 dilutions in 1xTris-EDTA (TE) buffer. 100 μL of standard or cell/lysis sample was introduced into a 96 well-plates followed by 100 μL of 1xTE to each relevant well. This was put in the dark for 5 minutes before fluorescence readings were carried out. The fluorescence was determined at 485 nm excitation and 535 nm emission using Synergy II BioTek plate reader. The previous study stated value of 7.7 pg of DNA per chondrocyte was used to approximate cell number (Kim et al., 1988).

2.5.2 Live/dead assay

The cell viability was observed with the aid of a Confocal Laser Scanning Microscope (CLSM, Olympus Fluoview FV 1200 with Fluoview software (4.1 version)) after staining with the Live/Dead Assay Kit. The viability of the cells was evaluated by the manufacturer's instructions. Calcein-AM ester dye was used fluorescently labelling viable cells in green, while the nucleus of dead cells was stained with Propidium Iodide dye (into red).

`

Cell culture media were taken out from samples, and the samples were washed with PBS and then immersed in the staining solution encompassing 10 μM Calcein-AM and 1 μM Propidium Iodide. They were later incubated for 20 minutes in the dark with 5% CO_2 and at 37°C. The samples were washed twice with PBS and immediately imaged using confocal laser scanning Microscope.

2.6 Total sulphated glycosaminoglycan contents assessment

Total GAG production was evaluated using 1,9-dimethylmethylene blue (DMMB) dye following the established protocol (Farndale et al., 1986). DMMB regent was made by the dissolution of 4 mg of DMMB in 250 mL of solution containing 0.58 g sodium chloride (NaCl), 0.75g glycine and 2.08 mL of 0.1M hydrochloric acid (HCL) dissolved in 248 mL of dH_2O. Standard (0-40 μg/mL) was made by dissolving bovine tracheal chondroitin sulphate in dH_2O. 100 μL of cell lysis sample or culture media or standard was introduced into a 96 well-plates and then 200 μL/ well DMMB to all wells was added. The absorbance of the solution in the plate was read immediately at 530 nm with using Synergy II BioTek plate reader.

2.7 Synchrotron FTIR spectroscopy

Synchrotron FTIR data were acquired from Diamond Light Source (Oxford), B22. The station is equipped with a Hyperion 3000 microscope (Bruker) and a Bruker 80V FTIR spectrometer, combining with liquid nitrogen powered 100 x 100 μm^2 MCT/A detector. A 36x Schwarzschild objective was used to obtain the spectra and images.

2.7.1 Sample preparation and cytospining

Prior to the cytospining process for cells encapsulated within hydrogel, the hydrogel was removed by heating up the samples in hot water bath (45°C) for 45 seconds. The resultant was centrifuged at 750 g for 2 minutes, and the cells pellets were resuspended in 0.9% NaCl. Cell suspensions were cytospun onto ZnS slides for 2 minutes at 1000 rpm using a cytofunnel and filter card. As soon as

`

the cells had been dumped on ZnS slides, samples were placed in a petri dish and fixed using 4% Paraformaldehyde (PFA).

2.7.2 Spectral collection

The system is accomplished by Opus software (Bruker). Typically, cytospun cellular samples were measured using a 10 X10 μm aperture, focusing the beam centrally onto nuclei region or peripheries of a cell. Spectral features were determined using former experiment measurements. Afterwards, a standard resolution of 4 cm^{-1} was used, 256 repetition scans per sample spectrum were taken as co-added scan from a single point and background measurement to maximise the signal to noise ratio and improve the resolution. Background measurements were taken every 30 cells spectral collection from areas of the substrate that were free of any sample material. Transmission mode was use for all measurements, using a ZnS substrate, 0.5 mm thick. For each sample, 30 - 40 cells were measured.

2.7.3 Data processing and analysis

The Unscrambler software (Version X, Camo, Oslo, Norway) was used to process the FTIR spectra to correct the baseline (linear-offset), and the spectra were also normalised (Standard Normal Variate (SNV)) and smoothed (Savitzky-Golay). Initially, the spectra were cut off to the area of interest for each analysis. The spectra were cropped to the region of 2700-3100 cm^{-1} that covers the lipid region, and for the fingerprint region, the spectra were cut off to 1000-1800 cm^{-1}. The SNV normalisation was performed after the baseline correction, which involves subtracting the mean spectrum and then dividing by the standard deviation for each spectrum. This helps to remove the effect of sample thickness as well as any baseline offset that may occur, and then the spectra were smoothed by applying Savitzky-Golay filter function.

The Unscrambler software (version X, Camo, Oslo, Norway) was also used to perform Principle Component Analysis (PCA). Loading plots indicate how much a variable contributes to each PC.

`

The same software was also used to visualise the spectra after it has been interpreted by the support software used to acquire the data at Synchrotron facilities (Opus, Bruker).

2.8 Cryostat sectioning

Experimental samples or articular cartilage tissue directly from bovine as a 'positive control' were embedded in optimal cutting temperature (OCT) compound. Then samples were cut using a standard cryostat (Bright, United Kingdom) into 10 μm thick sections on poly-L-lysine coated slides and kept in -20°C freezers.

2.9 Histologic analysis

2.9.1 Tri-lineage staining to confirm the MSCs phenotype

- **Alizarin red**

Alizarin red staining was used to confirm the osteogenic differentiation of MSCs. Before staining, 1% of Alizarin red solution was prepared in dH_2O and filtered using a 2 μm filter. The pH of the solution was set at pH 4. After 21 days culture; media was removed, and samples were washed in PBS and fixed by formalin. The samples were stained with Alizarin red solution for 5 minutes at room temperature. The stain was removed and washed three times in dH_2O. Calcium depositions were stained red (positive).

- **Oil Red O**

Adipogenic differentiation was characterised using Oil Red O prepared in 60% isopropanol and filtered using 2 μm filters. Formalin was removed entirely after the sample fixation, and the samples were washed twice with dH_2O. Oil Red O staining solution was added to the samples for 15 minutes at room temperature. The samples were washed three times in dH_2O and were rinsed with 60% isopropanol after removing the staining solution. Lipid formation appeared as small red droplets due to the differentiated MSCs in the adipocytes.

`

- **Toluidine blue staining**

In the tri-lineage study, the GAG production was evaluated using toluidine blue to characterise chondrogenic differentiation. 4% toluidine blue staining solution was prepared by dissolved 4g of toluidine blue in 100 mL of 0.1 M sodium acetate buffer solution. After 21 days culture; culture media was aspirated, and samples were washed in PBS and fixed in formalin at room temperature for 30 minutes. The samples were then stained with 4% toluidine for 10 minutes at room temperature, and the stain was removed, after which the samples were washed three times with distilled water. The total GAG stained with toluidine Blue.

2.9.2 Alcian blue staining

Alcian blue was used to characterise the GAG production where 0.1% (w/v) alcian blue staining solution was prepared by dissolving 0.1 g of alcian blue powder in 3% acetic acid (3 mL Glacial Acetic Acid + 97 mL dH_2O). The solution was appropriately dissolved and paper-filtered. At terminate culture points, the culture media was removed from the well, and each well was washed with PBS and fixed in formalin at room temperature overnight. The samples were then stained with 0.1% alcian blue (pH 1) for 15 minutes at room temperature. The stain was removed, and the samples were washed three times with dH_2O.

In this study for 3D samples toluidine blue has been used because the alcian blue stained the background gel strongly more than the toluidine blue, which may cause artificial staining.

2.10 Immunofluorescence assays

Immunofluorescence technique allows certain proteins in cells or tissue sections to be assessed through the binding of specific antibody conjugated to the fluorescent substrate. In this study immunofluorescence staining was conducted using primary antibodies against the following components in the pericellular matrix (PCM) and extracellular matrix (ECM): collagen VI (goat

`

polyclonal IgG), collagen II (mouse monoclonal IgG), aggrecan (rabbit polyclonal IgG), collagen I (rabbit monoclonal IgG) and HtrA1 (mouse polyclonal IgG).

Three samples for each culture group were fixed with 4% PFA at room temperature for 30 minutes. All samples were subjected to an unmasking treatment before the staining to develop the fluorescence detects the proteins following an established protocol (Wang et al., 2008). For detection of collagen VI, collagen II and collagen I samples were initially treated with 2 mg/mL testicular hyaluronidase (Hyase) by dissolving 2 mg of bovine Hyase in 1 mL of Tris-saline buffer at pH 5.0 (0.024 g trizma HCL with 0.08 g NaCl and 10 mL dH_2O). As regard aggrecan, the samples were initially treated with 25 mU mL^{-1} chondroitinase ABC by dissolving 0.2 U chondroitinase ABC in 1 mL of 0.1 M Tris-acetate buffer at pH 8.0 (0.121 g Tis base and 10 mL dH_2O) to generate 'stubs' of unsaturated disaccharides on the proteoglycan core proteins and to unmask epitopes. For HtrA1 detection, the samples were pre-treated with 25 mU/mL chondroitinase ABC and 2 mg/mL testicular hyaluronidase. The samples were washed three times with PBS containing 2% Bovine serum albumin (BSA) after treatment. These treated samples were then incubated with the primary antibodies and labelled with the fluorescein isothiocyanate (FITC)-conjugated secondary antibody for collagen VI and aggrecan, while tetramethylrhodamin (TRITC)-conjugated secondary antibody for collagen II, collagen I and HtrA1 and finally contrast stained with 4, 6-Diamidino-2-phenylindole (DAPI) to label the nuclei. DAPI (diluted 1:100 with PBS) was added for 20 minutes at room temperature. This was followed by three washes with PBS. Articular cartilage was used as a positive control. The samples in which primary antibodies were absent were assessed as negative controls.

All samples were observed using a confocal laser scanning microscope. Articular cartilage was used as a positive control. Primary antibodies were omitted for negative controls. All cells were evaluated using the same exposure time, gain, and offset camera settings, so that the immunofluorescence intensity was directly comparable among the groups for each given antibody.

`

2.11 Semi-quantification of cell morphology and staining intensity

Cell aspect ratio (length/width) of live cell images was used to assess the semi-quantification of cell morphology by using the image analysis using ImageJ software (1.51j 4). The longest chord of each cell was set as length, and the width was determined as perpendicular dimension to the length. At least 12 cells in each five randomly nominated areas for three biological samples were selected for the calculation. The mean values were collected and plotted for each group and at three culture time points. ImageJ software was also used to semi-quantify the intensity of staining. Five randomly selected areas from three images were chosen for each group. By using ImageJ software, the interest staining area and a region that has no stainig as a background were selected, and then the integrated intensity function was chosen. The total staining intensity was calculated according following formula: staining intensity = integrated density measurements – background measurements and the mean intensity were schemed for different groups and at different culture time points. Primary antibodies were omitted for negative controls. All cells were evaluated using the same exposure time, gain, and offset camera settings, so that the immunofluorescence intensity was directly comparable among the groups for each given antibody.

2.12 Western blotting

Protein in each sample was extracted after certain culture time point by digesting them in Radioimmunoprecipitation (RIPA) lysis buffer containing 1X protease and phosphatase inhibitor cocktail. The digestion buffer was kept on ice for 30 minutes, and then samples were centrifuged for 10 minutes at 11000 g at 4°C. The supernatant was then removed and stored at -20°C.

The protein concentration was measured by the bicinchoninic acid (BCA) protein method. Bovine serum albumin (BSA) standards were prepared at concentrations between 0 and 2 mg/mL. BCA reagent was prepared by adding 4% copper (II) sulphate pentahydrate solution to BCA solution in the ratio of 1:50, and 100 µL of the reagent was added to either 10 µL of each BSA standard or 5

`

μL of each lysate diluted in 5 μL RIPA buffer. Lysates were incubated for 30 minutes at 37°C, and then the A570 was determined using Synergy II BioTek plate reader. A protein standard curve was evaluated according with BSA standard values. Then, the protein concentration in each lysate was calculated by using the calibration curve.

A total volume of each lysate sample was calculated using the BCA assay containing 30 ug proteins and was added to 5 μL of a mixture of 150 μL of 1X NuPAGE sample and 7.5 μL of β-mercaptoethanol. To denature the protein content of the sample, the solution was heated for 15 minutes at 80°C in thermal cycler (OmniGene, United Kingdom).

A NuPAGE 4 -20 % Bis-Tris gel was loaded with 30 μg protein per well, and NOVEX® sharp pre-stained protein ladder (10 μL) was also loaded onto the gel. Samples were run in 1X BupH™ Tris-HEPES-SDS running buffer under a voltage of 70 V for 90 minutes. After that, the samples were transferred into an Amersham Hybond P 0.45 PVDF with 1X Novex® Tris-Glycine SDS Buffer for 90 minutes under a voltage of 30V.

After transferring has been completed, the membrane was washed three times by 1x TBST and was later blocked with 5% skim milk for one hour at room temperature and incubated overnight at 4°C with primary antibodies against collagen II (1:400), collagen I (1:400) and aggrecan (1:400).The membranes were then washed twice 1x TBST and incubated with corresponding HRP-conjugated secondary antibodies (1:4000) for one hour at room temperature. After washing the membranes three times by 1x TBST for ten minutes, signals were visualised using the FluroChem system (Bio-Techne). The membrane was washed three times by 1x TBST. The membrane was blocked in 5% skim milk, followed by the addition of the GAPDH (1:5000) primary antibody and washed three times by 1x TBST), and then incubated with (1:5000) HRP conjugated for 1 hour. Semi-quantitative measurement for proteins expressions using western blot was determined using ImageJ software by measurement the intensity in each band area and then normalize it to the loading control.

`

2.13 Scanning electron microscopy

A Hitachi S4500 SEM was used to view the images of the nanofiber scaffolds, where the specimens were coated with gold and imaged at an accelerating voltage of 15 kV. ImageJ software was used to determine the fibre diameters in analysing the SEM images (Wimpenny et al., 2012). The cross-sections of individual fibres were measured using a calibrated, line drawing tool. Two separate nanofibre subsamples were examined in at least three different areas, and about 50–200 fibres were measured for each sample.

2.14 Optical coherence tomography

Optical coherence tomography (OCT) is an imaging technique that uses coherent light (they have a constant phase difference and the same frequency, and the same waveform) to capture micrometre-resolution, two- and three-dimensional images from within optical scattering media (e.g., biological tissue). The light from a low-coherence source is split in two by the coupler with each part traveling along a separate arm of the interferometer, the reference and the sample arm. The light backscattered from the reference mirror and from the sample recombine at the coupler and generates an interference pattern, which is recorded by a single point detector.

The micro-channel dimensions in the scaffolds and the morphology of the assembled acellular or cellular 3D hybrid zonal constructs were assessed using optical coherence tomography (OCT; Telesto II, Thorn lab, USA). It works with the wavelength centred at 1300 nm providing approximately 1 mm image penetration.

2.15 Mechanical testing

An electro force model 3200 (BOSE, United Kingdom) (Figure 2.7) testing machine that was equipped with a 22-N load cell operated at a crosshead speed of 0.05 mm/sec was used to measure the mechanical properties of individual and assembled zonal scaffolds in uniaxial compression

`

testing. The dimension of the specimens dimension was measured as 1 cm X 1 cm for individual samples with a thickness of 0.5 mm for individual zonal scaffold and 0.6 mm for a 3D full zonal scaffold. The stress-strain curves were used to determine the compression modulus and the ultimate compression strength, which was taken as the maximum stress. Compression modulus was determined as the slope from the linear region of the stress–strain curve between 0.1 and 0.5 strain and the applied forces have been converted into stress with samples' area (Stress = Force/Area). The height difference between samples has been considered in the strain values which were obtained from the displacement divided by initial height (Strain = Δ Length/Length0), where the ultimate compression strength was taken as the maximum stress (Engineering toolbox/ Stress, Strain and Young's Modulus, 2011).

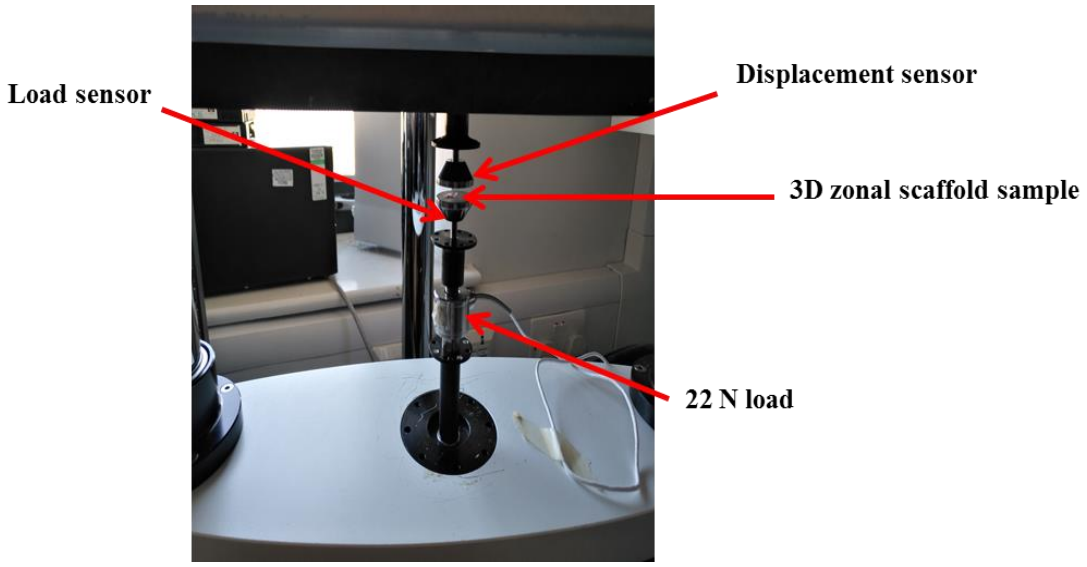

Figure 2.7: Compression mechanical test for different zonal scaffolds

Mechanical strength through ball indentation test was performed for a hydrogel mixture optimisation. Several ratios of agarose and HA respectively were made (0:10; 0.5:9.5; 1:9; 2:8), after which the mixture solution was placed on 1 cm^2 ring filter paper which was then inserted between two transparent plastic rings (20 mm) separately and held between two parallel flat metal plates with circular opening and tightened by a number of metal screws. These samples were

`

positioned on to a translation platform (Figure 2.8.A) and a plastic ball (1.23 mg) was placed on the centre of the sample to induce the deformation. The images of deformation were taken by long focal distance microscope which was connected with CCD camera linked to computer (Figure 2.8.B).

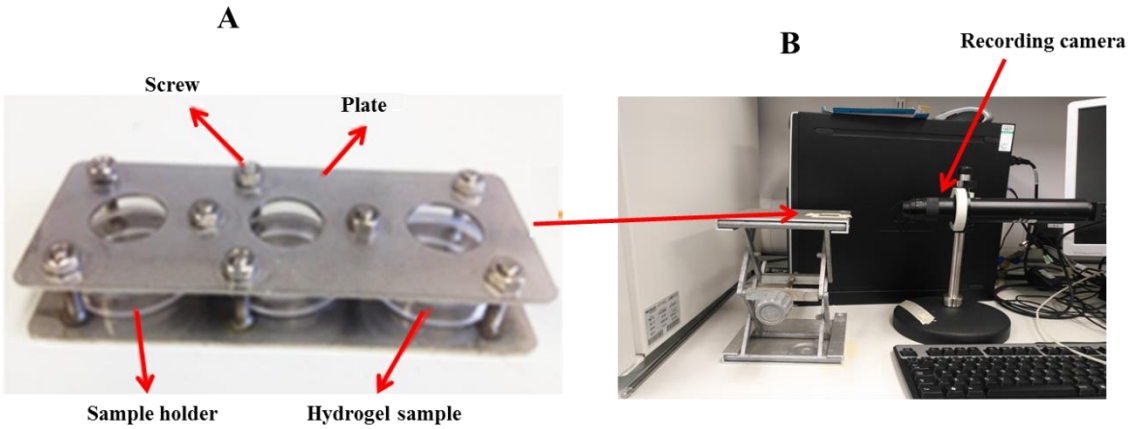

Figure 2.8: Ball indentation test for hydrogel mixture optimisation.

2.16 Statistical analysis

Four independent experiments have been run with three different chondrocyte preparations. The sample numbers in each independent experiment were triplicates. For statistical analysis, results are expressed as the mean ± standard deviation. Error bars on graphs indicate standard deviations (SD). The one-way analysis of variance (ANOVA) followed by Tukey post-tests was performed to determine statistical significance with significance defined as $p < 0.05$. All statistical analyses were performed using SPSS software.

`

Chapter 3 : Two-dimensional co-culture models of cartilage cells and mesenchymal stromal cells to study the enhancement of collagen VI and extracellular matrix production

`

3.1 Introduction

The role and degradation of PCM in culture

In the native articular cartilage tissue, a chondron is defined as a chondrocyte surrounded by a pericellular matrix. The PCM is rich in proteoglycans, collagen II and VI. Collagen VI is exclusively present in PCM. Hence, the "gold standard" for defining a chondron is the detection of collagen VI in associated cells (Poole et al., 1997). The PCM plays a significant role in the metabolic activity of the chondrocyte as well as the mechanical signalling from and to the extracellular matrix via cell-matrix interactions (Poole, 1987; Chang and Poole, 1997).

Enzymatically extracted chondrons adhering to hard substrates in monolayer will change their morphology from a rounded shape to a fibroblastic shape. This morphological change accompanied the loss of PCM up to day 7 in culture (Lee and Loeser., 1998, Larson et al., 2002). Enzymatically extracted chondrocytes lose their PCM during isolation process (Bonaventure et al., 1994; Stewart et al., 2000) and undergo phenotypic changes faster than a chondron during 2D culture (Lee and Loeser., 1998).

MSC and cartilage cell co-culture models

In the literature, co-culture studies of articular chondrocytes or chondrons with mesenchymal stem cells have provided evidence of increased ECM production (Qing et al., 2011; Levorson et al., 2014). According to Qing et al., (2011) chondrogenic properties (collagen II and aggrecan) were enhanced by the co-cultures of rabbit chondrocytes and rabbit MSCs in monolayer for 21 day culture. Levorson et al., (2014) confirmed the cartilaginous ECM-like (collagen II and GAGs) production was prompted in a xenogeneic co-culture model using rabbit MSCs and bovine chondrocytes within a nonwoven fibrous substrate. However, up till now, there have been no systematic studies to reveal whether MSC co-culture with cartilage cells makes reservation of PCM and what the associated mechanism (s) are.

`

Previous co-culture studies have tried to determine the effects of different ratios of chondrocytes or chondrons to MSCs in monolayer culture. As yet, there was no agreement but there were data to suggest that disparities between ratios could influence cell function, proliferation and even MSC differentiation (Qing et al., 2011; Walenda et al., 2010). The previous study also stated that collagen II and GAG production levels were higher in co-culture groups with a larger chondrocyte ratio to MSCs (chondrocyte: MSC; 4:1, 2:1 and 1:1). The optimal ratio of chondrocytes and MSCs in monolayer co-culture seemed to be 2:1 and 1:1 at day 7 culture (Qing et al., 2011). Previous work showed that a 1:1 ratio of chondrocytes to MSCs was capable of producing similar quantities of cartilage-like ECM as cultures of chondrocytes alone (Levorson et al., 2014). In another study, the 50% to 90% ratios of chondron/MSC cultures showed higher GAG production compared with chondron culture alone (Bekkers et al., 2013).

The potential influence of HtrA1to PCM degradation

To study the effect of co-cultures, particularly on the impact of the PCM as chondrogenic capacity, a biological marker which allows us to monitor the intactness of the PCM over time in culture is crucial. Collagen VI is the right marker. Interestingly, collagen VI cannot be digested by collagenase (during enzymatic extraction) and matrix metalloproteinases (during cartilage breakdown in OA), but it can be digested by serine proteases (Lee et al., 1997). Over the last decade, workers have considered whether upregulation of the serine proteinase, High Temperature Requirement A1, HtrA1, contributes to PCM disruption using human OA cartilage and mouse arthritic models (Polur et al., 2010; Hou et al., 2013). In one study (Polur et al., 2010) which used mouse knee cartilage, the relationship between HtrA1 and collagen VI was investigated. It was reported that collagen VI was degraded when chondrocytes secreted HtrA1, indicating that the PCM may be digested by HtrA1. Essentially, collagen VI disappeared from the PCM when HtrA1 was expressed. This interesting finding suggests that to test the integrity of the PCM can be through the use of HtrA1 as a “degradation” marker.

`

3.2 Objectives

The main aims of this chapter are to establish a xenogenic co-culture model of bovine chondrons, chondrocytes and rat MSCs, to determine whether MSCs play a role in the enhancement of chondrogenic capacity and PCM maintenance, and to define the optimal ratio of cell types. HtrA1 was utilised as a marker to reveal the potential working mechanisms of MSC in the co-culture. This study has used monoculture of chondrons and chondrocytes and MSCs to generate baseline data.

3.3 Materials and methods

3.3.1 Cell isolation and expansions

Bovine chondron and chondrocytes were used with passage 0 and passages 1 (P0, P1) exclusively. P1 and P2 rat MSCs was used. The cell isolation and culture details have been included in Chapter 2, Section 1.

Tri-lineage differentiation assays were conducted to confirm the multipotency of the used MSCs. The detailed MSC culturing for differentiation was explained in Chapter 2, Section 1.3. To confirm positive differentiation of each lineage, specific histochemical-staining was undertaken, as described in Chapter 2, Section 9. 1.

3.3.2 Experiments design and set up

Bovine articular chondrocytes (CY) and chondron (CN) at P0 and P1 were cultured in 2D monoculture or co-culture with rat MSCs. The ratios of chondrocytes or chondron to MSC were indicated in Table 3.1. All cultures were conducted in 48 well-plates at a seeding density of $1x10^4$ cells/well in DMEM or α-MEM supplemented media. The cultured was for 7 days and culture media were changed every three days. Details are described in Chapter 2, Section 1.

`

Table 3-1: Description of experimental groups with cell types and seeding densities

Experimental group	**Chondrocytes per well**	**Chondrons per well**	**MSCs per well**
CY	10,000	-	-
CY 80	8,000	-	2,000
CY50	5,000	-	5,000
CY20	2,000	-	8,000
CN	-	10,000	-
CN80	-	8,000	2,000
CN50		5,000	5,000
CN20		2,000	8,000
MSC	-	-	10,000

3.3.3 Cell morphology monitoring

The effect of all cell variables and culture time on cell morphology in monoculture and co-culture were monitored with an optical microscope (Olympus, Japan) attached to a CCD camera (1X 2-SLP, Micropublisher S-ORTV, Japan). Image-Pro Insight software was used to acquire the images. The cell morphology was semi-quantified by calculation of cell aspect ratio (length/width) of live cell images through the image analysis using ImageJ software as described in Chapter 2, Section 11.

3.3.4 Biochemical assays

At the end of the culture period, the experimental samples were digested by papain solution as described in Chapter 2, Section 4. The cells number was characterised by using PicoGreen DNA assay as explained in Chapter 2, Section 5.1. The GAG production was assessed by using DMMB

`

assay which was clarified in Chapter 2, Section 6. Overall the normalised value of GAG content per cell was calculated as well based on GAG content and cell number.

3.3.5 Histological analysis of GAG production

The GAG production in monocultures and co-cultures on all variables and different time points were assessed by Alcian blue staining as described in Chapter 2, Section 9.2.

3.3.6 Immunolocalisation of key PCM and ECM components

Immunostaining was used to identify the presence and distribution of PCM and ECM components (collagen II, collagen VI) and HtrA1, following the protocol described in Chapter 2, Section 10. Whole samples were stained using the same protocol. Semi-quantification of the cell morphology and the GAG and PCM component concentration was conducted based on the staining intensity across the groups and culture time by ImageJ analysis software as described in Chapter 2, Section 11.

3.4 Results

3.4.1 Tri-lineage differentiation of MSCs

The MSCs grown in chondrogenic media showed the positive staining for sGAG with toluidine blue dye; and cells in osteogenic media showed positive staining by Alizarin red dye for calcium deposition as the bright red nodules; and cells in adipogenic media were stained positively by the Oil Red O displaying lipid droplet formation (Figure 3.1).

`

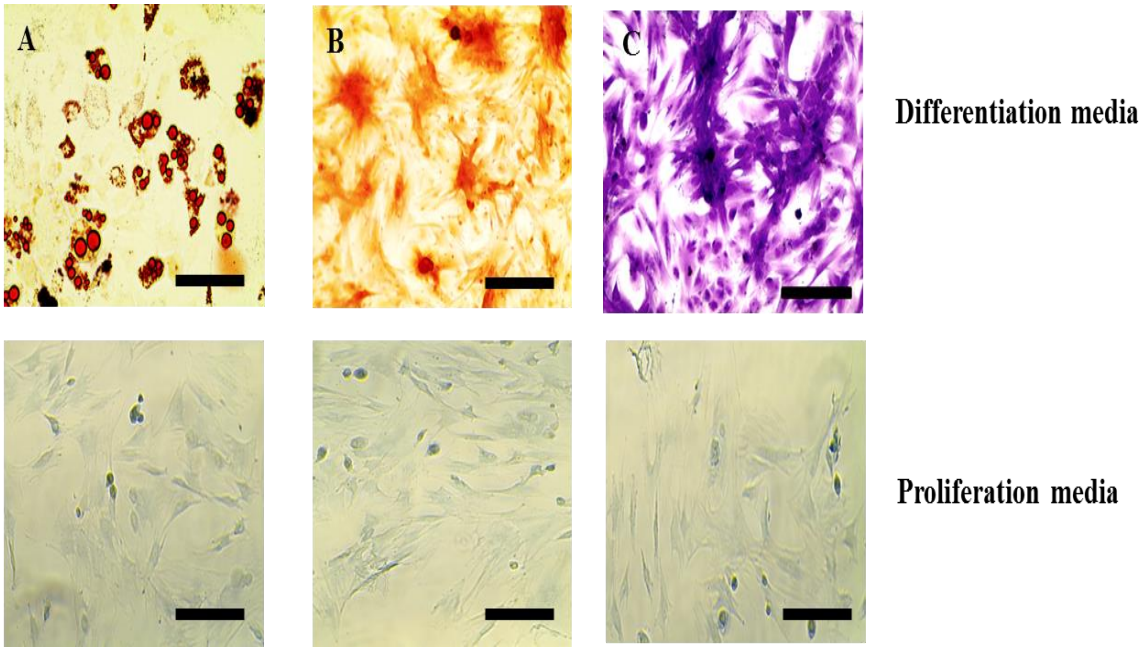

Figure 3.1: Illustration of Tri-lineage staining images after 21 days culture of the MSCs.

(A) Adipose differentiated cells (Red oil staining); (B) Osteoblast differentiated cells (Alizarin red); (C) Chondrogenic differentiated cells (Toluidine Blue). Scale bars represent 150 µm.

3.4.2 Cell morphology

3.4.2.1 Cell morphology in two-dimensional monocultures

In 2D monocultures the cell morphology was observed up to passage 1 (Figure 3.2). At P0 (Figure 3.2.A, day 1) chondrocytes and chondrons revealed a mostly rounded morphology while the MSCs had a spread spindle morphology. At the last culture time point, MSCs and chondrocytes had appeared as fibroblast-like spindle morphology while chondrons still maintained some of round shape. At P1 (Figure 3.2.B, day 1) all of the cell types had similar fibroblastic-like morphologies.

In order to quantify the differences in cell morphology between chondrons and chondrocytes throughout culture time and passage number, live cell images were taken, and these images were analysed to estimate cell aspect ratio (length/width, Figure 3.2.C). At day 1, chondrons and chondrocytes showed a round shape, corresponding to an aspect ratio value of 1. For both chondrons and chondrocytes, their aspect ratio increased at days 5 and further at day 7. MSC

`

showed much higher aspect ratio for all culture time points. Cells at passage number 1 showed high aspect ratio for both chondrocytes and chondron with fibroblast-like spindles morphology along the culture time. MSC kept spread morphology.

3.4.2.2 Cell morphology in two-dimensional co-cultures

Cell morphology of co-cultures was then estimated. For all MSC ratios, chondrons seemed to maintain a more rounded morphology whilst chondrocytes a more elongated morphology (Figures 3.3.A and B). At ratio 50:50, the morphology maintained the round shape for both chondrocytes and chondron during the first three days culture. After 7 days culture, the morphology slightly changes to elongated shape with some of round cell shape. The morphology of chondrons and chondrocytes at the ratio 20:80 or 80:20 co-cultures developed similarity to that of 50:50 ratio samples but with les round shape cells along cultures days.

Figures 3.3.C and 3.3.D showed the co-culture ratios 50:50 and 80:20 with MSc and chondrocytes or chondrons at P1. In general, chondrons and chondrocytes in all co-culture ratios presented similarity on their morphology along the three-time points i.e. elongated cell morphology. At day 7 both chondrons and chondrocytes became narrowed and extremely elongated cell morphology.

Compared to monocultures, co-culture samples seemed to improve chondrogenesis for all ratios of MSC and chondrons. Initially, MSC and chondrons seemed to have a low aspect ratio which increased significantly at day 7. At passage number 1, cells showed high aspect ratio; MSC kept spread morphology, also chondrocytes and chondron had fibroblast-like spindles morphology along the culture times.

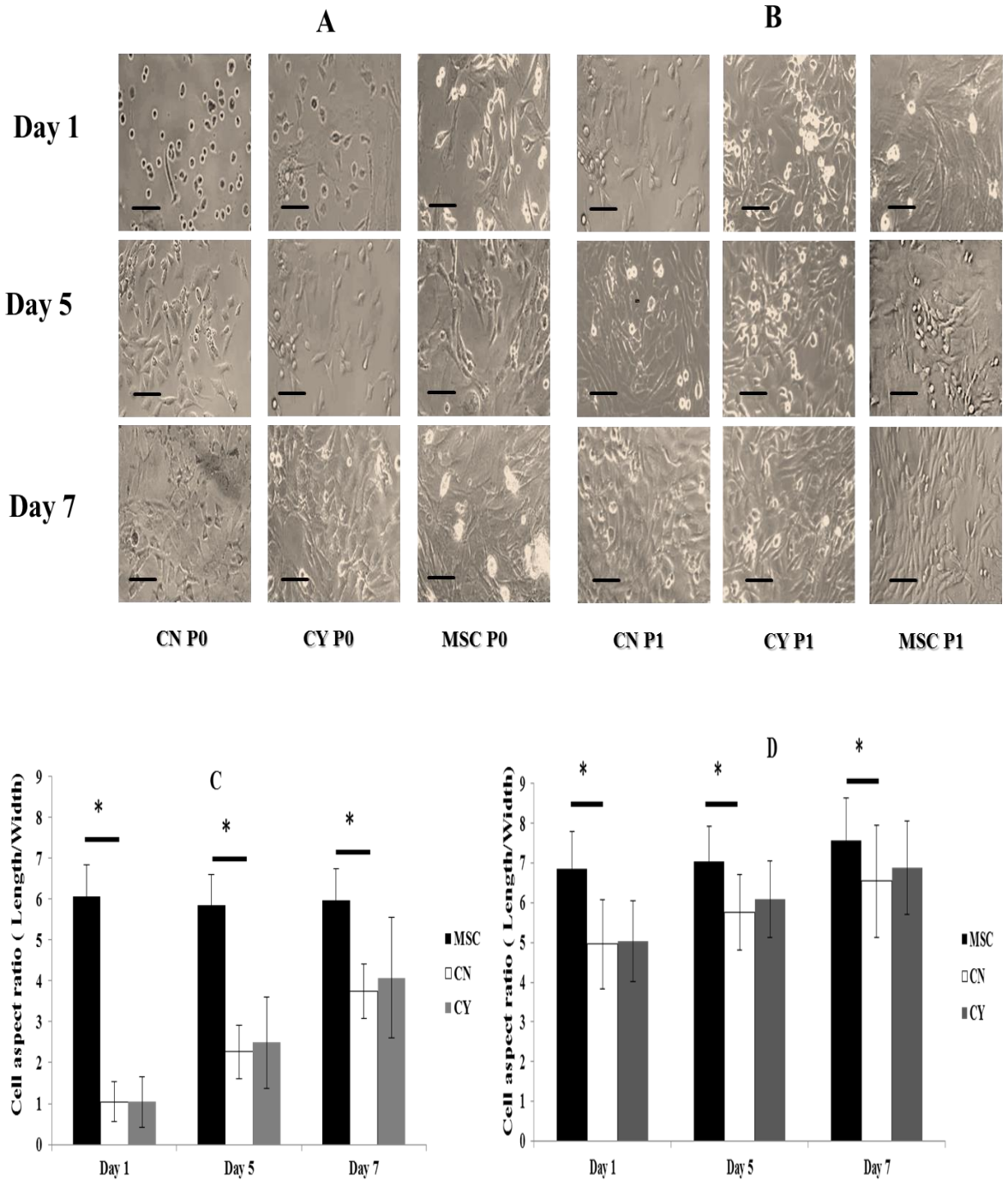

Figure 3.2**:** Cell morphology of chondrons (CN), chondrocytes (CY) and MSCs in monoculture at Days 1, 5 and 7 at (A) P0 and (B) P1. The scale bars represent 80 µm. (C) and (D) represented the cell aspect ratio analysis of P0 and P1 respectively chondron (CN) and chondrocyte (CY) in monoculture at days 1, 5, and 7. Data are expressed as mean ± SD (n = 3). *$p < 0.05$.

`

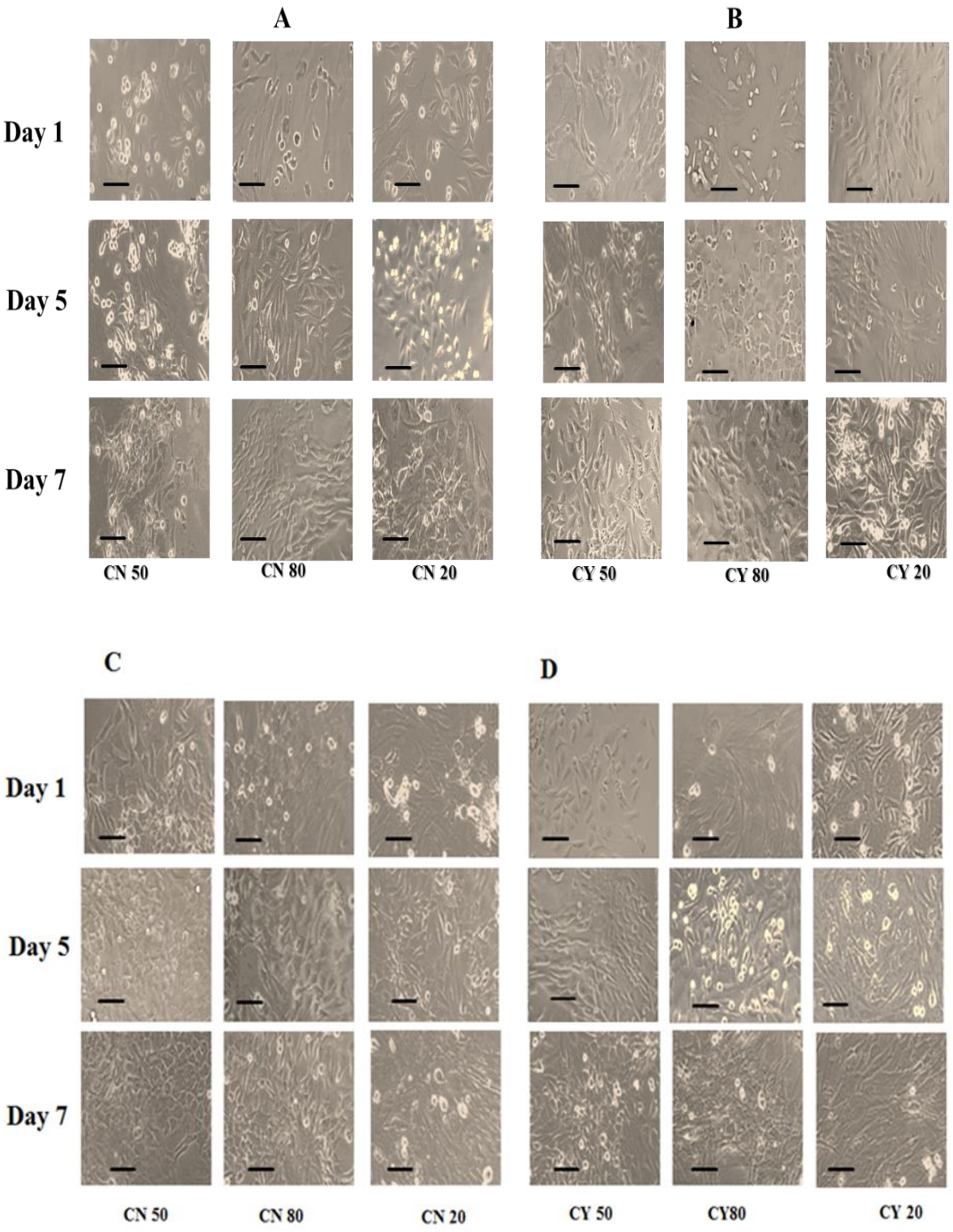

Figure 3.3: Cell morphology of co-culture of chondrons (CN, Panel A, P0) or chondrocytes (CY, Panel B P0), (CN, Panel C, P1) or chondrocytes (CY, Panel D P1) with MSCs.The scale bars represent 80 μm.

`

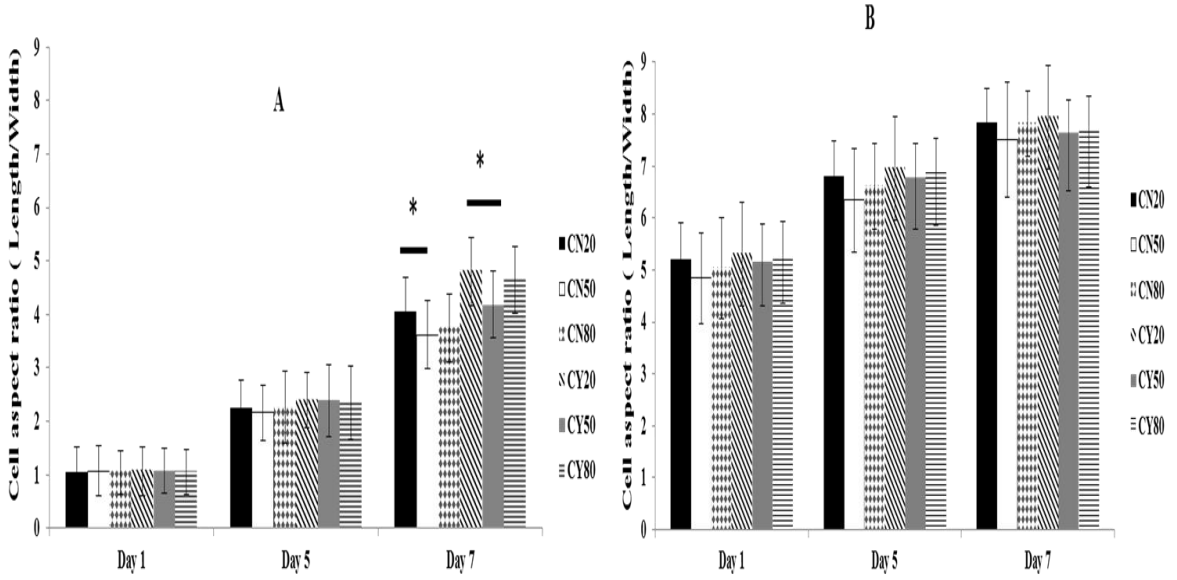

Figure 3.4: representive the cell aspect ratio analysis of P0 and P1 respectively chondron (CN) and chondrocyte (CY) in co-culture at days 1, 5, and 7. Data are expressed as mean ± SD (n = 3). *$p <$ 0.05.

3.4.3 Total sulphated GAG production and cell number

The total amount of sulphated GAG accumulated in cells in monoculture was assessed by DMMB at days 1, 3, 5 & 7 culture (Figures 3.4. A and B). At passage 0 and passage 1, the MSCs did not produce sulphated GAGs whilst the chondrons and chondrocytes accumulated a small amount of sulphated GAGs.

Cell number at different culture conditions were assessed by DNA contents (Figures 3.5.A and B). At passage 0 and passage 1, it became clear that cell number increased along the culture time, whilst chondron at P0 in different time points had lower cell number than chondrocyte samples ($p<0.05$). MSC exhibited highest cell number along culture. However, at P1 the cell number of chondrocytes and chondrons showed similar increase pattern ($p>0.05$). Both chondron and chondrocytes had much higher cell number at P1 than at P0.

Normalised data confirmed that sulphated GAG production per cell decreased with time and passage which was to be expected in monoculture conditions (Figures 3.6.A and B). GAG production was determined to be 16.8±0.61 pg/cell and 15.4±0.13 pg/cell for chondrons and

`

chondrocytes on day 1, and 10.0±0.45 pg/cell and 10.0±0.51 pg/cell on day 7, respectively. Figure 3.7 shows MSC and chondron co-cultures increased GAG production. The highest increase was in the samples with 50% MSC ratio ($p<0.05$), but the GAG production per cell decreased with time and passage.

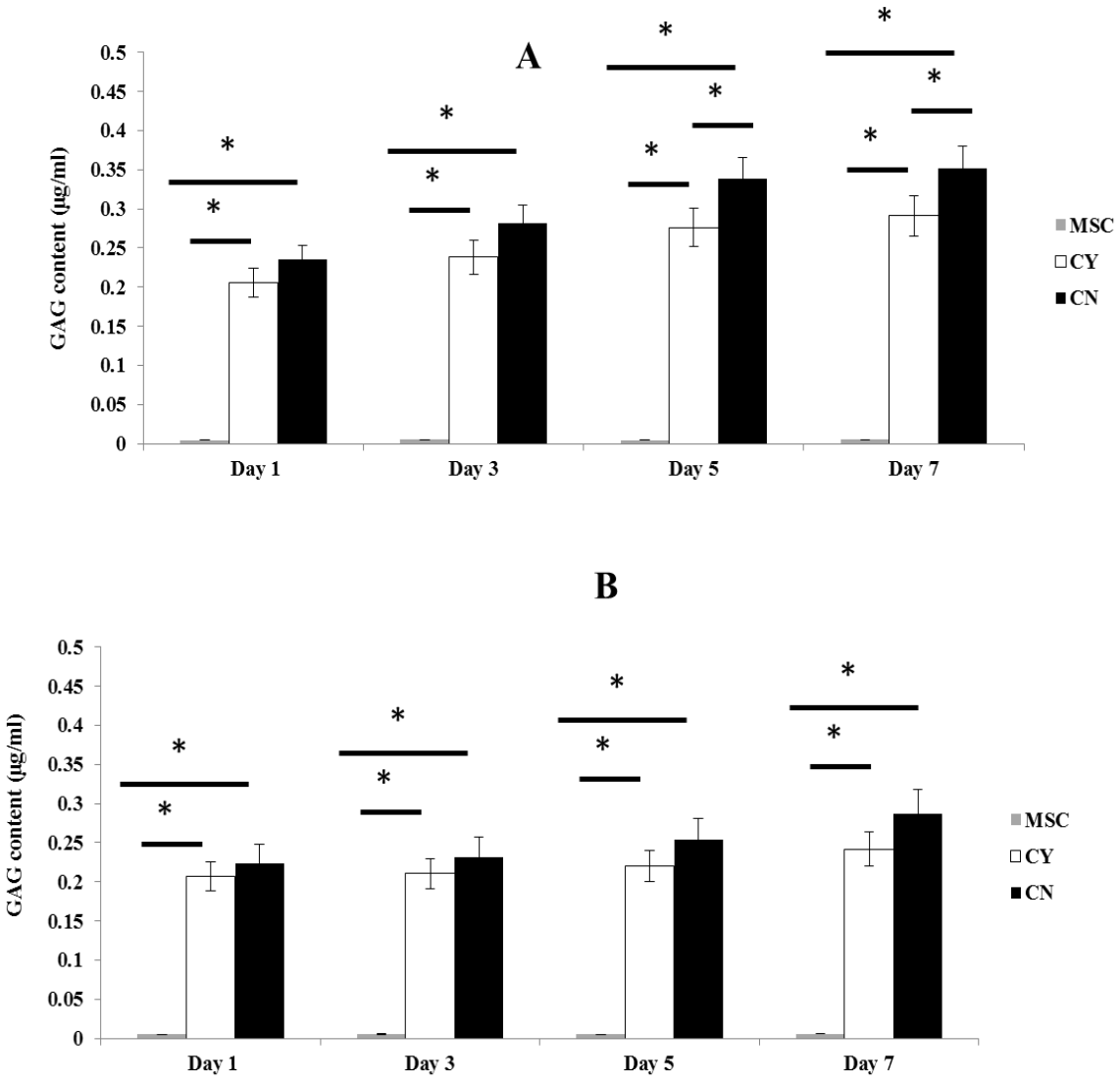

Figure 3.5: sGAG of chondron (CN), chondrocyte (CY), or MSC in monoculture at days 1, 3, 5, and 7 at P0 (panels A) and P1 (panels B). Data are expressed as mean ± SD (n = 3). *$p < 0.05$

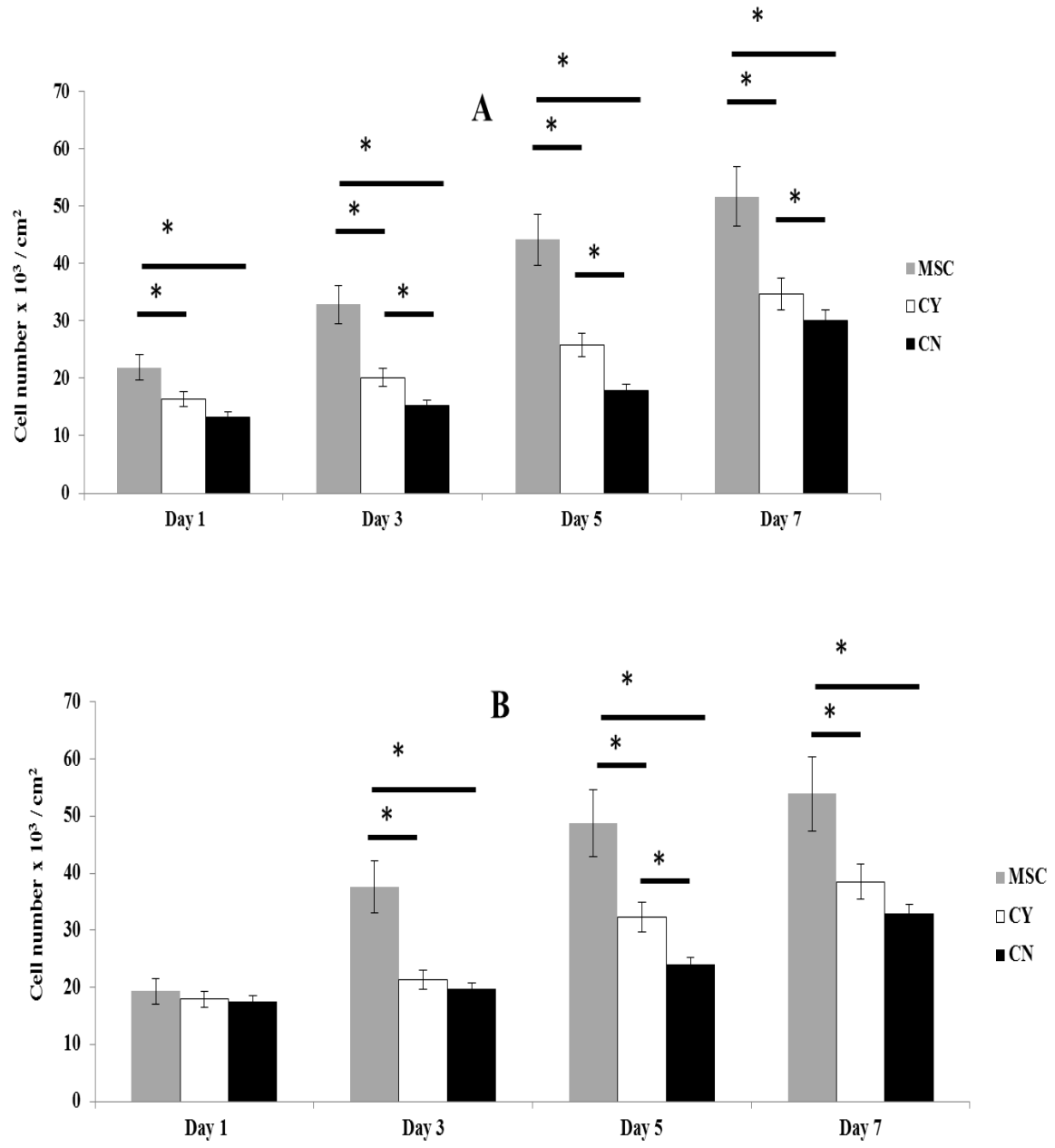

Figure 3.6: Cell number of chondron (CN), chondrocyte (CY), or MSC in monoculture at days 1, 3, 5, and 7 at P0 (panels A) and P1 (panels B). Data are expressed as mean ± SD (n = 3). *$p < 0.05$.

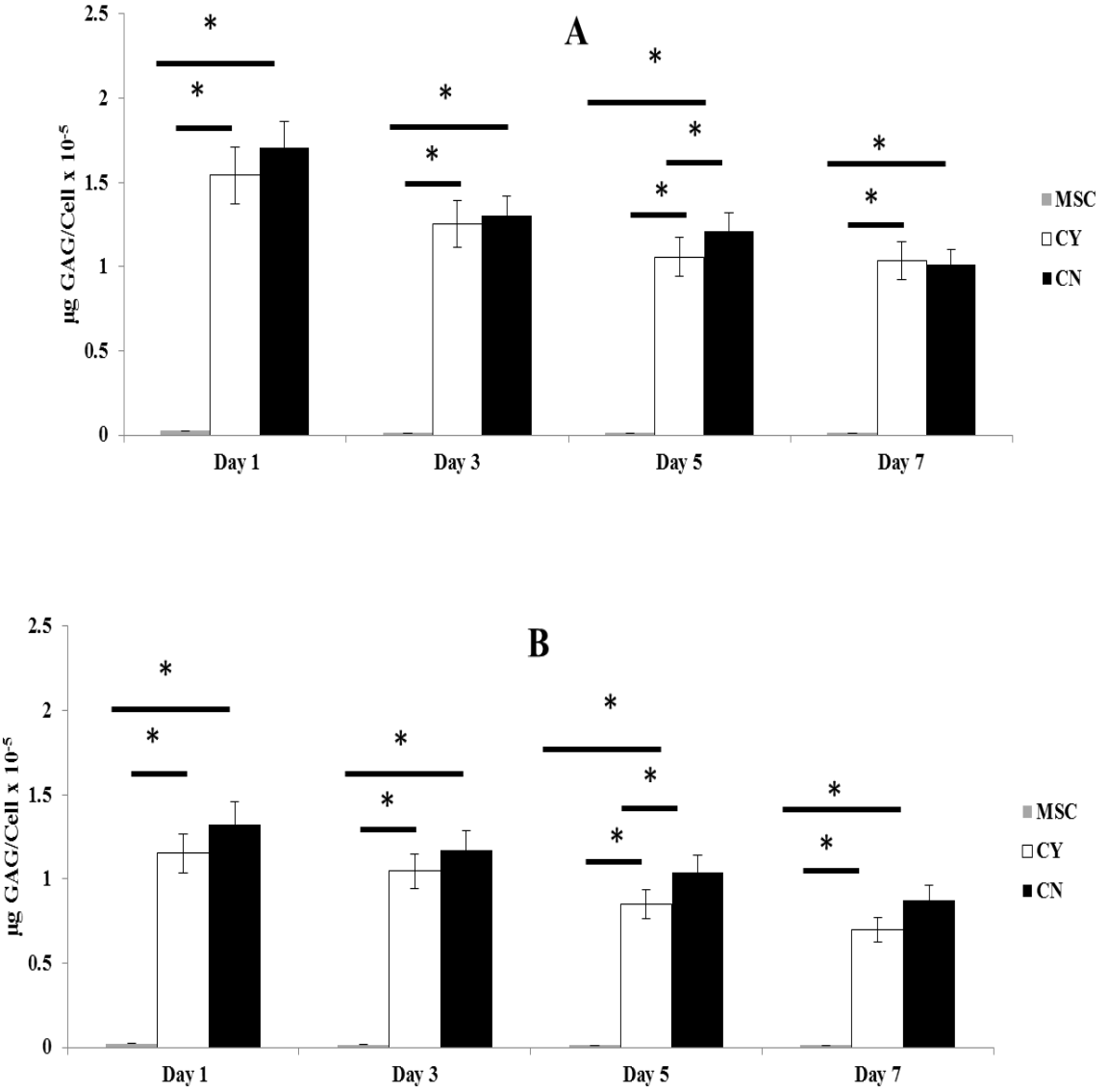

Figure 3.7: Total sGAG production normalised to cell number of chondron (CN), chondrocyte (CY), or MSC in monoculture at days 1, 3, 5, and 7 at P0 (panels A) and P1 (panels B). Data are expressed as mean ± SD (n = 3). * $p < 0.05$.

`

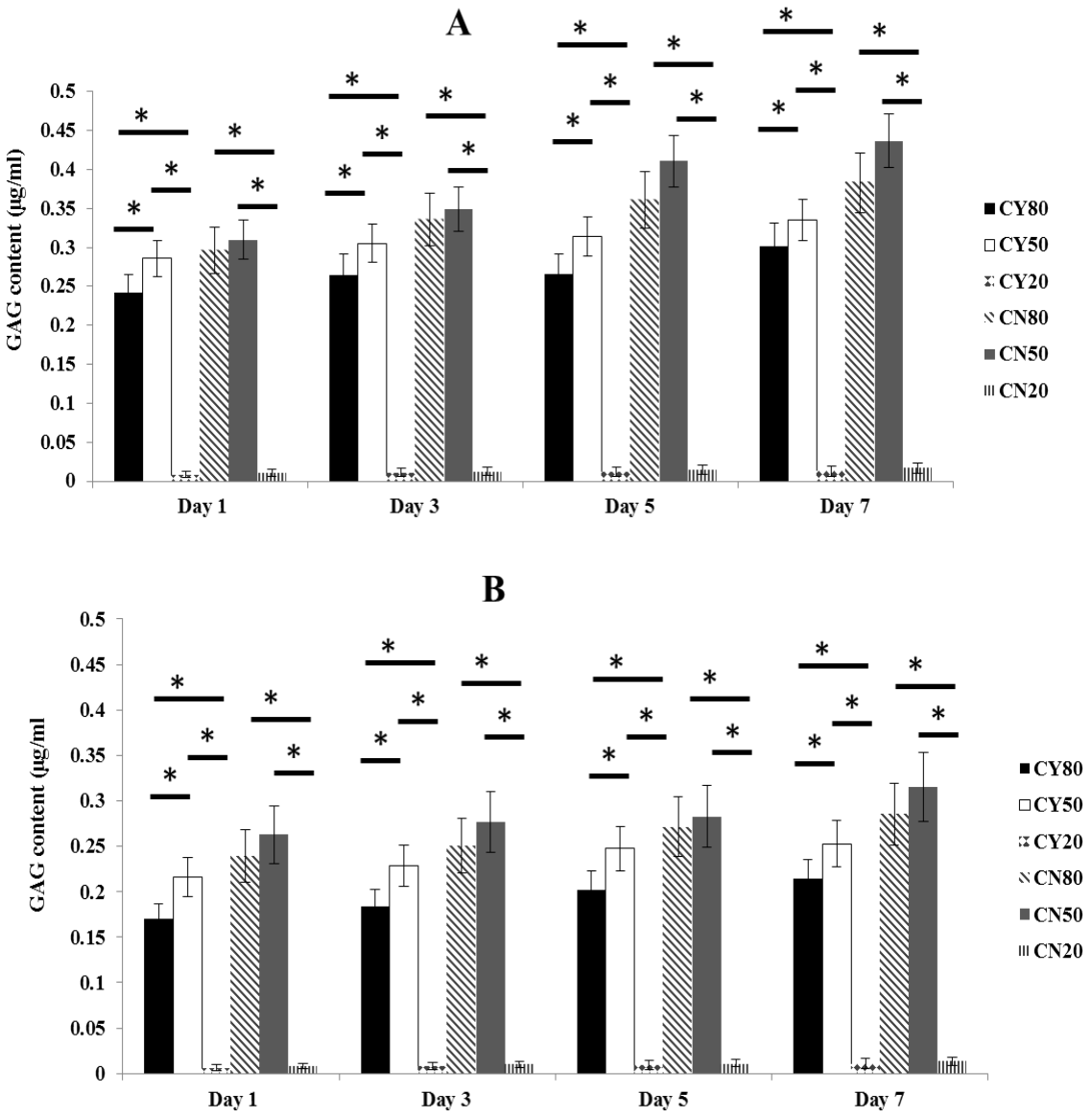

Figure 3.8: sGAG of chondron (CN), chondrocyte (CY), or MSC in co-culture at days 1, 3, 5, and 7 at P0 (panels A) and P1 (panels B). Data are expressed as mean ± SD (n = 3). * $p < 0.05$.

`

For the co-culture samples, the chondrocytes co-culture represented a slight higher cell number than chondron at P0 during different culture times ($p<0.05$). However, at passage 1 the cell number of chondrocytes and chondrons showed similar value along different time points ($p>0.05$) and the higher MSC ratio sample (20:80) showed the highest cell numbers during the culture than other two ratio samples (Figures 3.8.B and C). In agreement with the measurements from monoculture, the normalised GAG production in co-cultures reduced with time and passage (Figure 3.9). For the chondrocytes-MSC co-cultures, the GAG production was similar to monocultures, whilst for chondrons-MSC co-cultures the production of GAG was higher compared to monocultures. Chondrons-MSC co-culture ratio 50:50 showed the highest increase compared to the monocultures. The normalised values showed an increase from 16.8 ± 0.61 to 18.5 ± 0.54 pg/cell on day 1, and 10.0 ± 0.45 to 11 ± 0.38 pg/cell on day 7.

The sGAG products appearing in the media showed slightly different pattern. The chondrocytes demonstrated higher total amount of GAGs accumulated and released into the surrounding media than in cells; whilst chondrons exhibited more GAGs in cells than in released GAGs into media (Figure 3.10). Herein, chondron has retained the GAGs along culture time and reduced to leach out into the surrounding media comparing with chondrocytes culture in both mono and co-cutlers.

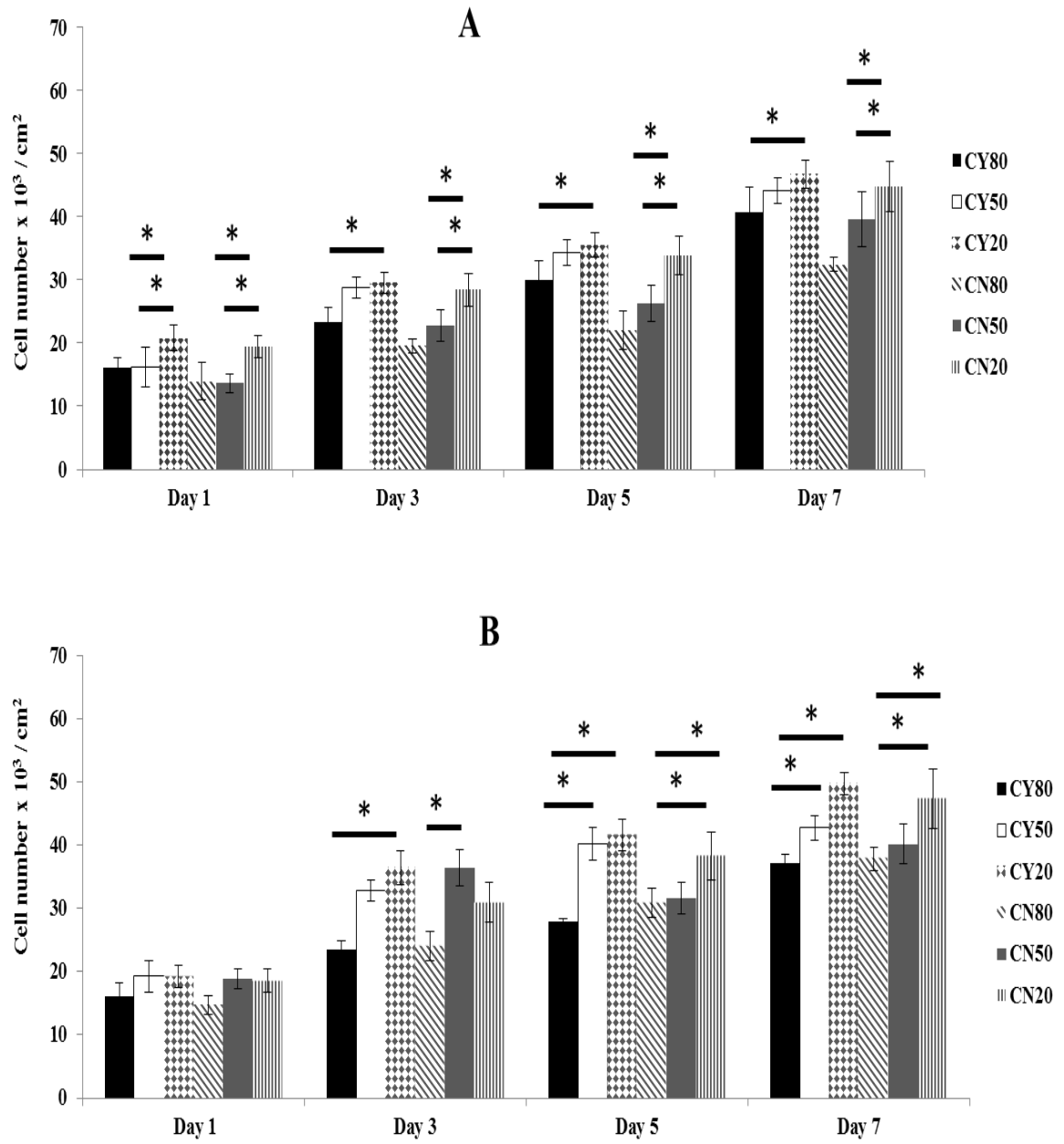

Figure 3.9: Cell number of chondron (CN), chondrocyte (CY), or MSC in co-culture at days 1, 3, 5, and 7 at P0 (panels A) and P1 (panels B). Data are expressed as mean ± SD (n = 3). * $p < 0.05$.

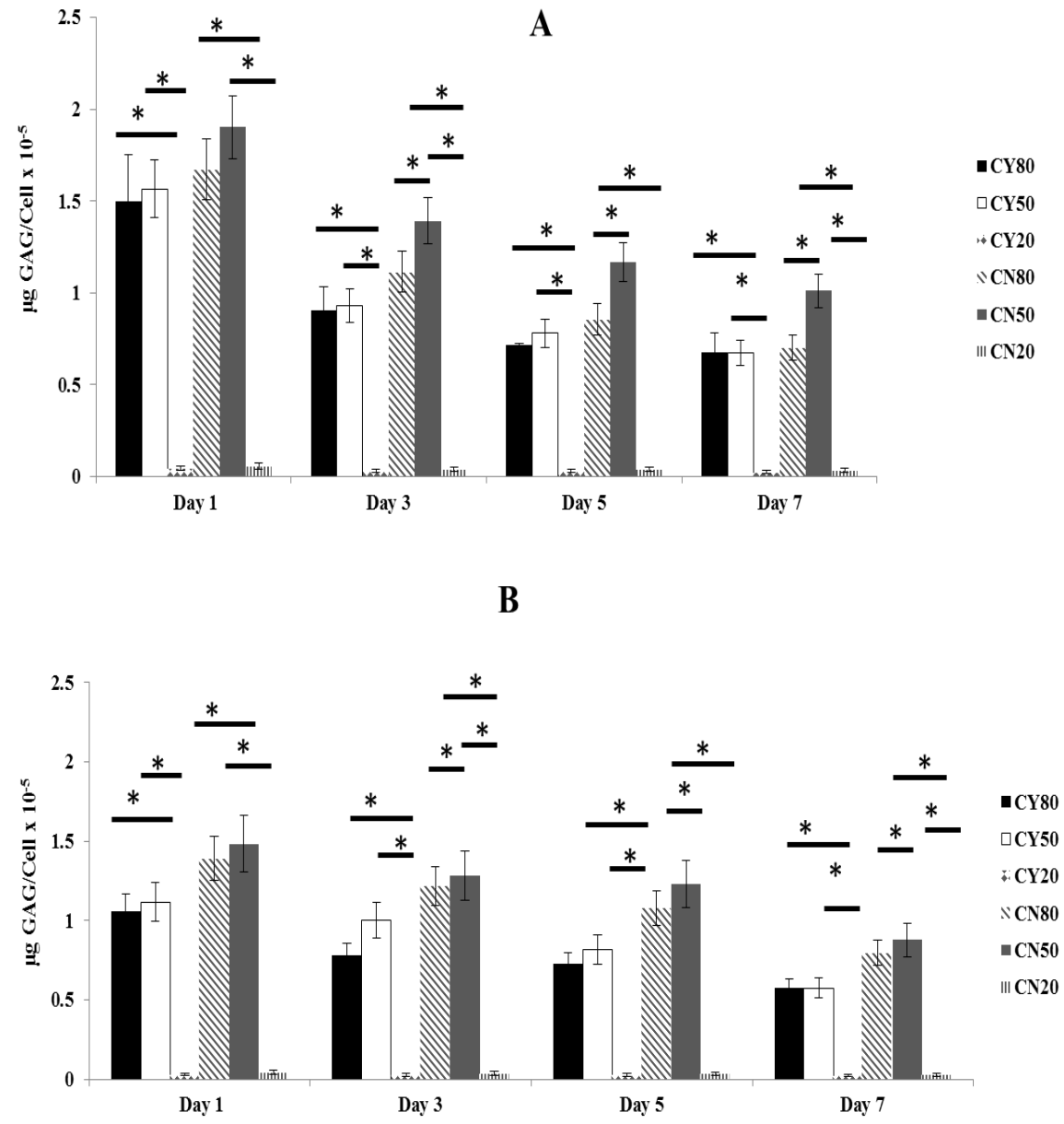

Figure 3.10**:** Total sGAG production normalised to cell number of chondron (CN), chondrocyte (CY), or MSC in co-culture at days 1, 3, 5, and 7 at P0 (panels A) and P1 (panels B). Data are expressed as mean ± SD (n = 3). * $p < 0.05$.

`

The data in Figures 3.4-3.9 are re-plotted into Figures 3.11 and 3.12 to visualise GAG value and cell number changes versus culture time between the mono and co-culture.

In general, the total GAG production in CN samples both mono- and co-culture samples (P0) were higher than corresponding CY samples in each culture time points. The production (or accumulated) rate of the total GAG in CN samples was higher than corresponding CY samples manifesting as the higher slope shown in Figures 3.11A and B, and Figures 3.12A and B.

When addition of MSC with 50% and 20% ratio, the total GAG production increased in comparison to mono-culture samples (all corresponding values in co-culture samples were above those of mono-culture samples). The increased rate in CN sample was much higher than in CY samples manifesting as the higher slope shown in Figures 3.11A and B, and Figures 3.12A and B. Clearly, 50% MSC addition was better than 20% addition in both CN and CY samples. However, the enhancement extent of 50% and 20% addition was larger in CN samples than in CY samples. 20% MSC addition in CY samples exhibited very close total GAG values to mono-type culture samples.

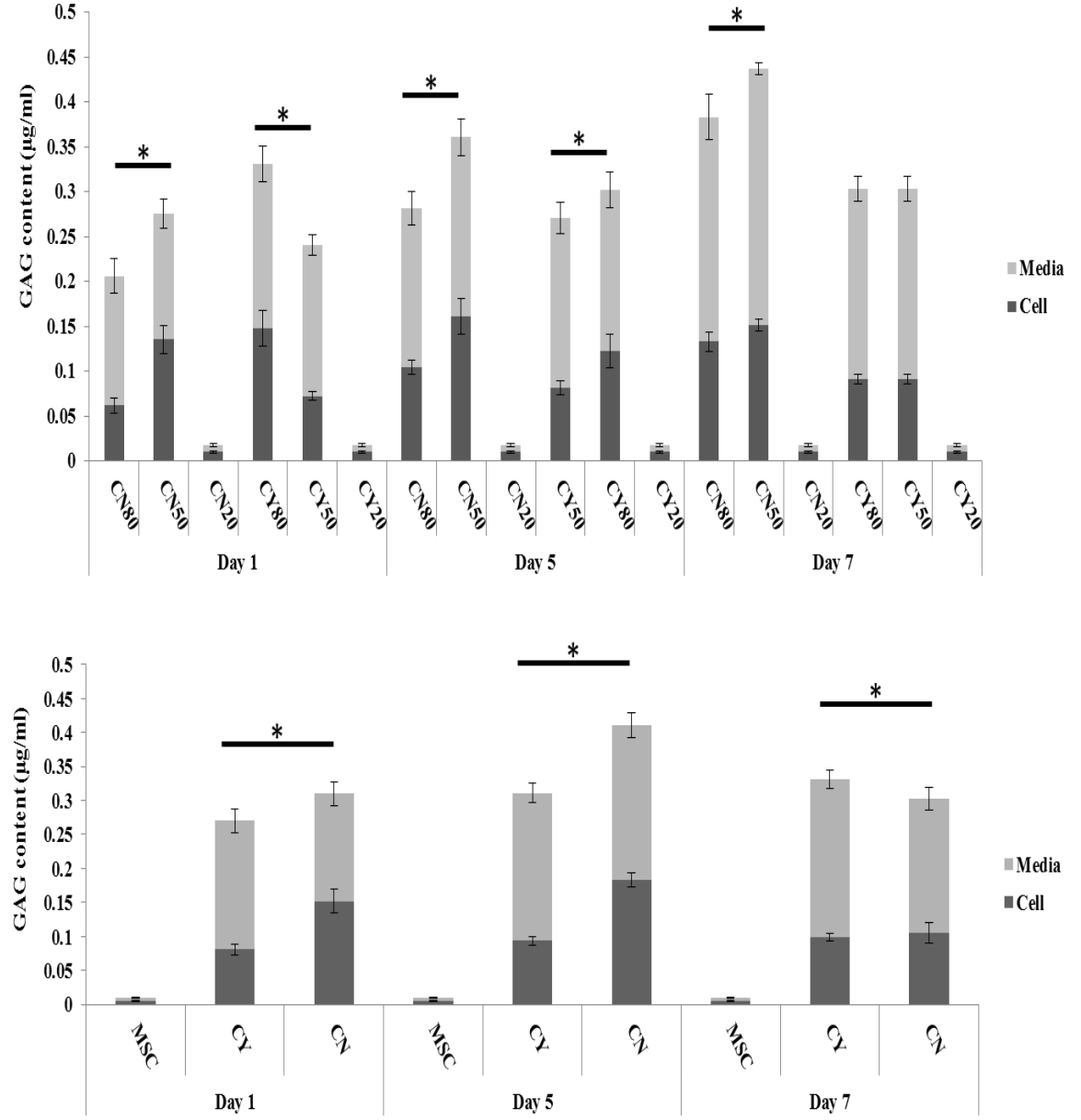

Figure 3.11**:** sGAG production in media and in cells for monoculture (chondron (CN) and chondrocyte (CY)) and co-culture with 20, 50, and 80% of MSC ratio at day 1, 3, 5, 7 cultures with P0 cells.* $p < 0.05$.

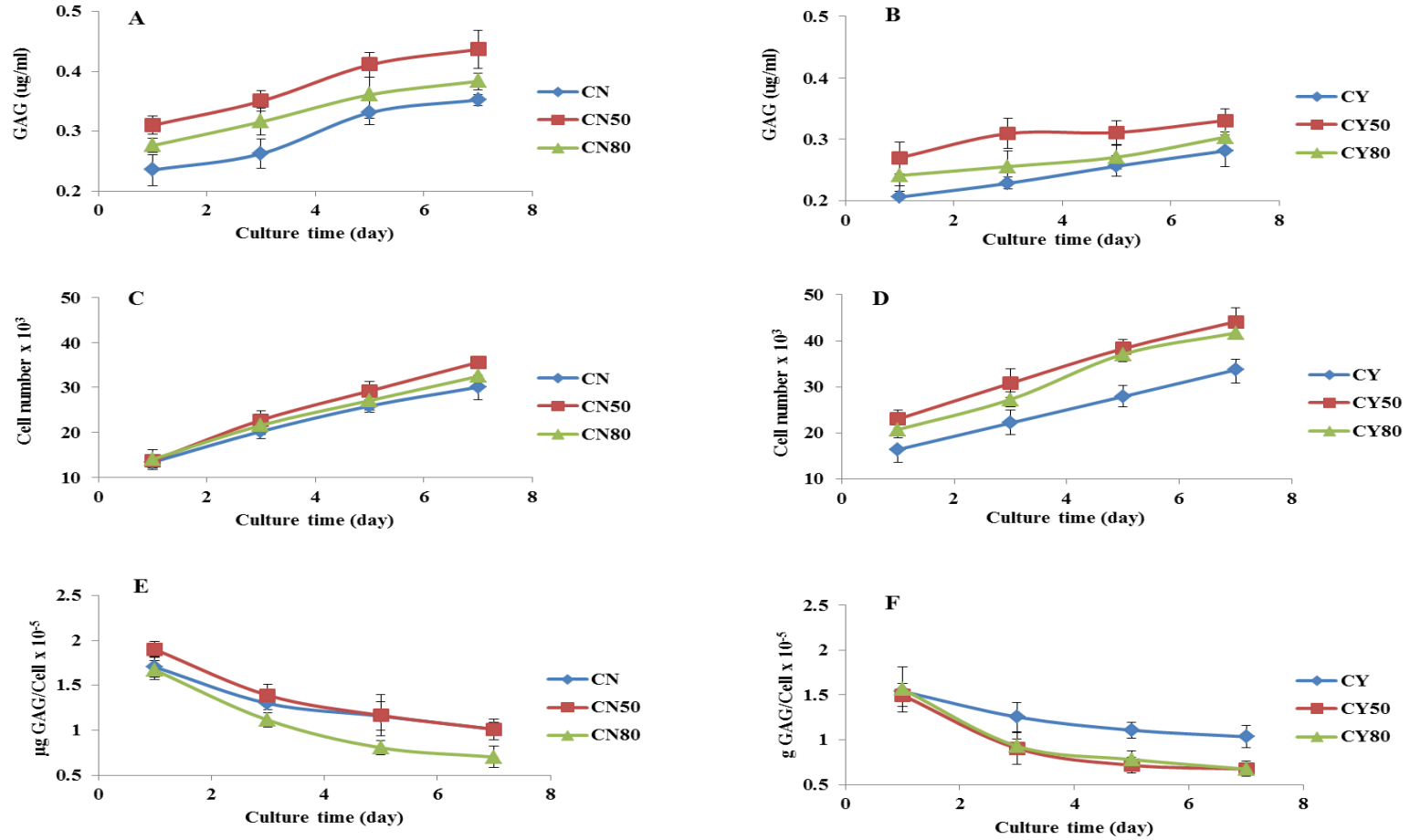

Figure 3.12**:** sGAG production versus culture time. A) and B) the total sGAG mass; C) and D) the cell number; E) and F) total sGAG production normalised to cell number. A), C) and E) are for chondron mono- and co-cultures; B), D) and F) are for chondrocyte mono and co-cultures at days 1, 3, 5, 7 cultures using P0 cells. Data are expressed as mean ± SD (n = 3).

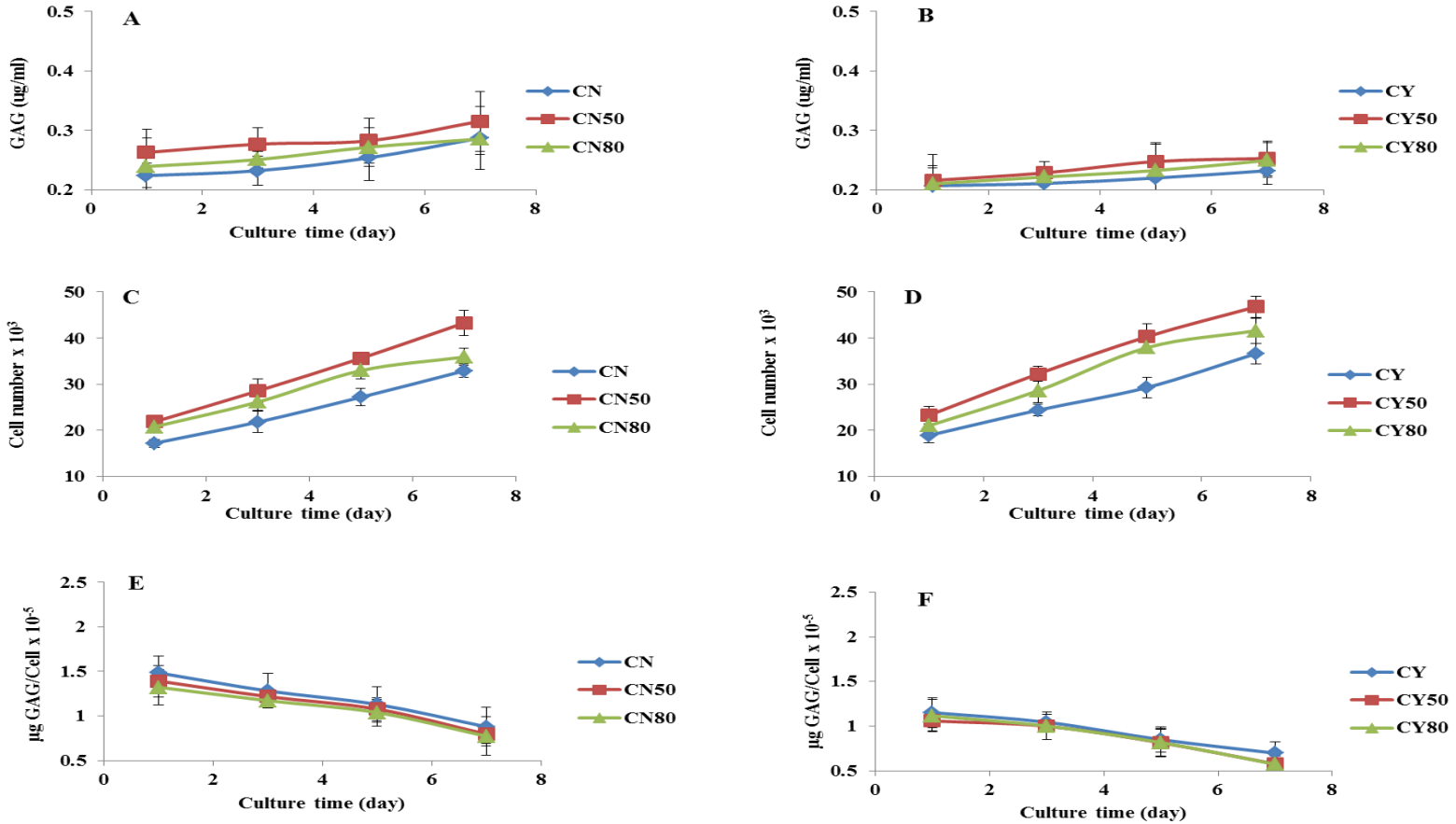

Figure 3.13: sGAG production versus culture time. A) and B) the total sGAG mass; C) and D) the cell number; E) and F) total sGAG production normalised to cell number. A), C) and E) are for chondron mono- and co-cultures; B), D) and F) are for chondrocyte mono and co-cultures at days 1, 3, 5, 7 cultures using P1 cells. Data are expressed as mean ± SD (n = 3).

`

3.4.4 Histological analysis of proteoglycans

3.4.4.1 Histological analysis of proteoglycans in two-dimensional monocultures

Alcian blue was used to detect proteoglycans and GAGs (Fig 3.13). The staining showed no detectable levels for MSCs. P0 chondrons showed a more intense staining compared to chondrocytes (Figure 3.13A), with the intensity increasing along culturing time. The staining appeared similar for both P1 chondrons and chondrocytes and overall lower when compared to P0 samples (Figure 3.13B). ImageJ was used to quantify the intensity of staining for P0 and P1 samples (Figure 3.13D).

By using ImageJ Analysis software, the GAG staining intensity between the groups and culture time for P0 and P1 cells samples was semi-quantified as showed in Figures 3.13C and D. At all culture time points, chondrons had a higher GAG production than P0 chondrocytes samples. The GAG intensity increased constantly along the culture, with day 7 having a significantly higher amount of GAGs than day 5 and day 1. At passage 1, the amounts of GAGs produced by both chondrons and chondrocytes were similar, and there was only a slight increase over prolonged culture.

`

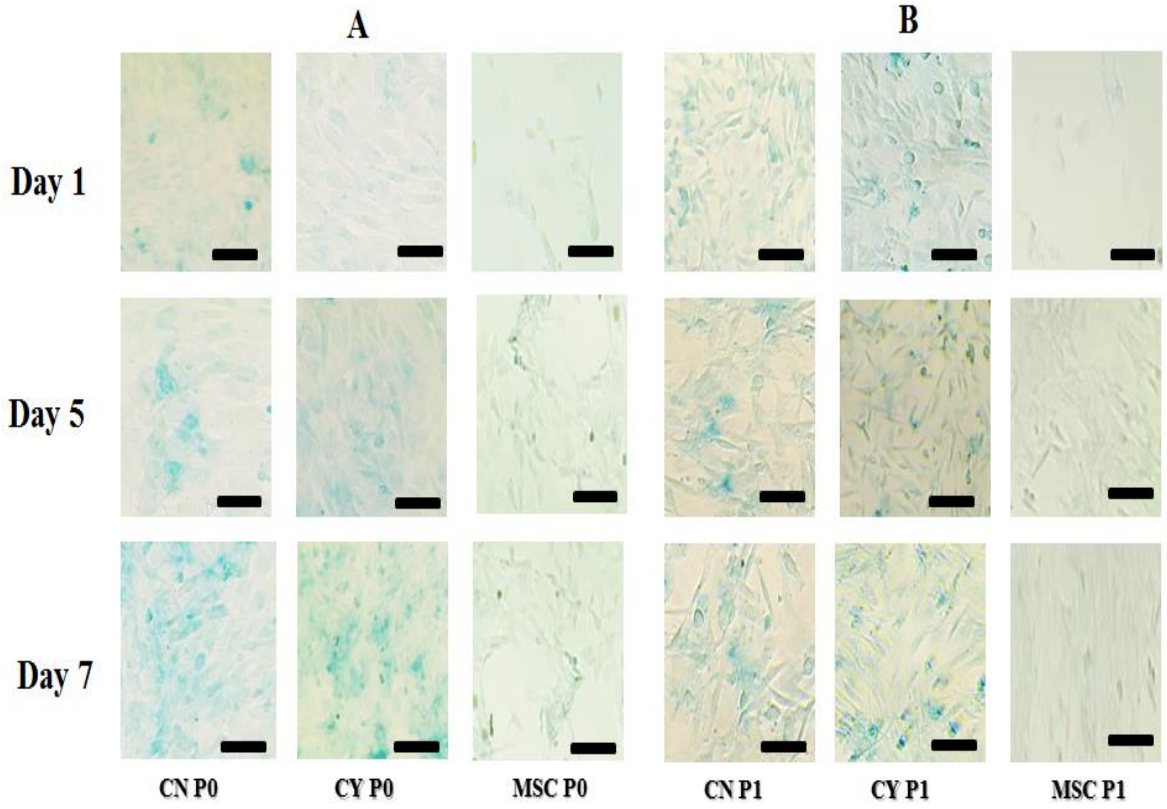

Figure 3.14: Representative images of alcian blue stained monocultures of chondrons (CN), chondrocytes (CY), or MSC at days 1, 5, and 7 cultures; A) at P0 and B) at P1. The scale bars represent 150 μm.

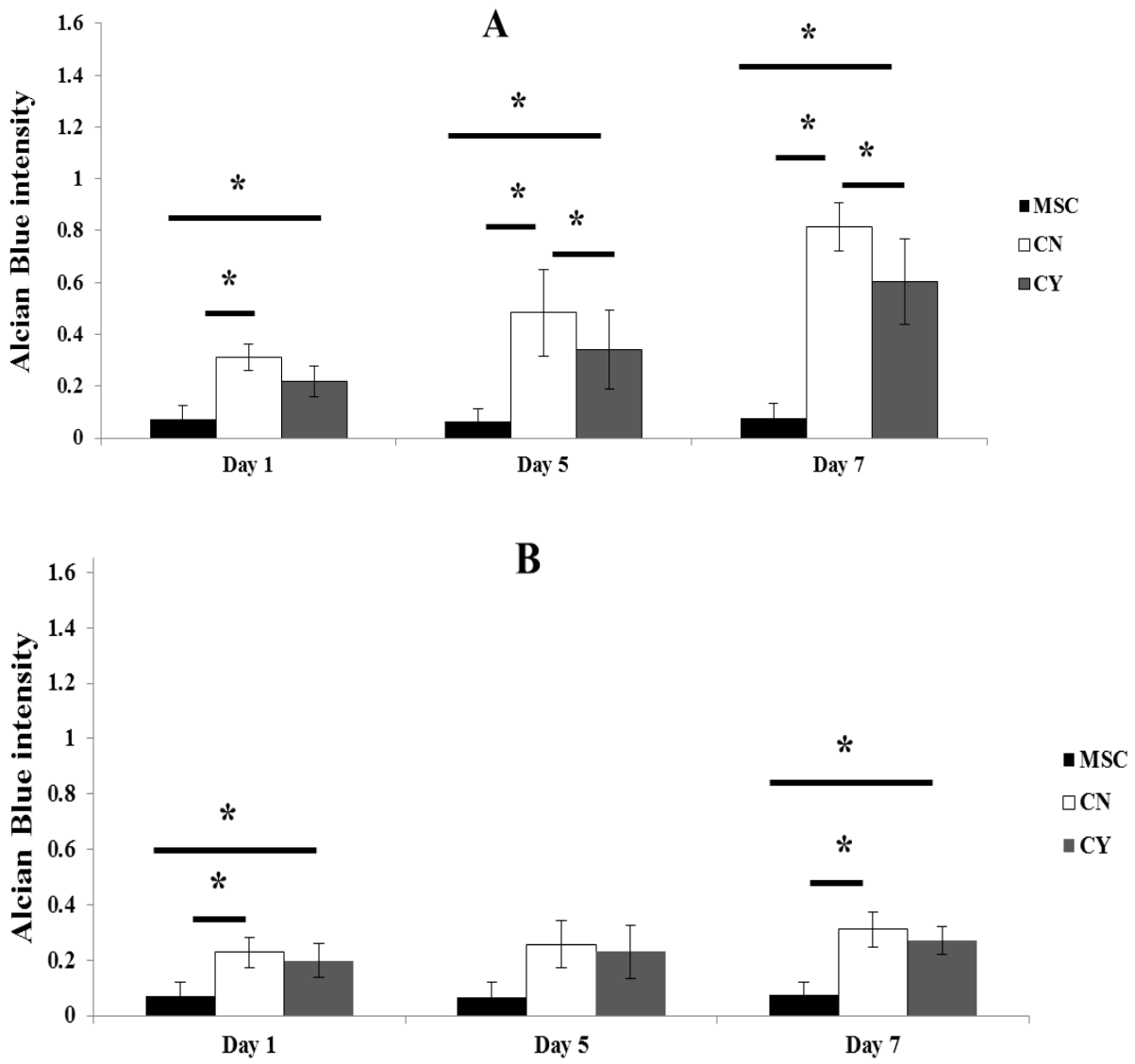

Figure 3.15: Representative quantification of alcian blue staining intensity of chondron (CN), chondrocyte (CY), and MSC in monoculture at days 1, 5, and 7 culture: A) at P0 and B) at P1. Data are expressed as mean ± SD (n = 3). *$p < 0.05$.

`

3.4.4.2 Histological analysis of proteoglycans in two-dimensional co-cultures

Figure 3.14A and B show the co-culture staining for P0 and P1 cells by alcian blue. Chondrocyte co-cultures had less staining for GAG and proteoglycans than chondron co-cultures, and the highest staining intensity was found in a 50:50 co-culture. At all culture time points as well as all cell ratio samples, the GAG staining intensity (Figures 3.14C and D), which was quantitatively measured with the ImageJ software, showed that the amount of GAGs produced in MSC–chondron co-culture was significantly higher than that in MSC–chondrocyte co-culture. The staining intensity continuously increased along the culture time, such that the GAGs at day 5 and day 1 were significantly less than that of day 7. The highest GAG production was found in the co-culture samples containing 50% MSC and 50% chondrons or chondrocytes, while high MSC ratio samples (consisting of 20% chondrons or chondrocytes) had the lowest GAG production. While the staining intensity of chondrons and chondrocytes was similar for all culture points and cell ratio samples of P1 cells, the staining was less intense for P0 samples.

`

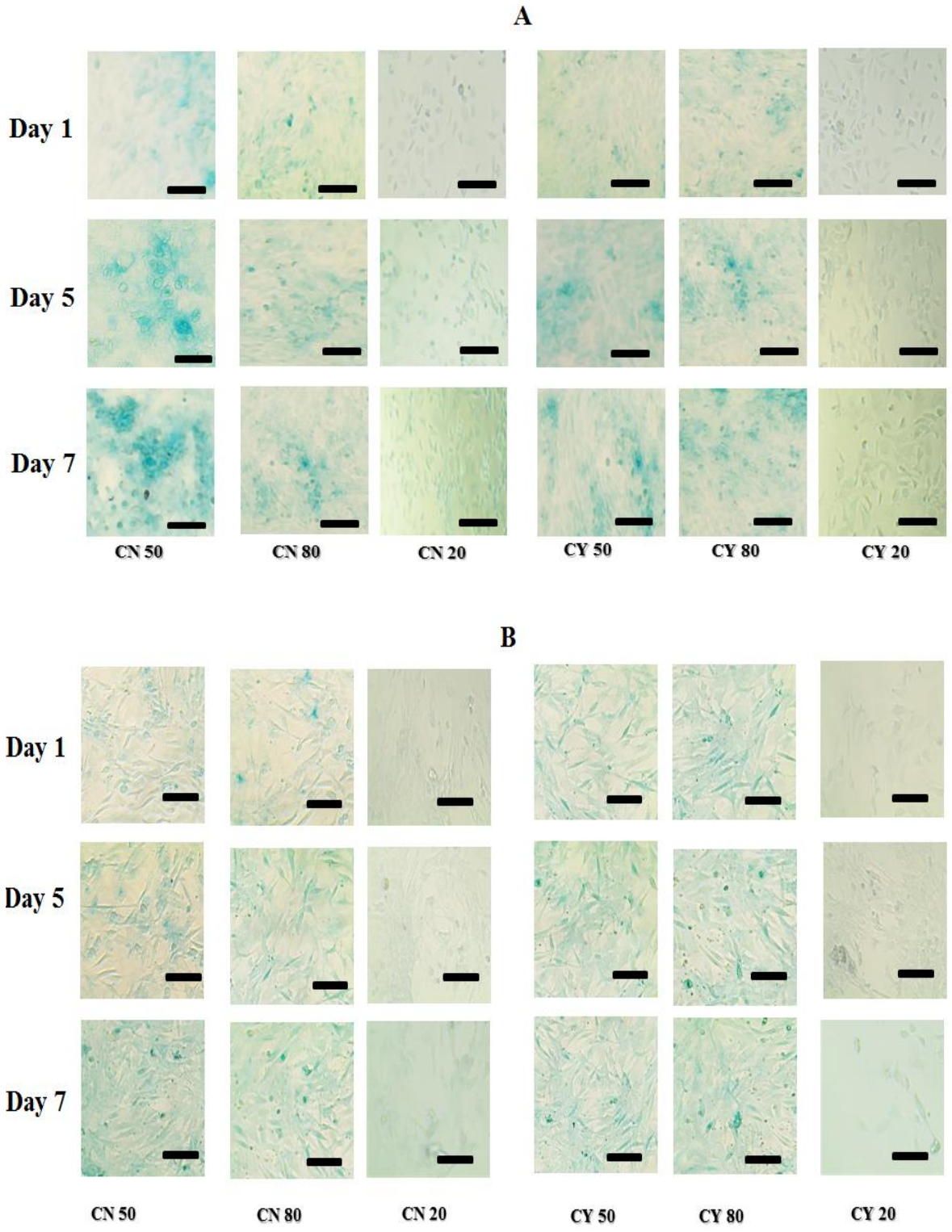

Figure 3.16: Representative images of alcian blue stained chondrons (CN) or chondrocytes (CY) with MSC in co-culture at days 1, 5, and 7 culture; A) at P0 and B) at P1. The scale bars represent 150 μm.

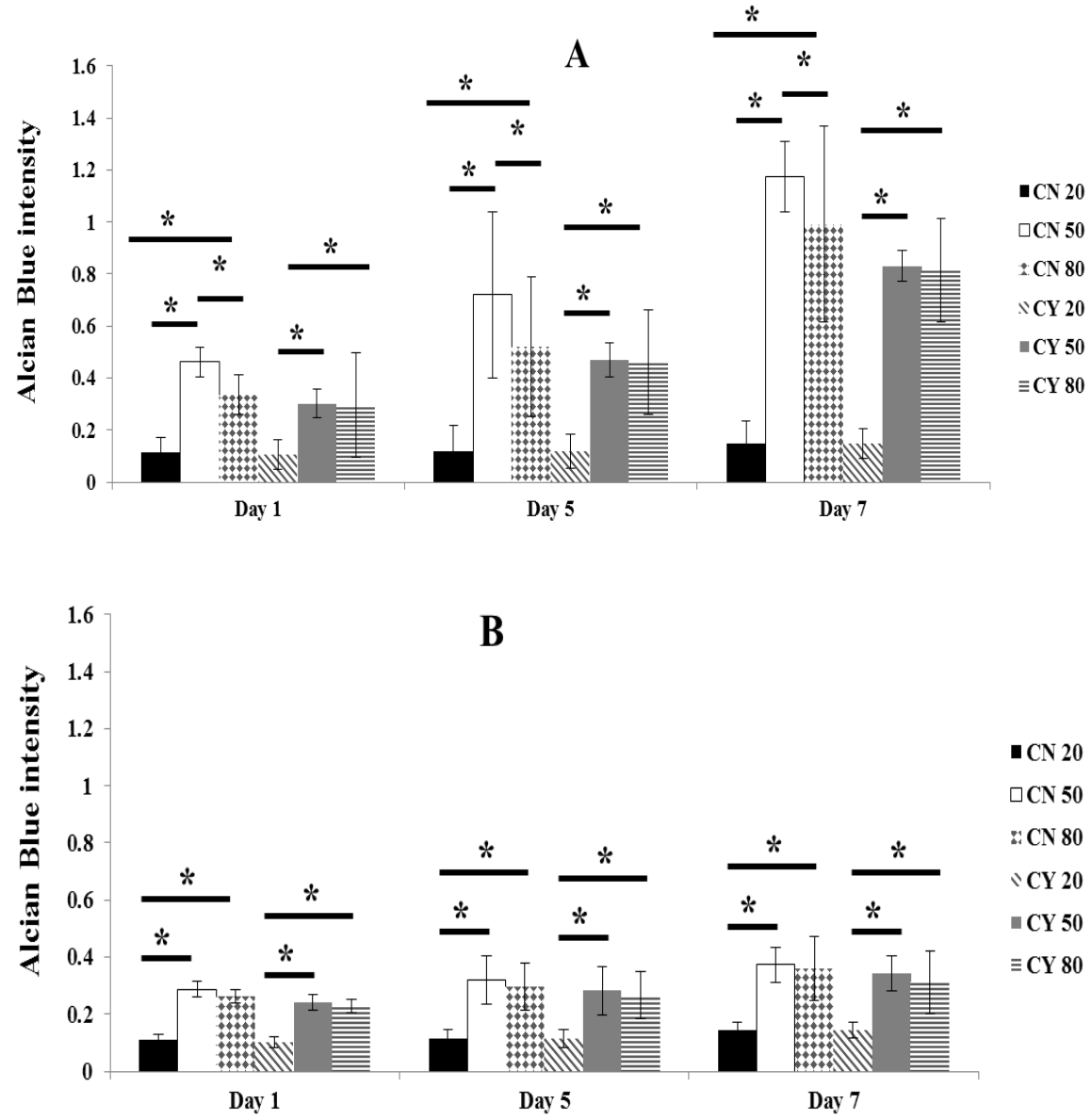

Figure 3.17: Representative quantification of alcian blue staining intensity of chondron (CN), chondrocyte (CY), and MSC in co-noculture at days 1, 5, and 7 culture: C) at P0 and D) at P1. Data are expressed as mean ± SD (n = 3). *$p < 0.05$.

`

3.4.5 Expression of key PCM and ECM components

3.4.5.1 Expression of key PCM components in two-dimensional monocultures

Figure 3.15 displayed the PCM and ECM components markers in the monocultures through immunofluorescence staining. MSCs had no any expression of all PCM markers. Collagen II staining intensity was detectable around P0 chondrons and P0 chondrocytes with chondrons expression more at all the culture time points. Collagen II showed accumulated deposition along culture i.e. the latest culture day expressed more than the first culture day. A dramatic difference was found in the production of high collagen II content at passage 0 cells compared to the other passages cells. At passage 1, collagen II expression was presented albeit less intense. Collagen VI, exclusively located in the PCM, was only detected in the chondron cultures. By day 7 (P0), collagen VI staining was lost under the present culture condition. There was no expression at all at P1 chondrons and chondrocytes. Immunofluorescence staining for HtrA1 was absent for chondrons and chondrocytes of both P0 and P1 cells at day 1 but present at day 5 and 7 with accumulated deposition along extended time in culture. At P1, chondrocytes showed stronger HtrA1 staining than the chondrons at the same culture time points. The staining pattern of HtrA1 was inverse to collagen VI staining in P0 chondron. These data were confirmed by comparison with both negative and positive controls using both isolated cells and full-depth bovine articular cartilage. The semi-quantification of staining intensity among the groups was presented in Figure 3.16, which correlated well with the immunofluorescent stained images (Figure 3.15).

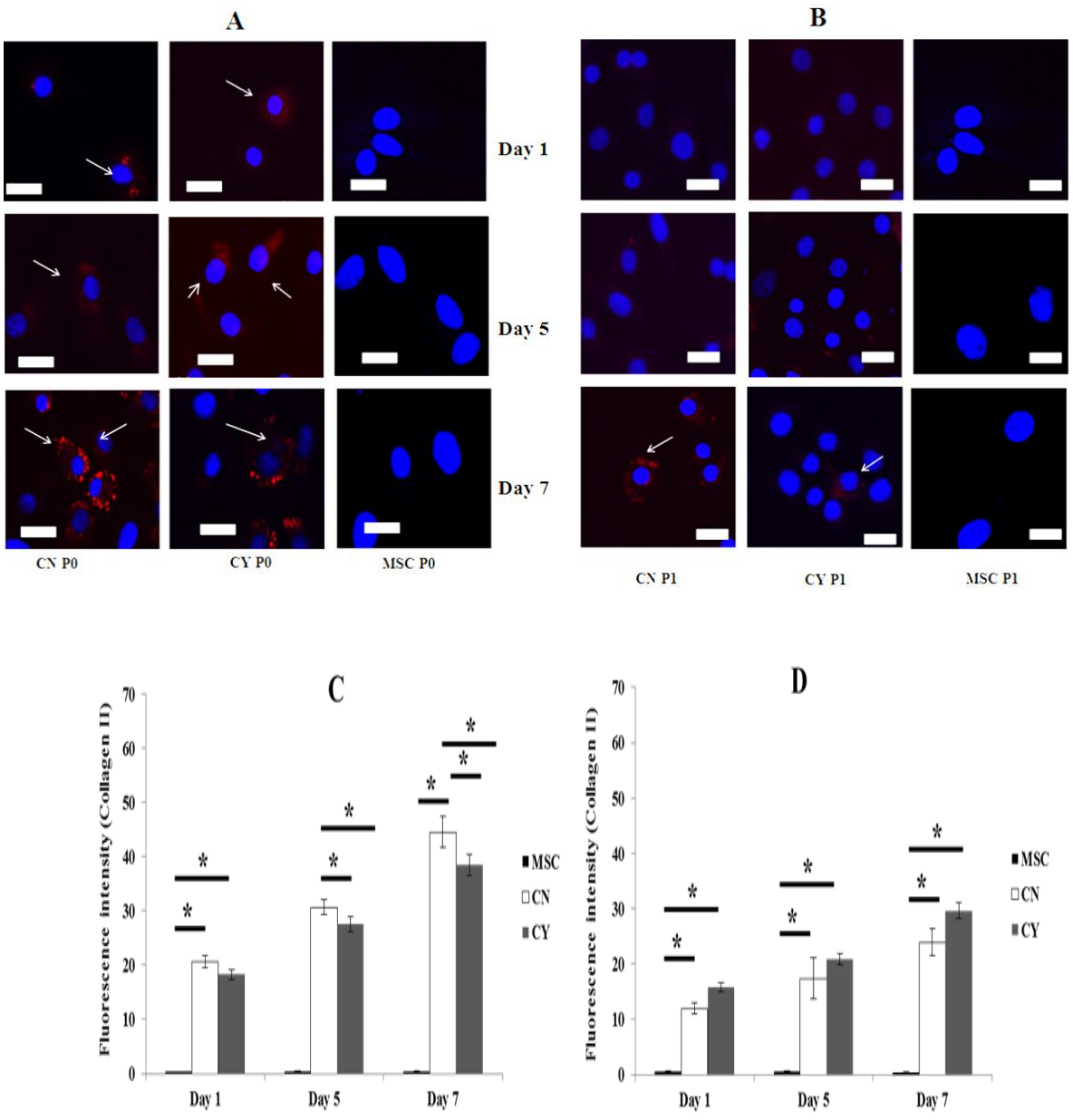

Figure 3.18: Representative immunofluorescent stained images of chondrons (CN), chondrocytes (CY), or MSCs in monoculture at days 1, 5, and 7 at P0 (panels A) and P1 (panels B). The cells were collagen II (red; The cells were counter-stained by DAPI (blue). The white arrows indicate positive staining. The scale bars represent 20 μm. Immunofluorescent stained intensity analysis of chondron (CN), chondrocyte (CY), and MSC in monoculture at days 1, 5, and 7 at collagen II; C for P0 cells and D for P1 cells. Data are expressed as mean ± SD (n = 3). * $p < 0.05$.

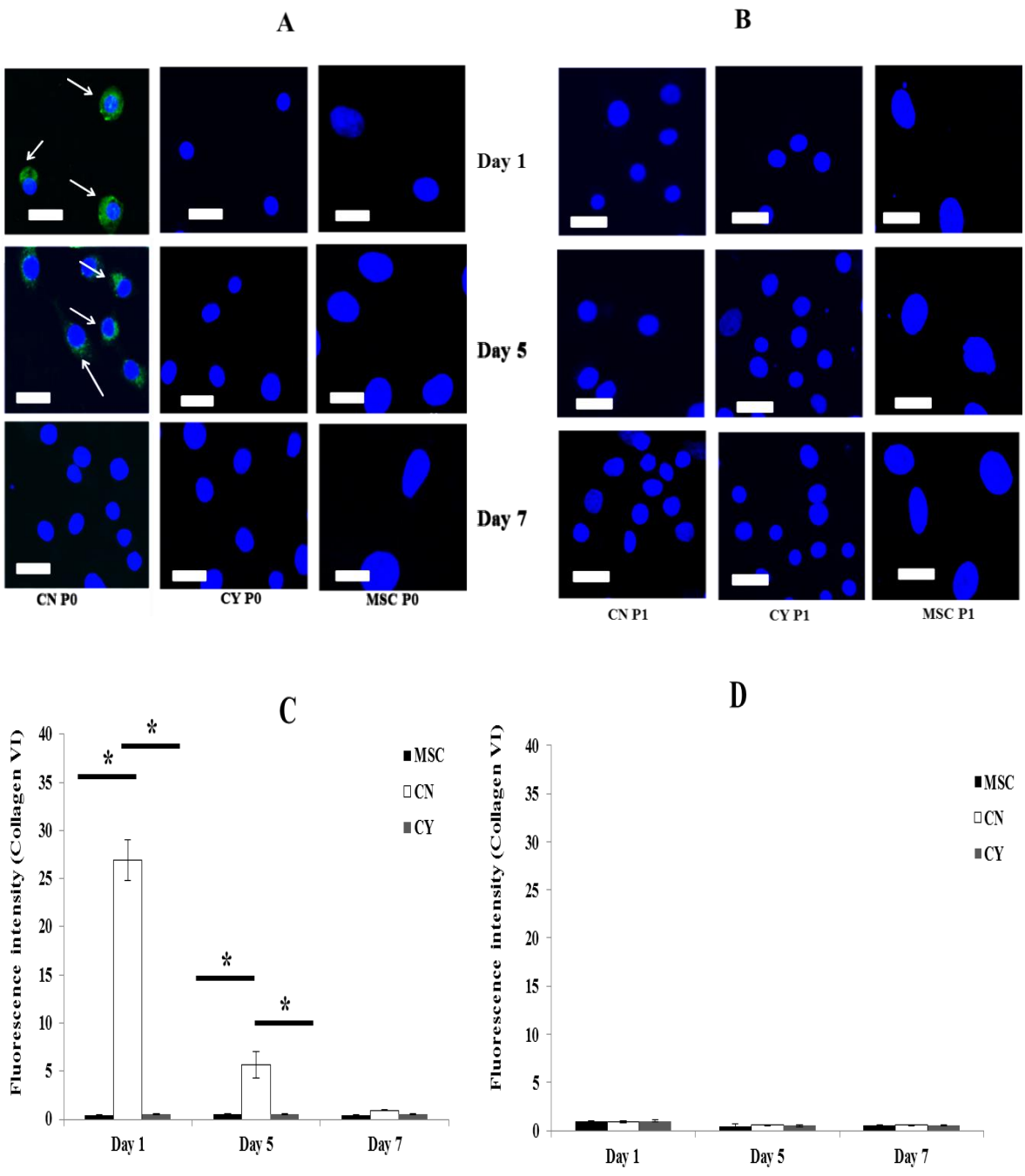

Figure 3.19**:** Representative immunofluorescent stained images of chondrons (CN), chondrocytes (CY), or MSCs in monoculture at days 1, 5, and 7 at P0 (panels A) and P1 (panels B). The cells were collagen VI (green the cells were counter-stained by DAPI (blue). The white arrows indicate positive staining. The scale bars represent 20 μm. Immunofluorescent stained intensity analysis of chondron (CN), chondrocyte (CY), and MSC in monoculture at days 1, 5, and 7 at collagen VI; C for P0 cells and D for P1 cells. Data are expressed as mean ± SD (n = 3). *$p < 0.05$

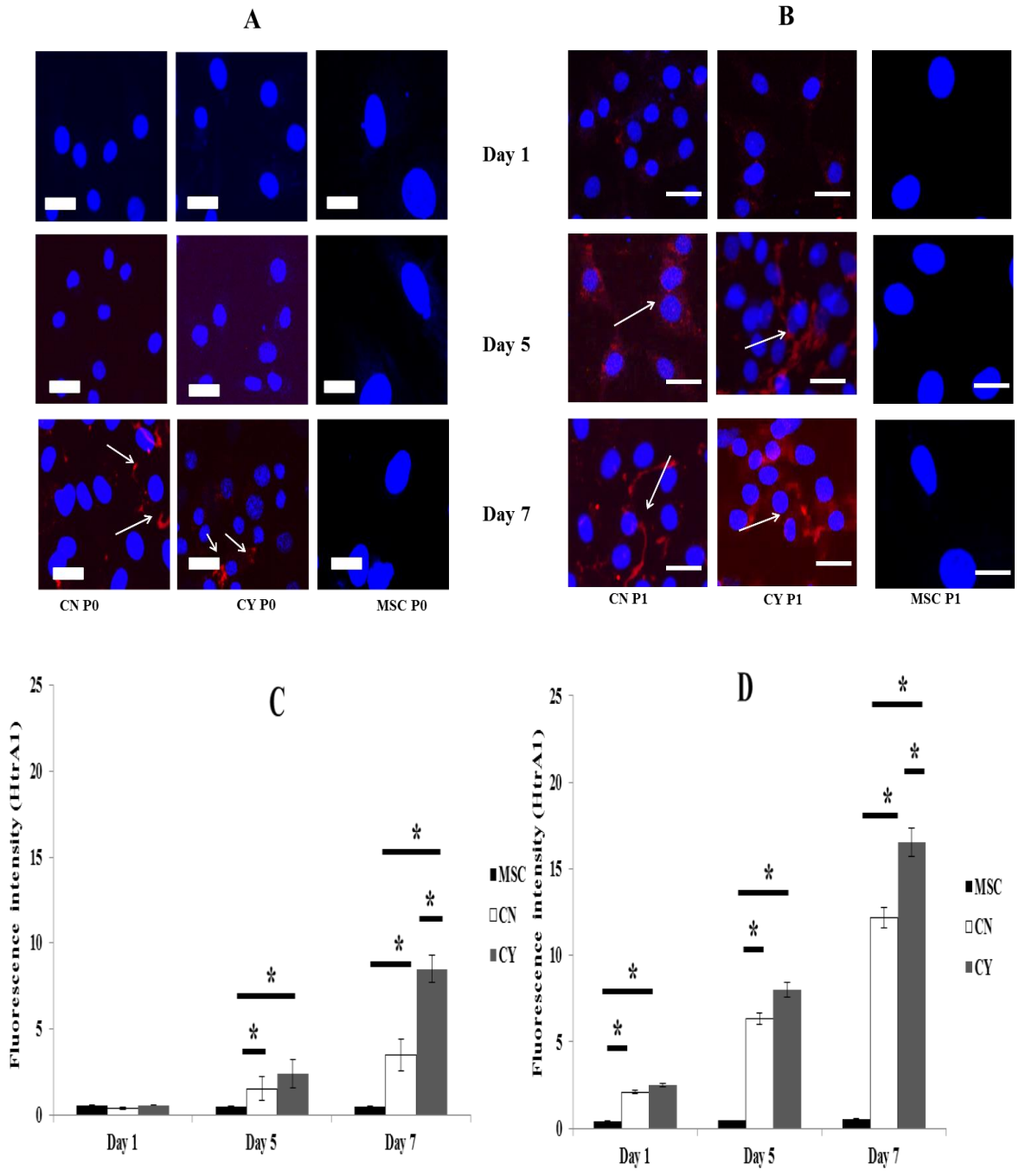

Figure 3.20**:** Representative immunofluorescent stained images of chondrons (CN), chondrocytes (CY), or MSCs in monoculture at days 1, 5, and 7 at P0 (panels A) and P1 (panels B). The cells were HtrA1 (red; the cells were counter-stained by DAPI (blue). The white arrows indicate positive staining. The scale bars represent 20 μm. Immunofluorescent stained intensity analysis of chondron (CN), chondrocyte (CY), and MSC in monoculture at days 1, 5, and 7 at HtrA1; C for P0 cells and D for P1 cells. Data are expressed as mean ± SD (n = 3). * $p < 0.05$.

`

3.4.5.2 Expression of key PCM and ECM components in two-dimensional co-cultures

At any culture time points or cell ratio, collagen VI staining was absent for the chondrocyte: MSC co-culture groups. In contrast, collagen VI was identified for all time points and ratios (Figure 3.17) for all chondron: MSC co-cultures when using P0 chondrons. The 50% chondron: MSC co-cultures had a highest collagen VI staining which matched with the alcian blue staining (Figure 3.9). P1 chondrons and chondrocytes had no any expression of collagen VI at all.

Along culture time, P0 chondrocyte and chondron co-cultures revealed increasing in collagen II staining intensity. The 50% ratio co-culture had the most intense staining. There was no influence on collagen II expressions for the co-culture with P1 cells. HtrA1 staining intensity was lower in all chondrons and chondrocytes co-culture ratios than monoculture. At 50% chondron: MSC co-cultures along all culture time points there were no detectable staining of HtrA1. The distinct staining intensity was in the chondrocyte: MSC co-cultures samples at day 7. At passage 1, the co-culture presented significant low expression of HtrA1 in compared to the mono-culture. There was weak expression of HtrA1 at day 7. The semi-quantification of staining intensity is presented in Figure 3.18, which correlated well with the immunofluorescent stained images (Figure 3.16).

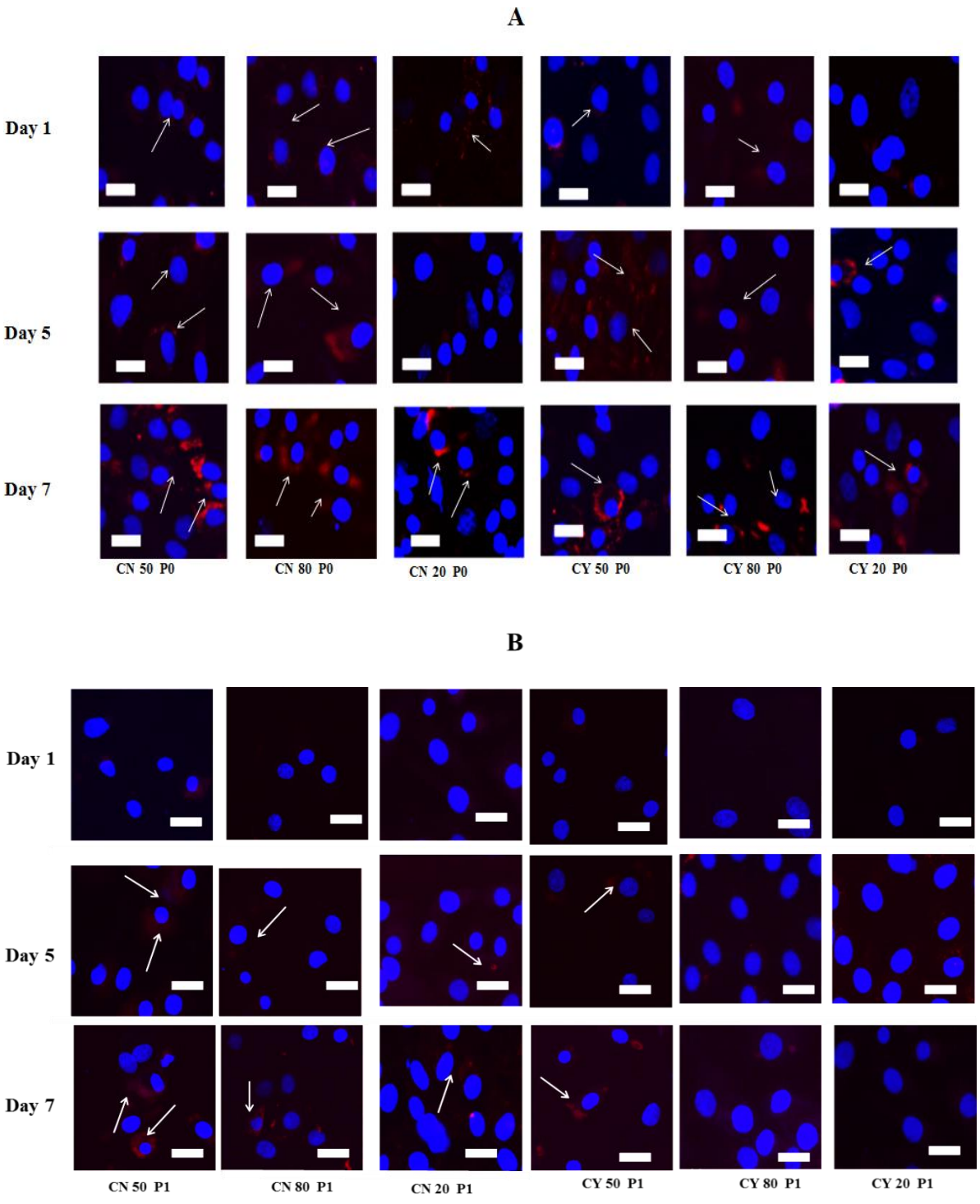

Figure 3.21: Representative immunofluorescent stained images of chondrons (CN), chondrocytes (CY), or MSCs in co-culture at days 1, 5, and 7 at P0 (panels A) and P1 (panels B). The cells were collagen II (red; the cells were counter-stained by DAPI (blue). The white arrows indicate positive staining. The scale bars represent 20 μm.

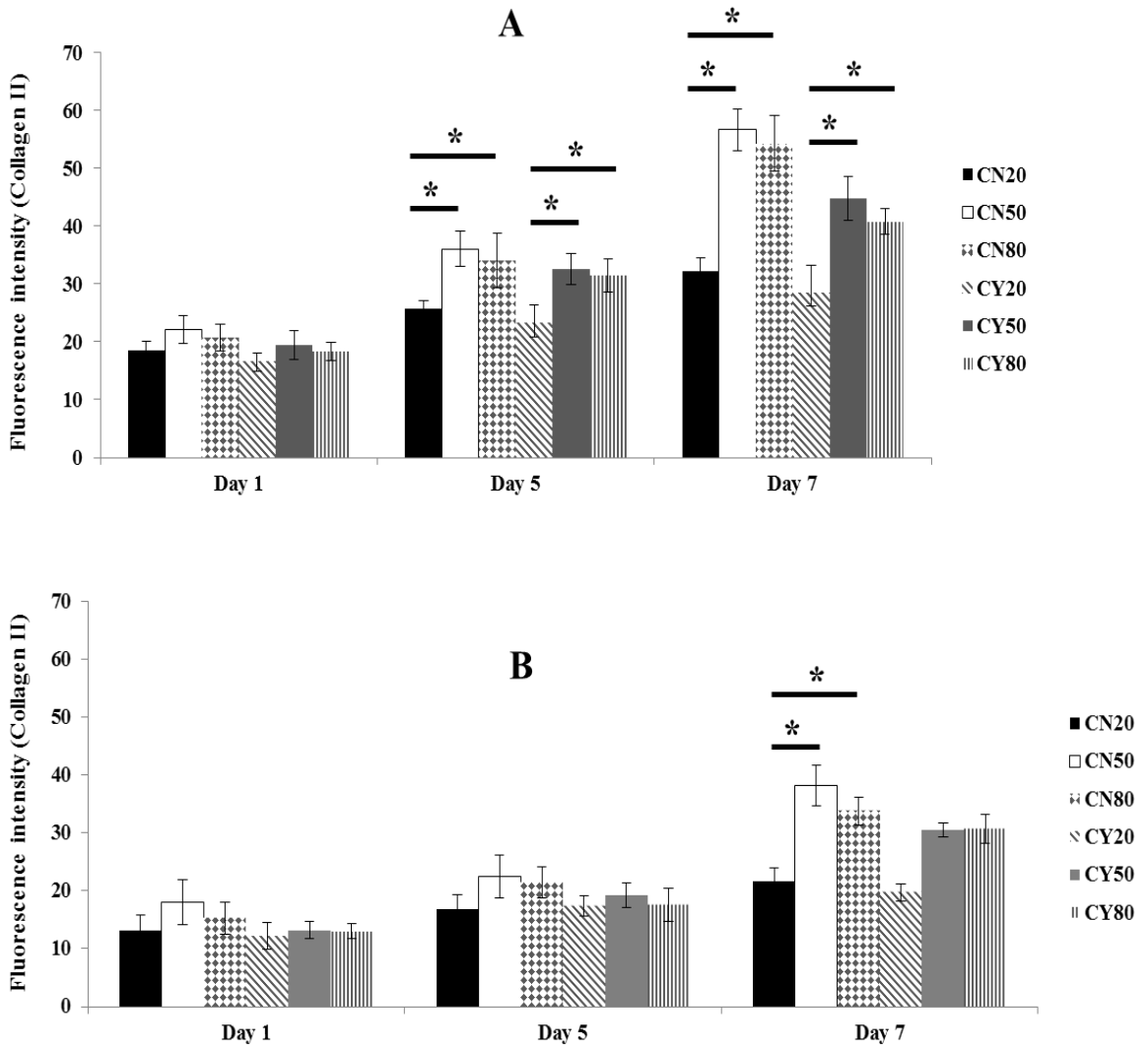

Figure 3.22: Representative Immunofluorescent stained intensity analysis of chondron (CN), chondrocyte (CY), and MSC in co-culture at days 1, 5, and 7 at collagen II; A for P0 cells and B for P1 cells. Data are expressed as mean ± SD (n = 3). *$p < 0.05$

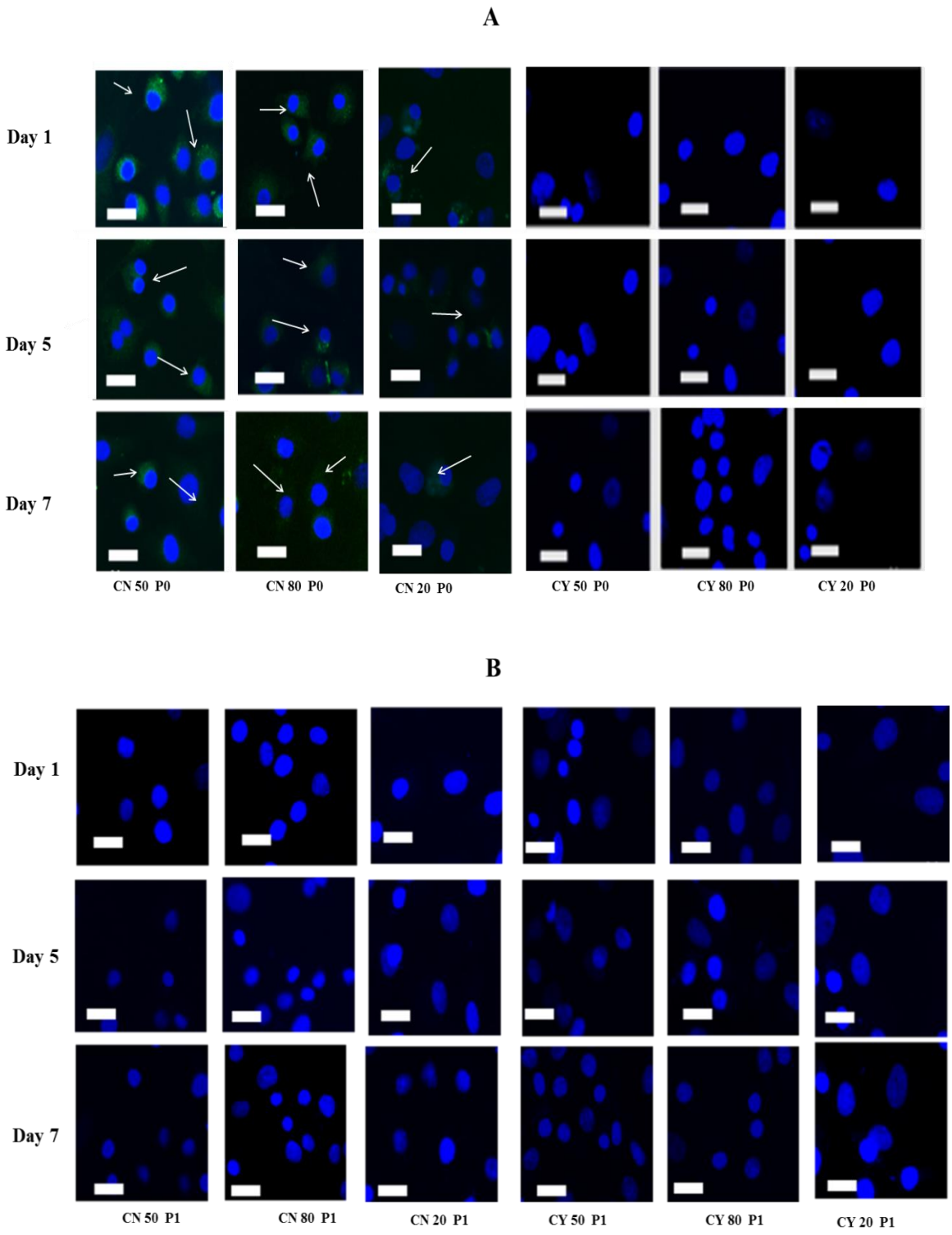

Figure 3.23: Representative immunofluorescent stained images of chondrons (CN), chondrocytes (CY), or MSCs in co-culture at days 1, 5, and 7 at P0 (panels A) and P1 (panels B). The cells were collagen VI (green; the cells were counter-stained by DAPI (blue). The white arrows indicate positive staining. The scale bars represent 20 μm.

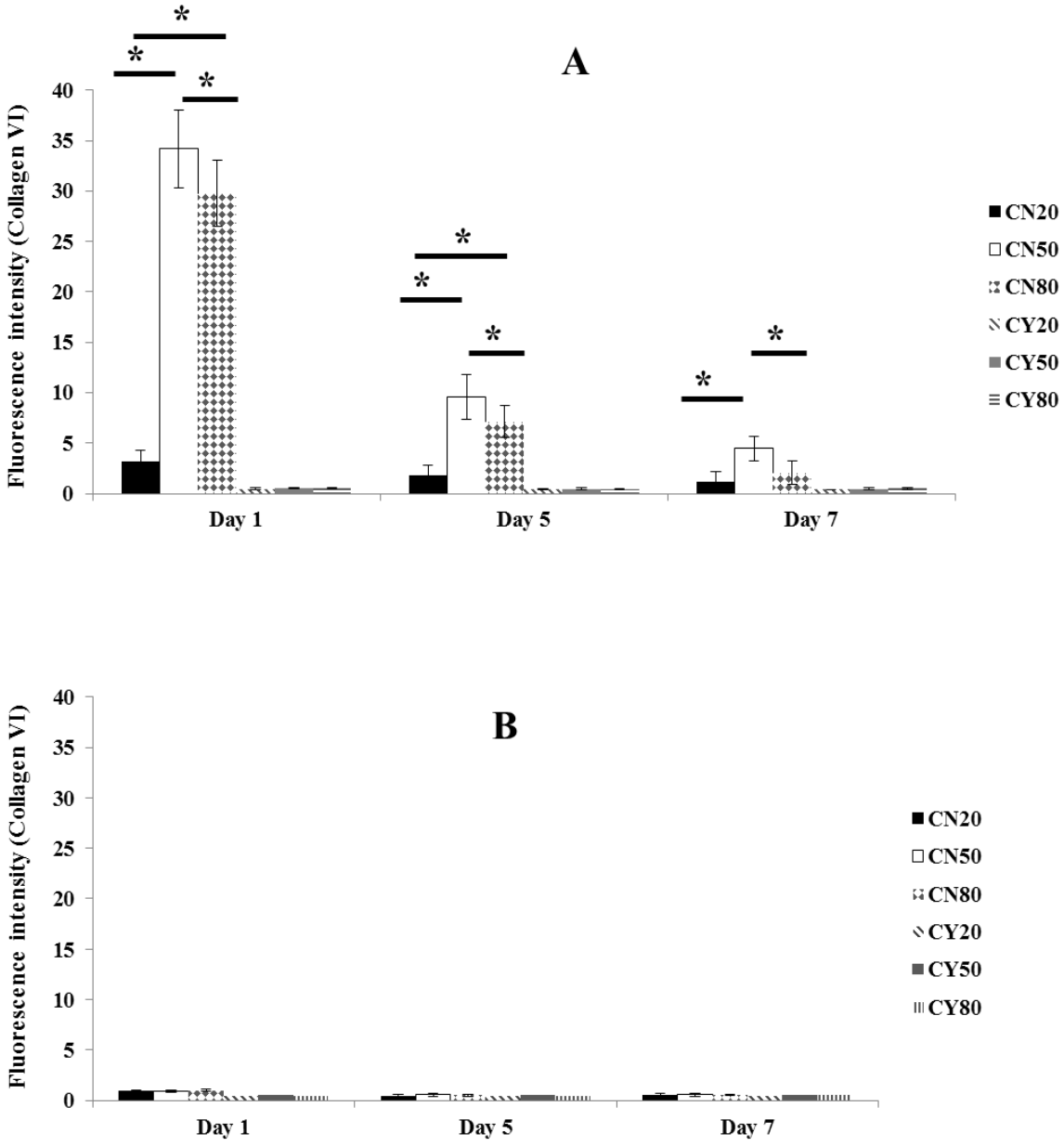

Figure 3.24: Representative Immunofluorescent stained intensity analysis of chondron (CN), chondrocyte (CY), and MSC in co-culture at days 1, 5, and 7 at collagen VI; A for P0 cells and B for P1 cells. Data are expressed as mean ± SD (n = 3). *$p < 0.05$

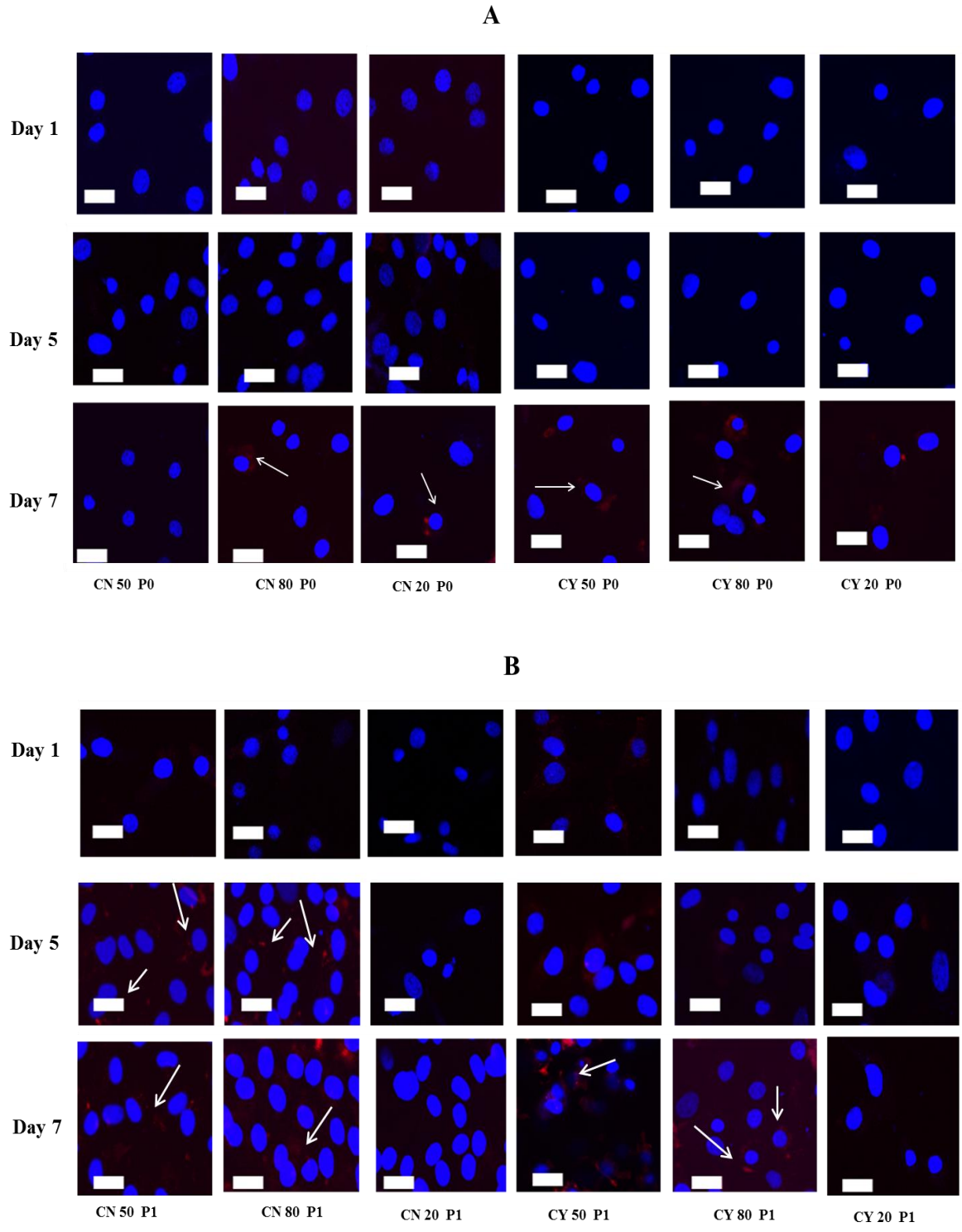

Figure 3.25**:** Representative immunofluorescent stained images of chondrons (CN), chondrocytes (CY), or MSCs in co-culture at days 1, 5, and 7 at P0 (panels A) and P1 (panels B). The cells were HtrA1 (red; the cells were counter-stained by DAPI (blue). The white arrows indicate positive staining. The scale bars represent 20 μm.

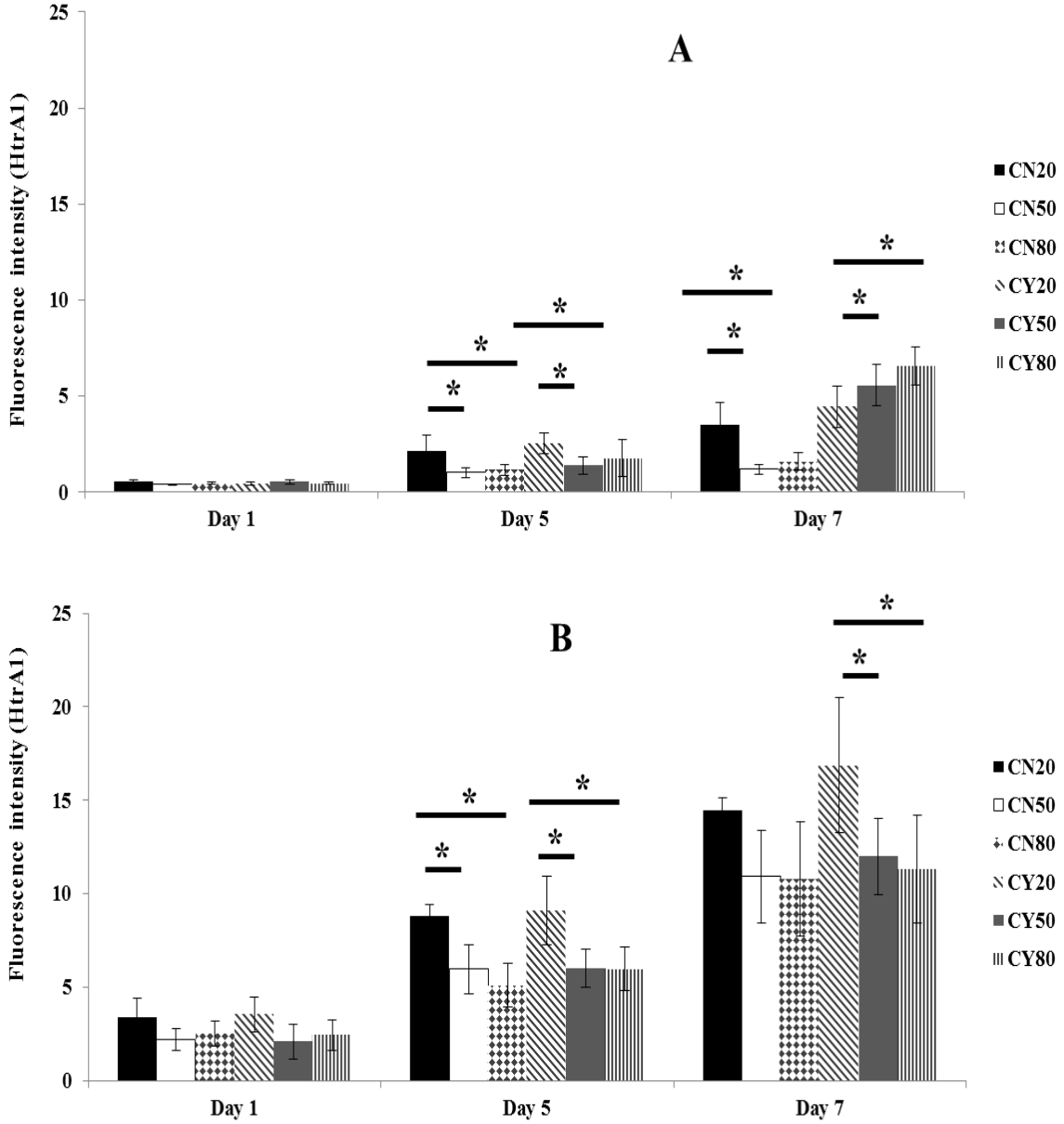

Figure 3.26: Representative Immunofluorescent stained intensity analysis of chondron (CN), chondrocyte (CY), and MSC in co-culture at days 1, 5, and 7 HtrA1 ; A for P0 cells and B for P1 cells. Data are expressed as mean ± SD (n = 3). *$p < 0.05$

`

3.5 Discussion

The chondrogenic capacity was assessed by cell morphology, the production rate of ECM (GAG and collagen II) and the presence of PCM (collagen VI) as the markers. Current study showed that the monolayer culture using hard substrate were unable to maintain the cartilaginous phenotype, and chondrocytes and chondron lose their phenotype from rounded to fibroblast-like spindle shapes with less collagen II and GAGs synthesis along 7 day culture duration. Co-culture of MSCs with chondrons enhanced ECM matrix production, as compared to chondrocyte or chondron monocultures. The co-culture of MSCs with chondrons appeared to decelerate the loss of the PCM as determined by collagen VI expression as compared to chondrons monoculture, whilst the expression of HtrA1 demonstrated an inverse relationship to that of the collagen VI.

Chondron has a higher chondrogenic potential than chondrocytes

This study has demonstrated that chondrons have higher chondrogenic potency than chondrocytes along culture duration regarding round shape morphology maintenance and ECM production; in terms of more accumulated GAG and collagen II production (8% and 11 % more in GAG and collagen II respectively). The higher ECM production in chondron culture in comparison to chondrocytes, which have no PCM, further confirms that PCM is an important source of chondrogenic signals for cartilage regeneration. Also, it has been shown in previous reports that chondrons have higher chondrogenic potency than chondrocytes (Larson et al., 2002; Bekkers et al., 2013).

PCM degradation process in 2D culture

It is demonstrated that PCM was very fragile and sensitive to culture condition. The dramatically changed surrounding of cartilage cells during culture influenced PCM's regeneration or preservation. Chondrocytes in both mono and co-cultures demonstrated that there was no PCM formation at any time points. While chondron in monoculture lost the native PCM gradually within

`

the culture duration; PCM was lost by day 7, whereas the co-culture chondron with MSC delayed the PCM degradation. The current study demonstrated that monolayer culture environment had no ability to preserve or rebuild PCM even with the co-culture of MSC if the culture plate was a hard substrate. It was confirmed that monolayer culture drove chondrocytes and chondron differentiation to fibroblast-like cell phonotype. It is speculated that without 3D microenvironment which mimic the native ECM and stabilise/accumulate newly formed PCM was the main cause for PCM lost by 7 day culture. Collagen VI staining had shown a clear picture for the degradation process. These observations have been supported by previous studies (Lee and Loeser., 1998, Larson et al., 2002).

The effect of co-culture and MSC ratios

In the co-culture, it is likely that bi-directional interactions occurred between cartilage cells and MSCs. It has been reported that chondrocyte secrete factors such as transforming growth factor-beta (TGF-β1), and bone morphogenetic proteins (BMP-2) (Bian et al., 2012; Wu et al., 2012) and these could induce chondrogenesis of MSCs and ECM production in vitro (Zhang et al., 2009; Lettry et al., 2010; Wu et al., 2012). In other studies it has been suggested that MSCs secrete chondrogenesis growth factors stimulating chondrocytes and therefore increasing cartilage matrix formation and proliferation matrix (Tsuchiya et al., 2004; Lettry et al., 2010; Levorson et al., 2014). Hence the ratio of MSC and cartilage cells in co-culture will influence the overall chondrogenic outcome.

Three different ratios of MSC and cartilage cells were used in this study, which was believed to induce distinct influence on chondrogenic capacity in chondron and chondrocytes. In 80:20 MSC and chondrocytes or chondrons ratio, MSCs were dominated cell population with lower chondrogenic impact due to the low number of cartilage cells. While the 20:80 MSC and chondrocytes or chondrons ratio had prevailed cartilage cells number, then the MSCs exerted less effect. Optimally, 50:50 MSC and chondrocytes or chondrons ratio had a balance between the two types of cell populations which allowed exchanging the signalling to maintain the chondrogenic

`

phenotype longer for cartilage cells and induce more MSCs to differentiate into chondrogenic lineage cells. Our results confirmed that 50:50 ratio had the maximum enhancement on chondrogenesis.

Reduction of HtrA1 production in co-culture

There is a gap in the understanding of PCM degradation in co-culture. As a secreted member of the trypsin family of serine proteases, HtrA1 has the capability to degrade the PCM (Polur et al., 2010). It has been reported that chondrocytes, expressing HtrA1 in mouse OA joints, do not produce collagen VI, which implies the disruption of the PCM (Hou et al., 2013). Whereas, in a mouse OA joint collagen VI was detected in the PCM while HtrA1 expression was absent (Polur et al., 2010). The current study demonstrated the same inverse relationship between the expression of HtrA1 and collagen VI. Interestedly, at the same condition as monoculture (culture time points), chondron co-culture with MSC samples had lower level HtrA1 expression. 50% chondron: MSC co-cultures did not show staining of HtrA1 at all culture time points, but the samples of chondrocyte: MSC co-cultures at day 7 had the highest staining intensity. At passage 1, the co-culture showed significant low expression of HtrA1 in compared to the monoculture. There was indistinct expression of HtrA1 at day 7. Hence, it is hypothesized that the presence of HtrA1 could be crucial to the degradation of collagen VI. The integrity of PCM could be preserved through protecting collagen VI by inhibition or inactivation of HtrA1 production. Thus, we speculate that the presence of MSCs in co-culture directly or indirectly inhibits the production of HtrA1, which results in the preservation and promotion of PCM.

The advantage of the current xenogeneic co-culture model

A major setback associated with studies on co-culture is that a large number of cells is required, which cannot be gathered from the patient samples obtained at surgery. A large number of consistent chondrons is difficult to isolate from limited supplies of cartilage tissue. To avoid the

`

issue of cell numbers, well characterised bovine chondrocytes and chondrons were used alongside rat MSC in this study because it is very difficult to get bovine MSCs.

Xenogeneic co-culture models using the bovine chondrocytes and either rat or rabbit MSCs have been successfully used by some other groups without any immune response or different inverse outcome (Levorson et al., 2014; Meretoja et al., 2014). Therefore, the xenogeneic co-culture model using rat MSCs and bovine cartilage cells will generate sufficient cells to clarify the effect on collagen VI. We have developed a xenogeneic co-culture model using rat MSCs to avoid the issue of the low yield of chondrons from small "off cuts" of patient tissue. It offers a valuable insight into chondrocyte and chondron co-cultures as well as the tool for classification of mechanism of MSC.

3.6 Conclusion

In conclusion, the monolayer culture system demonstrated an inability to maintain the chondrogenic phenotype, and chondrocytes and chondron changed their morphology from rounded to fibroblast-like spindle shapes. Also, it was confirmed that chondrons had higher chondrogenic potential than chondrocytes regarding GAG production and collagen II expression.

Co-culture of MSCs with chondrons enhanced ECM matrix production, as compared to chondrocyte or chondron monocultures. The co-culture of MSCs with chondrons appeared to decelerate the loss of the PCM as determined by collagen VI expression, whilst the expression of HtrA1 demonstrated an inverse relationship to that of the collagen VI. The ratio of 50:50 of MSCs in co-culture with chondrons presented the highest potential for better cartilage regeneration. Together this implies that MSCs directly or indirectly inhibited HtrA1 activity. However, PCM could not be preserved or regenerated in 2D culture even starting from chondron, and co-culture with MSCs if the culture plate was a hard 2D substrate which stimulated chondrocytes and chondron differentiation to fibroblast-like cells.

`

Chapter 4 : Three-dimensional cartilage tissue models to study PCM maintenance and regeneration

`

4.1 Introduction

The role of 3D environment in chondrogenic potential and in PCM regeneration and preservation

The maintenance or rebuilding of the PCM has a significant influence on cell-matrix interaction and function of cartilage engineered tissue (Vonk et al., 2010; Zhang et al., 2014). However, the PCM can be destroyed during dissection and *in vitro* culture (Larson et al., 2002). The results in chapter 3 showed that both chondrocytes and chondrons lose the chondrogenic phenotype and reduced their production of collagen II and GAGs within 1 week monolayer culture. In addition, the monolayer culture study suggested that cartilage cells have a reduced ability to preserve or rebuild their PCM, even when co-cultured with MSCs.

Hydrogels due to their high tissue-like water content, tuneable physical properties, homogenous cell distribution, high permeability for nutrients and waste products, have been developed for several tissue engineering applications (Tan et al., 2010; Eslahi et al., 2016). There is much evidence to show that preserving the chondrogenic phenotype can be achieved by culturing the chondrocytes and chondrons in a hydrogel environment (Chang and Poole, 1997; Dimicco et al., 2007; Vonk et al., 2010). This is due to the fact that hydrogels have a 3D network which is similar in structure to that of the native ECM (Eslahi et al., 2016). Through the use of hydrogels, chondrocytes can be stimulated to produce cartilage-specific matrix, where the hydrogel preserves the newly-produced matrix to allow accumulation of ECM-related content (Aleksander-Konert et al., 2016; Eslahi et al., 2016).

Using the well characterised agarose system, Chang and Poole (Chang and Poole, 1997) cultured chondrocytes for 24 h producing aggrecan, decorin, and fibronectin. A week later, the chondrocytes were surrounded by a ring of PCM containing collagen VI. Vonk et al. (2010) reported that chondrons retained their PCM whilst cultured in a well-defined alginate system for up to 25 days.

`

By comparison, chondrocytes needed a block of time to first rebuild their PCM, and then mature it. If these cells were going to be re-implanted into a cartilage defect, then there would be at least a 25 day delay whilst they caught up with the chondrons.

In the literature, co-culture studies of articular chondrocytes or chondrons with mesenchymal stem cells have provided evidence of increased ECM production (Qing et al., 2011; Levorson et al., 2014). According to Levorson et al., (2014) confirmed the cartilaginous ECM-like (collagen II and GAGs) production was prompted in a xenogeneic co-culture model using rabbit MSCs and bovine chondrocytes within a nonwoven fibrous substrate. Previous studies have stated that enhancement in ECM production by chondron and human MSCs in co-cultures for 4 weeks of pellet culture (Bekkers et al., 2013). However, up till now, there have been no systematic studies to reveal whether MSC co-culture with cartilage cells makes reservation of PCM and what the associated mechanism (s) are.

The gap of knowledge to be filled

To date, most research has focused on PCM maintenance or regeneration within 3D microenvironment hydrogels. The field needs some systematic studies designed to investigate and compare multi-factor effects in 3D culture environment which could influence the efficiency of PCM maintenance or regeneration. For example, we need to explore co-cultures with MSCs since we have preliminary evidence to suggest that this approach can promote better PCM maintenance.

Synchrotron microFTIR as a new tool to analyse PCM maintenance and regeneration

ECM and PCM formation and maturation were usually monitored as well through a range of difference approaches such as metachromasia, biochemistry and immunolocalisation techniques. For example, metachromatic stains such as toluidine blue and alcian blue have been widely used to detect the presence of GAGs and their associated proteoglycans (mainly aggrecan). The dimethylmethylene blue assay is widely used for the quantitation of total sulphated GAGs but it

`

can be inaccurate due to interference from polyanions. Metachromasia only provides a crude assessment and it provides a limited amount of information. Biochemical assays such as total collagen analysis or Western blotting using immunolocalisation have been utilised to assess protein accumulation (mainly collagen type II but also collagen VI). These techniques are useful but to characterise both articular cartilage and chondrons at the microscale level it will be necessary to develop additional techniques which can resolve micron-scale structural changes and difference during chondrocyte culturing.

Components of biological structures like human tissue and cells can be studied using Fourier Transform Infrared (FTIR) microspectroscopy (microFTIR). The advantage of using FTIR technique is that a single spectrum can reveal various important biomolecules simultaneously such as lipids, proteins, carbohydrates and nucleic acids. Each biomolecule produces its spectral signature depending on the nature of the bonds and concentrations of the molecules (Barth, 2009). Using a synchrotron source for FTIR provides a more powerful tool for cells and tissue study because of the high brightness which enables using smaller aperture to identify the spatial heterogeneity of biomolecules in single cells with as small as 5 micrometres apertures (Miller et al., 2005). Synchrotron microFTIR offers spatial distribution mapping and chemical structure detection at the micron scale, when integrating chemical analysis specificity with microbeam precision (Deegan, et al., 2015). FTIR offers non-destructive identification tool with less sample preparation and provides integral information for the spatial distribution of proteins presence, proteoglycan contents and concentration and lipids.

Several studies have recently been conducted on infrared spectroscopy on articular cartilage tissue and engineered constructs. Camacho et al., (2001) presented univariate parameters to quantify collagen and proteoglycan contents in articular cartilage. The amide I (1584 - 1720 cm^{-1}) was shown to correlate with the collagen content, and the carbohydrate region (984-1140 cm^{-1}) correlate with the proteoglycan content in pure compound mixtures of collagen and aggrecan

`

(Camacho et al., 2001). Potter et al., (2001) used FTIR spectral imaging, coupled with multivariate data processing to study the spatial distribution of ECM components in native cartilage tissue and 3D cartilage tissue, generated by chick sternal chondrocytes in a hollow fibre bioreactor (Potter et al., 2001). The FTIR data analysis showed that tissue-engineered cartilage had more collagen and less proteoglycans than the native cartilage.

A study reported that proteoglycans quantification could be enhanced by normalising the spectra of carbohydrate region by that of amide I in tissue-engineered cartilage, which reduced the thickness variation in the cartilage tissue sections (Kim et al., 2005). A statistically significant correlation was obtained between the FTIR spectral data and alcian blue staining. However, there was no study to assess the evolution process of PCM formation in tissue engineered cartilage constructs by FTIR. There was no synchrotron microFTIR study to map spatial distribution of chemical compositions of newly generated PCM in a tissue engineering cartilage model.

4.2 Objectives

This study aims to define the 3D culture environments that facilitate the preservation, regeneration and stabilisation of PCM by investigating and comparison of multi-factors such as; hydrogel types, presence of MSCs, culture medium types and culture duration in parallel. The non-destructive technique, the synchrotron microFTIR technique, would be explored to observe the PCM formation and cellular evolution of cultured cartilage cells in the 3D tissue-engineered cartilage models.

4.3 Materials and methods

4.3.1 Cell isolation and expansions

Bovine chondron and chondrocytes were used with passage 0 (P0) exclusively. P1 rat MSCs was used. The cell isolation and culture details have been included in Chapter 2, Section 1.

`

4.3.2 Experiments design and set up

Four cell groups containing monoculture, chondrocytes (CY), chondron (CN), and co-culture with mesenchymal stromal cells (MSC) in the ratio of 50:50 were prepared based on the 2D culture outcomes (chapter 3) for this study. All groups used basal (Bas) or chondrogenic (Ch) medium, respectively, and the cartilage cells were encapsulated with HA and agarose (ag) hydrogels in separate experimental groups. All samples were cultured in 96 well-plates. For hydrogel embedding, 75 µl of hydrogel mixture was cast first. After gelation, cells were seeded at a seeding density of $5x10^3$ cells/well (Table 4.1), and allowed to attach at 37˚C for 2 hours. Following 75 µl of hydrogel solution was filled in the well. The formed construct was incubated with basal or chondrogenic media (Table 2.1) and cultured up to 21 days at 37˚C and 5% CO_2. The cell morphology, cell number, total sulphated glycosaminoglycan (sGAG) content and the immunolocalisation of key PCM/ECM components were assessed on day 1, 7, 14 and 21.

`

Table 4-1: Description of experimental groups with cell types and seeding densities

Experimental group	Chondrocytes per well	Chondrons per well	MSCs per well	Mediums
CY (HA)	**5,000**	**-**	**-**	**Chondrogenic**
				Basal
CY50 (HA)	**2,500**	**-**	**2,500**	**Chondrogenic**
				Basal
CN (HA)	**-**	**5,000**	**-**	**Chondrogenic**
				Basal
CN50 (HA)	**-**	**2,500**	**2,500**	**Chondrogenic**
				Basal
CY (ag)	**-**	**5,000**	**-**	**Chondrogenic**
				Basal
CY50 (ag)	**2,500**	**-**	**2,500**	**Chondrogenic**
				Basal
CN (ag)	**-**	**5,000**	**-**	**Chondrogenic**
				Basal
CN50 (ag)	**-**	**2,500**	**2,500**	**Chondrogenic**
				Basal

4.3.3 Cell viability

A standard live/dead cell staining kit was used to assess cell survival in hydrogel capsules. The protocols with set up details were detailed in Chapter 2, Section 5.2.

`

4.3.4 Cell morphology monitoring

The cells and clusters morphology in monocultures and co-cultures on all variables and different time points were imaged with an optical microscope attached to a CCD camera.

4.3.5 Biochemical assays

Papain solution was used to digest the experimental samples at the end of the culture periods for PicoGreen DNA assay and DMMB assay as described in Chapter 2, Section 4, Section 5.1 and, Section 6 respectively. The normalised value of total GAG content per cell was calculated as well based on GAG content and cell number.

4.3.6 Histology

Hydrogel was removed by incubation for 45 seconds in a 40˚C water bath. The molten solution was centrifuged at 750 g; cells that were to be encapsulated on hydrogel were re-suspended in 0.9% NaCl. Cell suspensions were cytospun onto slides for 1 minute at 700 rpm. Once the cells had been deposited on slides, samples were fixed with 4% (v/v) formalin at room temperature for 30 minutes, and then stained for deposited sGAG using toluidine blue staining. The staining protocol details were included in Chapter 2, Section 9.1.

4.3.7 Immunolocalisation of key chondrogenic markers

Immunostaining was used to identify the presence and distribution of PCM and ECM components (collagen type II, collagen type VI) and HtrA1. Immunostaining staining was conducted using the protocols described in Chapter 2, Section 10. Intact samples were stained and staining intensity was observed by a confocal microscopy.

4.3.8 Semi-quantification of GAG and immunofluorescence staining intensity

The intensity of toluidine blue and immunofluorescence staining were semi-quantified using ImageJ software following the protocols detailed in Chapter 2, Section 11.

`

4.3.9 Synchrotron FTIR spectroscopy

For FTIR measurement, cytospun samples were prepared according to a described protocol in Chapter 2, Section 7. Five different groups were prepared; isolated chondron, isolated chondrocytes, and chondrocytes cultured in HA hydrogel with basal medium at days 7, 14 and 21.

Synchrotron FTIR data were acquired from Diamond Light Source (Oxford). Principle Component Analysis (PCA) was performed with loading plots to show the variation in FTIR spectra according to variation in culture conditions. The protocol details can be found in Chapter 2, Section 7.3.

4.4 Results

4.4.1 Cell cluster morphology

The shape of the cell clusters was assessed at different culture time points; 1, 7, 14 and 21 days (Figure 4.1). In monoculture, after 24 hours culturing both chondrocytes and chondrons displayed a rounded morphology in different hydrogel materials and media types. By day 7, both chondrocytes and chondrons showed a remarkable distinction within HA and agarose hydrogels. Chondrocytes and chondrons showed small spread round clusters within HA hydrogel, but they showed big clusters close to each other with less spreading in agarose hydrogel with both chondrogenic and basal media. At day 14, the appearance of the clusters changed dramatically; cell clusters presented a round shape with the slight spread. At 21 days, all of the cells in different groups tended to aggregate together as dense clusters. The Co-culture results showed variations in cell clustering. At the end of the first day, chondrons demonstrated a spread and rounded morphology in different hydrogel materials and media types. By contrast, chondrocytes formed small irregular clusters in close proximity to each other. Through the time course, both chondrocytes and chondrons clustered in a similar manner within both HA and agarose hydrogels at monoculture but with dense and smaller clusters with chondrogenic media. The co-culture samples at day 14 displayed a dense cluster with less spread comparison to monoculture.

`

A

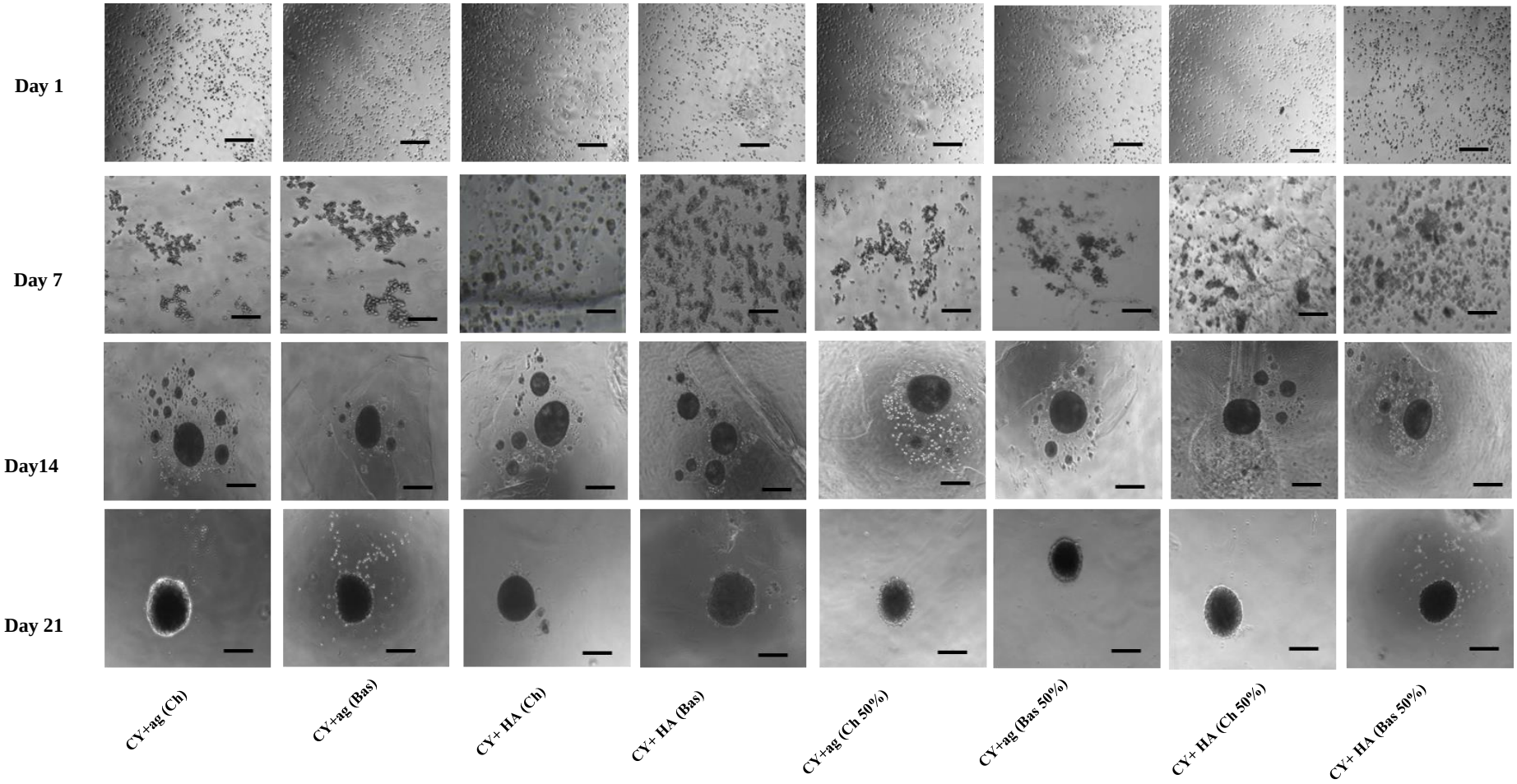
Day 1
Day 7
Day14
Day 21
CY+ag (Ch)
CY+ag (Bas)
CY+ HA (Ch)
CY+ HA (Bas)
CY+ag (Ch 50%)
CY+ag (Bas 50%)
CY+ HA (Ch 50%)
CY+ HA (Bas 50%)

`

B

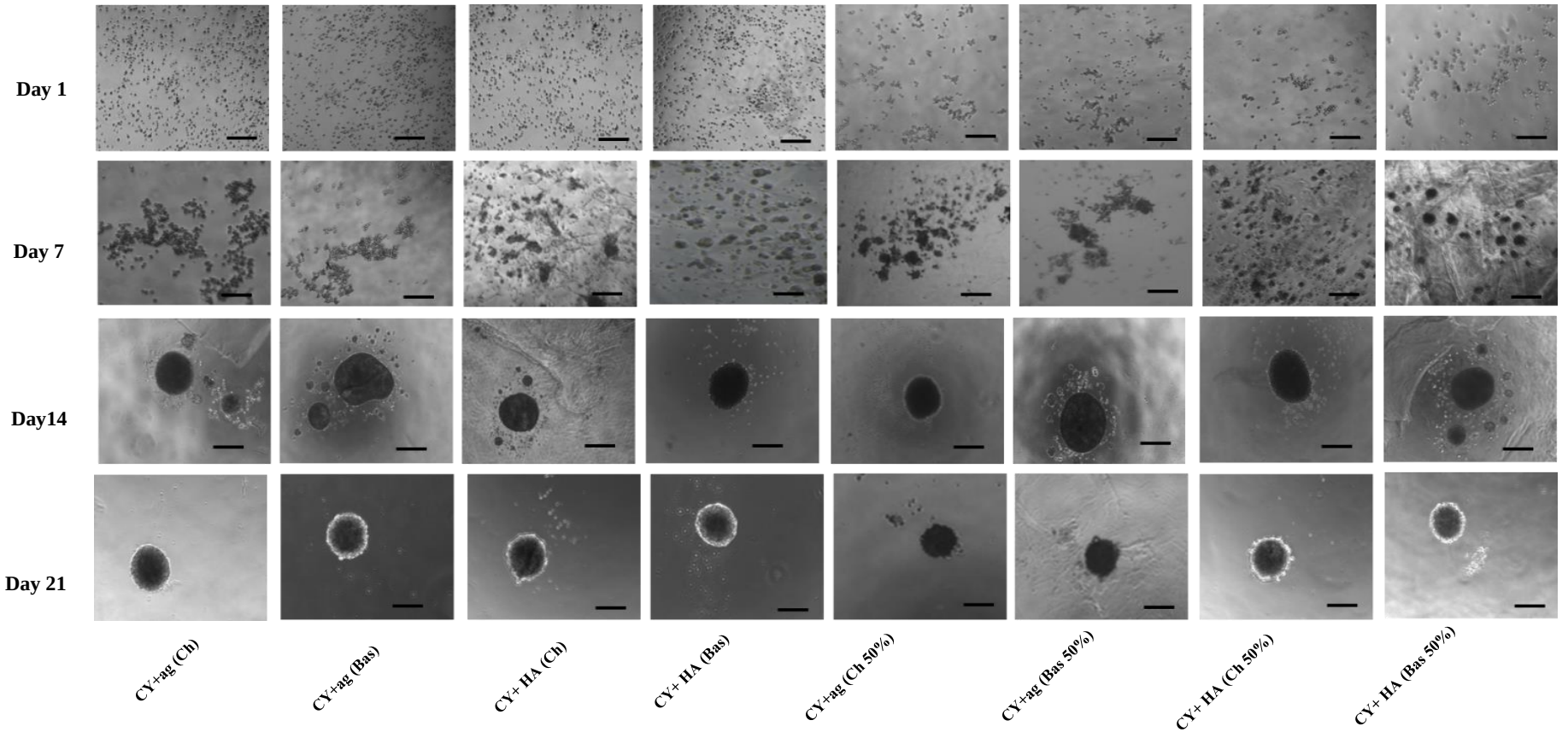

Figure 4.1: Cell morphology in mono and co-cultures within hyaluronic acid (HA) and agarose (ag) hydrogels under chondrogenic (Ch) and basal (Bas) mediums at Days 1, 7, 14 and 21 with/without 50% MSC with (A) chondron (CN) and (B) chondrocytes (CY). The scale bars represent 150 µm.

`

4.4.2 Cell viability and cell number

Figure 4.2 shows the live/dead cell images on the constructs taken by confocal microscopy at different time points; 1 and 21 days. The viable cells fluoresced green and the non-viable cells fluoresced red. Based on the image observation, by the first day all the cells in both chondron and chondrocytes in mono and co-cultures were viable and there were no dead cells. By the day 21 most cells were viable, and there were only a few dead cells detected within the agarose hydrogel than HA hydrogel, and monoculture has less dead cells in comparison to co-culture. Also, chondron cultures contained less dead cells comparing to chondrocytes.

Figure 4.3 shows that co-culture had a higher cell number in comparison with monoculture of both chondron and chondrocytes constructs. Also, the chondrocytes had higher cell number than the chondrons within the time in both mono and co-cultures. The HA hydrogel demonstrated a significantly higher cell number than the agarose hydrogel ($p < 0.05$) at different time points in both chondrogenic and basal mediums. Over time, the HA hydrogel had a higher proliferation rate in comparison with agarose which had almost the same cell number across the time course. Regarding media types, cell number was higher in a basal media culture in HA hydrogel in both chondron and chondrocytes mono and co-cultures ($p < 0.05$). Chondrogenic media culture showed that cell number and the proliferation rate decreased after day 7 in both mono and co-cultures.

`

A

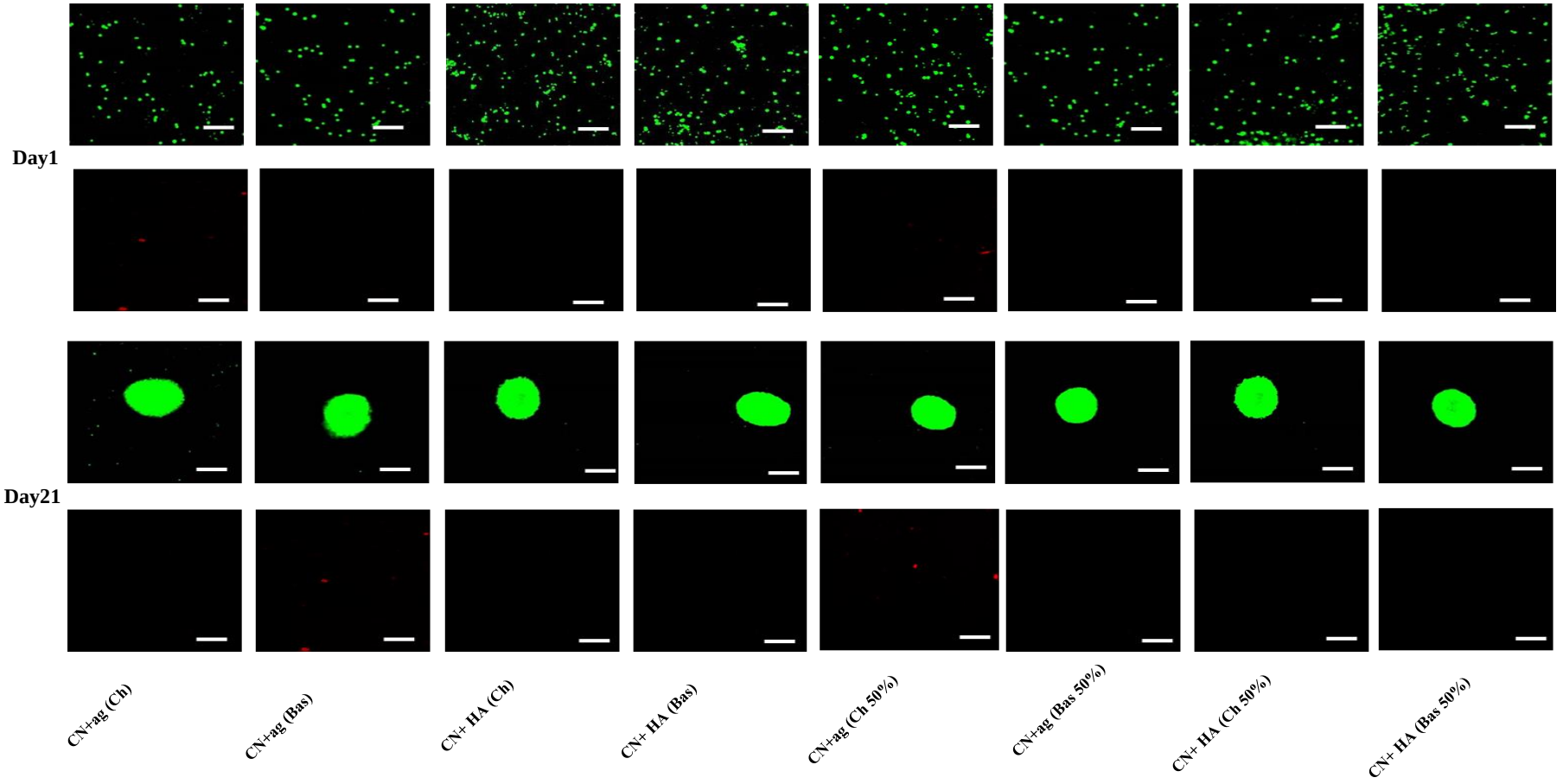
Day1
Day21
CN+ag (Ch)
CN+ag (Bas)
CN+ HA (Ch)
CN+ HA (Bas)
CN+ag (Ch 50%)
CN+ag (Bas 50%)
CN+ HA (Ch 50%)
CN+ HA (Bas 50%)

`

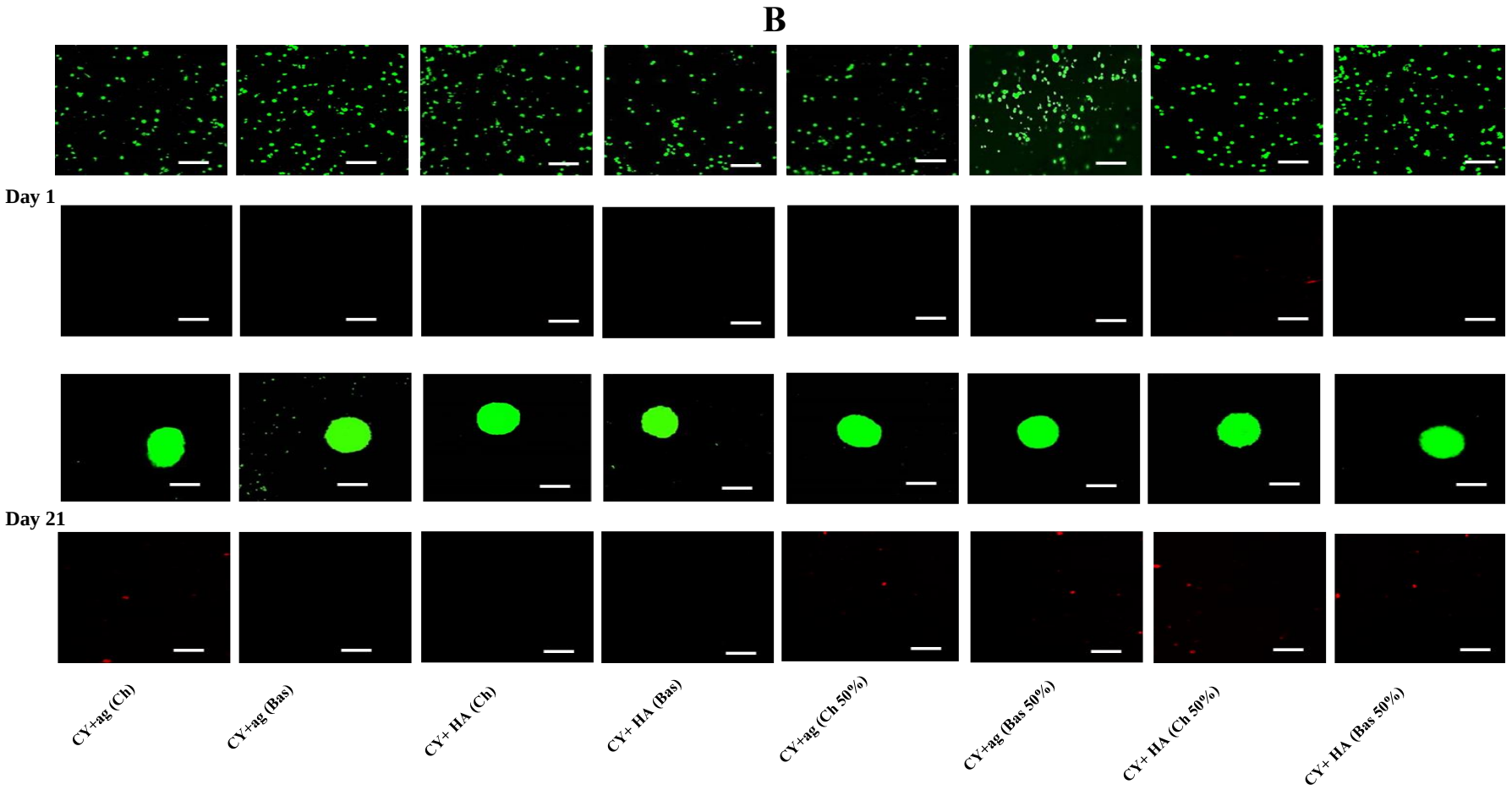

.

Figure 4.2: The live and dead staining of cartilage cells in mono and co-cultures within hyaluronic acid (HA) and agarose (ag) hydrogels, under chondrogenic (Ch) and basal (Bas) mediums at Days 1 and 21 with/without 50% MSC with (A) chondron (CN) and (B) chondrocytes (CY). Green represented live cells, red dead cells. The scale bars represent 100 μm.

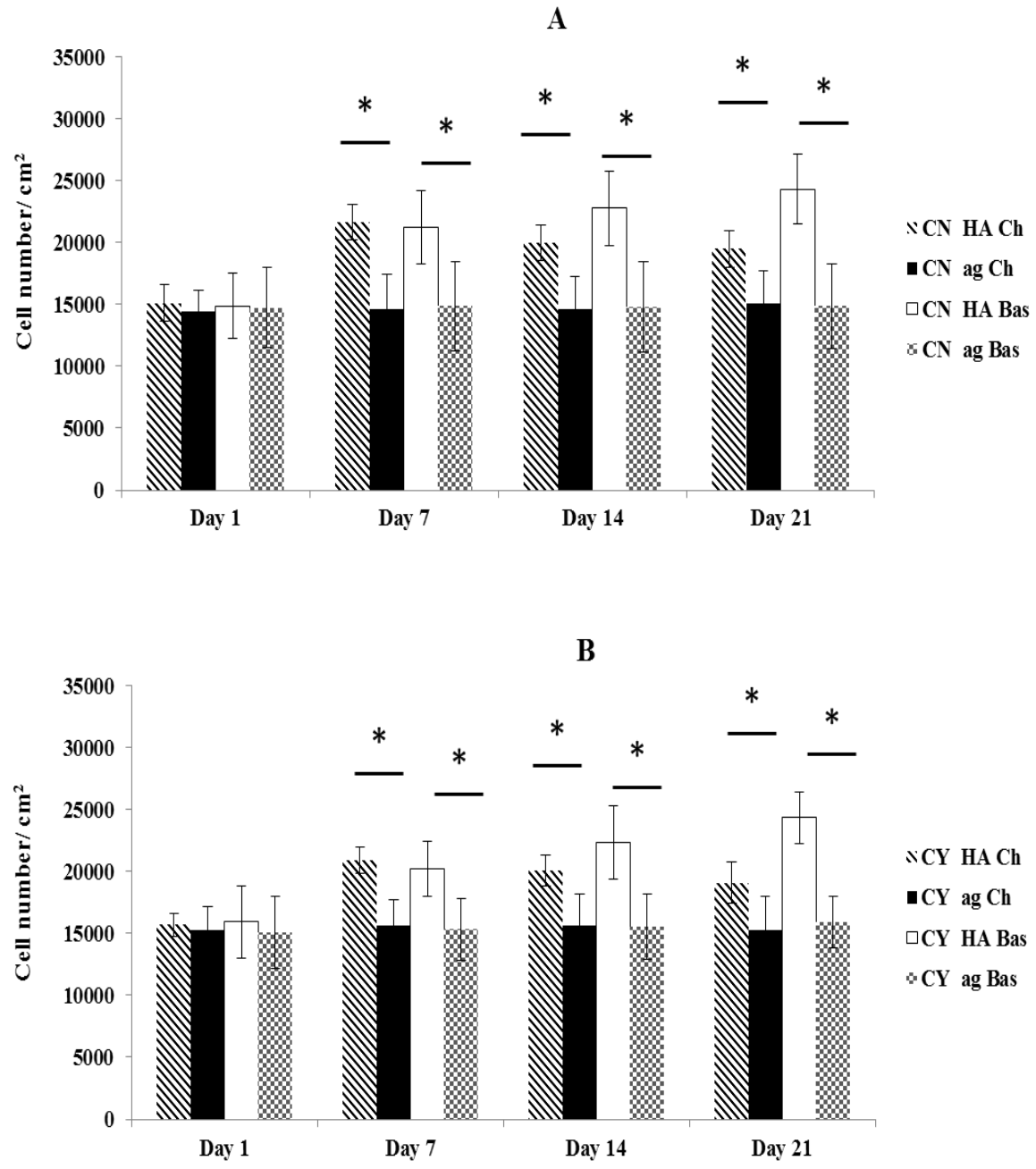

Figure 4.3: Cell number in monoculture with hyaluronic acid (HA) and agarose (ag) hydrogels under chondrogenic (Ch) and basal (Bas) media at Days 1, 7, 14 and 21 at (A) chondron (CN) and (B) chondrocytes (CY). Data are expressed as mean ± SD (n =3).

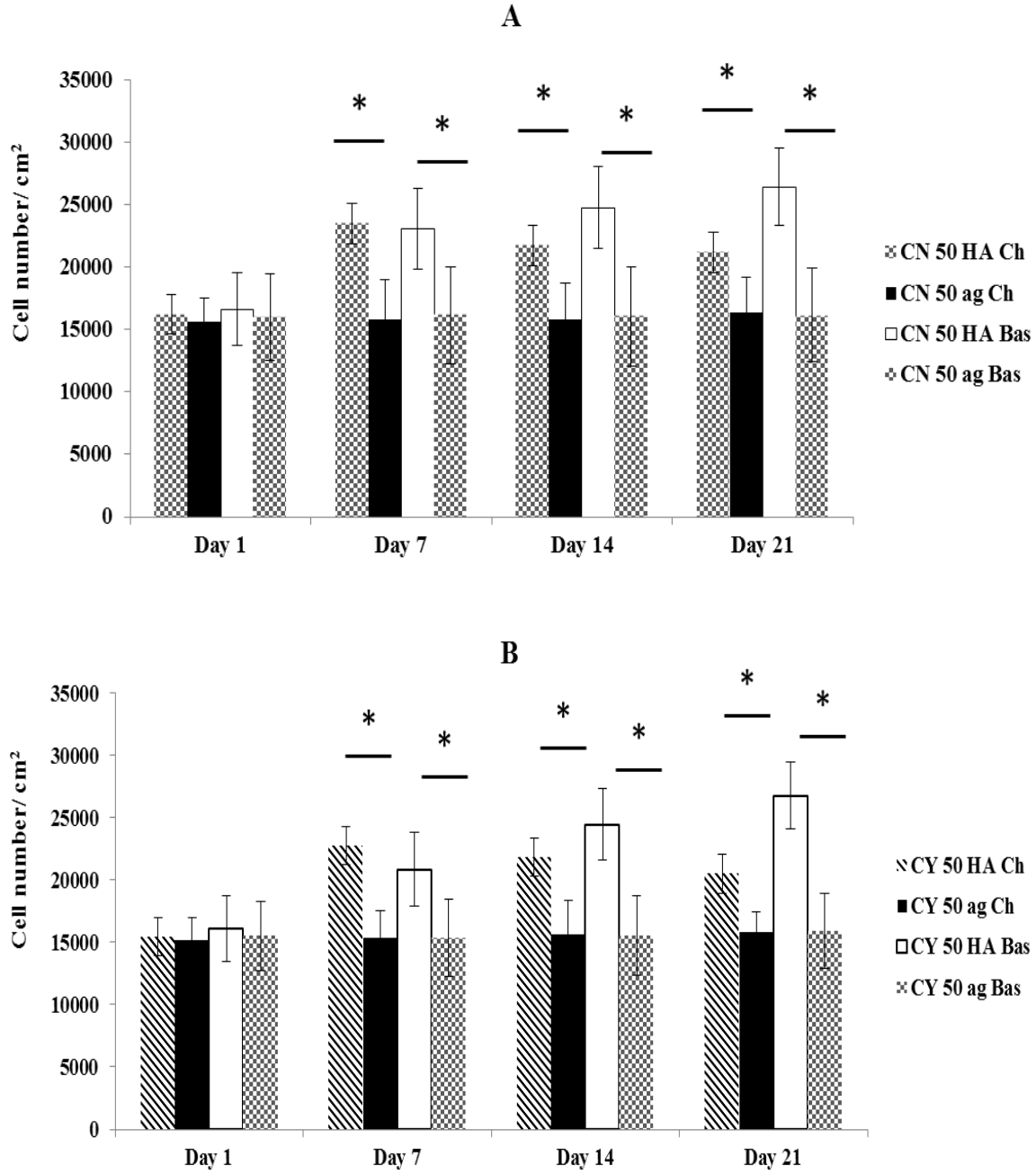

Figure 4.4: Cell number in co-culture with hyaluronic acid (HA) and agarose (ag) hydrogels under chondrogenic (Ch) and basal (Bas) mediums at Days 1, 7, 14 and 21 using 50% MSC with (A) chondron (CN) and (B) chondrocytes (CY). Data are expressed as mean ± SD (n =3).

`

4.4.3 Total sulphated GAG production

Figures 4.5 and 4.6 demonstrate the accumulated sGAG in mono and co-cultures for both chondron and chondrocytes constructs using different hydrogel materials and media types at different culture time points; 1, 7, 14 and 21 days. Co-culture enhanced the GAG production in comparison with monoculture in both chondron and chondrocytes constructs. Also, the chondron produced higher accumulated GAG than chondrocytes within the same time point in both mono and co-cultures ($p < 0.05$). HA hydrogel demonstrated higher GAG production than agarose hydrogel ($p < 0.05$) along different time points in both chondrogenic and basal media. The accumulated GAG increased with culture time. Chondrogenic medium culture showed enhancement and higher GAG production than basal medium culture in HA and agarose hydrogels in both chondron and chondrocytes in mono and co-cultures.

Normalised data confirmed that sGAG production per cell increased with time. Furthermore, MSC and chondron co-cultures significantly increased GAG production per cell ($p < 0.05$). The highest normalised GAG production (Figures 4.7 and 4.8) was in the samples with the HA gel, chondrogenic media and 50% MSC in both chondron and chondrocytes.

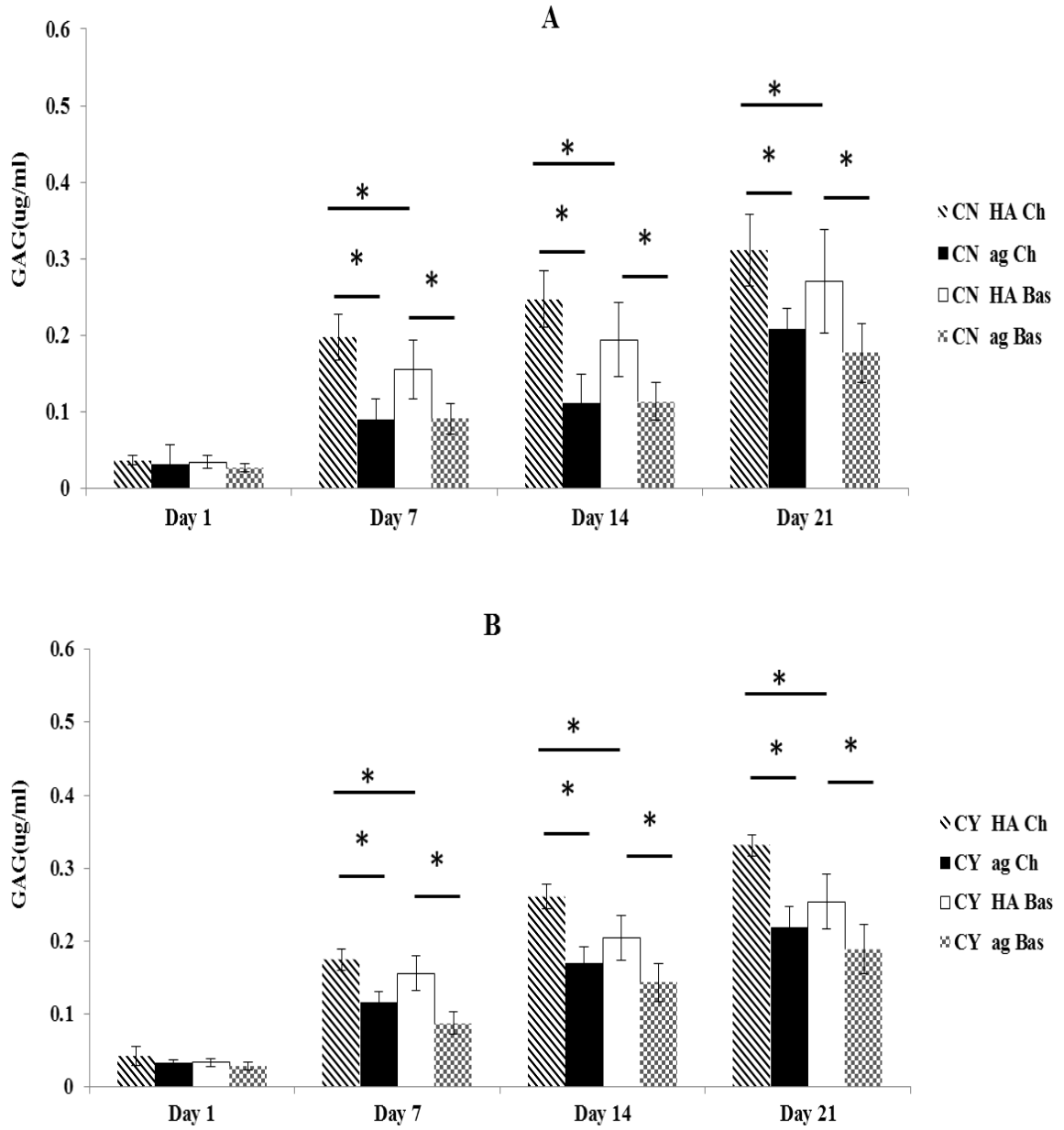

Figure 4.5: Total sGAG production in monoculture within hyaluronic acid (HA) and agarose (ag) hydrogels and chondrogenic (Ch) and basal (Bas) mediums at Days 1, 7, 14 and 21 at (A) chondron (CN) and (B) chondrocytes (CY). Data are expressed as mean ± SD (n =3). *$p < 0.05$

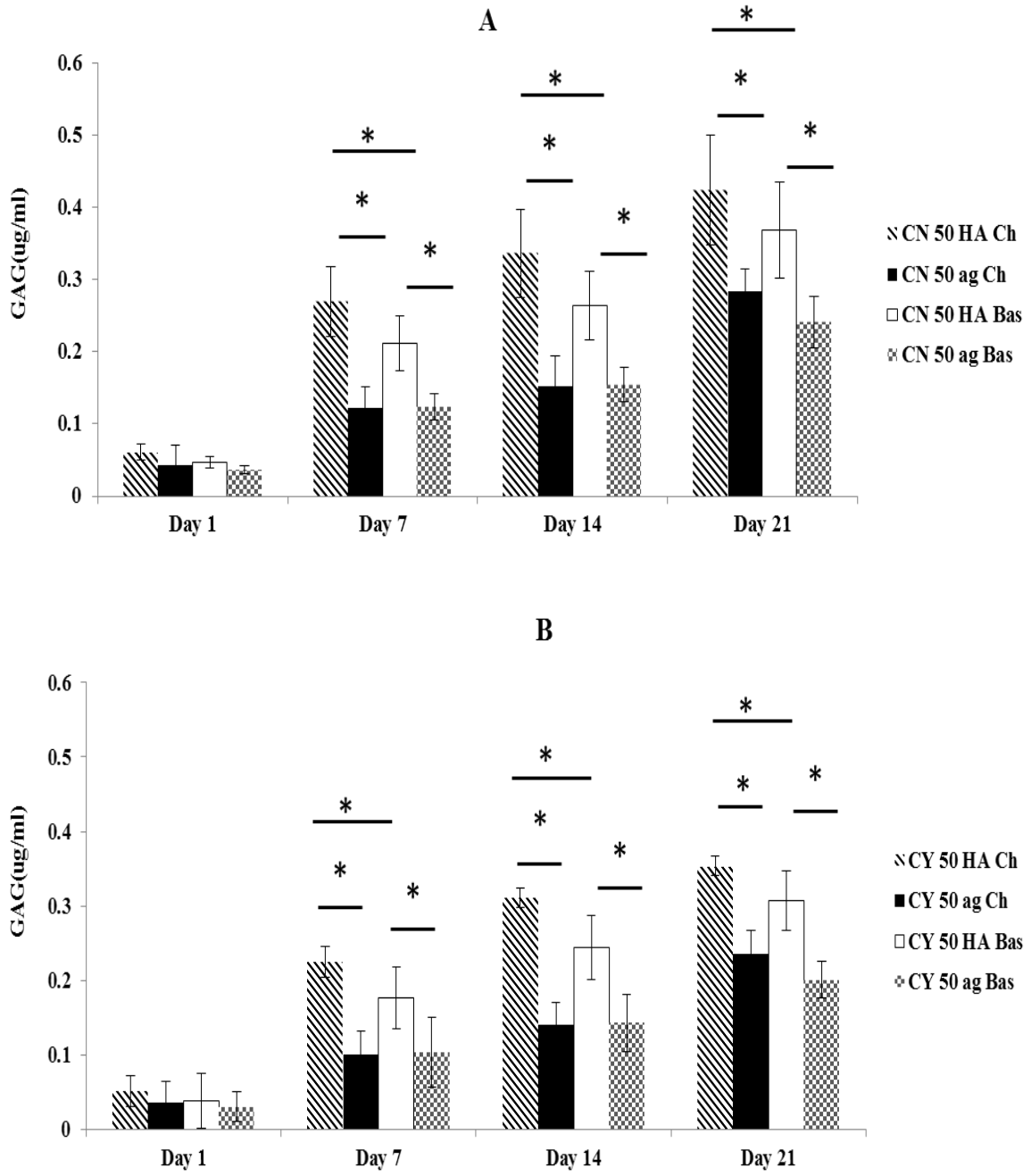

Figure 4.6: Total sGAG production in co-culture within hyaluronic acid (HA) and agarose (ag) hydrogels under chondrogenic (Ch) and basal (Bas) media at Days 1, 7, 14 and 21 using 50% MSC with (A) chondron (CN) and (B) chondrocytes (CY). Data are expressed as mean ± SD (n =3). *$p < 0.05$

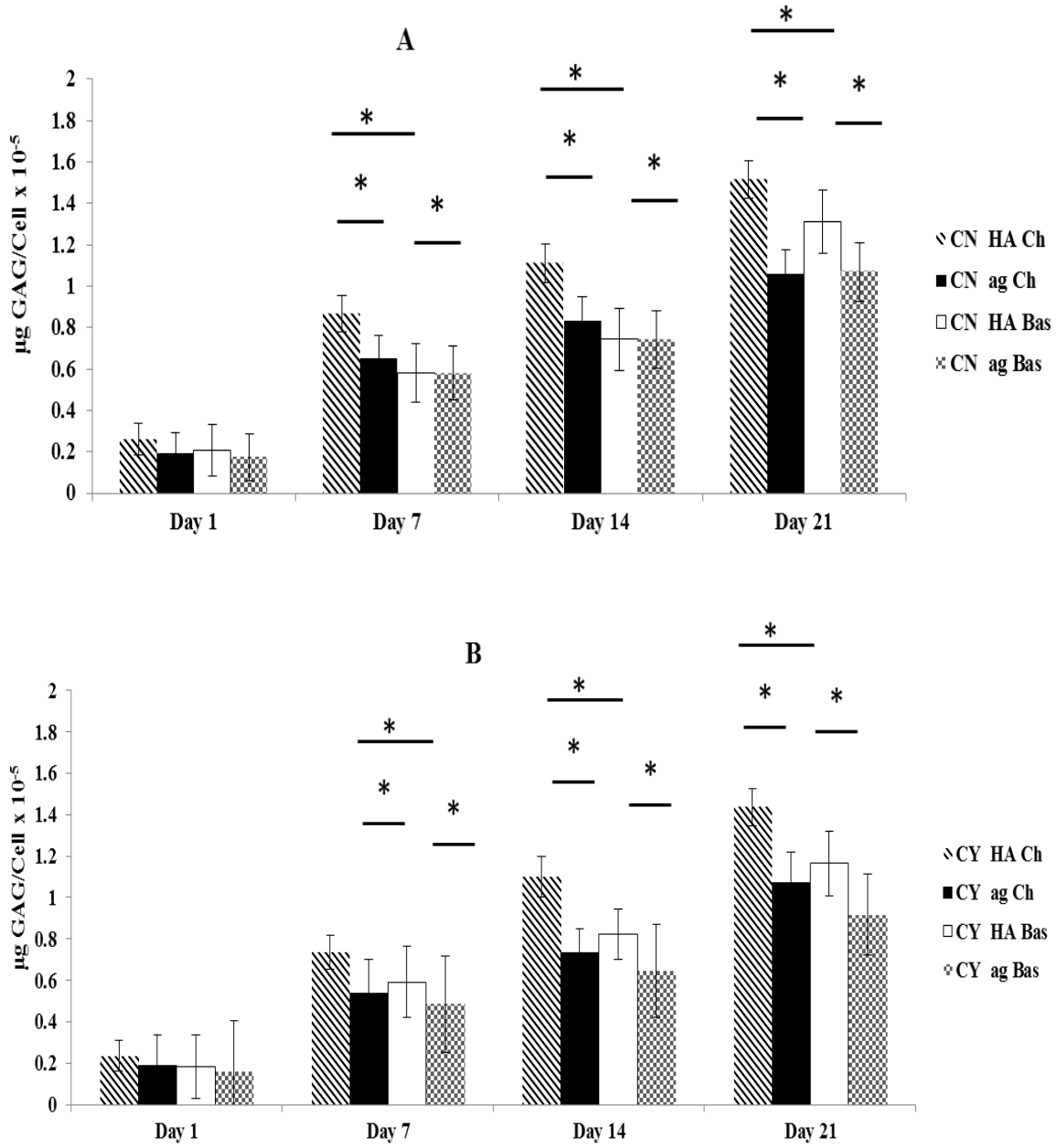

Figure 4.7: Total sGAG production normalised to cell number in monoculture within hyaluronic acid (HA) and agarose (ag) hydrogels and chondrogenic (Ch) and basal (Bas) media at Days 1, 7, 14 and 21 at (A) chondron (CN) and (B) chondrocytes (CY). Data are expressed as mean ± SD (n =3). *$p < 0.05$

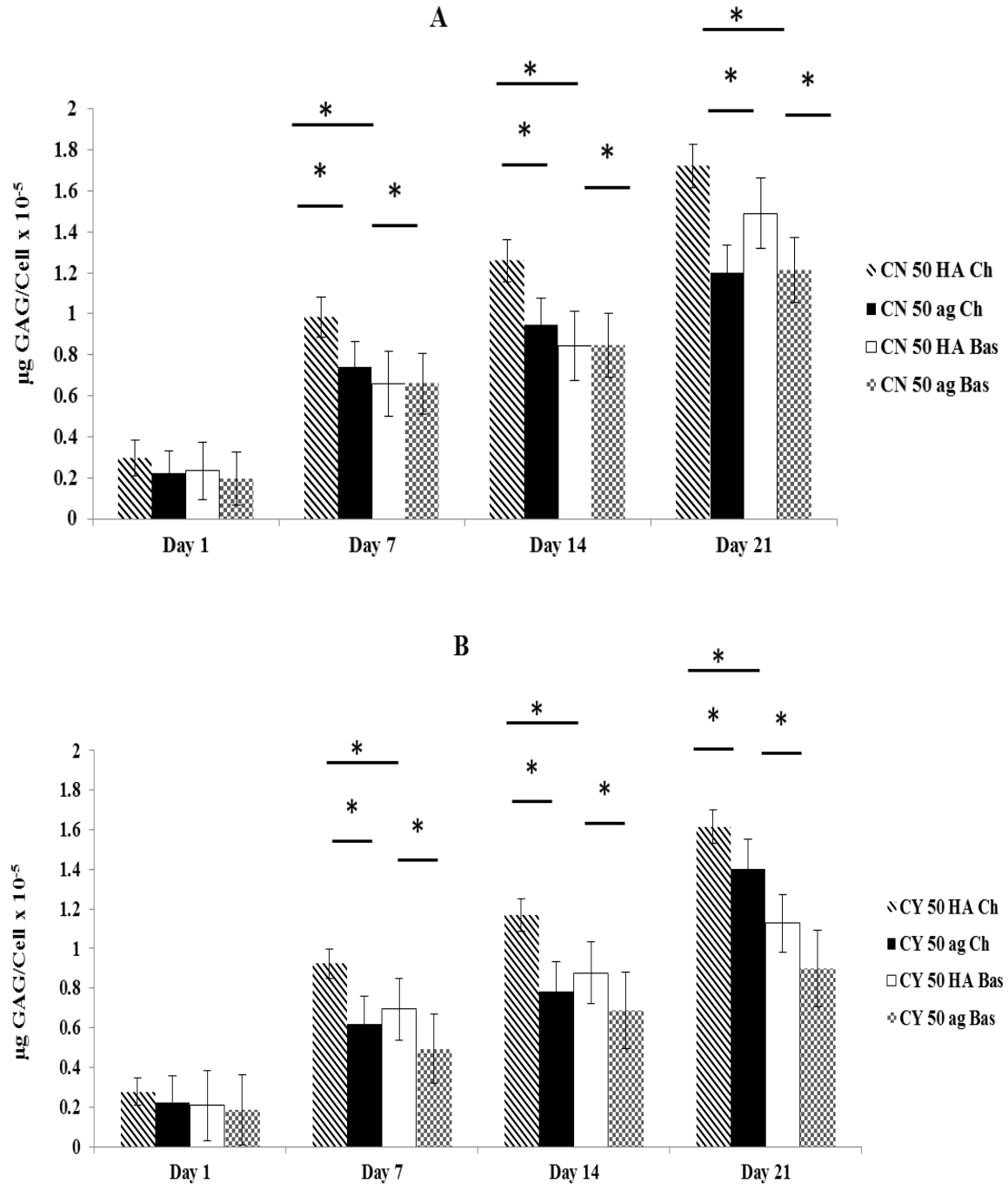

Figure 4.8: Total sGAG production normalised to cell number in co-culture within hyaluronic acid (HA) and agarose (ag) hydrogels under chondrogenic (Ch) and basal (Bas) media at Days 1, 7, 14 and 21 using 50% MSC with (A) chondron (CN) and (B) chondrocytes (CY). Data are expressed as mean ± SD (n =3). *$p < 0.05$

`

4.4.4 Histology

Each cultured sample was stained with toluidine blue to detect the presence and distribution of GAGs. Throughout the time course, GAGs increased in chondron and chondrocyte mono and co-cultures constructs (Figures 4.9 and 4.10). HA hydrogel showed more strongly stained than the agarose in mono and co-cultures. Furthermore, the samples cultured in chondrogenic media demonstrated more GAGs than basal media samples. Semi-quantification of the GAG staining intensity across the groups and culture time by ImageJ Analysis software was shown in Figure 4.10. It is shown that at monoculture and co-culture, chondrons presented higher GAG production than chondrocytes at all culture time points significantly and the intensity continuously increases along the culture with significant high GAG at day 21 and 14 than day 7 and 1. The semi-quantification of staining intensity correlated well with the total sulphated GAG (Figures 4.5 and 4.6).

`

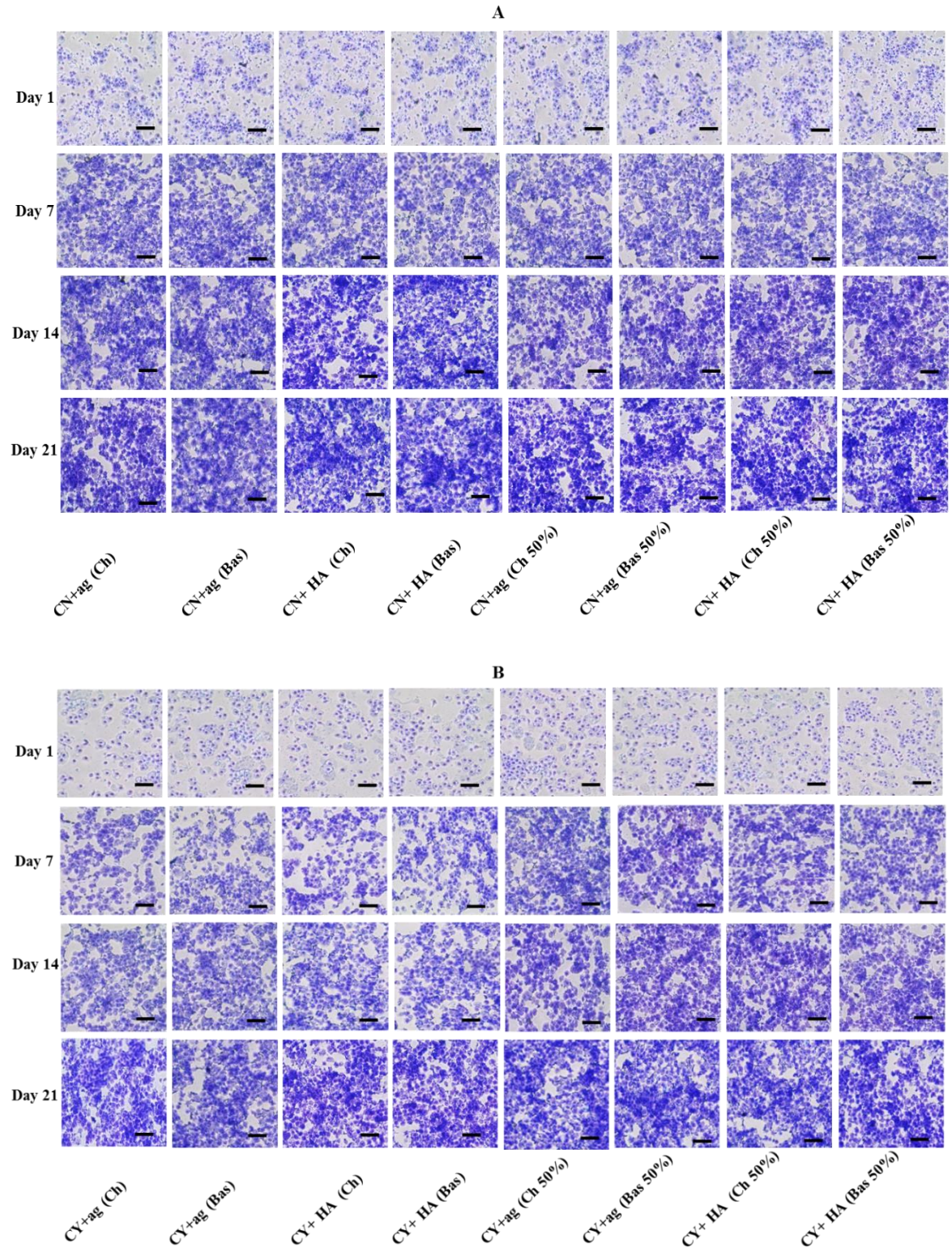

Figure 4.9: Representative toluidine blue stained in mono and co-cultures within hyaluronic acid (HA) and agarose (ag) hydrogels and chondrogenic (Ch) and basal (Bas) media at Days 1, 7, 14 and 21 with/without 50% MSC with (A) chondron (CN) and (B) chondrocytes (CY). The scale bars represent 100 μm.

`

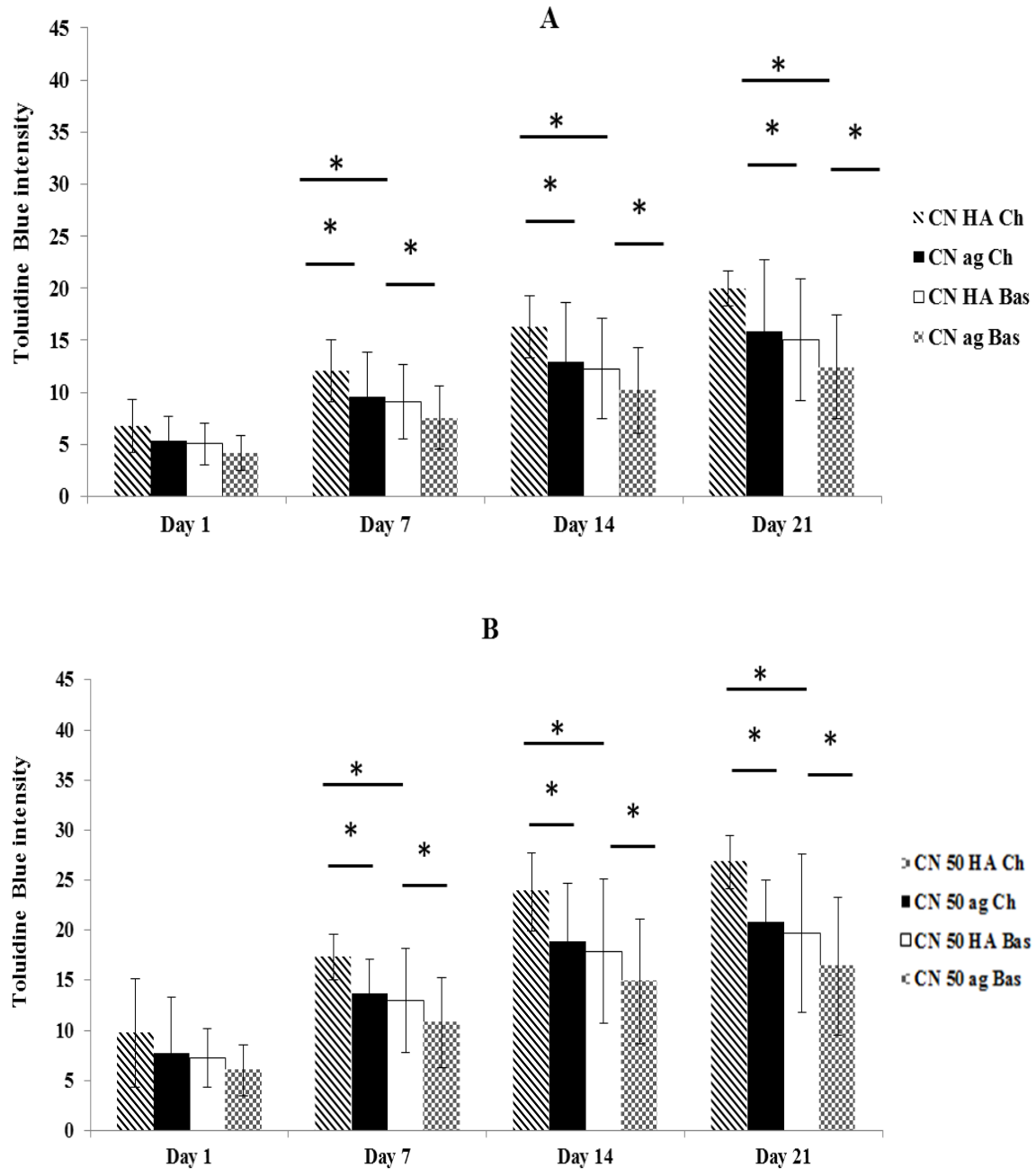

Figure 4.10: Representative semi-quantification of toluidine blue staining intensity in (A) chondron (CN) monoculture, (B) chondron co-culture within hyaluronic acid (HA) and agarose (ag) hydrogels and chondrogenic (Ch) and basal (Bas) media at Days 1, 7, 14 and 21. Data are expressed as mean ± SD (n =3). *$p < 0.05$

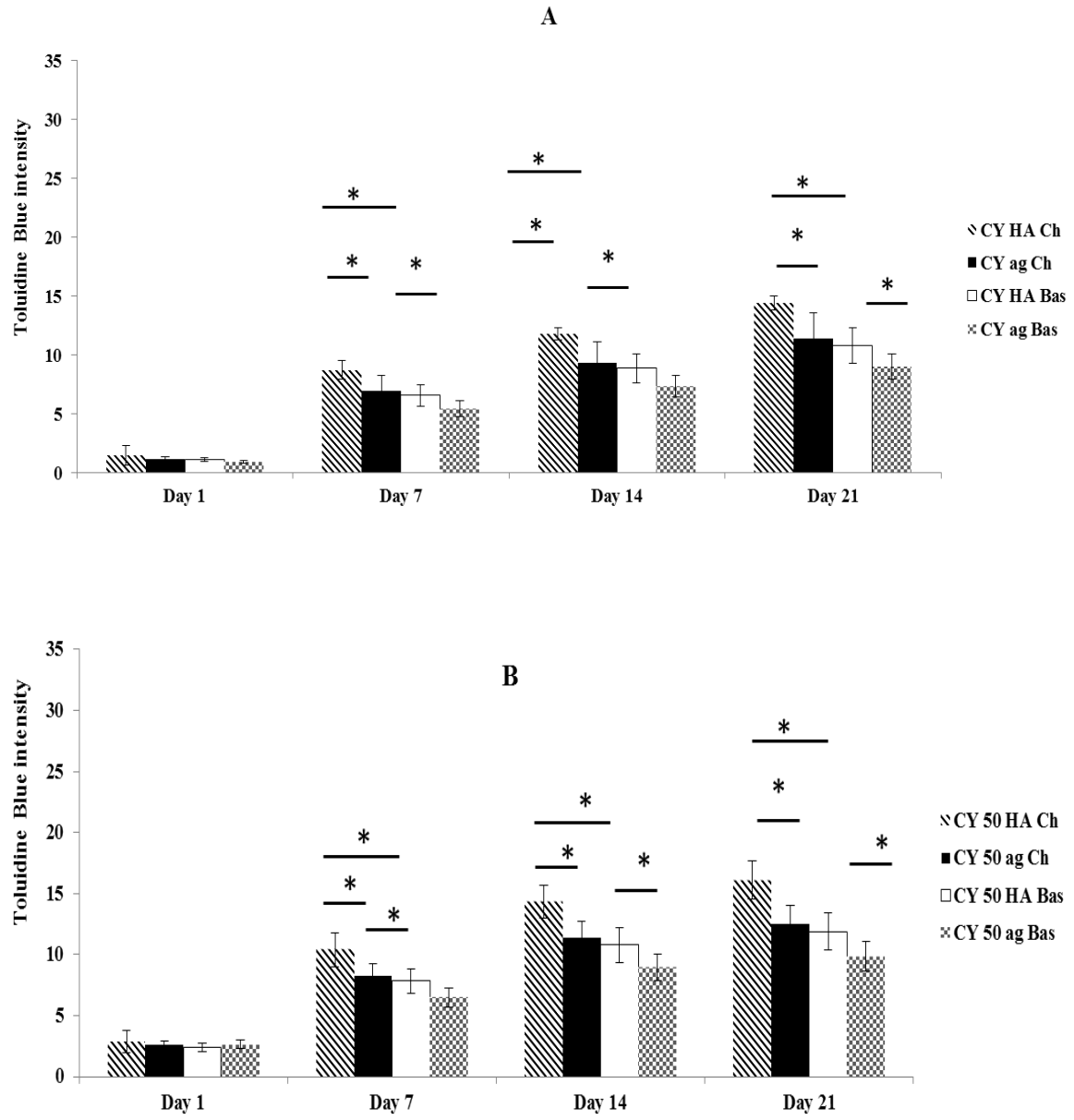

Figure 4.11: Representative semi-quantification of toluidine blue staining intensity in (A) chondrocytes (CY) monoculture, (B) chondrocytes (CY co-culture, within hyaluronic acid (HA) and agarose (ag) hydrogels and chondrogenic (Ch) and basal (Bas) media at Days 1, 7, 14 and 21. Data are expressed as mean ± SD (n =3). *$p < 0.05$

`

4.4.5 Expression of key PCM and ECM components

Immunofluorescence staining has been conducted to identify the essential PCM/ECM markers in the mono and co-cultures samples with different culture conditions at different time points using both chondron and chondrocytes.

Expression of collagen type VI and HtrA1

Figure 4.11 demonstrates collagen VI expression. It was clearly that collagen VI staining intensity and morphology were strongly dependent on the initial cartilage cells in the samples.

In chondron monocultures, collagen VI was presented and located around the cells from day 1 through whole culture period; but there was slight variation during the culture and reduction at the 21 day culture in agarose hydrogel. While for chondron co-culture with MSCs at day 7, 14 and day 21, there was no significant difference from the day 1 expression, also no difference with different culture conditions. The collagen VI staining was a dense, homogeneous and symmetric layer surrounding the cells in all chondron groups.

When using chondrocytes monoculture, there was no collagen VI detection at day 1 at all conditions, but detected collagen VI expression at day 7 under HA condition. It became apparent that cell surfaces were stained positively for collagen VI at day 14 under agarose hydrogel. Co-culture of MSC and chondrocytes increased overall collagen VI expression level; most importantly, the samples at all conditions expressed collagen VI from day 7 including under agarose gel condition. The expression of collagen VI increased in all conditions along culture time with HA condition showing the highest collagen VI. By the end of the culture period (3 weeks) the presence of a clear collagen VI stained region surrounding the chondrocytes with a little difference between mono and co-cultures and between HA and agarose hydrogels was obviously. However, the morphology of collagen VI staining layer in chondrocytes was quite different from that in chondron. Fragment and spotting appearance made distinction of the newly formed collagen VI from native

`

one. The semi-quantification of staining intensity correlated well with staining imaging of the collagen VI expression.

Figure 4.13 showed immunofluorescence staining of HtrA1. Generally, HtrA1 staining had a lower expression in co-culture than monoculture across chondrons and chondrocytes at different culture conditions. The HtrA1 staining was absent in co-culture of chondron and chondrocytes in different culture conditions at day 1 and day 7, but in monoculture there was visible HtrA1 staining at day 7. At day 14 co-culture, cells showed low and indistinct expression of HtrA1, but with considerable visible staining at monoculture. The immunofluorescence staining for HtrA1 at day 1 but present at day 7 and 21 with accumulated deposition with extended time in culture. Figure 4.14 presented the semi-quantification of HtrA1 staining, which corresponded with immunofluorescent staining for HtrA1.

`

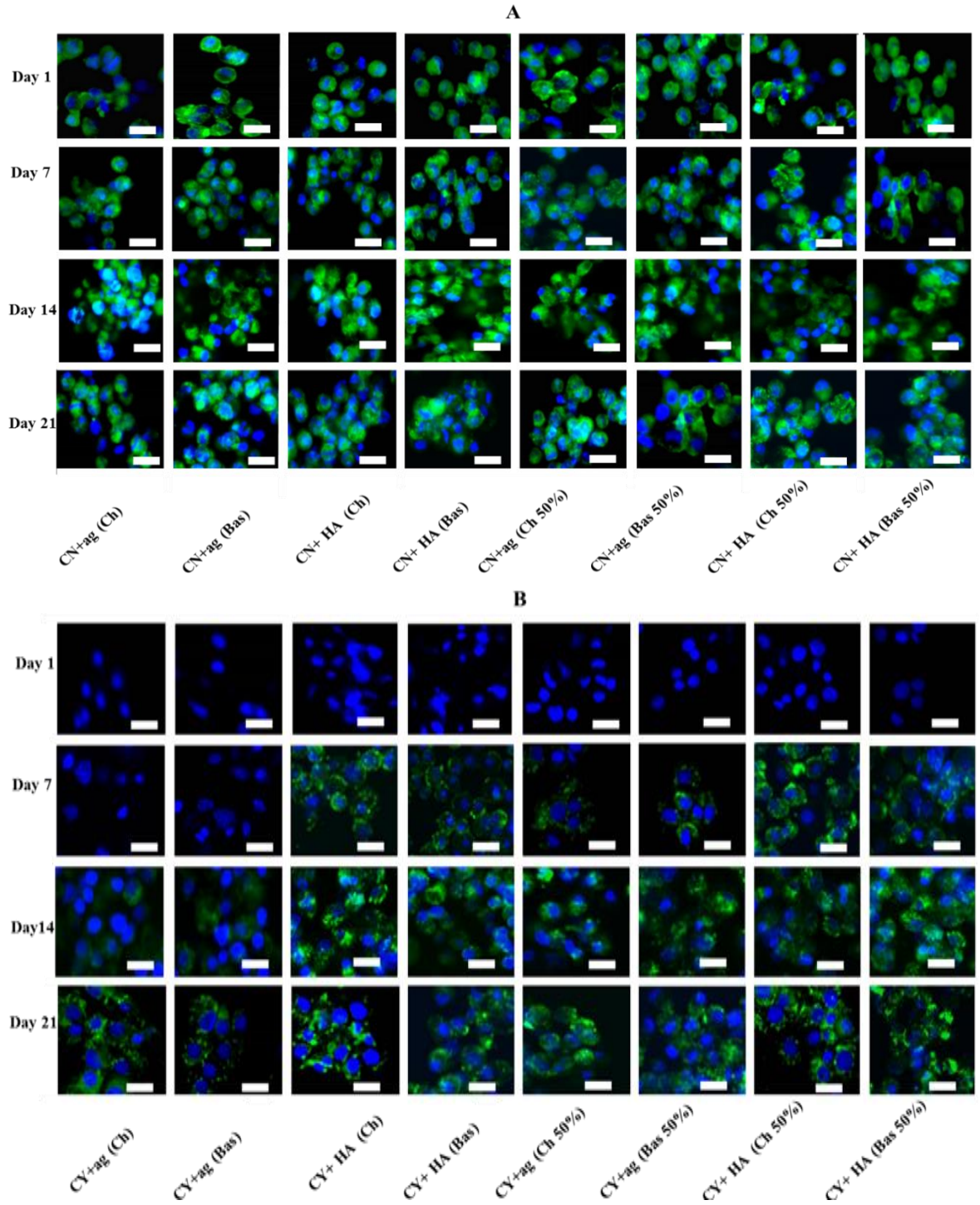

Figure 4.12: Representative collagen VI immunofluorescent stained in mono and co-cultures within hyaluronic acid (HA) and agarose (ag) hydrogels under chondrogenic (Ch) and basal (Bas) media at Days 1, 7, 14 and 21 with and without 50% MSC with (A) chondron (CN) and (B) chondrocytes (CY). The scale bars represent 20 μm.

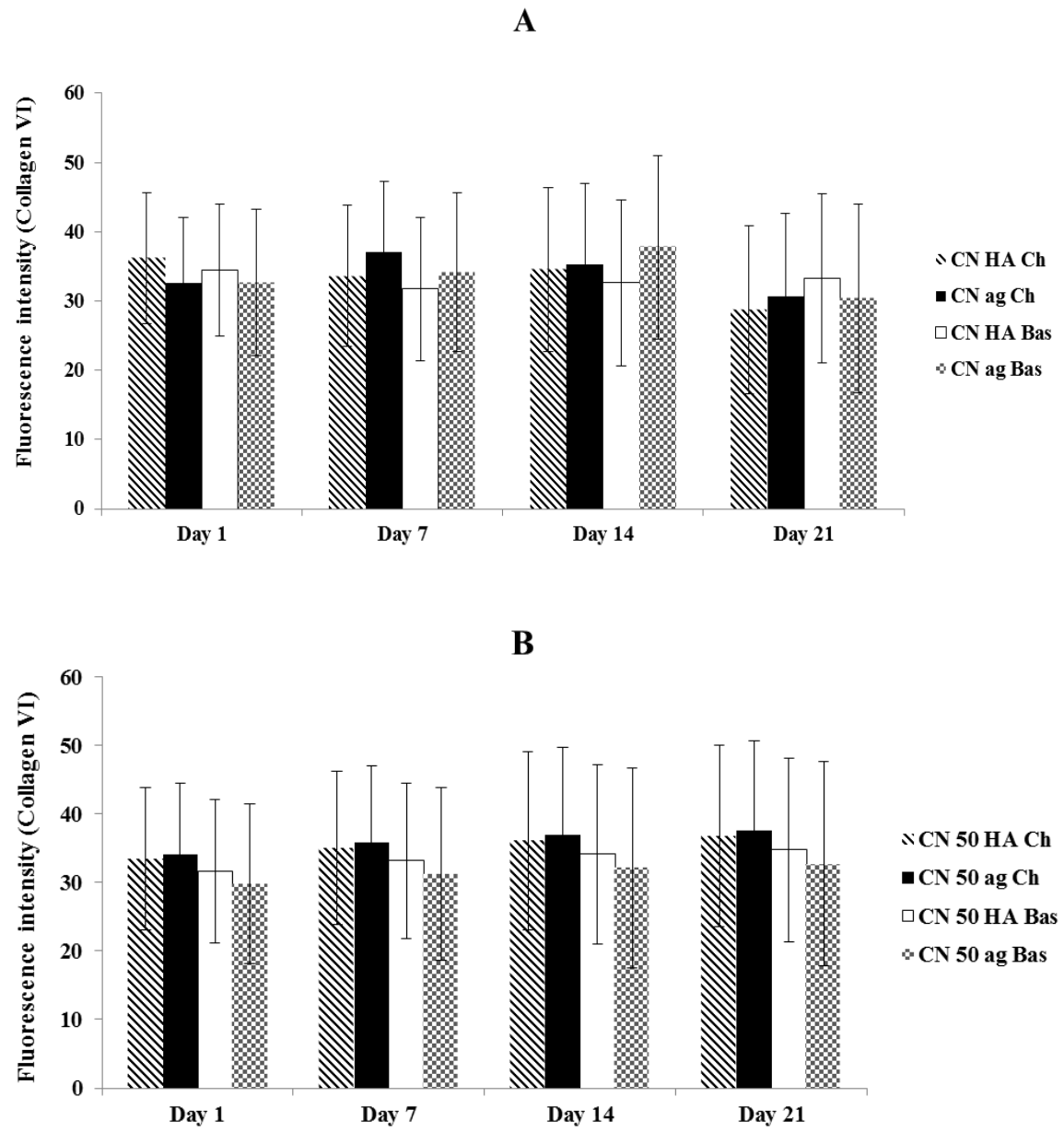

Figure 4.13: Representative semi-quantification of collagen VI immunofluorescent staining intensity in (A) chondron (CN) monoculture, (B) chondron co-culture within hyaluronic acid (HA) and agarose (ag) hydrogels and chondrogenic (Ch) and basal (Bas) media at Days 1, 7, 14 and 21. Data are expressed as mean ± SD (n =3). *$p < 0.05$

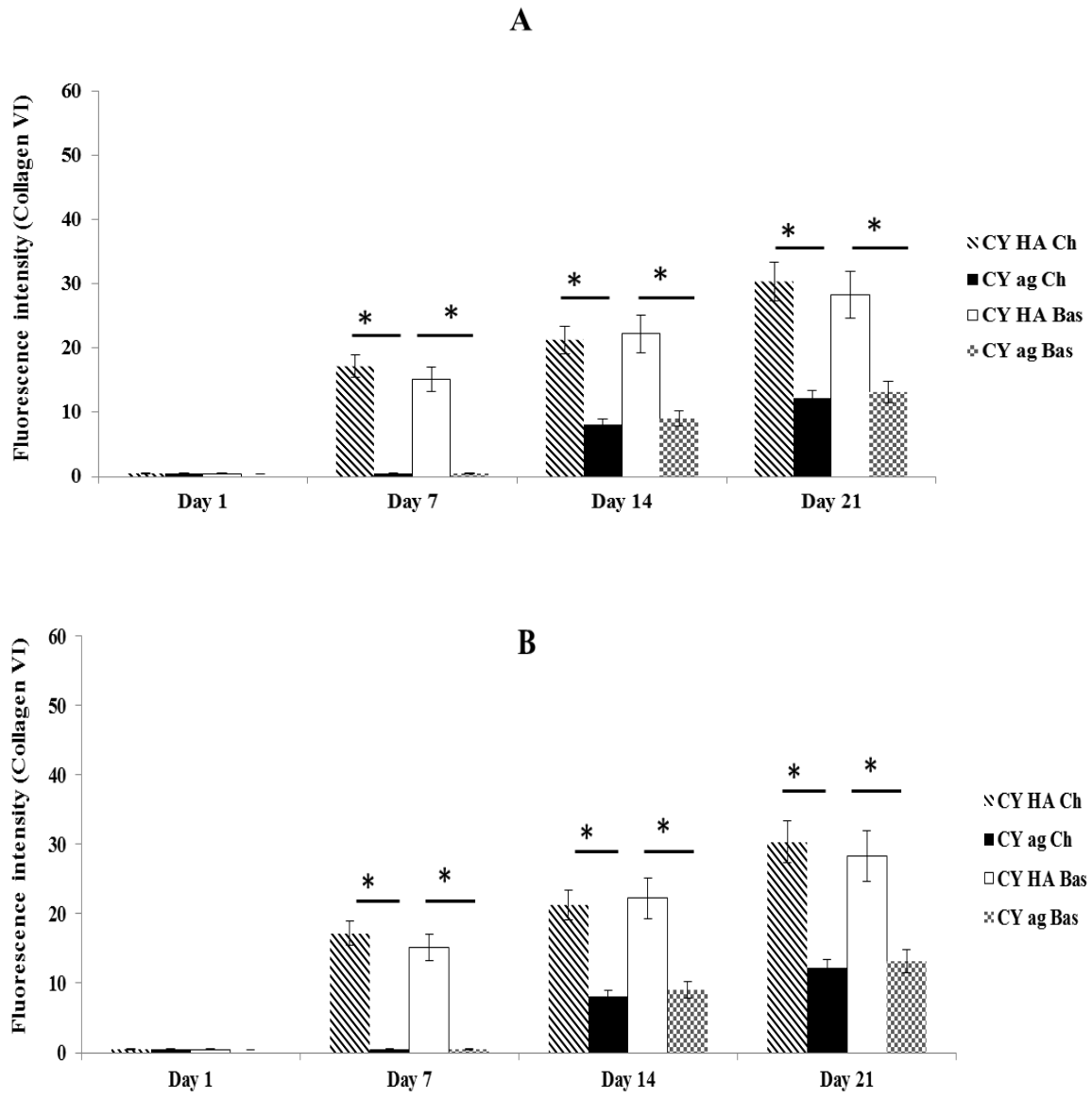

Figure 4.14:Representative semi-quantification of collagen VI immunofluorescent staining intensity in (A) chondrocytes (CY) monoculture, (B) chondrocytes co-culture within hyaluronic acid (HA) and agarose (ag) hydrogels and chondrogenic (Ch) and basal (Bas) media at Days 1, 7, 14 and 21. Data are expressed as mean ± SD (n =3). *$p < 0.05$

`

Expression of collagen type II

Both chondron and chondrocyte in mono and co-cultures showed fluorescent staining for collagen II (Figure 4.15) under all different culture conditions and the expression increased along the culture time points. There was different staining intensity of collagen II under HA hydrogel and agarose in mono and co-cultures but the difference was not significant. HA hydrogel generated higher collagen II than agarose samples. Furthermore, chondrogenic media demonstrated expression enhancement for collagen II with higher fluorescent staining than basal media. It was expected that the staining for collagen type II in 50% chondron: MSC co-cultures was more intense than in monocultures for both chondron and chondrocytes, with chondron co-culture expressing higher value. Semi-quantification of the collagen II staining intensity across the groups and culture time by ImageJ Analysis software was shown in Figure 4.16 with consistent conclusion as the staining images.

`

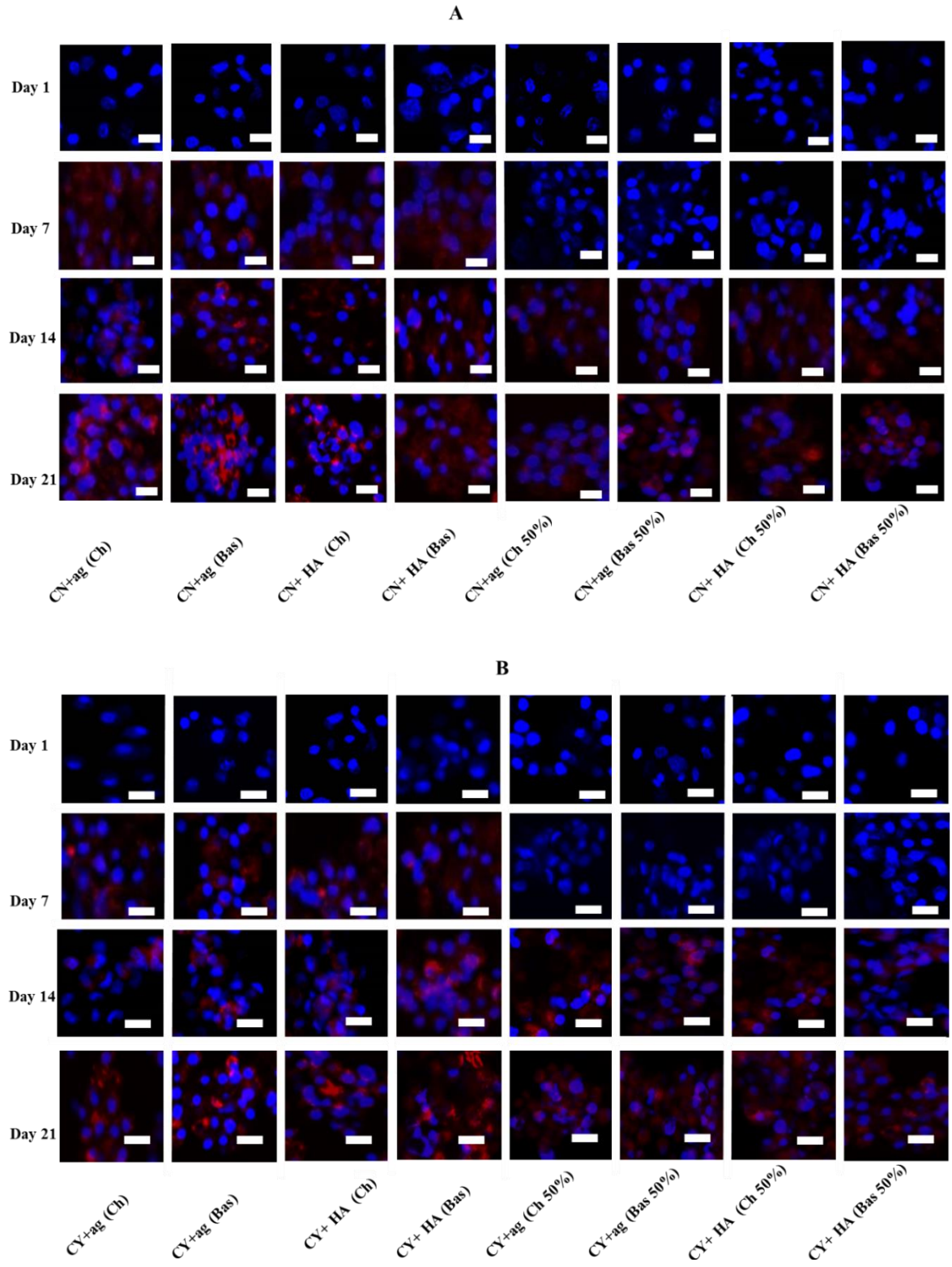

Figure 4.15: Representative HtrA1 immunofluorescent stained in mono and co-cultures within hyaluronic acid (HA) and agarose (ag) hydrogels and chondrogenic (Ch) and basal (Bas) mediums at Days 1, 7, 14 and 21 at (A) chondron (CN) and (B) chondrocytes (CY). The scale bars represent 20 μm.

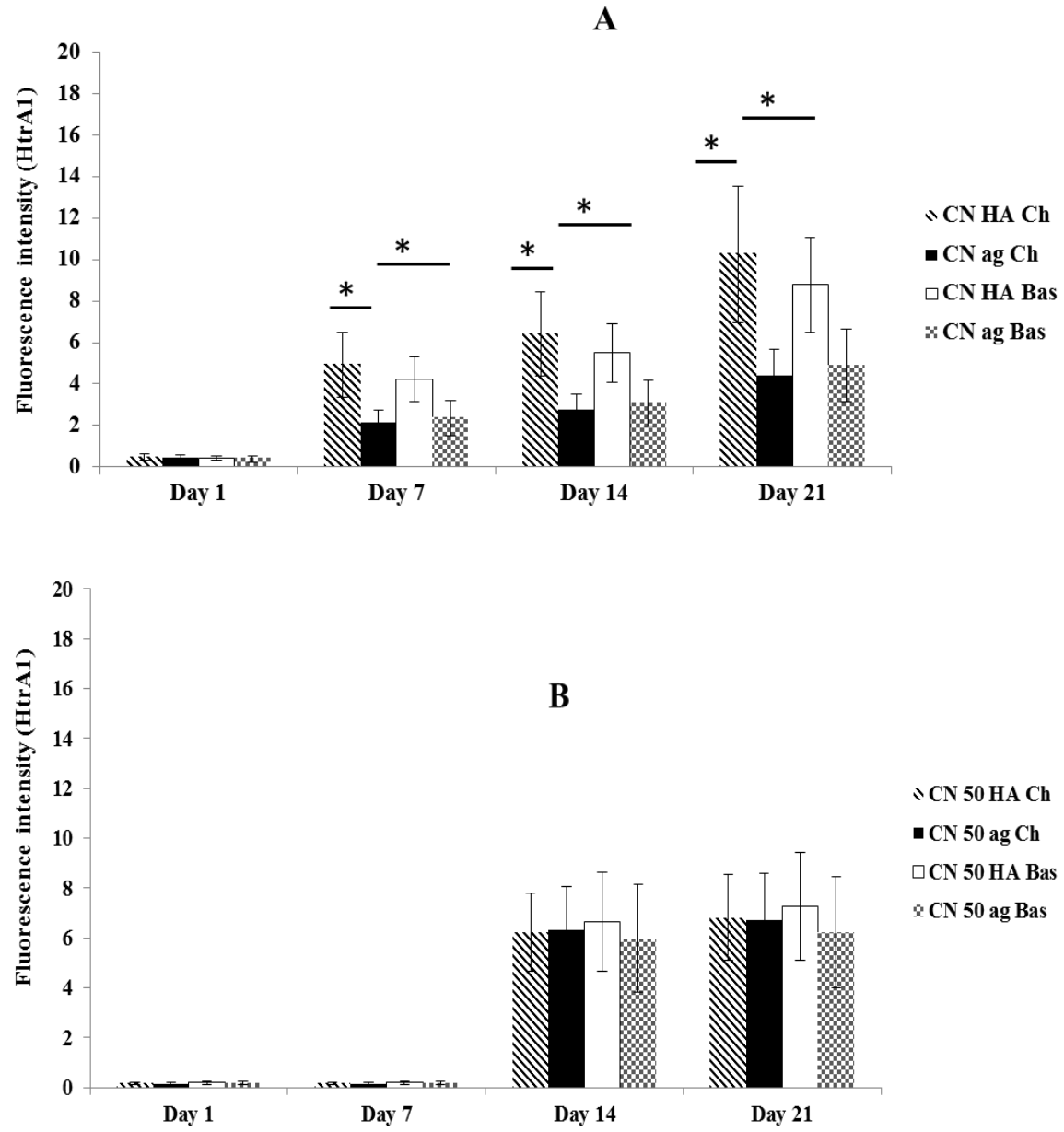

Figure 4.16: Representative semi-quantification of HtrA1 immunofluorescent staining intensity in (A) chondron (CN) monoculture, (B) chondron co- within hyaluronic acid (HA) and agarose (ag) hydrogels and chondrogenic (Ch) and basal (Bas) media at Days 1, 7, 14 and 21. Data are expressed as mean ± SD (n =3). *$p < 0.05$

`

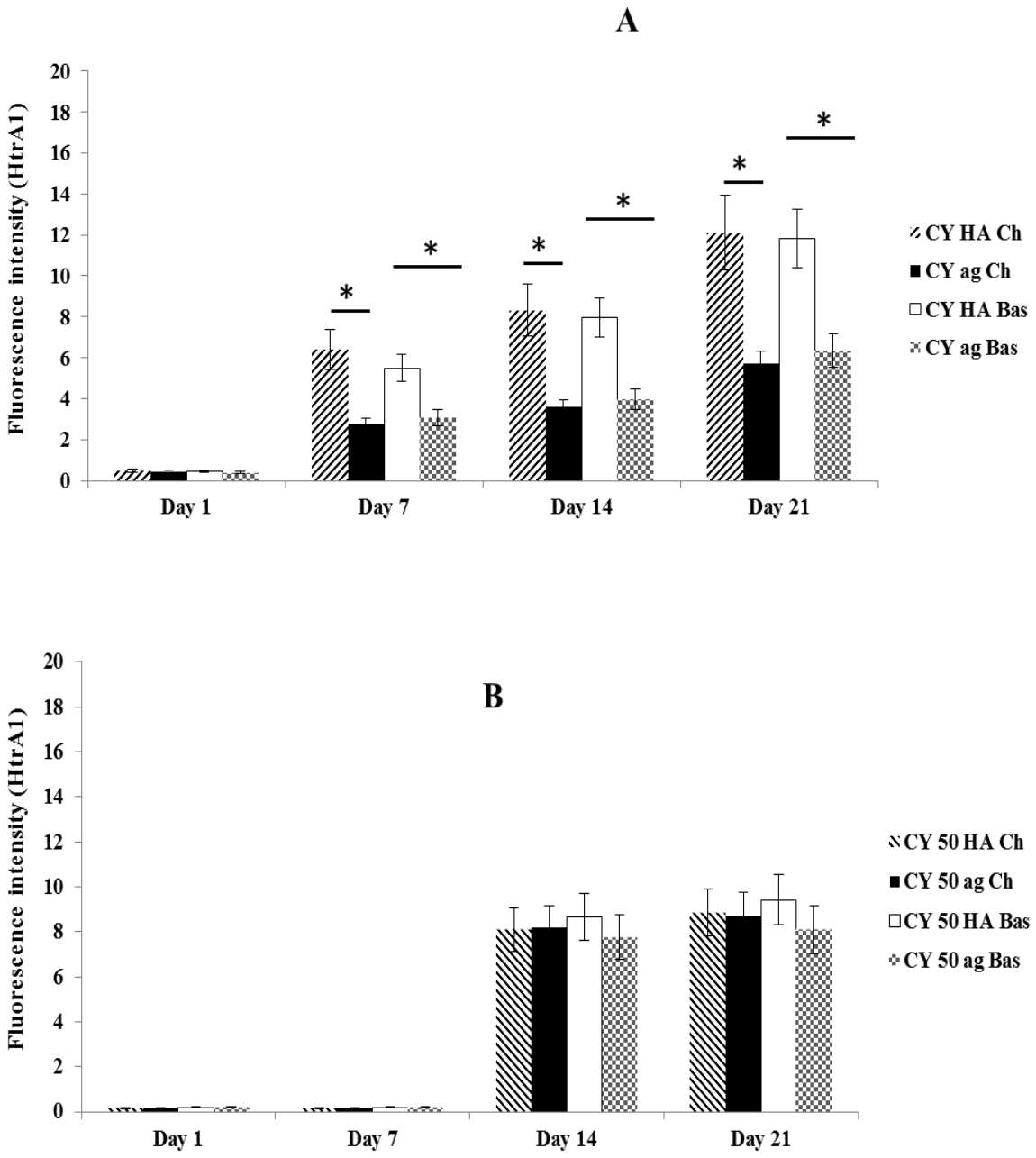

Figure 4.17: Representative semi-quantification of HtrA1 immunofluorescent staining intensity in (A) chondrocytes (CY) monoculture, (B) chondrocytes co-culture within hyaluronic acid (HA) and agarose (ag) hydrogels and chondrogenic (Ch) and basal (Bas) media at Days 1, 7, 14 and 21. Data are expressed as mean ± SD (n =3). *$p < 0.05$

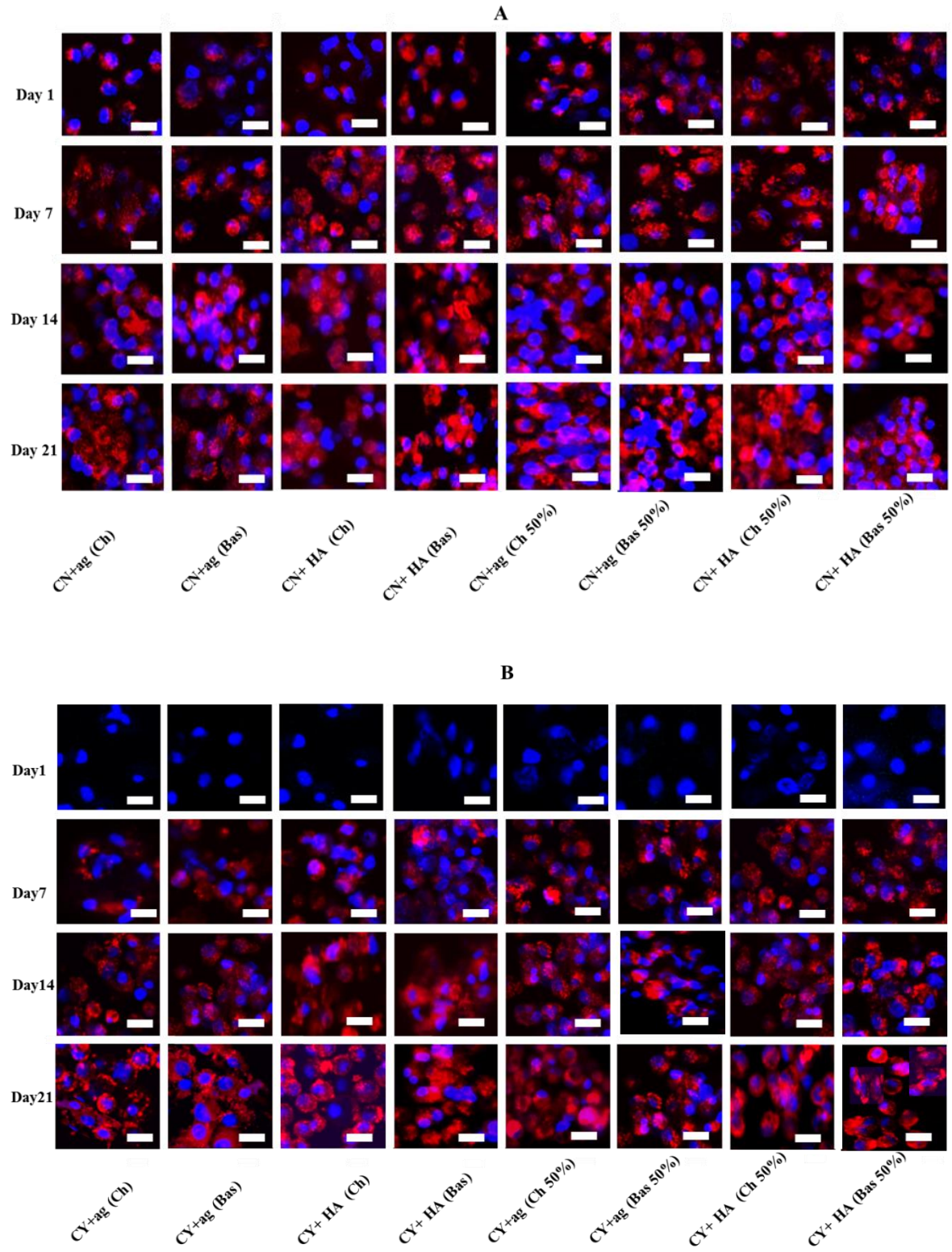

Figure 4.18: Representative collagen type II immunofluorescent stained in mono and co-cultures within hyaluronic acid (HA) and agarose (ag) hydrogels and chondrogenic (Ch) and basal (Bas) media at Days 1, 7, 14 and 21 with 50% MSCs with (A) chondron (CN) and (B) chondrocytes (CY). The scale bars represent 20 μm.

`

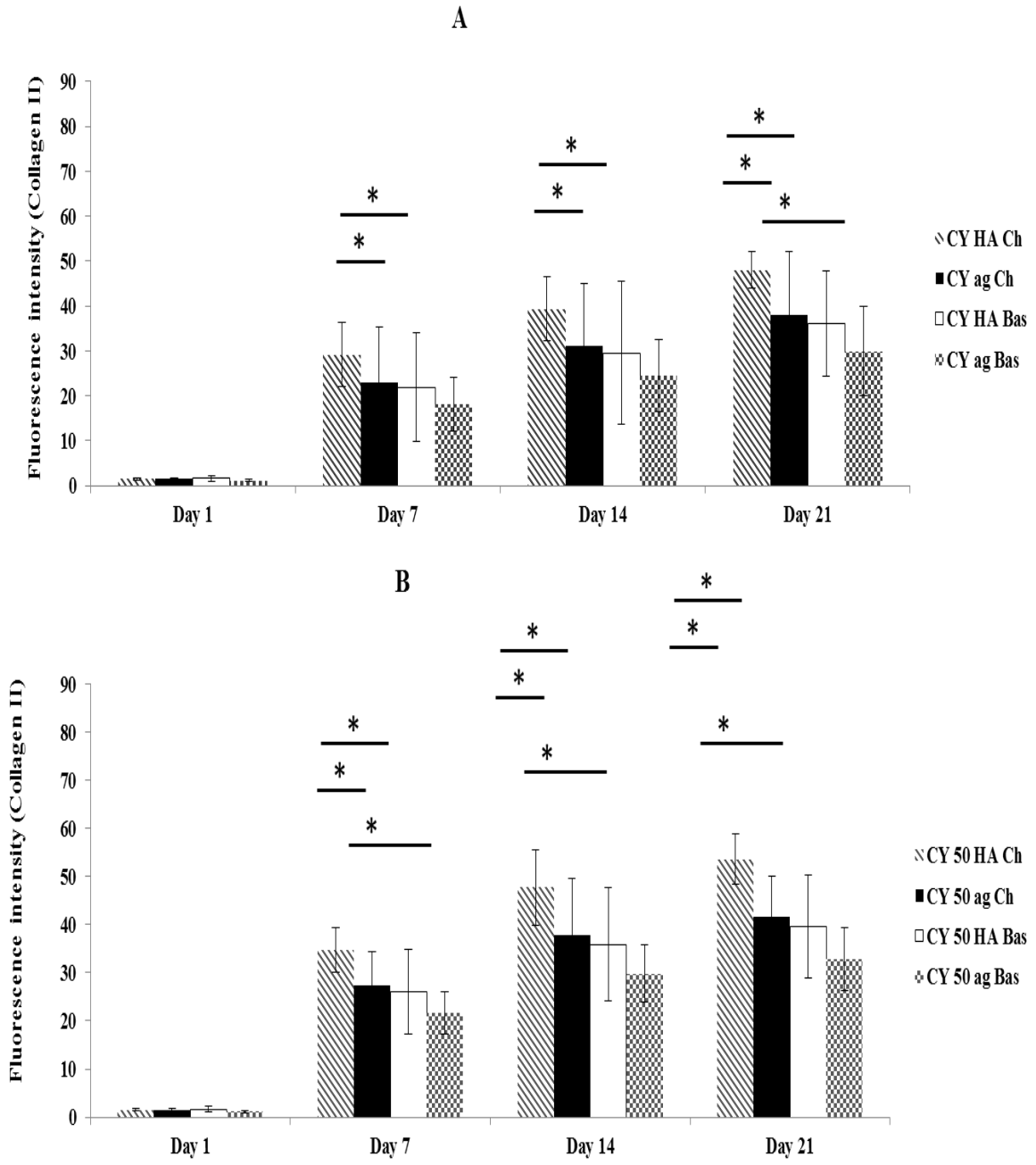

Figure 4.19 Representative semi-quantification of collagen VI immunofluorescent staining intensity in (A) chondron (CN) monoculture, (B) chondron co-culture within hyaluronic acid (HA) and agarose (ag) hydrogels and chondrogenic (Ch) and basal (Bas) media at Days 1, 7, 14 and 21. Data are expressed as mean ± SD (n =3). *$p < 0.05$

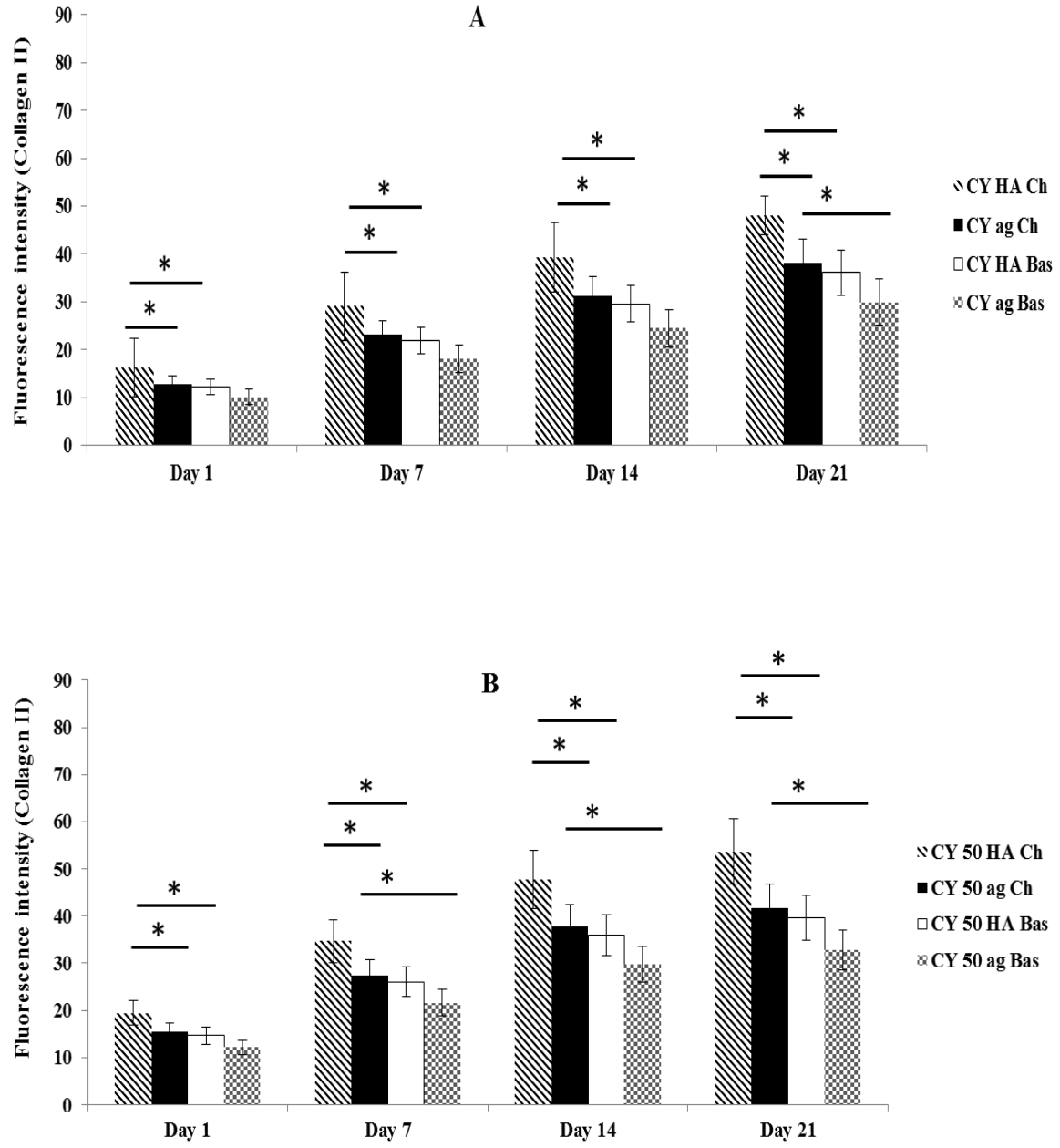

Figure 4.20: Representative semi-quantification of collagen II immunofluorescent staining intensity in (A) chondrocytes (CY) monoculture, (B) chondrocytes co-culture within hyaluronic acid (HA) and agarose (ag) hydrogels and chondrogenic (Ch) and basal (Bas) media at Days 1, 7, 14 and 21. Data are expressed as mean ± SD (n =3). *$p < 0.05$

`

4.4.6 FTIR Analysis of chondrocytes grown in HA hydrogel

As earlier stated, each biomolecule will produce its own spectral signature based on the nature of the bonds and their concentration in an individual spectrum. A typical spectrum of a biological sample is presented in Figure 4.17.

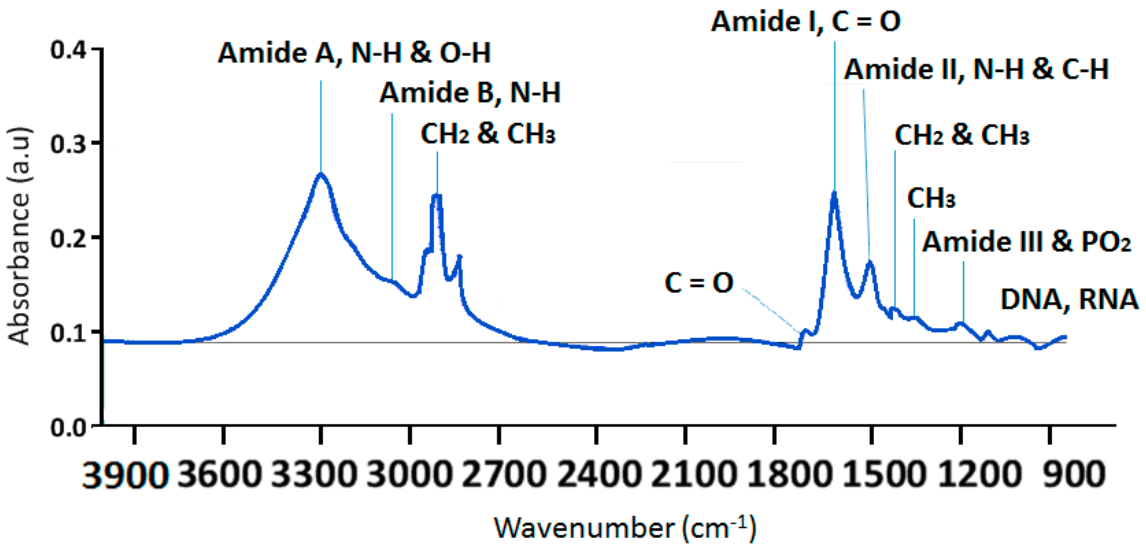

Figure 4.21: A typical FTIR spectrum of a cell showing the absorbance bands for phosphate, carbonate, and protein amide bonds. (Taken from De Ninno et al., 2010).

A FTIR spectrum analysis can be divided into two regions; fingerprint region which correlates explicitly with protein and proteoglycan content. Another region is lipid region which relates to cell number in general. Figure 4.18 showed the mean spectra of different experimental groups for fingerprint region (1000–1800cm^{-1}). Each the mean spectra were produced from at least 40 spectra, or 30 cells.

`

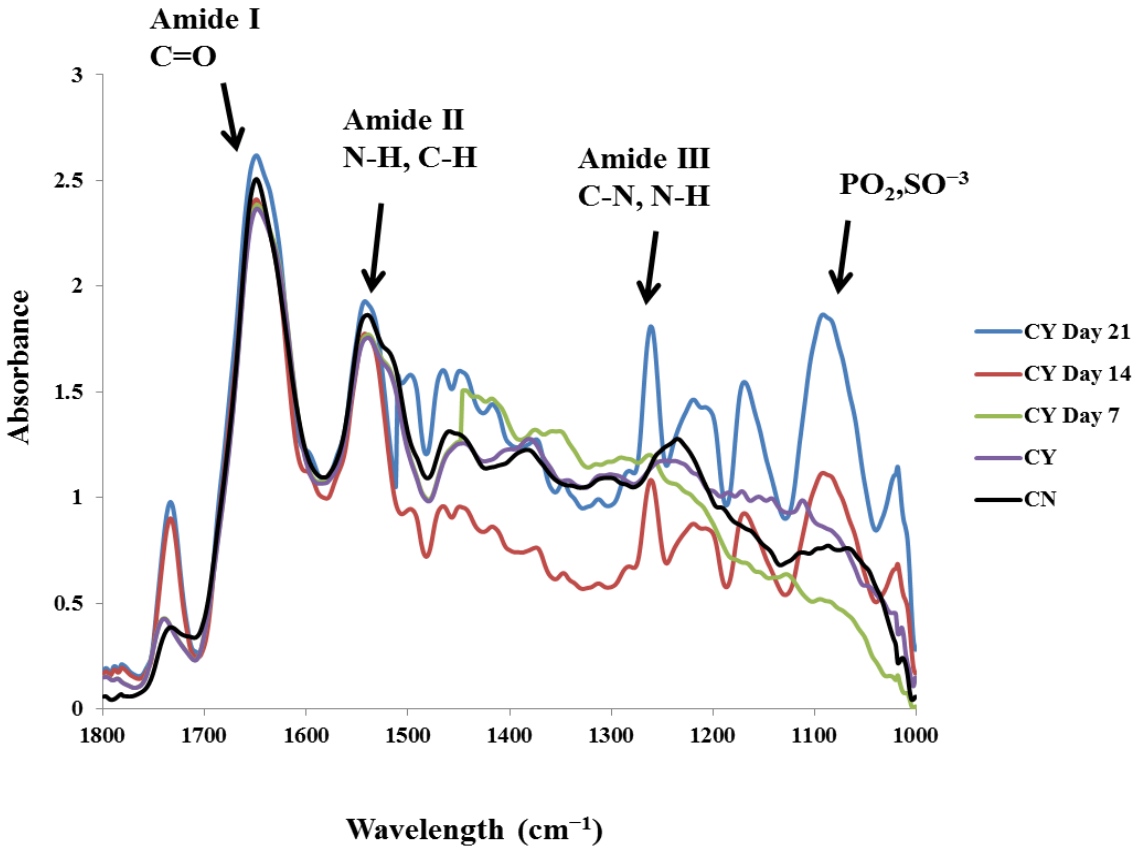

Figure 4.22: Mean spectra at fingerprint region for different experimental groups; controls: bovine chondron (CN), chondrocytes (CY); cultured chondrocytes in HA hydrogel at day 7, day 14, and day 21.

Clearly, the means plot displayed spectral variation between the culture samples and controls (native chondron and chondrocytes), also the chondrocytes culture duration (day 7, 14 and 21). To extract the main difference between groups and controls, the Unscrambler Software (Version X, Camo, Oslo, Norway) was used to analyse the acquired spectra by using PCA analysis. PCA and loading plots were used to visualise the differences between the spectra and where those differences are.

`

A

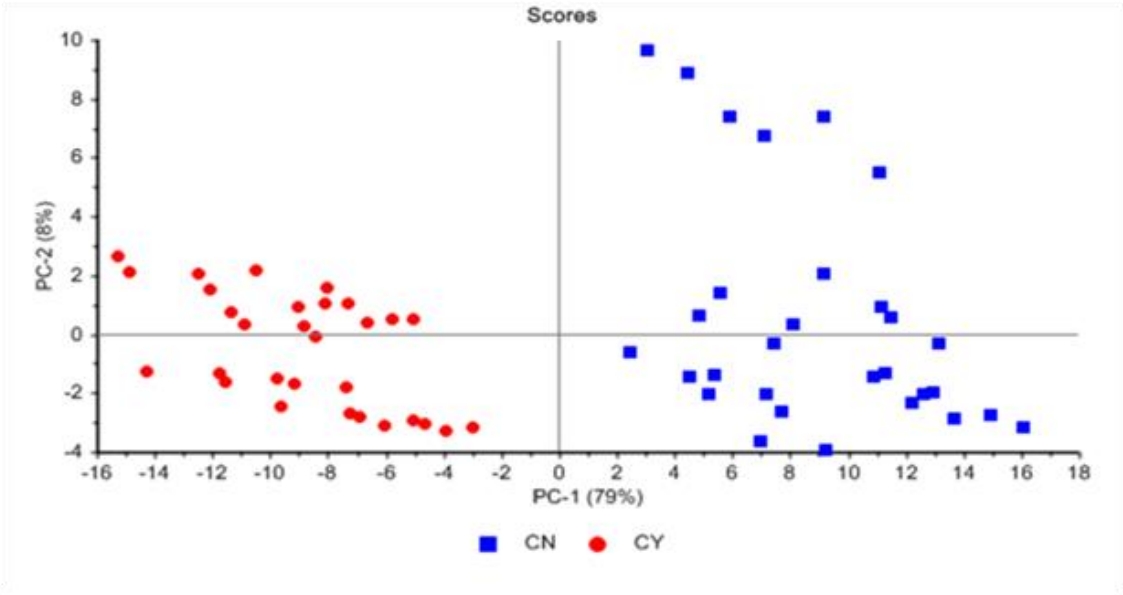

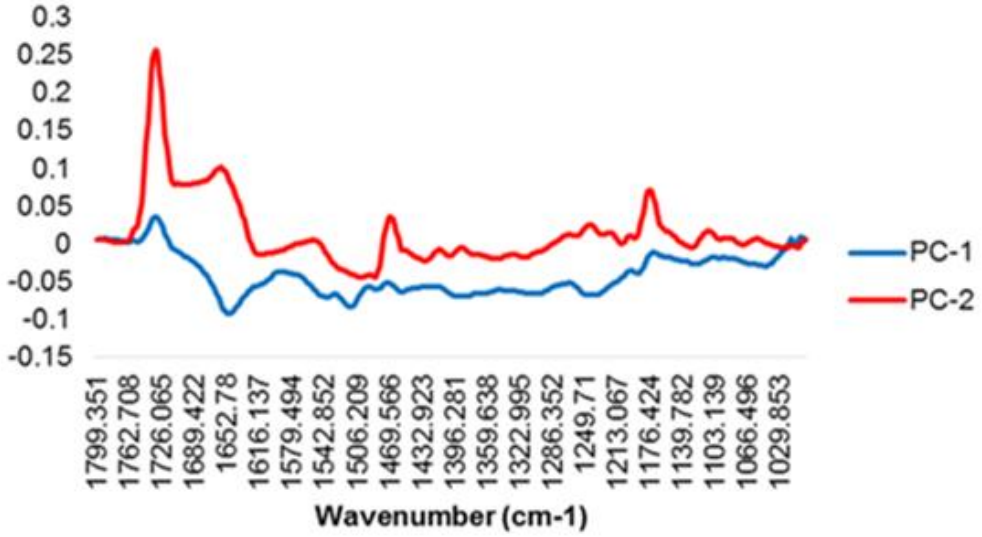

`

B

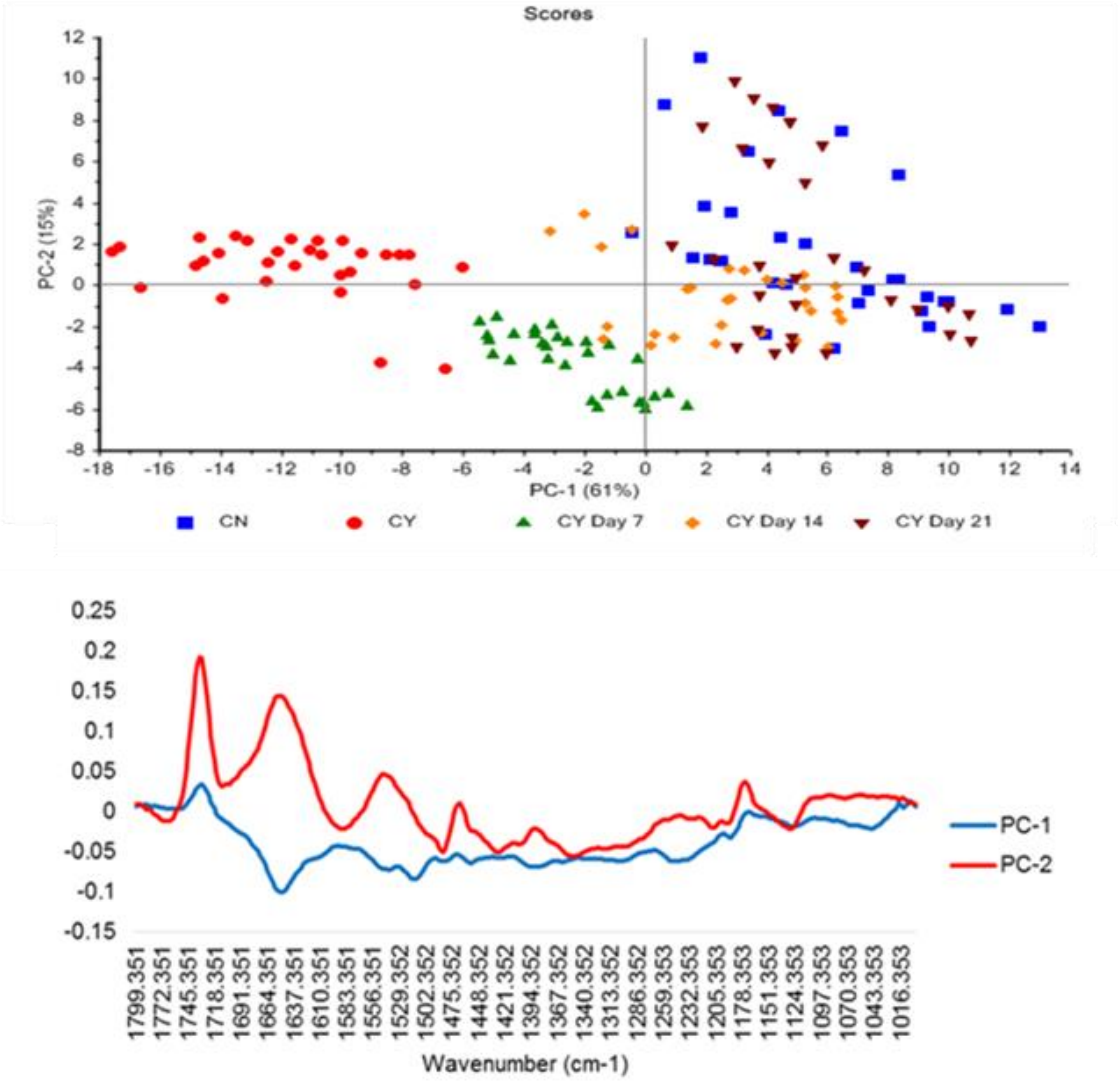

Figure 4.23: PCA scores and the loading lines at fingerprint region for different experimental groups; A) chondron (CN) vs chondrocytes (CY); B) chondron (CN) vs chondrocytes (CY) and chondrocytes (CY) with culture time points; day7, day14 and 21.

The PCA scores and loadings plot of spectra displayed a clear spectral clustering between CY and CN samples (Figure 4.19. A), also the chondrocyte constructs cultured at day 7, day 14 and day 21 samples (Figure 4.19. B).

Figure 4.19. B showed that CY and day 7 PCA scores had major separation from CN, day 14 and day 21 samples. In addition, there was no considerable separation between CN and day 21 samples.

`

Figure 4.20 shows the mean spectra for different experimental groups for lipid region (3100–2700cm^{-1}).

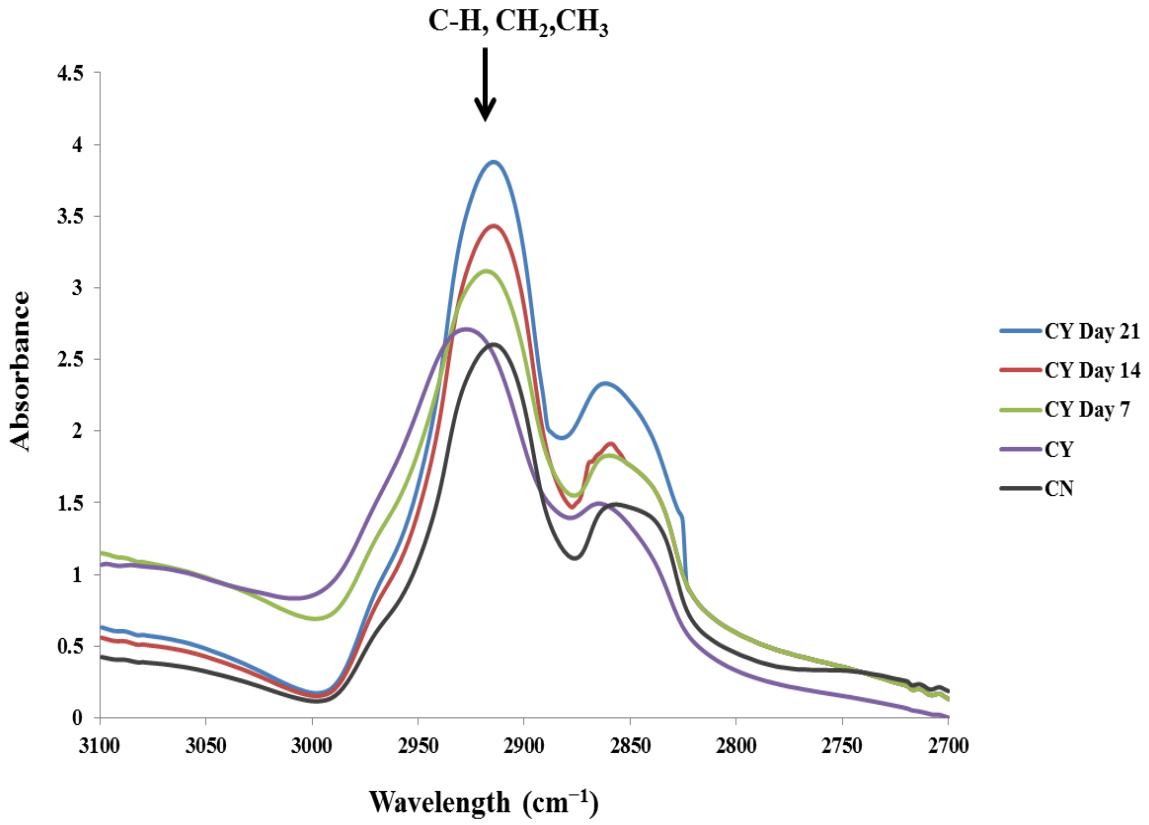

Figure 4.24: Mean spectra at lipid region for different experimental groups, chondrocytes cultured at day 7, day 14, and day 21.and control groups (bovine chondron (CN), chondrocytes (CY)).

`

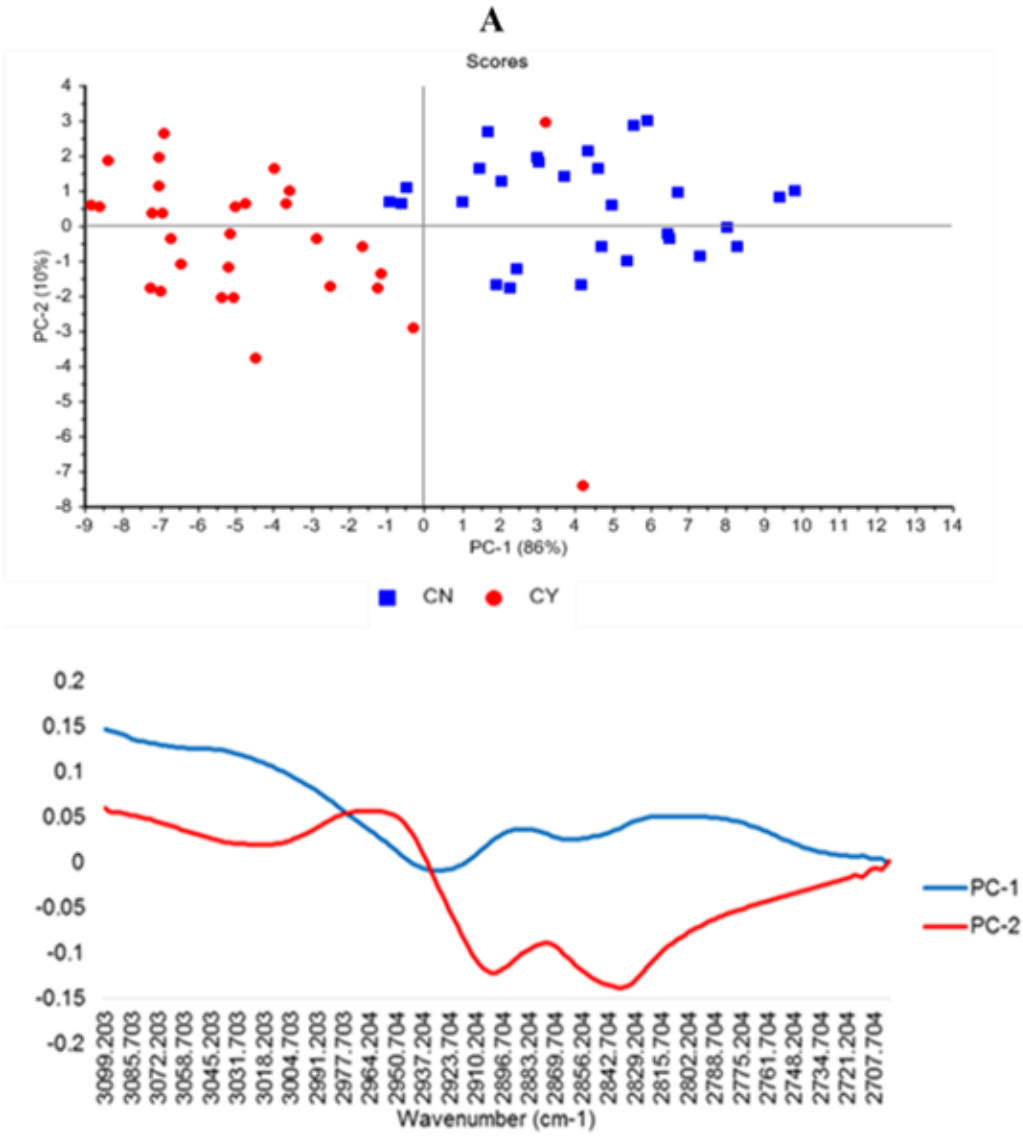
A
Scores
PC-2 (10%)
PC-1 (86%)
CN
CY
0.2
0.15
0.1
0.05
0
-0.05
-0.1
-0.15
-0.2
3099.203
3085.703
3072.203
3058.703
3045.203
3031.703
3018.203
3004.703
2991.203
2977.703
2964.204
2950.704
2937.204
2923.704
2910.204
2896.704
2883.204
2869.704
2856.204
2842.704
2829.204
2815.704
2802.204
2788.704
2775.204
2761.704
2748.204
2734.704
2721.204
2707.704
Wavenumber (cm-1)
PC-1
PC-2

`

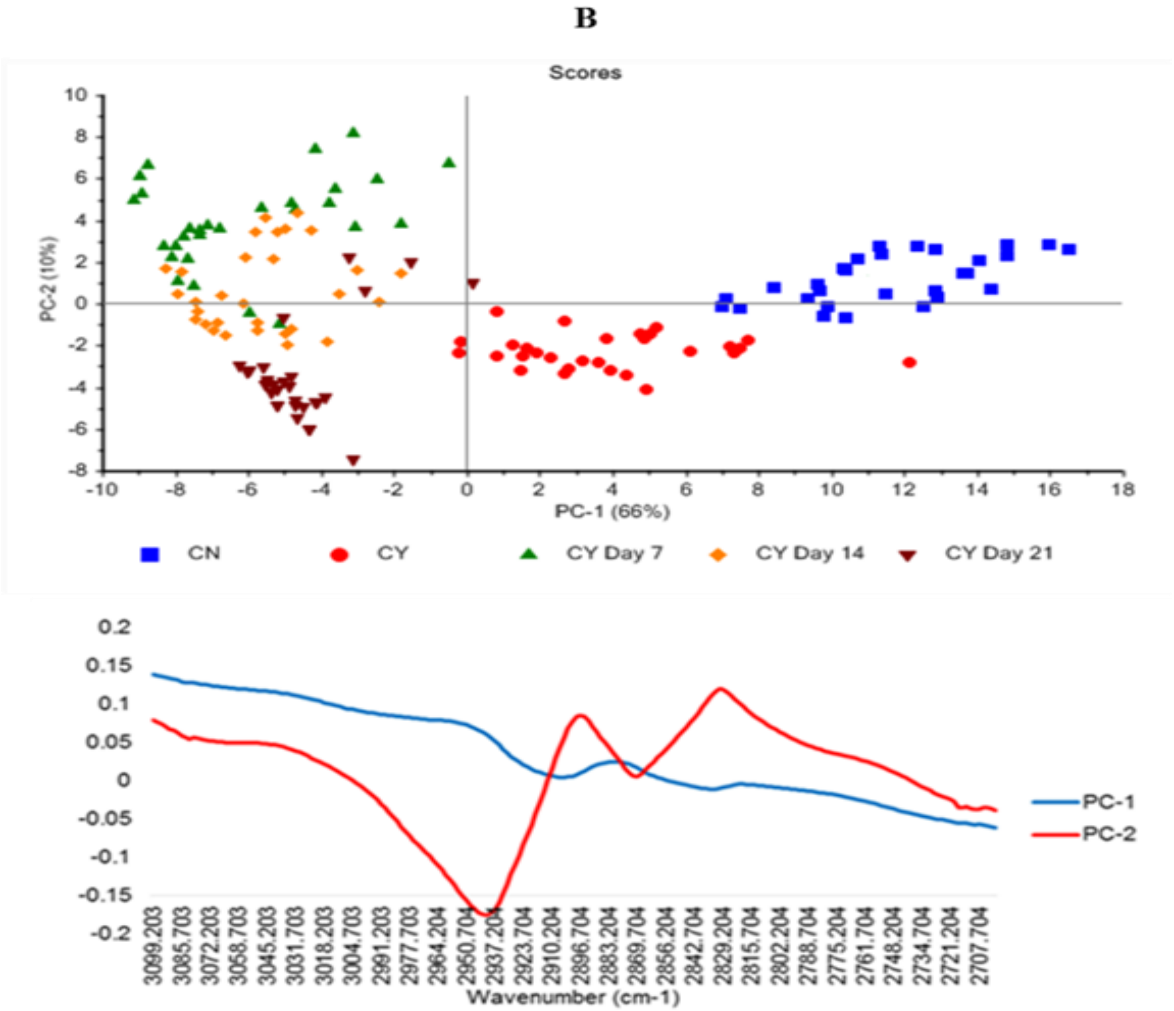

Figure 4.25: PCA scores and the loading lines at lipid region for different experimental groups; A) Chondrocytes (CY) vs chondron (CN); B) Chondron (CN) vs chondrocytes (CY) and chondrocytes (CY) with culture time points; day7, day14 and 21.

The PCA scores and loadings plot of spectra demonstrated certain overlapping between chondrocytes and chondron (Figure 4.21.A). Figure 4. 21. B revealed a distinct difference in PCA scores between controls (chondrocytes and chondron) from experimental samples of day 7, 14 and 21 cultures.

`

4.5 Discussion

This study demonstrated that 3D culture environment (HA and agarose hydrogels) can preserve the native PCM during culturing of chondrons, as well as regenerate PCM in chondrocytes within 3 weeks culture at different culture conditions; mono or co-culture with MSC, with different medium types, and hydrogel types. The newly formed PCM marked by collagen VI expression in chondrocytes which were cultured within the 3D environment have been detected in both co- and monocultures, under agarose and HA hydrogel with varied concentrations, and the variation was culture condition dependent. Basal and chondrogenic culture media influenced the expression of cartilage-specific ECM markers but did not affect collagen VI synthesis. In addition, it has been confirmed that the synchrotron microFTIR technique by analysis of spectra in both lipid and fingerprint regions can reveal indirectly the PCM formation and cellular evolution of cultured chondrocytes in 3D hydrogel environment non-destructively.

Chondron has a higher chondrogenic potential than chondrocytes

The retention of the native PCM has been reported to affect the metabolic activity of the chondrocytes (Vonk et al., 2010). A key marker of the PCM microenvironment is collagen VI (Poole et al., 1987), which is known to interact with various matrix macromolecules such as collagen II and decorin (Bidanset et al., 1992), proteoglycan and hyaluronan (Kielty et al., 1992). In addition, collagen VI has been shown in previous studies to interact with the integrin receptors of chondrocytes (Salter et al., 1992; Loeser, 2014). This implies that collagen VI plays a dual role, one of which is creating macromolecular interactions to ensure the structural and functional integrity of the chondron, the other is to mediate cell surface anchorage and signalling potential between the chondrocyte and its pericellular microenvironment. In this light, it would be logical to use collagen type VI as a key detection indicator for the structural and functional integrity and maturation of matrix in tissue engineered cartilage.

`

This study has been shown that the culturing chondrons formed a more cartilage-like ECM (collagen II and GAG) and led to better hyaline cartilage production on a 3D hydrogel microenvironment than the chondrocytes along all culture conditions. This strongly suggests that the PCM is an effective source of chondrogenesis. The preserved PCM indicating by strong collagen VI staining in all chondron included groups explained the higher ECM productions in the groups. Although we use different species, the trend in results concur with Vonk et al. (2010) study in which goat's chondrons and chondrocytes were cultured for 25 days in alginate beads, and it has been demonstrated that maintaining the native chondrocyte's PCM enhanced the cartilage markers (collagen type II and GAG) production.

HA has a better chondrogenic potential than agarose

Cell-matrix interaction plays an important role in the proliferation, differentiation and survival of chondrocytes (Svoboda, 1998). In this study, a round cell shape and cluster of cartilage cells was found in HA and agarose hydrogels culture with the increase of cluster size with culture time. Overall in this study, both hydrogels culture (HA and agarose) supported the deposition of cartilage-specific matrix markers including GAGs, collagen II and the unique marker of PCM collagen VI, which promoted rebuilding cartilaginous–like ECM, but HA hydrogel culture had higher chondrogenic potency than agarose hydrogel culture in all culture conditions in terms of more accumulated GAG and collagen II production (13% and 10 % more in GAG and collagen II respectively for chondrocytes samples at day 21(Figure 4.6 and Figure 20)).

The chemical and physical environments of ECM in native cartilage can be better mimicked by using highly hydrated hydrogels. Thus, hydrated hydrogels serve as an ideal cellular microenvironment for maintaining chondrogenic phenotype and cell proliferation (Aleksander-Konert et al., 2016; Eslahi et al., 2016). A specific subset of known integrins is produced by each cell type, which controls the interactions between the cells and their microenvironment (Hynes, 1992). Agarose hydrogel has no cell adhesion motifs to support direct cell anchorage as it prevents

`

the absorption of adhesive proteins from the environment (Steward et al., 2011). Thus, agarose can maintain the round shape of chondrocytes if it is used to encapsulate chondrocytes (Kuhtreiber et al., 1999). HA found natively in cartilage tissue, has been studied for decades (Yoo et al., 2005). Chondrocytes in native articular cartilage tissue demonstrated round shape morphology and clustered in small groups (Hunziker et al., 2002). HA is known to interact with chondrocytes via various surface receptors including CD44. This surface receptor bound to HA and triggers chondrocytes to retain their original morphology and phenotype, an area that is still not fully understood (Yoo et al., 2005).

MSCs promoted chondrogenesis

Herein, co-culture MSCs with both chondron and chondrocytes had a higher GAG and collagen II production in comparison with their monoculture in 3D hydrogel conditions. There were potentially two impact pathways through which the presence of MSCs in co-culture enhanced the formation of the PCM and ECM.

This chondrogenic enhancment is considered to be the result of signaling via direct cell–cell contacts, as well as secreted factors generated by MSCs and chondrocytes. Chondrocyte-secreted factors such as TGF-β1 and BMP-2 may promote chondrogenesis of MSCs *in vitro* (Bian et al., 2012; Wu et al., 2013). Another study demonstrated that articular chondrocytes secreted parathyroid hormone-related protein which can inhibit hypertrophy of chondrocytes or MSCs during chondrogenesis (Fischer et al., 2010). Other studies have hypothesised that MSCs secreted TGF-β1 and BMP-2 growth factors regularly from cultured MSC. The increased cartilage matrix formation and proliferation rate was explained due to stimulation of the chondrocytes by MSCs (Tsuchiya et al., 2004; Lettry et al., 2010; Levorson et al., 2014). There is a gap in the understanding of PCM degradation in co-culture. As a secreted member of the trypsin family of serine proteases, HtrA1 has the capability to degrade the PCM (Polur et al., 2010). It has been reported that chondrocytes, expressing HtrA1 in mouse OA joints, do not produce collagen VI,

`

which implies the disruption of the PCM (Hou et al., 2013). Whereas, in a mouse OA joint collagen VI was detected in the PCM while HtrA1 expression was absent (Polur et al., 2010). Uniquely, we speculate that MSCs directly or indirectly suppressed the production of HtrA1, or generated inhibitors for HtrA1 in co-culture, which led to the preservation and promotion of PCM integrity. In chapter 3, it was revealed clearly that the monolayer co-culture of chondrons and MSCs reduced the HtrA1 production. This pathway hypothesis was confirmed with the 3D culture by the immunostaining results. Figure 4.12 and 4.13 showed that there was an inverse relationship between HtrA1 and collagen VI expression in both chondron and chondrocyte mono and co-culture with MSCs. Overall, the presence of 50% MSCs enhanced cartilage cells' chondrogenic capacity.

Different effect of culture medium types on chondrogenesis

In order to enhance the chondrogenic capacity, the catabolic and anabolic processes of chondrocytes are known to be influenced by a defined medium of several growth factors which stimulate ECM production and promote the chondrogenesis of MSCs (Mackay et al., 1998; Fortier et al., 2011). There is no report, till date, whether the PCM integrity and production are affected by different culture medium, especially about the synthesis of collagen VI.

In this study, chondrogenic media showed enhancement in cartilage-specific matrix markers, i.e. GAGs and collagen II production using both hydrogels types and in both mono and co-cultures in comparison to basal media (11.5% and 14 % more in GAG and collagen II for chondrocytes samples at day 21 respectively (Figure 4.6 and Figure 20)), but both of mediums types had no influence in collagen VI syntheses. We speculated that chondrogenic media used in this study only supplemented with specific growth factors influencing on GAG and collagen II production but containing less specific stimulators on collagen VI synthesis.

The effect of culture time on PCM formation and maintenance

`

In contrast to 2D culture in chapter 3, mono and co-culture of chondrons in all 3D conditions in this chapter maintained PCM manifesting as the clear collagen VI staining from day 1 up to 21 days culture duration. Co-culture with MSCs did not only stabilise PCM expression but also increased its production as the increase of culture time (Figure 4.11).

Dramatic observation was the newly formed PCM in the culture of isolated bovine chondrocytes in mono and co-culture constructs. The new PCM exhibited a various deposition across the time course. The culture in HA hydrogel displayed the presence of collagen VI after 7 days in both mono and co-cultures with speckled stripe structures surrounding the chondrocytes, whilst agarose culture required 2 weeks to restore the PCM. With the co-culture of MSCs, thin layer of collagen VI appeared in agarose culture after 7 days. In all culture conditions, collagen VI expression increased with culture duration. By 14 day culture, all condition culture has detected collagen VI staining. However, chondron demonstrated dense and homogenous collagen VI staining, whilst chondrocytes staining showed a spotting and thin deposit of collagen VI staining along the culture duration. This study clearly showed that PCM regeneration was time-dependent and the newly formed PCM had different quality to native counterpart (Figure 4.12). Further investigation on the difference is required.

The current study outcomes are consistent with previous study. It has been reported collagen VI regeneration is a slow process, requiring time to accumulate collagen VI (Dimicco et al., 2007). Chang and Poole (1997) observed a narrow ring of collagen VI around the cells after 7 days when chondrocytes were cultured in agarose hydrogel, and an 11 week period was needed to remodel into a mature and native-like PCM. To confirm VI collagen present in chondron, Vonk et al compared chondron with chondrocytes culture. They found that in the chondrons, the type VI collagen was traced around the cells along culture duration. Some type VI collagens were found around the chondrocytes after 25 days of culture in alginate beads, but chondrocytes had a smaller amount of type VI collagen than that found around the chondrons (Vonk et al., 2010).

`

Synchrotron microFTIR as a new tool for observation of PCM and cellular evolution

Synchrotron microFTIR is a non-destructive analytic tool with less sample preparation request. It can provide spatial distribution of proteins, proteoglycan and lipids, and associated concentration within a single measurement. The PCA was performed as an unsupervised analysis that reduces large numbers of variables (microFTIR spectral vectors) into a few principle components (PC) (that are calculated from the covariance of the data set being analysed). Thus, it will be able to identify where there are differences in the data sets. Loading plots indicate how much a variable contributes to each PC. Hence PCA analysis can demonstrate where there are high levels of variance with a spectrum.

Synchrotron microFTIR offers spatial distribution mapping and chemical structure detection at the micron scale, when integrating chemical analysis specificity with microbeam precision. FTIR offers non-destructive identification tool with less sample preparation and provides integral information for the spatial distribution of proteins presence, proteoglycan contents and concentration and lipids.

However, there was no study to assess the evolution process of PCM formation in tissue engineered cartilage constructs by FTIR. There was no synchrotron microFTIR study to map spatial distribution of chemical compositions of newly generated PCM in a tissue engineering cartilage model.

Originally, the spectra were collected in peripheral and nucleus regions and aimed to distinguish them by the presence of PCM. Unfortunately, the used aperture was too large and we could not get the separated spectra well. However, when we mixed all peripheral and nucleus region spectra for each groups and analysed their similarity to control chondrons and chondrocytes groups.Originally, the spectra were collected in peripheral and nucleus regions and aimed to distinguish them by the presence of PCM. Unfortunately, the used aperture was too large and we could not get the

`

separated spectra well. However, when we mixed all peripheral and nucleus region spectra for each groups and analysed their similarity to control chondrons and chondrocytes groups.

There was the clear spectral difference between chondrocytes and chondron samples, also day 7, day 14 and day 21 samples. PCA scores for fingerprint region showed that chondrocytes and day 7 had major separation from chondron, day 14 and day 21 samples. However, there was no significant separation between chondron and day 21 samples (Figure 4.23). PCA score in lipid region showed no considerable difference between chondrocytes and chondron samples, but with the significant difference from samples of day 7, day 14 and day 21 (Figure 4.25).

As captured in the fingerprint region, the loadings showed similar spectra for PC1 and PC2, with the main differences occurring around 1550 cm^{-1} which implied that there were changes within amide II stretch, C-N stretch and N-H bend which correlated with collagen concentration (Camacho et al., 2001; Barth, 2009). The difference around ~ 1240 – 1310 cm^{-1} implied that there were changes within amide III band components of proteins C-N stretch, N-H bend, C-C stretch and SO^{-3} asymmetric stretching vibration of sulphated GAGs (Bychkov and Kuzmina, 1992; Camacho et al., 2001; Barth, 2009). The lipid region loadings displayed a difference at 3000 cm^{-1} which was indicative of CH_2 and CH_3 stretching and also at ~ 2950 and 2850 cm^{-1} which also indicated a change in the symmetrical C-H stretch of CH_2 within lipid membranes (Barth, 2009).

According to PCA scores, the cluster of day 14 and day 21 constructs with chondron indirectly demonstrated that chondrocytes cultured under the current conditions might generate chondron-like cell phenotype. The presence of PCM on day 14 and day 21, which contained collagen type VI and proteoglycan, could explain their similarity of spectra to chondron, not chondrocytes. These speculations were further supported by the PCA analysis in lipid region. The separation of chondron, chondrocytes, day 7, day 14 and day 21 were not strong as in fingerprint region because the change of the lipid region reflected cell number in general. These data shed light to reveal the

`

cellular evolution of cultured chondrocyte in tissue-engineered cartilage model by synchrotron microFTIR technique.

4.6 Conclusion

This work showed that 3D culture systems can maintain the chondrogenic phenotype and manifesting as identification of collagen VI in the culture which is the unique marker for PCM. In the HA cultures, PCM was observed after 7 days in both mono and co-cultures with speckled stripe structures surrounding the chondrocytes surface. The cultures required 2 weeks to restore the PCM. For agarose cultures, small scattered stippled layer around the chondrocyte of PCM appeared after 7 days in co- cultures and after 14 days in monocultures. PCM was restored after 3 weeks. In addition, the presence of MSC directly or indirectly suppresses the production of HtrA1, or generates inhibitors for HtrA1 in co-culture, which led to the preservation and promotion of PCM integrity.

It is revealed that the chondrogenic culture media enhanced the expression of cartilage-specific ECM markers in comparing with basal media but both of them had no preferred effect on PCM marker ‘collagen VI’ synthesis.

Synchrotron microFTIR technique can be used as a non-destructively technique to observe the PCM formation and cellular evolution of cultured chondrocytes in tissue-engineered cartilage model by analysis of spectral changes in both lipid and fingerprint regions.

`

Chapter 5 : Constructing and testing of hybrid zonal-specific scaffolds for better cartilage regeneration

`

5.1 Introduction

The nature zonal organisation in articular cartilage

Articular cartilage is anisotropic in nature and organised into distinct zones; there are at least three architectural zones (superficial, middle and deep) with striking variations between their structure, chondrocyte phenotype, ECM composition and mechanical properties (Aydelotte et al., 1988; Hunziker et al., 2002). In the superficial zone, chondrocytes are elongated as a result of the tightly packed collagen fibres which have a parallel orientation to the surface to dissipate high tensile strength; also the concentration of proteoglycans is low than that in middle and deep zones (Camarero-Espinosa et al., 2016). The middle zone contains rounded chondrocytes with a random collagen fibres orientation, and this zone has a large amount of proteoglycans. In this zone, the collagen fibres are randomly oriented to provide resistance to the multidirectional compressive force (Stockwell, 1979; Hunziker et al., 2002). The deep zone contains chondrocytes stacked in columns with radial collagen architecture and high proteoglycan concentration. This radial orientation provides cartilage with a high compressive stress resistance (Camarero-Espinosa et al., 2016).

Current techniques to mimic zonal organisation in cartilage tissue engineering

It is essential to produce articular cartilage with full functional capacity for patients with large cartilage defects. Replication of the zonal organisation of tissue-engineered cartilage is one of the multiple strategies to generate functional cartilage. Up till now, there are a small number of studies which sought out for zonal cartilage tissue engineering (Klein et al., 2003; Waldman et al., 2003; Ng et al., 2005; Malda et al., 2010; Steele et al., 2014). Approaches to mimic the zonal structure and function include cell-based, scaffold-based, a combination of cells and scaffold (Klein et al., 2009). Cell-based methods have typically replicated the native distribution of chondrocyte populations by the isolation of zonal chondrocytes and cultured in micro mass pellet or in a cell

`

culture insert (Klein et al., 2003; Waldman et al., 2003). In these studies, the chondrocytes have been employed in specific regions of a construct, and they have been shown to retain their zone-specific phenotype and secrete specific zonal ECM components such as aggrecan, collagen II and collagen X (Waldman et al., 2003; Malda et al., 2010). Other study has used multi-layered hydrogels to support cartilage production within different zonal sub-populations. Ng et al., (2005) took zonal populations of chondrocytes and seeded them into layers of 2% and 3% agarose. Steele et al., (2014) created a multi-zone cartilage construct by using electrospun polycaprolactone nanofibers. Analysis of the multi-zone scaffolds demonstrated region-specific variations in chondrocyte number, ECM composition, and chondrogenic gene expression.

Potential biomaterials to create new 3D zonal scaffolds

Electrospun nanofibres have been extensively studied and shown to have a great potential in tissue engineering (Kumbar et al., 2008). The fabrication of polymeric nanofibers by electrospinning has been used to mimic nanofibrous collagen matrices, which are found in articular cartilage ECM (Wise et al., 2014). Electrospun polylactic acid (PLA) nanofibres have been used widely for medical devices and in the field of musculoskeletal tissue engineering (Woodruff and Hutmacher, 2010) since PLA is an FDA-approved polymer. Hyaluronic acid (HA) is a major component of synovial fluid and cartilage, and has a high capacity to maintain chondrocyte phenotype (Collins and Birkinshaw, 2013), and it has promising biocompatibility, biodegradability, and non-immunogenicity (Yoo et al., 2005). Combination of electrospun nanofiber and HA as zonal scaffolds has not been tried previously.

5.2 Objectives

The aim of the study in this chapter is to design hybrid zonal-specific 3D scaffolds which can induce the formation of biomimetic zonal organisation and composition of ECM as in native articular cartilage tissue. Initially, the influence of individual scaffolds on both chondrocyte

`

morphology and ECM production in different zones is investigated. Aligned and randomly arranged nanofibers in combination with HA hydrogel are used to create the superficial and middle zones scaffolds, respectively. The HA hydrogel including defined micro-channels is used to mimic the characteristics of the native deep zone. All three zone constructs are combined into a single construct to assess the cell distribution and integrity of a full 3D zonal construct with a biomimetic zonal organisation.

5.3 Methods and materials

5.3.1 Cell isolation and expansions

Bovine chondrocytes were used with passages 1 (P1) to simulate the clinical application. The cell isolation and culture details have been included in Chapter 2, Section 1.1.

5.3.2 Fabrication of PLA nanofibers

PLA nanofibers were generated by electrospinning technique using 2% PLA solution. The fabrication protocols with set up details are described in Chapter 2, Section 3.

5.3.3 Fabrication of hydrogel scaffolds

Crosslinked HA hydrogel was used to generate deep zone or the base for individual zone. The reconstructed HA gel was used to stabilize nanofiber meshes in individual zones or assembled samples following the protocols described in Chapter 2, Section 2.2.

5.3.4 Fabrication and assembling of zonal constructs

5.3.4.1 Fabrication and assembling of individual zone constructs

Each individual zonal construct was produced using different combination of materials, where each was equipped with a different microstructure. In the fabrication of the superficial and middle zone constructs, an aligned and a randomly aligned PLA nanofiber meshes were placed respectively on a 1 cm^2 slice of crosslinked HA gel. The chondrocytes ($1x10^5$ per sample) were seeded onto the

`

hybrid scaffolds. 100 μl of the reconstituted HA gel and 2% (w/v) agarose hydrogel mixture in a ratio of 9:1 was applied to the scaffold surface to stabilize the cell and nanofiber position after 2 hours cell seeding. The deep zone construct was formed by crosslinking HA hydrogel (1 cm^2 X 0.6 mm) with micro-channels. Ten microscale channels/sample were made using micro needle (ϕ 400 μm) pass through HA hydrogel. Chondrocytes (10^4 cell/channel) were seeded into the channels of the scaffolds. The chondrocytes ($1x10^5$ per sample) seeding in the reconstituted HA gel without nanofiber and channels were fabricated as the negative control following above procedure. The samples were cultured in DMEM supplemented with 10% FCS and 1% L-glutamine and 1% penicillin-streptomycin at 37˚C in 5% CO_2 for 14 days.

5.3.4.2 Fabrication and assembling of the multiple zone construct

The layer-by-layer assembly method was used to form zonal construct (Yang et al., 2011). The hydrogel with micro-channels was placed on PTFE plate and was seeded with cells at cell density of 1 x 10^4/ channel. The samples were incubated for 2 hours at 37˚C, 5% CO_2 to allow the cells attachment. PLA random nanofiber meshes were placed on top of the hydrogel and 1 x $10^5/cm^2$ chondrocytes were seeded on nanofiber meshes. The cells were allowed to attach at 37^{o}C for 2 hours. 100 μl of the reconstructed HA hydrogel and 2% (w/v) agarose hydrogel mixture in a ratio of 9:1 were then loaded on top of the construct. The aligned nanofiber meshes were placed on top of the hydrogel. After that, the chondrocytes were seeded on nanofiber meshes at a cell density of 1 x $10^5/cm^2$. The cells were left for 2 hours in the incubator to allow for attachment. The formed 3D constructed samples were sealed by the reconstructed HA hydrogel, and thereafter incubated with supplemented DMEM mentioned previously and cultured for 14 days at 37˚C and 5% CO_2.

5.3.5 Characteraization of scaffolds

Nanofiber scaffolds were imaged using SEM. Fibre diameters were determined using ImageJ through the SEM images by the protocol described in Chapter 2, Section 13.

`

OCT was used to measure the micro-channel morphology and the dimension of assembled 3D hybrid zonal scaffold. The OCT utilizes the wavelength centred at 1300 nm, providing approximately 1 mm image penetration. 3D zonal hybrid scaffold was placed inside a covered round small Petri dish. 2-D images were taken to record the morphological properties of 3D zonal hybrid scaffold.

The mechanical properties of individual and assembled zonal scaffolds and the bovine cartilage tissue (positive control) and the HA gel alone construct (negative control) were measured in uniaxial compression testing using BOSE machine. The protocols with set up details can be found in Chapter 2, Section 15. Mechanical strength through ball indentation test was performed for the optimization of ratio of hydrogel mixture. The mixture gel in several ratios of agarose and HA were made (0:10; 0.5:9.5; 1:9; 2:8). The protocols with set up details are described in Chapter 2, Section 15.

5.3.6 Cell morphology monitoring

The morphology of chondrocytes on each 3D zonal scaffold at different time points was imaged with an optical microscope attached to a CCD camera. Image-Pro Insight software was used to acquire the images.

5.3.7 Cell viability

In order to assess cell survival in hydrogel capsules, a standard live/dead cell staining kit was used following the protocol described in Chapter 2, Section 5.2.

5.3.8 Biochemical assays

Papain solution was used to digest the experimental samples at the end of the culture periods as described in Chapter 2, Section 2.4 for PicoGreen DNA assay and DMMB assay in Chapter 2,

`

Section 2.5.1 Section 6 respectively. The normalised value of total GAG content per cell was calculated based on GAG content and cell number in each sample.

5.3.9 Immunolocalisation of key chondrogenic components

Immunostaining was used to identify the specific ECM markers, collagen II and aggrecan, within each zone constructs and collagen I was also carried out to further confirm the phenotype of cells. 3D visualisation of samples was achieved by scanning sections from bottom to top through a confocal microscopy. The z-stack of confocal microscope images with 20-μm intervals between each plane of the specimens throughout the thickness of 3D zonal scaffolds was reconstructed using Imaris 8.1 analysis software; which provided a tool to visualise the zonal structure in 3D constructs. Immunostaining was conducted using the protocol described in Chapter 2, Section 10. Intact samples were stained using this same protocol.

5.3.10 Western blotting

Western blotting was used to identify the production of specific ECM markers, collagen II, collagen I and aggrecan in the construct samples. The protein bands were shown with PVD membrane. Semi-quantitative measurement for proteins expressions using western blot was determined using ImageJ software. Western blotting was carried out according the protocol described in Chapter 2, Section 12.

5.4 Results

5.4.1 Optimization of mixture gel ratio

The pulverised crosslinked HA gel had poor mechanical property. It could not form stable and portable hydrogel as scaffolds. Hence small percentage of agarose was mixed with HA gel to reconstruct mechanical strong and stable hydrogel. To identify the lowest agarose percentage in the hydrogel mixture, hydrogels with different ratios of HA and agarose were prepared, and the mechanical strength was assessed by ball indentation test.

`

Figure 5.1 showed the ball indentation setting up to test different composition of the reconstructed gel, higher agarose percentage, and higher mechanical strength. The mixture gel with 95% HA plus 5% agarose could not withstand the metal ball and the ball penetrated the hydrogel layer immediately. 90% HA and 10% agrose mixture hydrogel was the mixture with the lowest agarose concentration withstands the metal ball loading for 30 minutes (Figure 5.1.A). Hence 90% HA plus 10% agarose reconstructed gel has been used for the rest of experiments in this chapter.

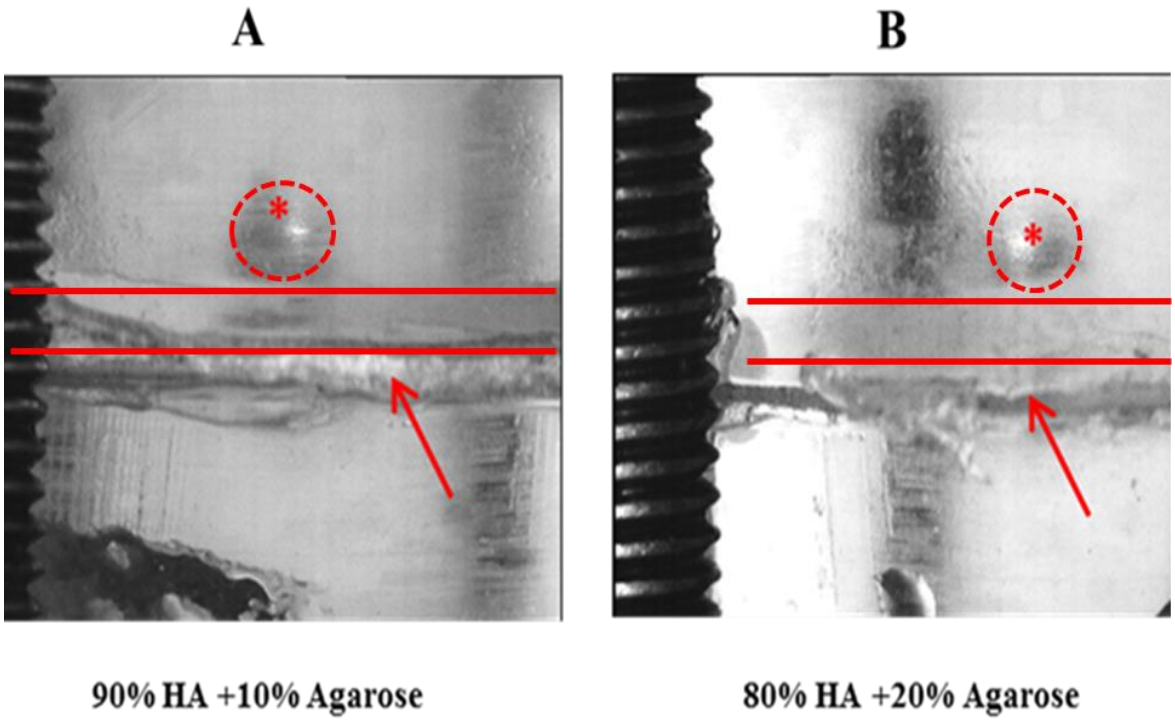

Figure 5.1: Microscopic side view images showing mechanical strength of HA and agarose mixture gel by ball indentation test in order to optimize the ratio of HA and agarose in the reconstructed gel. A) a mixture gel of 90% HA and 10% agrose. B) a mixture gel of 80% HA and 20% agrose. (*) and dash circle denote the metal ball, lines indicate the HA and agarose mixture hydrogel layer and arrows indicate filter paper as hydrogel support. The background is the free space.

5.4.2 Scaffold morphology and mechanical property

The SEM images (Figure 5.2.A, I, II) show the highly aligned and randomly arranged nanofiber meshes produced. The fibre diameter between the two types of fibres did not differ significantly (518±60 nm versus 486±80 nm, Table 5.1). Figure 5.2.A III clearly demonstrates the top view of

`

micorchannels in the deep zone, with an average channel diameter of 489 µm ±100, Table 1. Figure 5.2.B illustrates the cross section of individual scaffolds fabricated through the combination of electrospun fibre with HA hydrogel or HA hydrogel with the channels passed through the gel.

The cross-section of the assembled 3D zonal scaffold with zonal organisation; superficial, middle and deep zone was illustrated by using OCT imaging technique (Figure 5.3). This bottom-up, layer-by-layer assembly technique has created distinct zonal organization in a 3D scaffold, both aligned nanofiber (superficial zone) and random nanofibers (middle zone) were placed on top of the hydrogel with defined micro-channels.

The compression modulus was determined by the slope from the linear region of the stress–strain curve between 0.1 and 0.5 strain and the applied forces have been converted into stress with samples' area. The height difference between samples has been considered in the strain values which were obtained from the displacement divided by initial height, whilst the ultimate compression strength was taken as the maximum stress. It was demonstrated there was little variation of the compression modulus between superficial, middle and deep zones, and gel alone scaffold, but the full 3D zonal scaffold had about 22 % higher compression modulus than each of the individual scaffolds. However, all scaffolds had lower compression modulus than native cartilage tissue (Table 5.1). The representative load deformation curves were displayed in Figure 5.4.

`

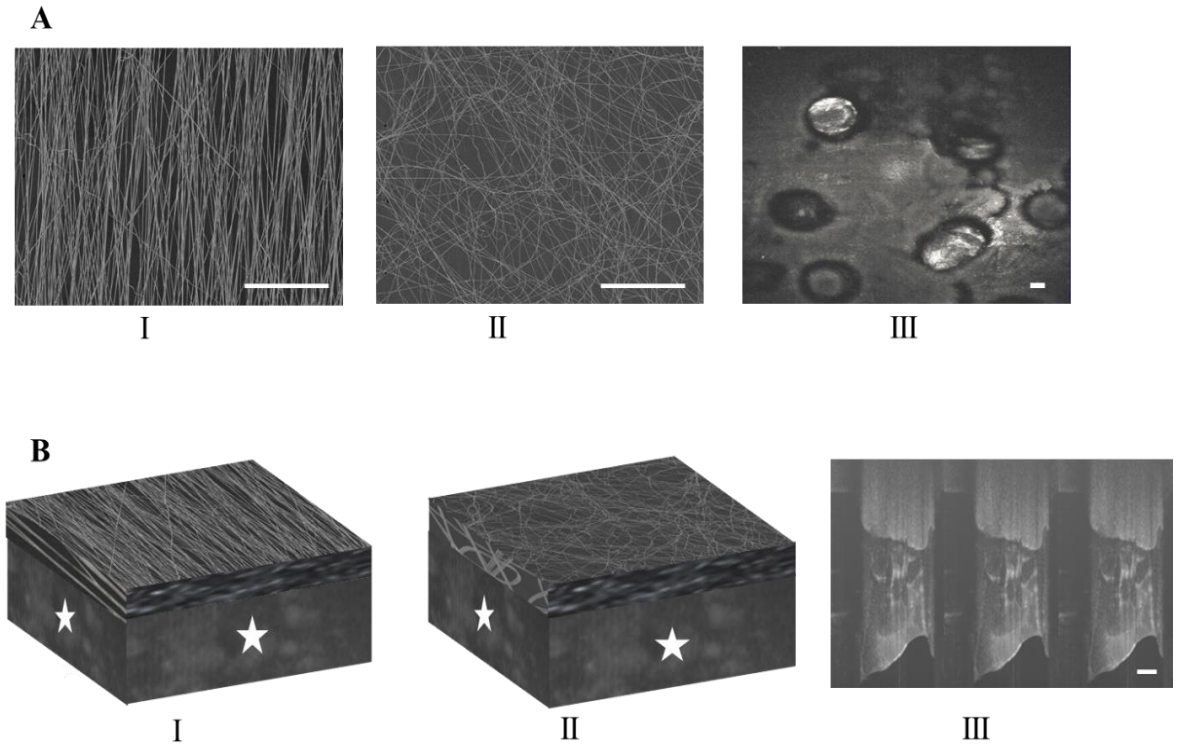

Figure 5.2: Morphology of individual scaffolds and hybrid scaffolds. (A) Top view images of individual 3D zonal scaffolds; (B) Side-view of individual 3D zonal scaffolds. I) aligned nanofibre and superficial zone; II) random nanofibre and middle zone (The insert is the high magnification for aligned and random nanofibres); and III the emtey channels in HA hydrogel and deep zone (The insert is the reconstructed z-staged image showing the vertical channels). SEM images for I, II; light microscope and OCT images for III. (*) denotes the HA hydrogel layer. Scale bar is 100 μm.

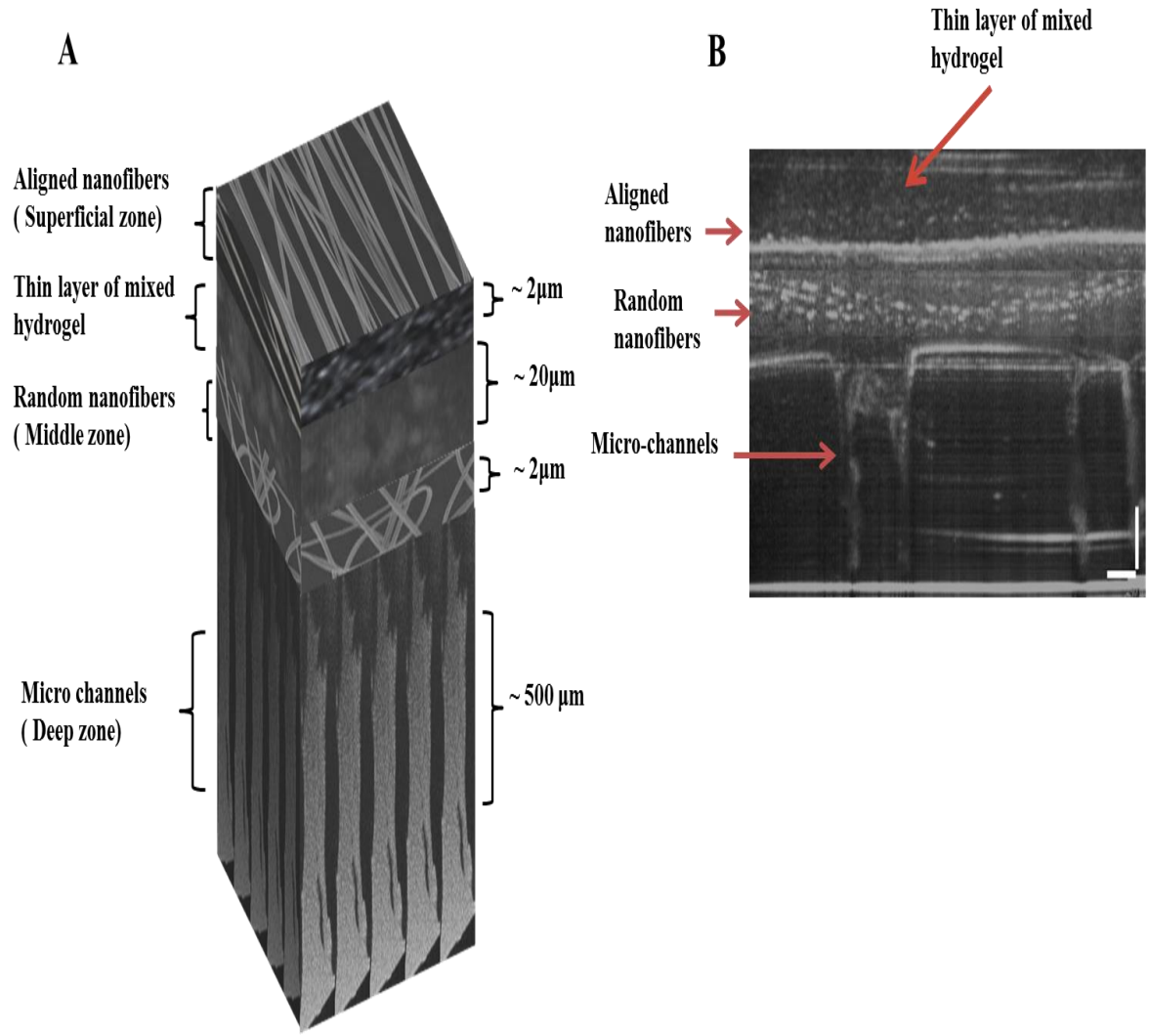

Figure 5.3: Morphology of assembled scaffolds and constructs (A) Schematic illustration of the assembled zonal scaffolds with corresponding thickness. (B) An OCT image of the assembled 3D zonal constructs showing the aligned nanofibre as superficial zone, random nanofibre as middle zone, and the vertical emtey channels as deep zone. Scale bar is 250 µm.

`

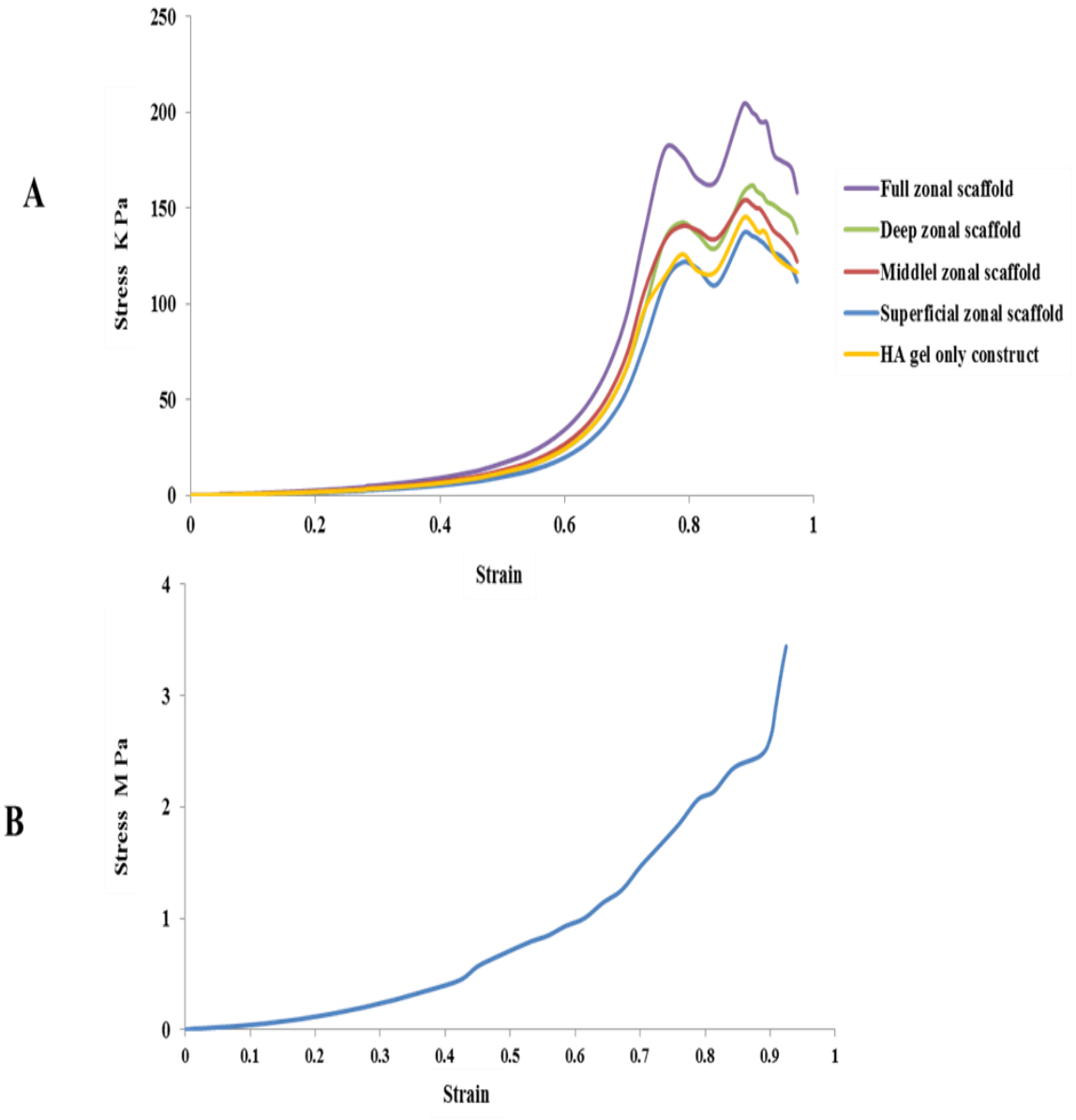

Figure 5.4: Representative Stress-strain curves. A) The three individual, assembled 3D zonal scaffolds, and HA gel alone construct (negative control). B) Bovine cartilage tissue (positive control).

`

Table 5-1: Physical parameters of the hybrid zonal scaffolds, HA gel alone scaffold and bovine cartilage tissue

Scaffold cartilage mimicking	**Scaffold orientation**	**Fiber and channel size (μm)**	**Ultimate compression stress (KPa)**	**Compression modulus (KPa)**
Superficial	Aligned (horizontal)	0.518± 0.06	143± 32.35	15.47± 3. 5
Middle	Random	0.486± 0.08	149± 28.11	16.16± 2.9
Deep	Vertical channels	489± 100	153± 12.41	15.85± 4.2
Full scaffolds construction	-	-	209± 40.35	25.12± 4.4
HA gel alone scaffold	-	-	145± 31.83	17.67± 3.8
Bovine cartilage tissue	-	-	3410 ± 983	570 ± 164

5.4.3 Chondrocyte morphology in individual constructs

Figure 5.5 illustrates the morphology of live chondrocytes on each 3D zonal construct. Within the superficial zone, it can be seen that the individual chondrocytes appeared to stretch along the aligned nanofibers from day 1 and developed a highly aligned morphology at 2 weeks. By contrast,

`

chondrocytes maintained their round shape in the random oriented nanofibers within the middle zone. The cells appeared to cluster together. Within the HA channels of the deep zone, the chondrocytes appeared to form vertical round shape cells stacking up within the channels.

`

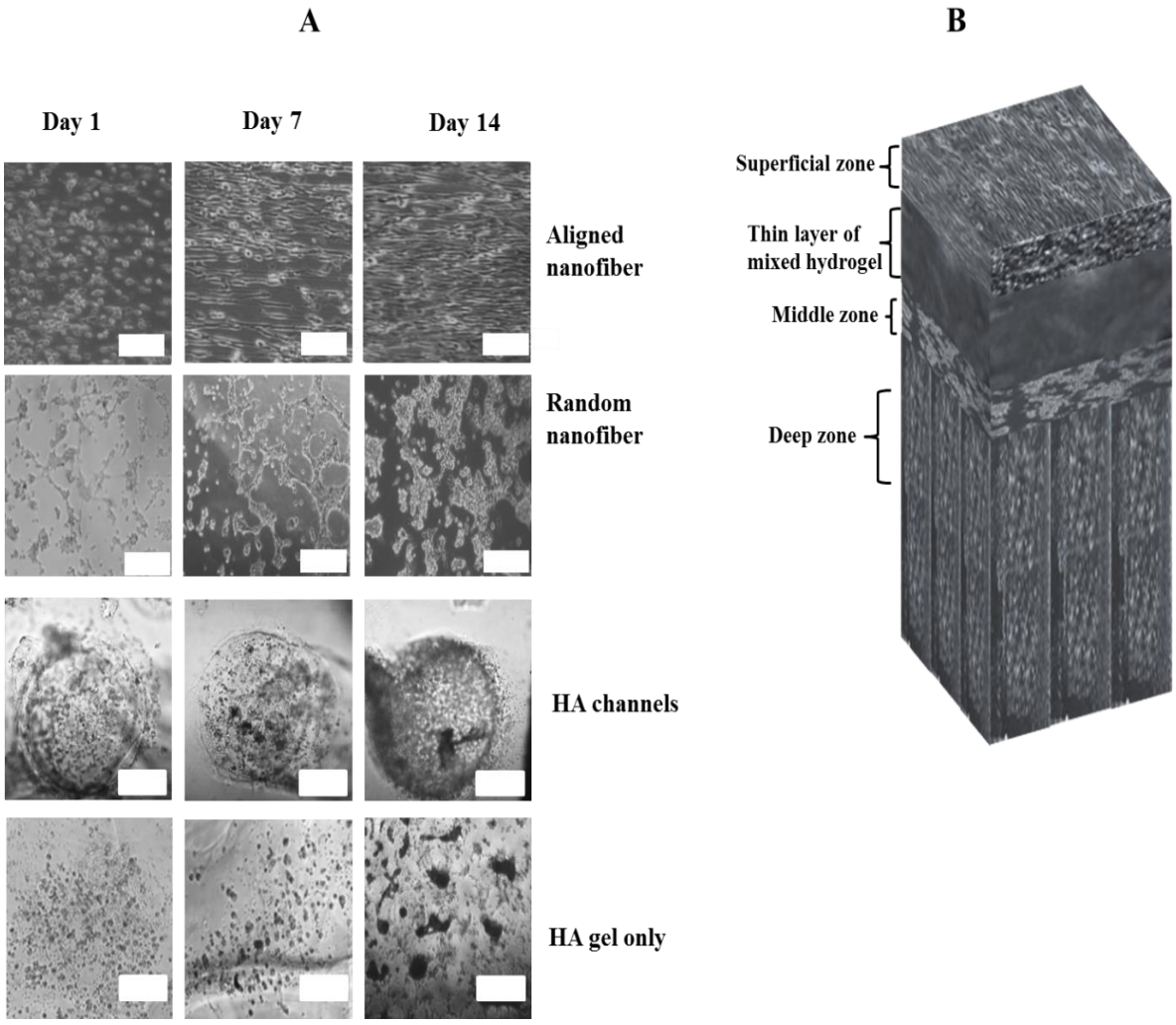

Figure 5.5: (A) Microscopic images of the live chondrocytes in the three separately cultured zonal scaffolds and HA gel alone constructs showing their morphology and orientation along culture at different time points (n = 3). Scale bar is 150 μm. (B) The schematic illustration the live chondrocytes morphology and orientation in the assembled three zonal scaffolds. Scale bar is 150 μm.

5.4.4 Cell viability

Figure 5.6 shows the live/dead cell images of constructs taken by confocal microscopy. Based on the image observation, all zonal constructs had high viable cells (most green stained cells) and low dead cells (few red cells). In addition, in the superficial zone constructs chondrocytes aligned longitudinally along the nanofibers. High cell viability was demonstrated in the control construct.

`

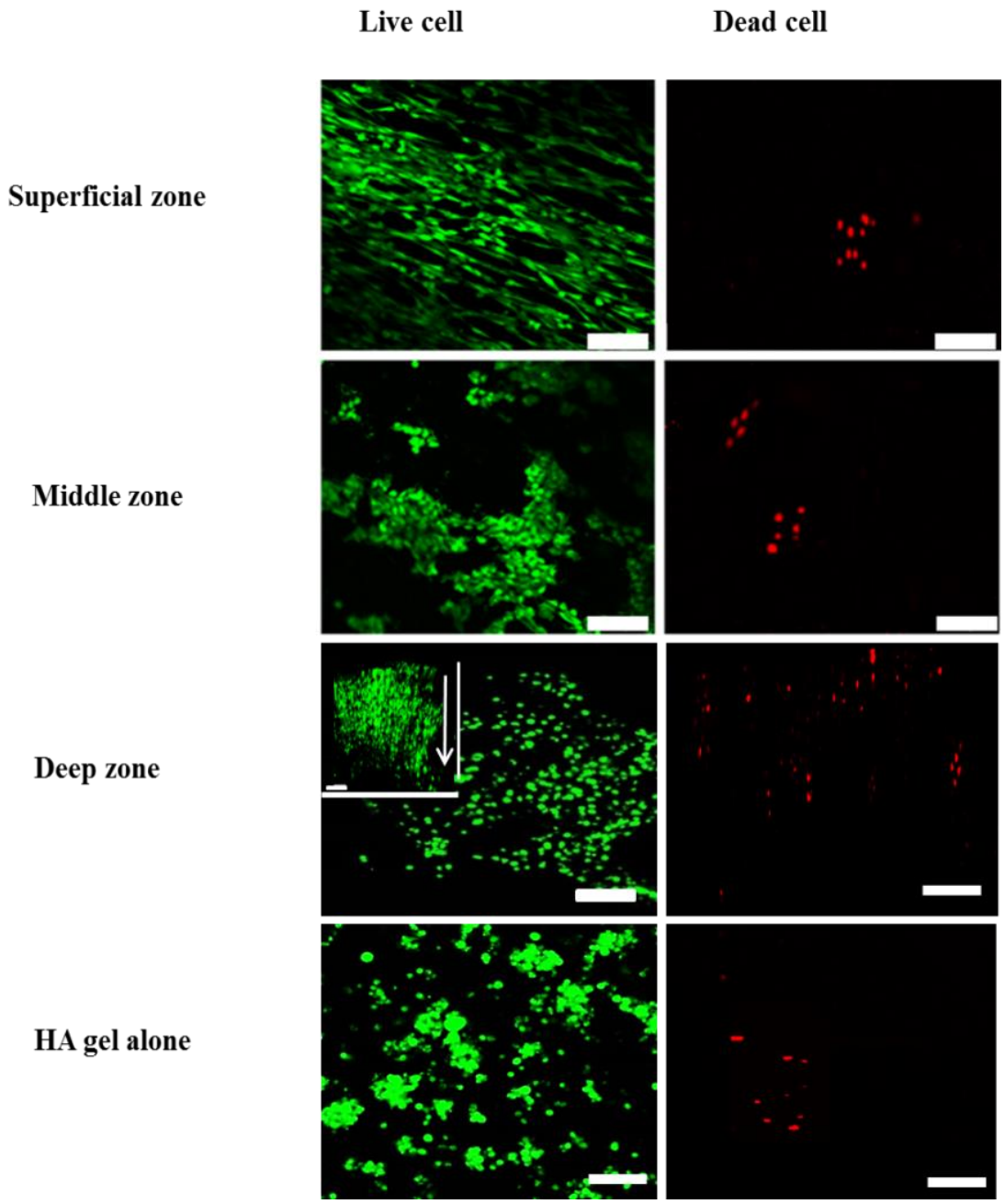

Figure 5.6: The live and dead staining images of chondrocytes in three separately cultured scaffolds and HA gel alone construct taken at day 14 culture. The insert is the reconstructed z-staged image showing the cells within the vertical channel, indicating channel direction by an arrow. Green indicates live cells, and red dead cells. Scale bar is 100 μm, (n=3).

`

5.4.5 Cell number

DNA quantitative assay was used to indicate the cell numbers. Figure 5.7 illustrates cell number in zonal constructs. It was demonstrated that at all culture time points, the HA gel alone, deep zone and middle zone scaffolds had almost the same cell number. However, the cell numbers were lower than that in the superficial zone scaffolds ($p < 0.05$).

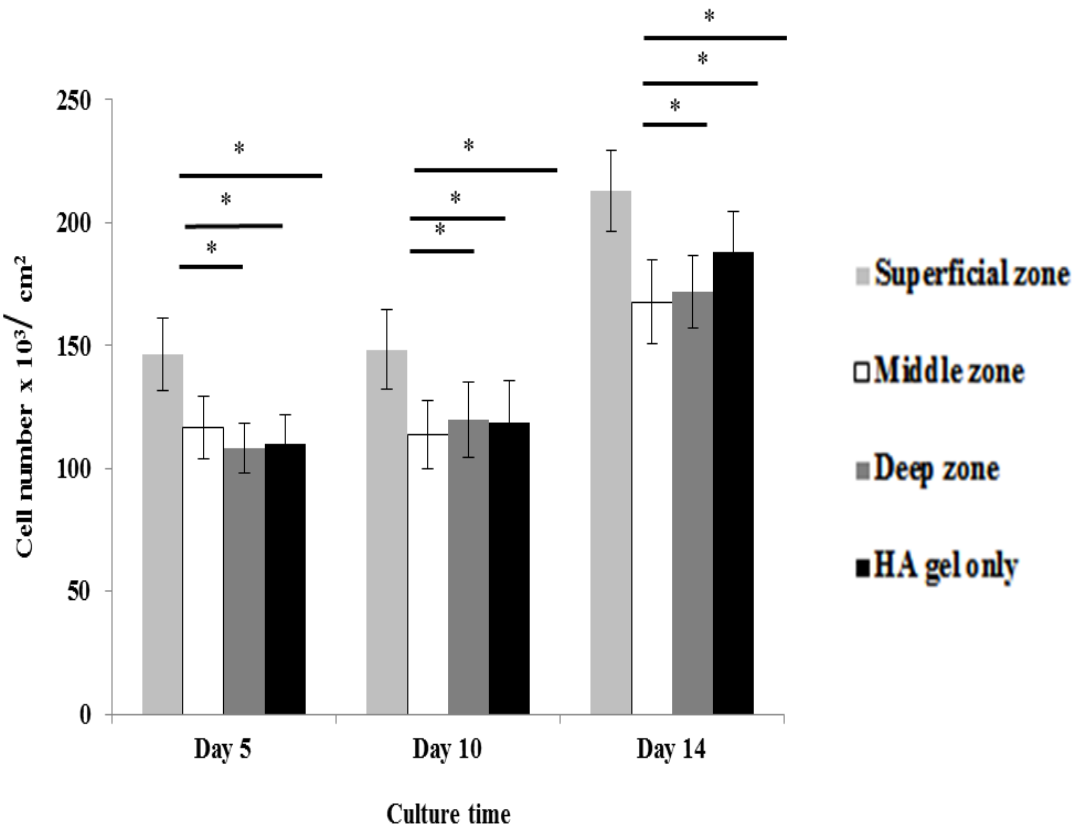

Figure 5.7: Cell number in three separately cultured scaffolds and HA gel only construct at Days 5, 10 and 14 culture. Data are expressed as mean ± SD (n = 3). *$p < 0.05$*

Total sulphated GAG content production

The total amount of sulphated GAG accumulated in the different 3D zonal scaffolds was quantified as shown in Figure 5.8. It is clear that the cells in HA gel alone, deep and middle zone scaffolds produced significantly higher GAG amounts than that in the superficial zone scaffold ($p<0.05$). The normalised GAG content (μg) per cell in different 3D nanofabricated zonal constructs is shown in

`

Figure 5.9. Seemingly, the GAG content with respect to DNA present was highest in the deep zone scaffold compared to the other zones, especially at later time points ($p<0.05$).

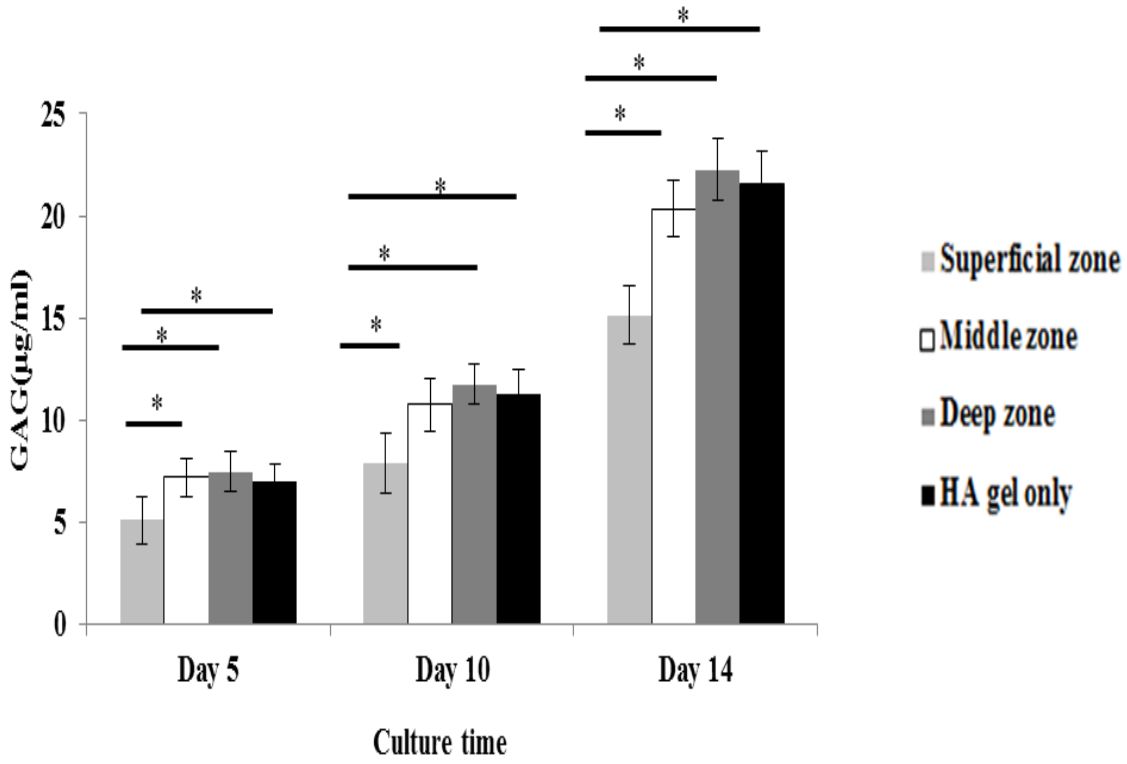

Figure 5.8: Total sGAG production in three separately cultured scaffolds and HA gel only construct at Days 5, 10 and 14. Data are expressed as mean ± SD (n = 3). *$p < 0.05$

`

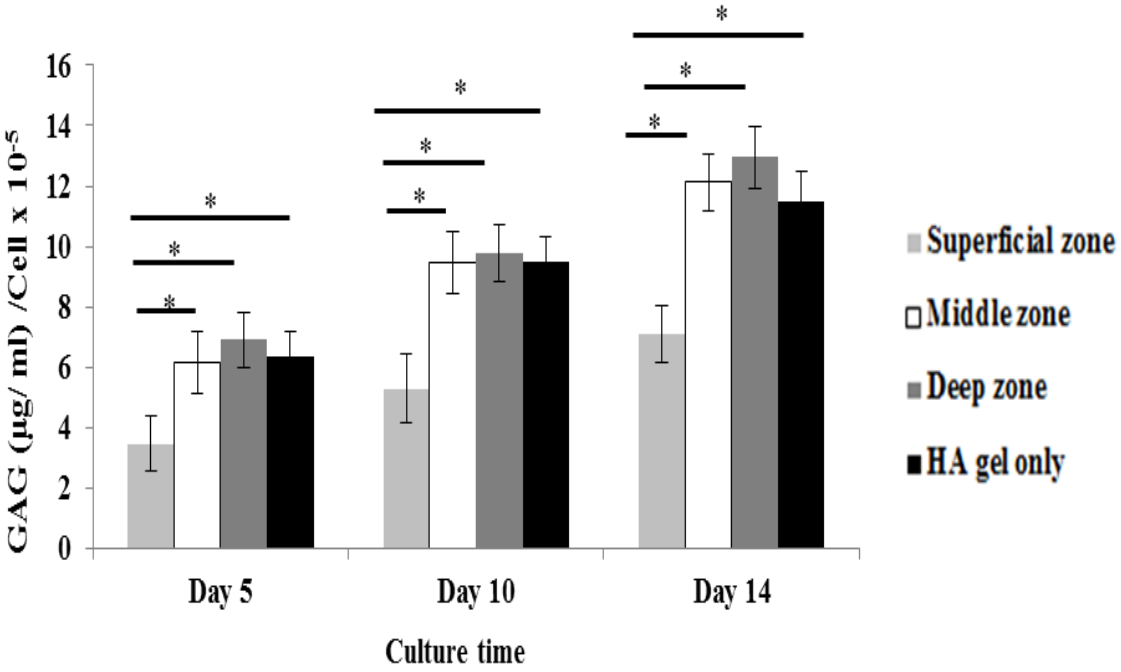

Figure 5.9: Total sGAG production normalised to cell number in three separately cultured scaffolds and HA gel only construct at Days 5, 10 and 14. Data are expressed as mean ± SD (n = 3). *$p < 0.05$

Expression of ECM components

Figure 5.10 shows the immunofluorescence staining for markers of ECM in individual 3D zonal constructs. Immunostaining for collagen I was also carried out to further confirm the phenotype of cells. It can be seen that the cells in superficial zone sample had the highest collagen I production whilst the lowest collagen II and aggrecan production. Middle and deep zone samples demonstrated higher collagen II and aggrecan expression than superficial zone. On the other hand, with regards to collagen I, the staining intensity decreased with the depth-dependent constructs, whereas to aggrecan, its expression increased with the depth-dependent constructs. For collagen II, the highest staining was seen in the middle zone samples and the lowest was observed in the superficial zone samples. However, production and secretion of collagen II were present in all scaffold types, which was not the case for collagen I staining. The staining images of native bovine cartilage samples showed the depth variation of collage I, II and aggrecan expression with collagen I expression in

`

superficial zone only; collagen II across all zones and strong aggrecan in middle and deep zones (Figure 5.11).

Western blot results in Figure 5.12.A showed the superficial zone samples produced higher collagen I and lower collagen II and aggrecan expression. Whilst the collagen II demonstrated higher level in middle zone scaffold with low collagen I expression. Aggrecan, one of the main markers of articular cartilage, showed high expression with depth; deep zone had the highest aggrecan and lowest collagen I concentration. The intensity of proteins expression (Figure 5.12.B) seemed to correspond to the Western blot results (Figure 5.12.A). The results were consistent to immunohistological staining.

To demonstrate that the chondrocytes could be incorporated and maintained in individual zonal scaffolds when assembling the individual zonal constructs into a construct, DAPI was used to label the cells first and the three-different zone constructs with labelled cells were assembled and further cultured for 14 days. The cross-sectional image and reconstructed 3D image of the assembled construct were shown in Figure 5.13. Both live/dead staining images and DAPI tracking image showed that the zonal structure was well maintained, and the cells were spread across the zones. Few red cells in live/dead staining assay demonstrated the high cell viability in the assembled constructs (Figures 5.13.A and B).

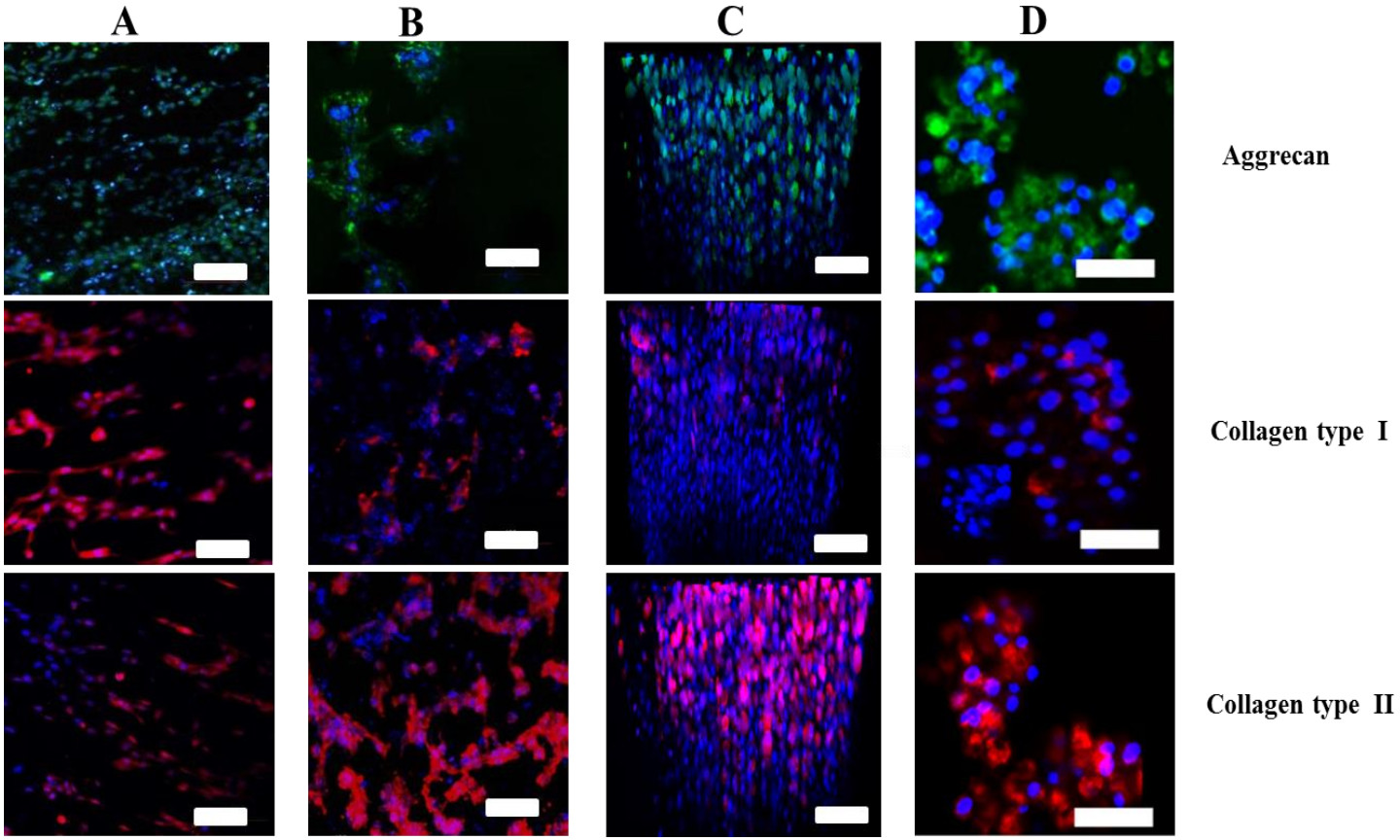

Figure 5.10: Immunostaining images of chondrocytes cultured in the three separate zonal scaffolds and HA gel only constructs: column A; superficial zone, column B; middle zone, column C; deep zone, column D; chondrocytes are grown in HA hydrogel. Blue: nuclei; green: aggrecan; red: collagen II or collagen I. Scale bar is 100 μm. (n=3, three independent experiments).

`

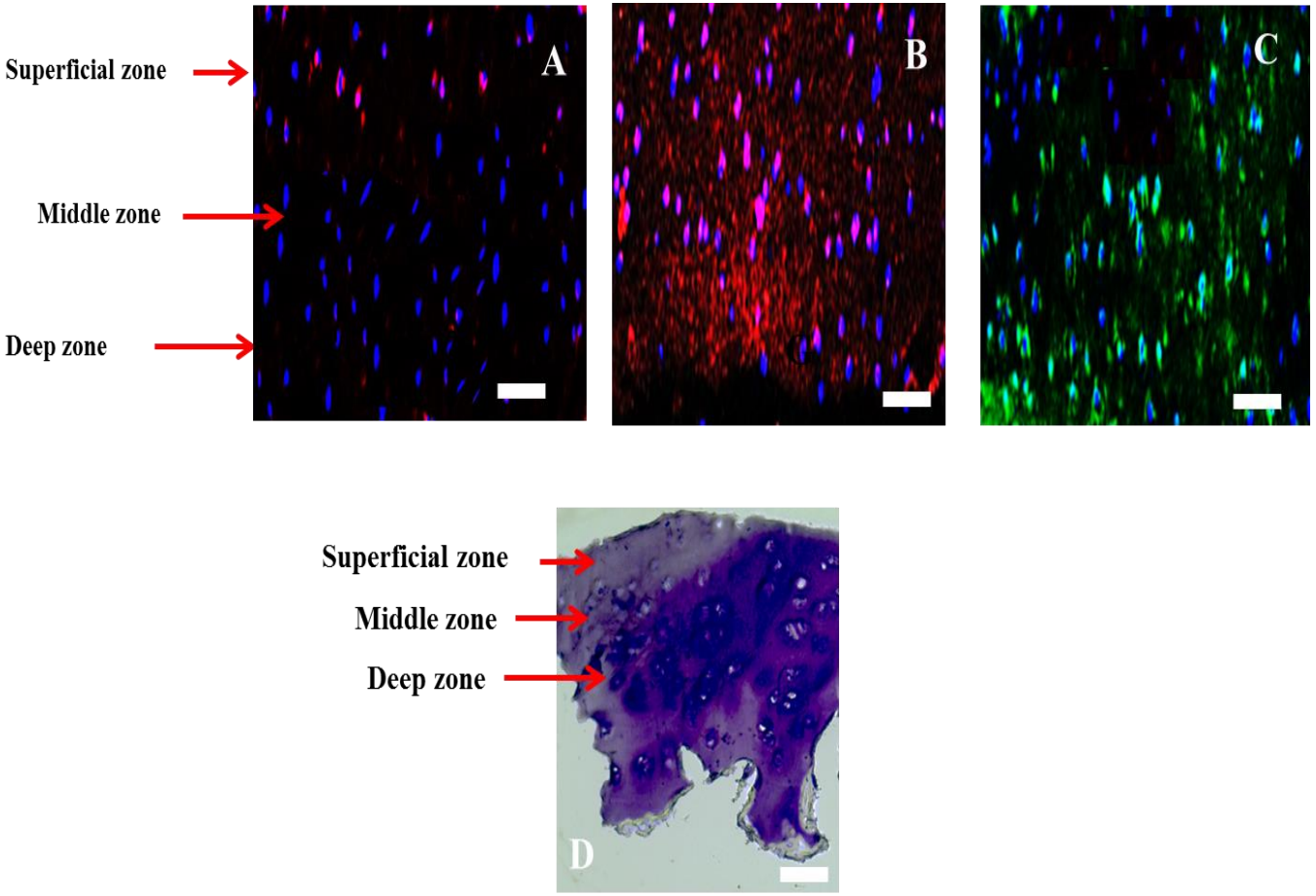

Figure 5.11: Illustration of Immunostaining images of freshly dissected bovine cartilage. (A) collagen I, (B) collagen II, (C) aggrecan, (D) Toluidine blue. Blue: nuclei; green: aggrecan; red: collagen II or collagen I; purple: GAG. Scale bar is 100μm.

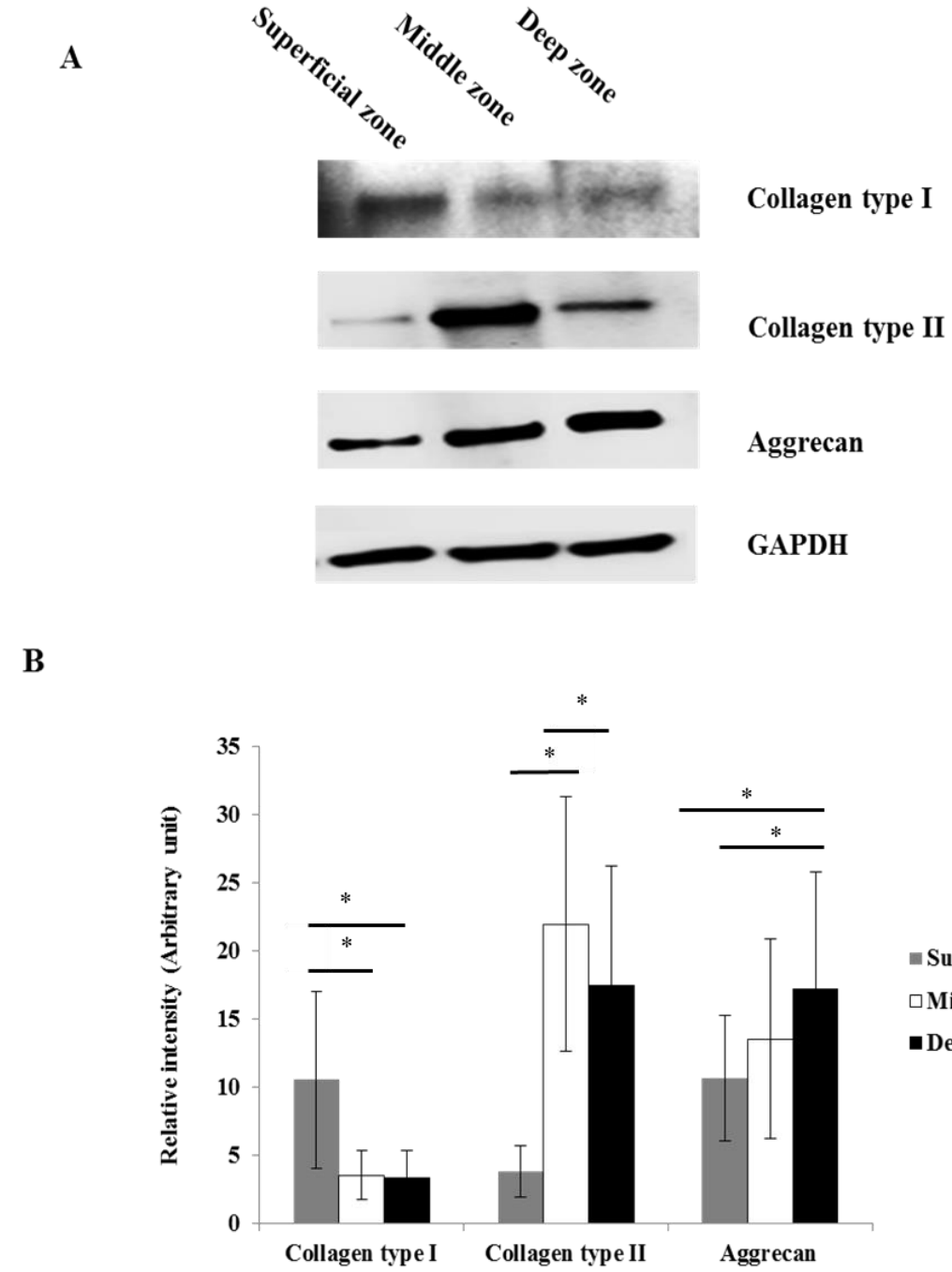

Figure 5.12: (A) Western blotting of collagens I and II and aggrecan expression of chondrocytes in the three zonal constructs after culturing for 14 days. (B) Representative semi-quantification of western blotting results and expression levels relative to the loading control (GAPDH). Data are expressed as mean ± SD (n = 3). *$p < 0.05$*

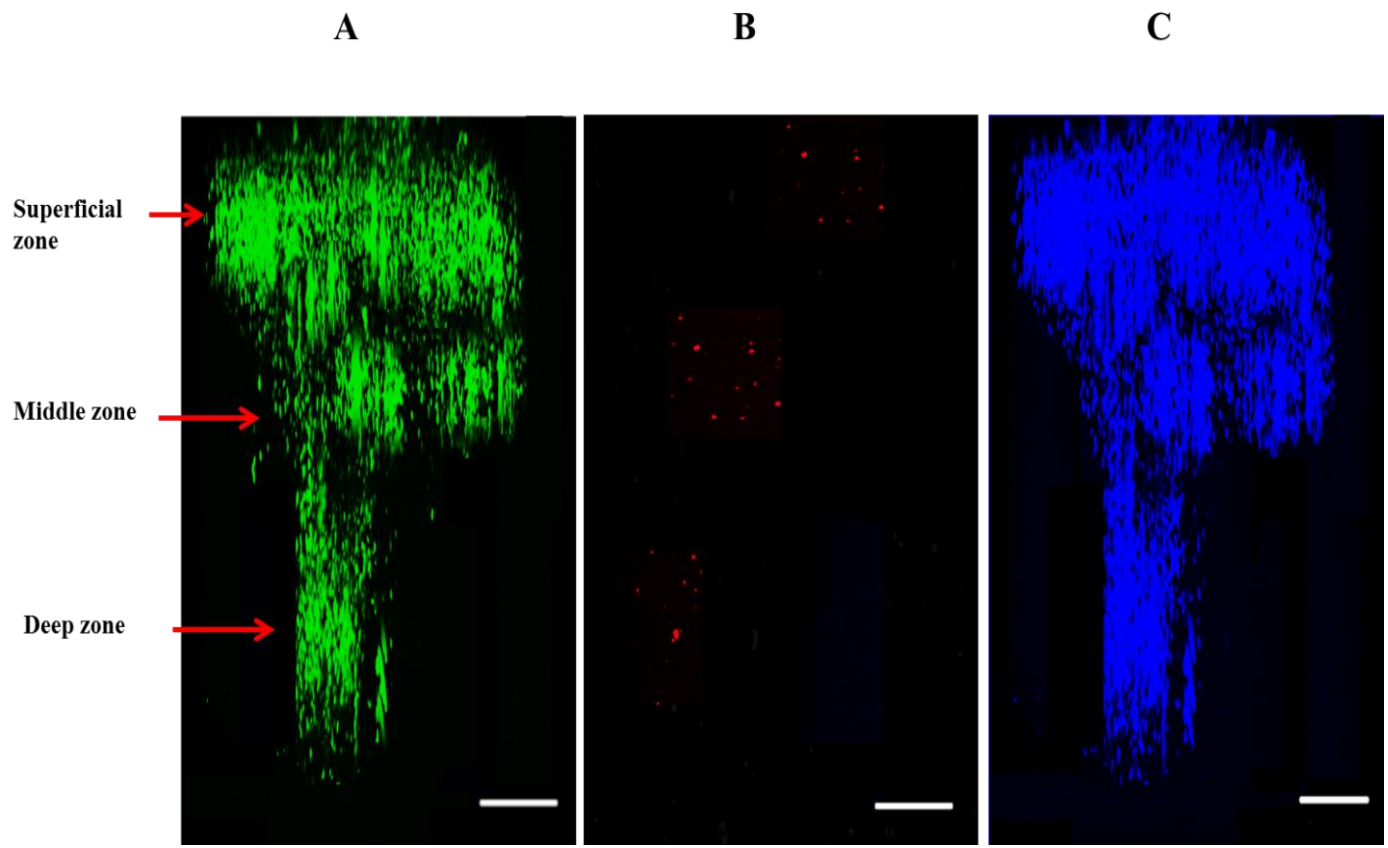

Figure 5.13: Reconstructed 3D images of DAPI labelled chondrocytes in the assembled 3D zonal scaffolds alongside live/dead kit staining covering the superficial, middle, and deep zones (presenting one vertical channel only). A) live cells (green); B) dead cells (red); C) DAPI (blue). Scale bar is 250 μm.

`

5.5 Discussion

The zonal organisation of scaffolds that mimics the organisation and the structure of cartilage tissue and potentially induce the synthesis of appropriate ECM within the separate zones could lead to long-term functionality in cartilage regeneration. There is no doubt that this is a complex challenge to tackle. In this study, hybrid cartilage scaffolds have been successfully fabricated, comprising PLA nanofiber and a HA hydrogel which appeared to provide appropriate zone-specific parameters mimicking microstructural organisation and inducing ECM production. The multiple imaging, biochemical and biomechanical assessments demonstrated that the seeded bovine chondrocytes responded to the scaffolds spatial orientation and arrangement. The current hybrid zonal-specific 3D scaffolds induced the formation of biomimetic zonal organisation and composition of ECM as found in native articular cartilage tissue. However, HA gel scaffolds only achieved randomly distributed round chondrocytes with homogeneous ECM distribution.

The 'contact guidance' from electrospun nanofibers triggers distinct cell arrangement

Articular cartilage has a heterogeneous arrangement of cells and ECM, which comprises rounded and orientated cells, demanding specific ECM fibres structure in defined regions. It has been confirmed that the electrospun nanofibres developed in this study could stimulate chondrogenic capacity selectively through providing a surface similar to the native zones of articular cartilage.

It has been reported that cytoskeletal morphology and orientation of ECM is tightly interrelated (Dalby et al., 2002; Tijore et al., 2018). The control of the orientation and the morphology of cells can be used to control the architecture of secreted ECM because the orientation of newly produced ECM follows the cytoskeletal shape. Inversely, artificial ECM with specific patterns on the cell culture substrates can induce the aligned cellular patterns through 'contact guidance' (Vrana et al., 2008; Wilson et al., 2012). Dalby et al. (2002) have documented that the ECM architectures and cytoskeletal orientation can be controlled by nanometre-scale structures. Work from our own group

`

(Wimpenny et al., 2012) further demonstrated that electrospun nanofibres facilitated the adhesion of chondrocytes and the regulation of their morphology.

The crosslinked HA hydrogel is chondrogenic

Hydrogels have a promising potential for tissue engineering applications due to their high-water content, tunable physical properties, able for homogeneous cell distribution, high permeability for nutrients and waste products of metabolism (Aleksander-Konert et al., 2016; Eslahi et al., 2016). Moreover, highly hydrated hydrogels can better mimic the chemical and physical environments of ECM and therefore are ideally cellular microenvironment for cell proliferation and differentiation (Tan et al., 2010).

The hydrogel for cartilage regeneration needs to have the capacity to maintain their chondrogenic capacity. HA found natively in cartilage tissue, has been studied for decades (Yoo et al., 2005). Chondrocytes in native articular cartilage tissue demonstrated round shape morphology and clustered in small groups (Buckwalter et al., 2005). HA is known to interact with chondrocytes via various surface receptors including CD44. This surface receptor bound to HA and triggers chondrocytes to retain their original morphology and phenotype, an area that is still not fully understood (Yoo et al., 2005). High aggrecan and collagen II production in the deep zone scaffold, channelled HA from this study supported that HA is highly chondrogenic.

Hybrid scaffolds mimic native zonal structure

In this study, nanofibers acted as a contact guidance platform to control cell morphology and matrix production as well as provided further evidence to show that the aligned and randomly orientated fibre morphology resulted in elongated and small clusters of round cells morphology respectively in superficial and middle zones scaffolds.

Chondrocyte phenotype is defined by a change in morphology and the alteration of crucial ECM components including collagen II and aggrecan (Bonaventure et al., 1994; Bobick et al., 2009).

`

This study showed the organisation of cell aggregates regulated the biochemical synthesis and ECM organisation. In the superficial zone, the aligned nanofibres produced elongated chondrocytes cells, which altered the cell phenotype to fibroblast-like phenotype with higher collagen I synthesis and the lowest collagen II, aggrecan and GAG. The middle zone scaffold maintained the round shape of chondrocytes with random clusters with higher collagen II, aggrecan and GAG production in comparison to superficial zone. Apparently, the orientation of electrospun fibres can be smartly used to regulate rather precisely chondrocytes' phenotype through their morphology from fully elongated to round cell shapes and variation of ECM synthesis. In the current study, we used crosslinked and reconstructed HA gel as the stable hydrate environment for chondrocytes in a prolonged culture period. The micro-channels were made through the HA hydrogel to mimicking the deep zone. In the deep zone scaffold, the chondrocytes formed round, columnar cell clusters with higher aggrecan and GAG production in comparison to superficial zone. Current data illustrated that HA can be utilised to control both ECM production and maintain chondrocyte morphology.

This study adapted a smart hybrid and sandwich style fabrication for zonal distinct constructs, which separately and synergistically has the potential to regulate a chondrocytes' phenotype, enabling chondrocyte elongation (superficial zone) or aggregation (random clusters in the middle zone and columnar clusters in the deep zone). The bottom hydrogel layer restricted cells attaching, which drove cells adhered and oriented along nanofiber meshes, whilst the top layer of hydrogel (reconstructed HA gel) provided the support necessary to stabilise the orientation of cells and nanofibers meshes. Altogether, combining of using a highly hydrated hydrogel, which has low protein affinity, with nanofibers, which have high cell attachment capacity, has the potential to lead to a clinically benefit product in the cell therapy of cartilage treatment. Hence, the adaptation of the two level control strategies in scaffold fabrication has the potential to create multiple zone cartilage regeneration. Different from other reports, this work has generated hydrated and full thick construct

`

with distinct ECM architecture and composition along depth (Klein et al., 2003; Malda et al., Ng et al., 2005; Steele et al., 2014).

5.6 Conclusion

This feasibility study confirmed that PLA nanofiber meshes with different alignment and micorchannels in an HA hydrogel could be used to create hybrid scaffold models. The current hybrid scaffolds induced chondrocyte alignment and generation of ECM as found in different zones of native cartilage, evidenced by the cell morphology and ECM component production level. The regulation of chondrocytes' aggregation state and skeleton morphology by nanofiber and micro-channels and maintaining of these morphologies in highly hydrate gel can become a facile technique to replicate zonal specific cartilage construct. The three zonal constructs can be assembled and kept intact during culture. Thus, this study presents new hybrid scaffolds and facile method for biomimetic cartilage regeneration.

`

Chapter 6 : General discussion, overall conclusion and future work

`

6.1 General discussion

The healthcare challenge to regenerate human articular cartilage is at an exciting point but there are some key issues which remain difficult but important steps. This PhD study has attempted to address key issues to further our understanding and to move the field forward. Isolated chondrocytes are not the ideal form of cartilage cells to produce cartilage ECM but they are the cells used in the recently NHS approved cartilage cell therapy (National institute for health and clinical excellence UK, 2017). They are ideal for treating small focal cartilage defects. However, the field needs to continue to move forward to find a better solution for large, full depth defects which affect both cartilage and bone. Freshly extracted chondrons form a more cartilage-like ECM than chondrocytes and their surrounding PCM is thought to maintain chondrocyte phenotype (Vonk et al., 2014; Zhang et al., 20014). The PCM is crucial for many functions including good ECM formation (Poole, 1997; Larson et al., 2002). The presence of a PCM has been shown to enhance matrix production by chondrocytes, suggesting that an intact PCM improves cartilage regeneration (Vonk et al., 2010). Herein, the data obtained in chapter 3 and 4 have provided evidence to support work performed by Lee and Loeser, (1998). Using bovine chondrocytes in a monolayer model, we have demonstrated that chondrons appeared to have better chondrogenic potential when compared to chondrocytes with respect to GAG, collagen II and collagen VI synthesis. Crucially, the PCM is important for ECM synthesis but it is a fragile structure.

Currently there is an equal weight of evidence suggesting that MSCs with or without other cell types are suitable for cartilage cell therapy. This was evidenced, for example, by the observational cohort study by Nejadnik et al, (2010) who reported that MSCs in cartilage repair were as effective as chondrocytes. Only recently, it has become clear that co-culture MSCs with articular cartilage cells offers an even great potential to cartilage growth.

A main impediment related to co-culture studies is that a large number of cells is required, which cannot be gathered from the patient samples obtained at surgery. A large number of consistent

`

chondrons is difficult to isolate from limited supplies of cartilage tissue. To avoid the issue of cell numbers, well characterised bovine chondrocytes and chondrons were used alongside rat MSC in this study because it is very difficult to get bovine MSCs. Xenogeneic co-culture models using the bovine chondrocytes and either rat or rabbit MSCs have been successfully used by some other groups without any immune response or different inverse outcome, but that immune reactions were not assessed (Levorson et al., 2014; Meretoja et al., 2014).

The phenotypic changes are considered to be the result of signalling via direct cell–cell contacts, as well as secreted factors generated by MSCs and articular cartilage cells (Bian et al., 2012, Levorson et al., 2014). The reciprocal effect has been used to explain the ratio effect when co-culture MSCs with cartilage cells in 2D model. 50:50 of MSC and cartilage cells produced better enhancement effect in ECM production in comparison to 20:80 and 80:20 ratio samples. In 80:20 MSC and chondrocytes or chondrons ratio samples, MSCs were dominated cell population with lower chondrogenic impact due to the low number of cartilage cells. While the samples with 20:80 MSC and chondrocytes or chondrons ratio had prevailed cartilage cells number, then the MSCs exerted less effect. 50:50 MSC and chondrocytes or chondrons ratio had a balance between the two types of cell populations which allowed exchanging the signalling to maintain the chondrogenic phenotype longer for cartilage cells and induce more MSCs to differentiate into chondrogenic lineage cells.

The PCM is believed to have chondrogenic potential evidenced by the enhanced ECM matrix production in co-culture of chondron and MSCs, as compared to chondrocyte or chondron monocultures. The co-culture of MSCs with chondrons appeared to decelerate the loss of the PCM as determined by higher collagen VI expression. However, the high chondrogenic potential will be lost if there are no appropriate cell growth and matrix protection environments even the presence of MSCs.

`

The HtrA1 secretory enzyme was suggested to degrade collagen VI in the PCM. The hypothesis was proved correct in this study deduced from the immunostaining results showing an inverse relationship between HtrA1 expressions and collagen VI concentration in the PCM. It is confirmed that the presence of MSC directly or indirectly suppresses the production of HtrA1 or generates inhibitors for HtrA1 in co-culture samples, which led to decelerate the loss of the PCM as determined by collagen VI expression.

Figure 6.1 illustrates the modelling and remodelling processes of PCM at different culture conditions in our 2D model based on the collagen VI staining outcome. The overall observation from this study was that monolayer culture could not preserve mature PCM nor regenerate PCM even co-culturing chondron with MSCs.

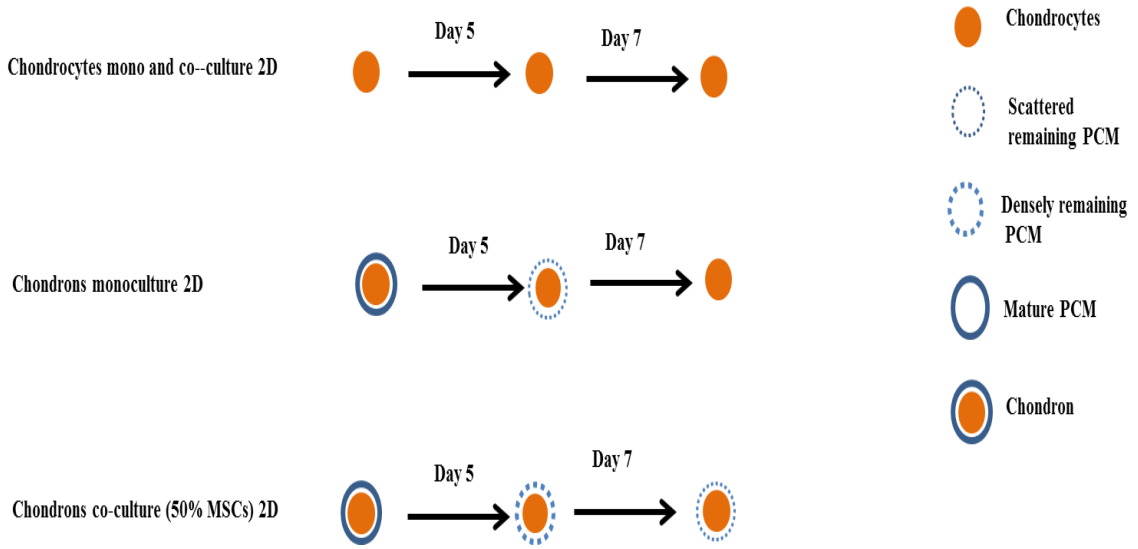

Figure 6.1: The schematic illustration of modelling and remodelling processes of PCM during different culture conditions in 2D culture models.

This study demonstrated that 3D culture environments as appropriate scaffold are essential conditions required to mimic the native ECM microenvironment which preserved existing PCM molecules; bound/stored newly produced PCM and enhanced the chondrogenic capacity during cartilage regeneration. Multiple factors in 3D culture including hydrogel types (hyaluronic acid versus agarose hydrogels); cartilage cell types (chondron versus chondrocytes); mono or co-culture

`

with MSC and different medium types affected the chondrogenic capacity assessed by the cell morphology, production rate of ECM (GAG production and collagen II expression) and the presence of PCM (collagen VI expression) (Figure 6.2).

This study confirms the newly formed PCM from isolated bovine chondrocyte culture has various deposition across mono and co-cultures, and HA and agarose hydrogels encapsulation along culture time. In the HA cultures, PCM was observed after 7 days in both mono and co-cultures chondrocytes with speckled stripe structures surrounding the chondrocytes surface (Figure 4.11). The cultures required two weeks to restore the PCM. For agarose cultures, small scattered stippled layer around the chondrocyte of PCM appeared after 7 days in co-cultures and after 14 days in monocultures. PCM was restored after three weeks. When using chondrons in 3D culture, PCM was maintained in all culture period and all the studied conditions. The co-culture with MSCs stabilized the PCM better than the monoculture.

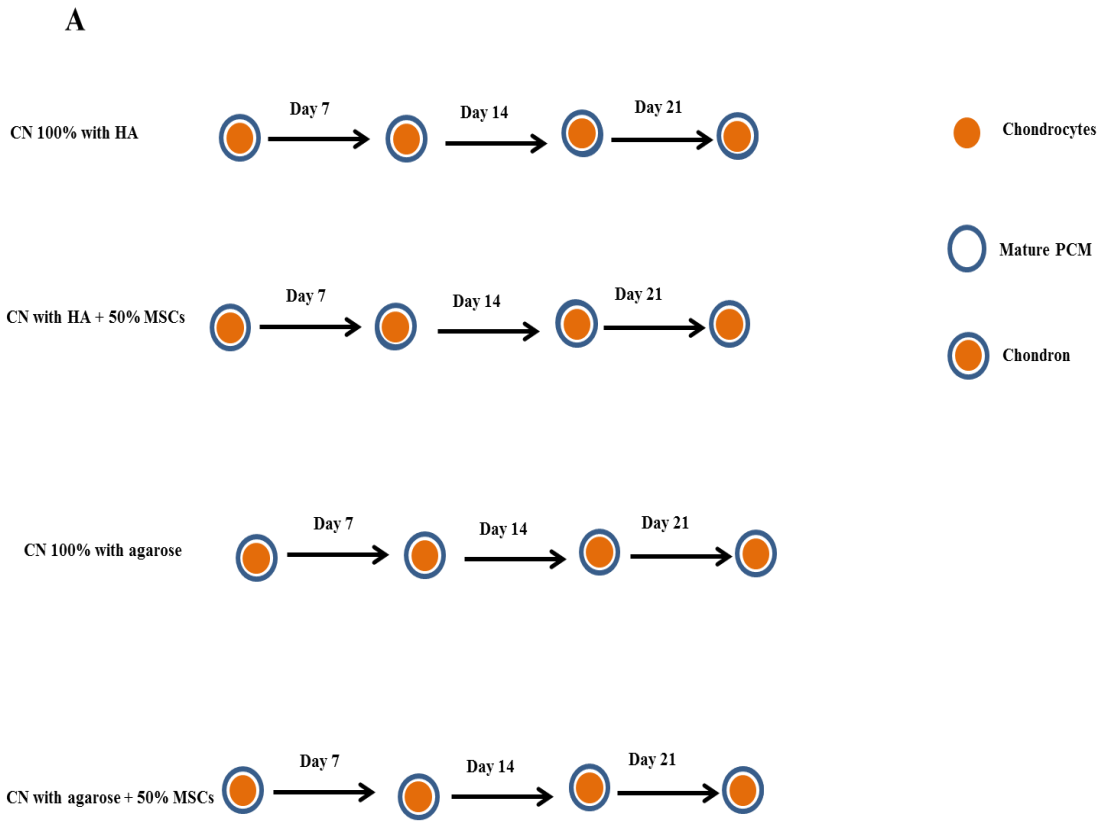

`

B

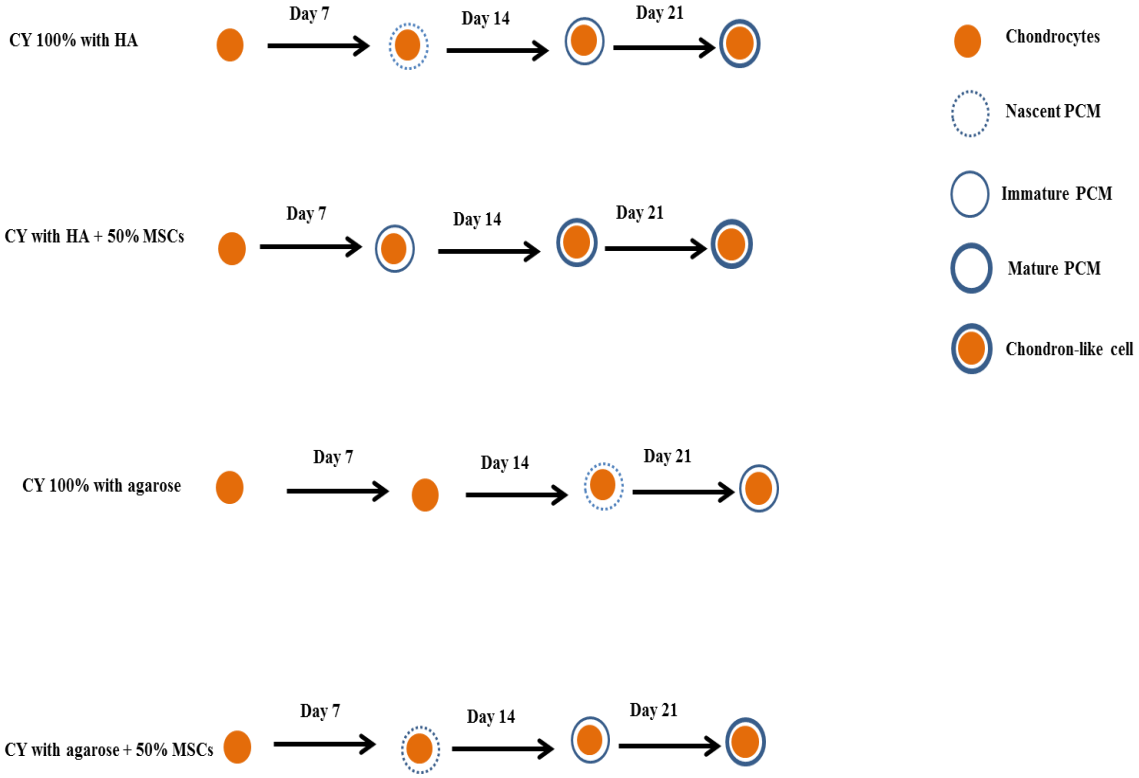

Figure 6.2: The schematic illustration of modelling and remodelling processes of PCM in 3D culturing with (A) chondron; (B) chondrocytes at different culture time points with different culture conditions.

Using a synchrotron source for FTIR provides a more powerful tool for cells and tissue study because of the high brightness which enables using lower aperture to identify the spatial heterogeneity of biomolecules in single cells with as small as 5 micrometre aperture. Also, synchrotron microFTIR offers spatial distribution mapping and chemical structure at the micron scale, when integrating chemical analysis specificity with microbeam precision.

The current study confirmed the multiple advantages of microFTIR. It is a non-destructively technique with less sample preparation and provides integral information for the spatial distribution and concentration of proteins, proteoglycan and lipids, which correlated to the PCM formation and cellular evolution of cultured chondrocytes in tissue-engineered cartilage models.

`

PCA scores showed changes in amide II which was related to protein structure and concentration. The spectral difference in the amide III band could be due to changes in SO^{-3} groups. Indirectly, PCA spectra of data showed that day 14 and 21 samples clustered to chondrons, indicating that chondrocytes cultured under these conditions could generate chondron-like cell morphology and PCM. Thus day 14 and 21 samples which contained collagen VI and more proteoglycan may explain the spectral similarity to chondrons but not to chondrocytes. PCA analysis in the lipid region further supported this hypothesis where the chondron and chondrocyte separated, but the separation was not as strong as compared to the fingerprint region on all three time points (day 7, 14, and 21). Synchrotron microFTIR spectroscopy and PCA can indeed help in better understanding the cellular evolution of cultured chondrocytes in tissue-engineered cartilage models involving subtle changes in protein types and proteoglycan concentration.

Cartilage can withstand large forces due to its complex structure and tissue organisation. Articular cartilage has an anisotropic zonal structure extending from the articular surface to the subchondral bone. The zones are variations in mechanical properties, cellular and extracellular matrix (Buckwalter et al., 2005). The goal of cartilage engineering is to generate in *vivo* recapitulated tissues with integrity and function by combining cells and scaffolds with chondrogenic ability. Although there are some success stories using this approach, there is little information on well organised constructs. Given the importance of recapitulation of in vivo tissues, it is imperative to engineer cartilage tissues with zonal structure and biofunction.

In this study, a hybrid and sandwich fabrication approach were employed for distinct zonal constructs allowing separate and synergistic regulation of chondrocyte phenotype (Figure 5.3). The model showed chondrocyte elongation in the superficial zone or chondrocyte aggregation in either the middle zone or deep zone (columnar clusters). The bottom layer of the hydrogel limited cell attachment and this drove cells to adhere and orient their somas alongside nanofiber meshes (Figure 5.5). In the top layer of the hydrogel (reconstructed HA gel), cell orientation was stabilised

`

on the nanofiber meshes. The aligned nanofiber mesh used in the superficial zone induced an elongated cell morphology, lower glycosaminoglycan (GAG) and collagen II production, higher cell proliferation and collagen I production than the cells in the middle zone scaffold. Within the middle zone scaffold, which comprised of a randomly orientated nanofiber mesh, the cells were clustered and expressed more collagen II. The deep zone scaffold induced the highest GAG production, the lowest cell proliferation and the lowest collagen I expression of the three zones. The combination of highly hydrated hydrogels with low protein affinity allowed chondrocyte chondrogenesis at the macroscopic level. By using nanofibers with their high cell attachment affinity, it is possible to control cell morphology at the zonal level. These characteristics will eventually speed up the cell therapy development where the maturation of therapeutic cartilage with the zonal organisation can be realised pre and post-implantation.

6.2 Overall conclusion

According to the results obtained it is concluded that both chondrons and MSCs enhanced ECM production and maintained PCM at the same time via MSCs' ability to delay the PCM destruction. The hypothesis that MSCs secreted inhibition factors for HtrA1 were supported by the finding of inverse expression of collagen VI to this enzyme, and HtrA1 was responsible for degrading PCM components. This study clearly demonstrated that 2D culture environment could not maintain or regenerate PCM even with MSC presence because the hard substrate (culture plate), induced chondrocytes and chondron differentiation to fibroblast-like cell phenotype. Without ECM microenvironment, which stabilise and accumulate newly formed PCM; matured PCM in chondron would lose during the 2D culture in short duration.

This work showed that 3D culture systems could maintain the chondrogenic phenotype of cartilage cells manifesting as the presence of collagen VI during the culture. The 3D culture preserved PCM in chondron from day 1 up to 21 day culture. In addition, the appearance of collagen VI in the

`

cultured chondrons was dense and homogenous; and co-culture with MSCs did not affect much the appearance and density of collagen VI.

3D culture of chondrocytes had ability to regenerate PCM manifesting as the gradual production of collagen VI along the culture. The variation of collagen VI concentration was strongly culture condition dependent. In contrast to collagen VI appearance in chondron culture, the newly formed collagen VI was spotted, less dense.

At the first day of culture, chondrocytes displayed no staining of collagen VI. By day 7, it was apparent that cell surfaces were staining positively within HA hydrogel in both mono and co-cultures with significant high expression in HA co-culture, while the agarose culture just showed a small scattered stippled layer around the chondrocyte in co-culture with no expression in monoculture at day 7. At day 14, collagen VI staining was found at all culture conditions including agarose monoculture. After 21 days the presence of a boundary of collagen type VI stained region surrounding the chondrocytes with a little change between mono and co-cultures for both HA and agarose hydrogels. Also, it is revealed that the chondrogenic culture media enhanced the expression of cartilage-specific ECM markers (collagen II and GAG) comparing with basal media, but both of them had no any effect on PCM marker ‘collagen VI’ synthesis. The best culture condition to generate high ECM/PCM content from chondrocyes was in HA hydrogel, using chondrogenic media and with 50% MSCs.

The study has developed a new non-destructively technique to observe the PCM formation and cellular evolution of cultured chondrocytes in tissue-engineered cartilage model by using the synchrotron microFTIR technique via analysis of spectral changes in both lipid and fingerprint regions.

Fingerprint region analysis for FTIR spectrum demonstrated that cultured chondrocytes might generate chondron-like cell morphology specifically at day 14 and day 21. The presence of PCM on day 14 and day 21, which contained collagen type VI and proteoglycan, could explain their

`

similarity of spectra to chondron, not to chondrocytes by PCA analysis. The spectrum analysis in lipid region further supported these speculations. Lipid region revealed that the separation of chondron, chondrocytes, day 7, day 14 and day 21 were not strong as in fingerprint region because the change of the lipid region reflected cell number most.

The current study confirmed that PLA nanofiber meshes with different alignments (aligned and random) and micro-channels in HA hydrogels could act as hybrid scaffolds which can induce distinguished chondrocyte alignment and ECM generation in three native cartilage zones. The three zonal constructs can be assembled and kept intact during culture. Both biological responses were evident at cell morphology and ECM production levels. Regulating chondrocyte aggregation, state, cytoskeletal morphology with nanofibers and micro-channels in highly hydrated hydrogels through the hybrid scaffolds become a simple technique to induce and generate zonal-specific structure of the cartilage. The aligned nanofiber mesh induced chondrocyte alignment and generation of ECM as found in the superficial zone, evidenced by the elongated cell morphology, low GAG production and collagen I production than the cells in the middle and deep zones scaffolds. The middle zone scaffold with randomly alignment nanofiber induced round chondrocyte clusters and expressed more collagen II. As a deep zone scaffold; the micro-channels in HA induced the highest aggrecan and GAG production and the lowest collagen I expression of the three zones.

6.3 Future work

The work described in this study has raised some approaches for future work, which could help in the cartilage tissue engineering.

Regarding the cell source, human cells could then be conducted instead of cross-species like bovine or rat cells, which is likely to provide the opportunity to mimic human articular cartilage tissue before they become clinically useful products.

`

Further characterisation could then be conducted to determine the mechanism behind the co-culture and direct cell-cell contacts signalling and identify the secreted factors generated by MSCs and chondrocytes or chondron.

With regard to the development of 3D nanofibre-hydrogel composite, further work is suggested to replicate full thickness native articular cartilage tissue, which could be achieved through bottom-up, layer-by-layer assembly method. The biological and biomechanical properties of the new cartilage constructs will be characterised thoroughly. It would be hoped that these improvements by incorporation of growth factors would further enhance the ECM-like cartilage.

Furthermore, it would be beneficial to determine the long-term stability and tissue formation over increased culture duration, HA concentration in the constructs and application of mechanical condition for the constructs which accelerate the ECM production are potential approaches to increase the mechanical property of the constructs.

Further work is suggested to study formation of PCM through different zones by using 3D nanofibre-hydrogel composite which is likely to provide functional engineered cartilage tissue.

`

References

Adams, J.C. and Watt, F.M., 1993. Regulation of development and differentiation by the extracellular matrix. Development, 117(4), pp.1183-1198.

Ahmed, T.A. and Hincke, M.T., 2010. Strategies for articular cartilage lesion repair and functional restoration. Tissue Engineering Part B: Reviews, 16(3), pp.305-329.

Aleksander-Konert, E., Paduszyński, P., Zajdel, A., Dzierżewicz, Z. and Wilczok, A., 2016. In vitro chondrogenesis of Wharton's jelly mesenchymal stem cells in hyaluronic acid-based hydrogels. Cellular & Molecular Biology Letters, 21(1), p.11.

Alexopoulos, L.G., Setton, L.A. and Guilak, F., 2005. The biomechanical role of the chondrocyte pericellular matrix in articular cartilage. Acta biomaterialia, 1(3), pp.317-325.

Archer, C.W. and Francis-West, P., 2003. The chondrocyte. The international journal of biochemistry & cell biology, 35(4), pp.401-404.

Arthritis Research UK 2013, OSTEOARTHRITIS IN GENERAL PRACTICE; Data and perspectives.Available:http://www.arthritisresearchuk.org/arthritis-information/data-andstatistics/osteoarthritis.aspx [2018, 03/03].

Ateshian, G.A., Soltz, M.A., Mauck, R.L., Basalo, I.M., Hung, C.T. & Lai, W.M. 2003, The role of osmotic pressure and tension-compression nonlinearity in the frictional response of articular cartilage, Transport in Porous Media, 50(1-2), pp. 5-33.

Aydelotte, M.B. & Kuettner, K.E. 1988, Differences between sub-populations of cultured bovine articular chondrocytes. I. Morphology and cartilage matrix production, Connective tissue research, 18(3), pp. 205-222.

Baharvand, H., 2014. Stem Cell Nanoengineering. John Wiley & Sons.

Balazs, E.A. and Denlinger, J.L., 1989. Clinical uses of hyaluronan. The biology of hyaluronan, 265, p.285.

`

Barnes, C.P., Sell, S.A., Boland, E.D., Simpson, D.G. and Bowlin, G.L., 2007. Nanofiber technology: designing the next generation of tissue engineering scaffolds. Advanced drug delivery reviews, 59(14), pp.1413-1433.

Barth, A. and Haris, P.I. eds., 2009. Biological and biomedical infrared spectroscopy (Vol. 2). IOS press.

Bayliss, M.T., Venn, M., Maroudas, A. and Ali, S.Y., 1983. Structure of proteoglycans from different layers of human articular cartilage. Biochemical Journal, 209(2), pp.387-400.

Bekkers, J.E., Tsuchida, A.I., van Rijen, M.H., Vonk, L.A., Dhert, W.J., Creemers, L.B. & Saris, D.B. 2013, Single-stage cell-based cartilage regeneration using a combination of chondrons and mesenchymal stromal cells: comparison with microfracture, The American Journal of Sports Medicine, 41(9), pp. 2158-2166.

Bian, L., Zhai, D.Y., Mauck, R.L. and Burdick, J.A., 2011. Coculture of human mesenchymal stem cells and articular chondrocytes reduces hypertrophy and enhances functional properties of engineered cartilage. Tissue Engineering Part A, 17(7-8), pp.1137-1145.

Bidanset, D.J., Guidry, C., Rosenberg, L.C., Choi, H.U., Timpl, R. and Hook, M., 1992. Binding of the proteoglycan decorin to collagen type VI. Journal of Biological Chemistry, 267(8), pp.5250-5256.

Bobick, B.E., Chen, F.H., Le, A.M. and Tuan, R.S., 2009. Regulation of the chondrogenic phenotype in culture. Birth Defects Research Part C: Embryo Today: Reviews, 87(4), pp.351-371.

Boeuf, S. and Richter, W., 2010. Chondrogenesis of mesenchymal stem cells: role of tissue source and inducing factors. Stem cell research & therapy, 1(4), p.31.

Bonaventure, J., Kadhom, N., Cohen-Solal, L., Ng, K., Bourguignon, J., Lasselin, C. & Freisinger, P. 1994, Reexpression of cartilage-specific genes by dedifferentiated human articular chondrocytes cultured in alginate beads, Experimental cell research, 212(1), pp. 97-104.

`

Braghirolli, D.I., Steffens, D. and Pranke, P., 2014. Electrospinning for regenerative medicine: a review of the main topics. Drug discovery today, 19(6), pp.743-753.

Brittberg, M., Lindahl, A., Nilsson, A., Ohlsson, C., Isaksson, O. & Peterson, L. 1994, Treatment of deep cartilage defects in the knee with autologous chondrocyte transplantation, New england journal of medicine, 331(14), pp. 889-895.

Brodsky, B.A.R.B.A.R.A. and Shah, N.K., 1995. Protein motifs. 8. The triple-helix motif in proteins. The FASEB journal, 9(15), pp.1537-1546.

Bruder, S.P., Fink, D.J. and Caplan, A.I., 1994. Mesenchymal stem cells in bone development, bone repair, and skeletal regenaration therapy. Journal of cellular biochemistry, 56(3), pp.283-

Buckwalter, J.A., Mankin, H.J. & Grodzinsky, A.J. 2005, Articular cartilage and osteoarthritis, Instructional Course Lectures-American Academy of Orthopaedic Surgeons. 54, pp. 465.

Burdick, J.A. and Prestwich, G.D., 2011. Hyaluronic acid hydrogels for biomedical applications. Advanced materials, 23(12).

Bychkov, S.M. and Kuz'mina, S.A., 1992. Study of tissue proteoglycans by means of infrared spectroscopy. Biulleten'eksperimental'noi biologii i meditsiny, 114(9), pp.246-249.

Camacho, N.P., West, P., Torzilli, P.A. and Mendelsohn, R., 2001. FTIR microscopic imaging of collagen and proteoglycan in bovine cartilage. Biopolymers, 62(1), pp.1-8.

Camarero-Espinosa, S., Rothen-Rutishauser, B., Foster, E.J. and Weder, C., 2016. Articular cartilage: from formation to tissue engineering. Biomaterials science, 4(5), pp.734-767.

Caplan, A.I., Elyaderani, M., Mochizuki, Y., Wakitani, S. and Goldberg, V.M., 1997. Principles of cartilage repair and regeneration. Clinical orthopaedics and related research, (342), pp.254-269.

Carvalho, A.d.M., Yamada, A.L.M., Golim, M., Álvarez, L., Jorge, L., Conceição, M., Deffune, E., Hussni, C.A. & Alves, A. 2013, Characterization of mesenchymal stem cells derived from equine adipose tissue, Arquivo Brasileiro de Medicina Veterinária e Zootecnia, 65 (4), pp. 939-945.

`

Cescon, M., Gattazzo, F., Chen, P. and Bonaldo, P., 2015. Collagen VI at a glance. J Cell Sci, 128(19), pp.3525-3531.

Chang, J. and Poole, C.A., 1997. Confocal analysis of the molecular heterogeneity in the pericellular microenvironment produced by adult canine chondrocytes cultured in agarose gel. The Histochemical journal, 29(7), pp.515-528.

Chu, W.C., Zhang, S., Sng, T.J., Ong, Y.J., Tan, W.L., Ang, V.Y., Foldager, C.B. and Toh, W.S., 2017. Distribution of pericellular matrix molecules in the temporomandibular joint and their chondroprotective effects against inflammation. International journal of oral science, 9(1), p.43.

Clair, B.L., Johnson, A.R. & Howard, T. 2009, Cartilage repair: current and emerging options in treatment, Foot & ankle specialist, 2(4), pp. 179-188.

Cohen, N.P., Foster, R.J. & Mow, V.C. 1998, Composition and dynamics of articular cartilage: structure, function, and maintaining healthy state, The Journal of orthopaedic and sports physical therapy, 28(4), pp. 203-215.

Collins, Maurice N., and Colin Birkinshaw. 2013, Hyaluronic acid based scaffolds for tissue engineering—A review. Carbohydrate polymers, 92 (2) pp.1262-1279.

Crockett, R., Grubelnik, A., Roos, S., Dora, C., Born, W. & Troxler, H. 2007, Biochemical composition of the superficial layer of articular cartilage, Journal of Biomedical Materials Research Part A, 82 (4), pp. 958-964.

Dahlin, R.L., Kasper, F.K. and Mikos, A.G., 2011. Polymeric nanofibers in tissue engineering. Tissue Engineering Part B: Reviews, 17(5), pp.349-364.

Dalby, Matthew J., Stephen J. Yarwood, Mathis O. Riehle, Heather JH Johnstone, Stanley Affrossman, and Adam SG Curtis. 2002, Increasing fibroblast response to materials using nanotopography: morphological and genetic measurements of cell response to 13-nm-high polymer demixed islands. Experimental cell research, 276 (1) pp. 1-9.

`

Deegan, A.J., Cinque, G., Wehbe, K., Konduru, S. and Yang, Y., 2015. Tracking calcification in tissue-engineered bone using synchrotron micro-FTIR and SEM. Analytical and bioanalytical chemistry, 407(4), pp.1097-1105.

De Ninno, A., Gerardino, A., Girarda, B., Grenci, G. and Businaro, L., 2010. Top-Down approach to nanotechnology for cell-on-chip applications. Biophysics and Bioengineering Letters, 3(2).

Dimicco, M.A., Kisiday, J.D., Gong, H. and Grodzinsky, A.J., 2007. Structure of pericellular matrix around agarose-embedded chondrocytes. Osteoarthritis and cartilage, 15(10), pp.1207-1216.

Drury, J.L. and Mooney, D.J., 2003. Hydrogels for tissue engineering: scaffold design variables and applications. Biomaterials, 24(24), pp.4337-4351.

Engineering toolbox/ Stress, Strain and Young's Modulus. 2011. Available: http:// www.engineeringtoolbox.com/stress-strain-d_950.html [2018, 04/04].

Enomoto, M., Leboy, P.S., Menko, A.S. and Boettiger, D., 1993. β1 integrins mediate chondrocyte interaction with type I collagen, type II collagen, and fibronectin. Experimental cell research, 205(2), pp.276-285.

Eslahi, N., Abdorahim, M. and Simchi, A., 2016. Smart polymeric hydrogels for cartilage tissue engineering: A review on the chemistry and biological functions. Biomacromolecules, 17(11), pp.3441-3463.

Eyre, D.R., 2004. Collagens and cartilage matrix homeostasis. Clinical orthopaedics and related research, 427, pp.S118-S122.

Farndale, R.W., Buttle, D.J. & Barrett, A.J. 1986, Improved quantitation and discrimination of sulphated glycosaminoglycans by use of dimethylmethylene blue, Biochimica et Biophysica Acta (BBA)-General Subjects, 883 (2), pp. 173-177.

Fischer, J., Dickhut, A., Rickert, M. and Richter, W., 2010. Articular chondrocytes secrete PTHrP and inhibit hypertrophy of mesenchymal stem cells in coculture during chondrogenesis. Arthritis Rheum, 62(9), pp.2696-2706.

`

Fortier, L.A., Barker, J.U., Strauss, E.J., McCarrel, T.M. and Cole, B.J., 2011. The role of growth factors in cartilage repair. Clinical Orthopaedics and Related Research®, 469(10), pp.2706-2715.

Fragonas, E., Valente, M., Pozzi-Mucelli, M., Toffanin, R., Rizzo, R., Silvestri, F. and Vittur, F., 2000. Articular cartilage repair in rabbits by using suspensions of allogenic chondrocytes in alginate. Biomaterials, 21(8), pp.795-801.

Frenkel, S.R. and Di Cesare, P.E., 2004. Scaffolds for articular cartilage repair. Annals of biomedical engineering, 32(1), pp.26-34.

Fuller, J.A. and Ghadially, F.N., 1972. Ultrastructural observations on surgically produced partial-thickness defects in articular cartilage. Clinical orthopaedics and related research, 86, pp.193-205.

Funayama, A., Niki, Y., Matsumoto, H., Maeno, S., Yatabe, T., Morioka, H., Yanagimoto, S., Taguchi, T., Tanaka, J. and Toyama, Y., 2008. Repair of full-thickness articular cartilage defects using injectable type II collagen gel embedded with cultured chondrocytes in a rabbit model. Journal of Orthopaedic Science, 13(3), pp.225-232.

Furumatsu, T., Tsuda, M., Taniguchi, N., Tajima, Y. & Asahara, H. 2005, Smad3 induces chondrogenesis through the activation of SOX9 via CREB-binding protein/p300 recruitment, The Journal of biological chemistry, 280(9), pp. 8343-8350.

García-Martínez, L., Campos, F., Godoy-Guzmán, C., del Carmen Sánchez-Quevedo, M., Garzón, I., Alaminos, M., Campos, A. and Carriel, V., 2017. Encapsulation of human elastic cartilage-derived chondrocytes in nanostructured fibrin-agarose hydrogels. Histochemistry and cell biology, 147(1), pp.83-95.

Garg, H.G. and Hales, C.A. eds., 2004. Chemistry and biology of hyaluronan. Elsevier.

Glass-Brudzinski, J., Perizzolo, D. and Brunette, D.M., 2002. Effects of substratum surface topography on the organization of cells and collagen fibers in collagen gel cultures. Journal of Biomedical Materials Research Part A, 61(4), pp.608-618.

Goessler, U.R., Bugert, P., Bieback, K., Baisch, A., Sadick, H., Verse, T., Klüter, H., Hörmann, K. and Riedel, F., 2004. Expression of collagen and fiber-associated proteins in human septal cartilage during in vitro dedifferentiation. International journal of molecular medicine, 14(6), pp.1015-1022.

Grieshaber, S.E., Jha, A.K., Farran, A.J. and Jia, X., 2011. Hydrogels in tissue engineering. In Biomaterials for Tissue Engineering Applications (pp. 9-46). Springer Vienna.

Guilak, F., Ratcliffe, A., Lane, N., Rosenwasser, M.P. & Mow, V.C. 1994, Mechanical and biochemical changes in the superficial zone of articular cartilage in canine experimental osteoarthritis, Journal of Orthopaedic Research, 12, (4), pp. 474-484.

Haddo, O., Mahroof, S., Higgs, D., David, L., Pringle, J., Bayliss, M., Cannon, S. & Briggs,

T. 2004, "The use of chondrogide membrane in autologous chondrocyte implantation", The

Knee, vol. 11, no. 1, pp. 51-55.

Hardingham, T.E., Fosang, A.J. & Dudhia, J. 1994, The structure, function and turnover of aggrecan, the large aggregating proteoglycan from cartilage, European journal of clinical chemistry and clinical biochemistry: journal of the Forum of European Clinical Chemistry Societies, 32 (4), pp. 249-257.

Hardingham, T.E., and Muir, H. (1972). The specific interaction of hyaluronic acid with cartilage proteoglycans Biochim. Biophys. Acta 279,401-405.

Hendriks, J., Riesle, J. and van Blitterswijk, C.A., 2007. Co-culture in cartilage tissue engineering. Journal of tissue engineering and regenerative medicine, 1(3), pp.170-178.

Hoemann, C.D., 2004. Molecular and biochemical assays of cartilage components. Cartilage and Osteoarthritis: Volume 2: Structure and In Vivo Analysis, pp.127-156.

Hou, Y., Lin, H., Zhu, L., Liu, Z., Hu, F., Shi, J., Yang, T., Shi, X., Zhu, M. & Godley, B.F. 2013, Lipopolysaccharide Increases the Incidence of Collagen-Induced Arthritis in Mice Through Induction of Protease HTRA-1 Expression, Arthritis & Rheumatism, 65 (11), pp. 2835-2846.

`

Hu, S.I., Carozza, M., Klein, M., Nantermet, P., Luk, D. and Crowl, R.M., 1998. Human HtrA, an evolutionarily conserved serine protease identified as a differentially expressed gene product in osteoarthritic cartilage. Journal of Biological Chemistry, 273(51), pp.34406-34412.

Hubbell, J.A., 1995. Biomaterials in tissue engineering. Nature Biotechnology, 13(6), pp.565-576.

Huber, M., Trattnig, S. and Lintner, F., 2000. Anatomy, biochemistry, and physiology of articular cartilage. Investigative radiology, 35(10), pp.573-580.

Hunziker, E.B., 1999. Articular cartilage repair: are the intrinsic biological constraints undermining this process insuperable?. Osteoarthritis and Cartilage, 7(1), pp.15-28.

Hunziker, E.B., Quinn, T.M. and Häuselmann, H.J., 2002. Quantitative structural organization of normal adult human articular cartilage. Osteoarthritis and Cartilage, 10(7), pp.564-572.

Hutmacher, D.W., 2000. Scaffolds in tissue engineering bone and cartilage. Biomaterials, 21(24), pp.2529-2543.

Hutmacher, D.W., 2000. Scaffolds in tissue engineering bone and cartilage. Biomaterials, 21(24), pp.2529-2543.

Hynes, R.O., 1992. Integrins: versatility, modulation, and signaling in cell adhesion. Cell, 69(1), pp.11-25

Ikada, Y., 2006. Challenges in tissue engineering. Journal of the Royal Society Interface, 3(10), pp.589-601.

Jackson, R.W. and Dieterichs, C., 2003. The results of arthroscopic lavage and debridement of osteoarthritic knees based on the severity of degeneration. Arthroscopy: The Journal of Arthroscopic & Related Surgery, 19(1), pp.13-20.

Jaiswal N, Haynesworth SE, Caplan AI and Bruder SP. Osteogenic differentiation of purified, culture-expanded human mesenchymal stem cells in vitro. Journal of Cellular Biochemistry 1997;64(2):295-312.

Jayakumar, R. and Nair, S. eds., 2012. Biomedical applications of polymeric nanofibers (Vol. 246). Springer Science & Business Media.

`

Johnstone, B., Alini, M., Cucchiarini, M., Dodge, G.R., Eglin, D., Guilak, F., Madry, H., Mata, A., Mauck, R.L., Semino, C.E. & Stoddart, M.J. 2013, Tissue engineering for articular cartilage repair--the state of the art, European cells & materials, 25 (2), pp. 248-267.

Jones, A.R., Gleghorn, J.P., Hughes, C.E., Fitz, L.J., Zollner, R., Wainwright, S.D., Caterson, B., Morris, E.A., Bonassar, L.J. & Flannery, C.R. 2007, Binding and localization of recombinant lubricin to articular cartilage surfaces, Journal of orthopaedic research, 25 (3), pp. 283-292.

Kielty, C.M., Whittaker, S.P., Grant, M.E. and Shuttleworth, C.A., 1992. Type VI collagen microfibrils: evidence for a structural association with hyaluronan. The Journal of Cell Biology, 118(4), pp.979-990.

Kim, M., Bi, X., Horton, W.E., Spencer, R.G. and Camacho, N.P., 2005. Fourier transform infrared imaging spectroscopic analysis of tissue engineered cartilage: histologic and biochemical correlations. Journal of biomedical optics, 10(3), p.031105.

Kim, Y., Sah, R.L., Doong, J.H. & Grodzinsky, A.J. 1988, Fluorometric assay of DNA in cartilage explants using Hoechst 33258, Analytical Biochemistry, 174 (1), pp. 168-176.

King, M.W., 2014. Integrative Medical Biochemistry: Examination and Board Review. McGraw Hill Professional.

Klein, T., Schumacher, B., Schmidt, T., Li, K., Voegtline, M., Masuda, K., Thonar, E. & Sah, R. 2003, Tissue engineering of stratified articular cartilage from chondrocyte subpopulations, Osteoarthritis and cartilage, 11(8), pp. 595-602.

Klein, T.J., Malda, J., Sah, R.L. & Hutmacher, D.W. 2009, Tissue engineering of articular cartilage with biomimetic zones, Tissue Engineering Part B: Reviews, 15, (2), pp.143-157.

Kock, L., van Donkelaar, C.C. & Ito, K. 2012, Tissue engineering of functional articular cartilage: the current status, Cell and tissue research, 347, (3), pp. 613-627.

Kontturi, L.S., Järvinen, E., Muhonen, V., Collin, E.C., Pandit, A.S., Kiviranta, I., Yliperttula, M. and Urtti, A., 2014. An injectable, in situ forming type II collagen/hyaluronic acid hydrogel

vehicle for chondrocyte delivery in cartilage tissue engineering. Drug delivery and translational research, 4(2), pp.149-158.

Kook, Y.M., Jeong, Y., Lee, K. and Koh, W.G., 2017. Design of biomimetic cellular scaffolds for co-culture system and their application. Journal of tissue engineering, 8, p.2041731417724640.

Kühtreiber, W.M., Lanza, R.P. & Chick, W.L. 1999, Cell encapsulation technology and therapeutics, Springer Science & Business Media.

Kumbar, S.G., James, R., Nukavarapu, S.P. and Laurencin, C.T., 2008. Electrospun nanofiber scaffolds: engineering soft tissues. Biomedical materials, 3(3), p.034002.

Landínez-Parra, N.S., Garzón-Alvarado, D.A. and Vanegas-Acosta, J.C., 2012. Mechanical behavior of articular cartilage. In Injury and Skeletal Biomechanics. InTech.

Lanza, R., Langer, R. and Vacanti, J.P. eds., 2011. Principles of tissue engineering. Academic press.

Larson, C.M., Kelley, S.S., Blackwood, A.D., Banes, A.J. and Lee, G.M., 2002. Retention of the native chondrocyte pericellular matrix results in significantly improved matrix production. Matrix biology, 21(4), pp.349-359.

Laurencin, C.T., Ambrosio, A., Borden, M. & Cooper Jr, J. 1999, Tissue engineering: orthopedic applications, Annual Review of Biomedical Engineering, 1, (1), pp. 19-46.

Lee, G.M. and Loeser, R.F., 1998. Interactions of the chondrocyte with its pericellular matrix. Cells Mater, 8, pp.135-149.

Lee, G.M., Poole, C.A., Kelley, S.S., Chang, J. and Caterson, B., 1997. Isolated chondrons: a viable alternative for studies of chondrocyte metabolism in vitro. Osteoarthritis and cartilage, 5(4), pp.261-274.

Leijten, J.C., Georgi, N., Wu, L., van Blitterswijk, C.A. and Karperien, M., 2012. Cell sources for articular cartilage repair strategies: shifting from monocultures to cocultures. Tissue Engineering Part B: Reviews, 19(1), pp.31-40.

Lettry, V., Hosoya, K., Takagi, S. and Okumura, M., 2010. Coculture of equine mesenchymal stem cells and mature equine articular chondrocytes results in improved chondrogenic differentiation of the stem cells. Japanese Journal of Veterinary Research, 58(1), pp.5-15.

Levorson, E.J., Santoro, M., Kasper, F.K. and Mikos, A.G., 2014. Direct and indirect co-culture of chondrocytes and mesenchymal stem cells for the generation of polymer/extracellular matrix hybrid constructs. Acta biomaterialia, 10(5), pp.1824-1835.

Li, W.J., Danielson, K.G., Alexander, P.G. and Tuan, R.S., 2003. Biological response of chondrocytes cultured in three-dimensional nanofibrous poly (ϵ-caprolactone) scaffolds. Journal of Biomedical Materials Research Part A, 67(4), pp.1105-1114.

Liu, J., Nie, H., Xu, Z., Niu, X., Guo, S., Yin, J., Guo, F., Li, G., Wang, Y. and Zhang, C., 2014. The effect of 3D nanofibrous scaffolds on the chondrogenesis of induced pluripotent stem cells and their application in restoration of cartilage defects. PloS one, 9(11), p.e111566.

Liu, Y., Zhou, G. and Cao, Y., 2017. Recent Progress in Cartilage Tissue Engineering—Our Experience and Future Directions. Engineering, 3(1), pp.28-35.

Loeser, R.F., 2014. Integrins and chondrocyte–matrix interactions in articular cartilage. Matrix Biology, 39, pp.11-16.

Loeser, R.F., Goldring, S.R., Scanzello, C.R. and Goldring, M.B., 2012. Osteoarthritis: a disease of the joint as an organ. Arthritis & Rheumatology, 64(6), pp.1697-1707.

Mackay, A.M., Beck, S.C., Murphy, J.M., Barry, F.P., Chichester, C.O. and Pittenger, M.F., 1998. Chondrogenic differentiation of cultured human mesenchymal stem cells from marrow. Tissue engineering, 4(4), pp.415-428.

Malda, J., Ten Hoope, W., Schuurman, W., Van Osch, G.J., Van Weeren, P.R. & Dhert, W.J. 2009, Localization of the potential zonal marker clusterin in native cartilage and in tissue-engineered constructs, Tissue Engineering Part A, 16, (3), pp. 897-904.

Malloy, K.M. & Hilibrand, A.S. 2002, Autograft versus allograft in degenerative cervical disease., Clinical orthopaedics and related research, 394, pp. 27-38.

`

Mankin, H. J., Ratcliffe, A., Iannotti, J. P., Buckwalter, J. A., and Mow, V. C. (2000). Chapter17 Articular Cartilage Structure, Composition, and Function. In Orthopaedic basic science :biology and biomechanics of the musculoskeletal system, Rosemont, ed. (Illinois: American Academy of Orthopaedic Surgeons), pp. 443-470.

Mankin, H.J. and Thrasher, A.Z., 1975. Water content and binding in normal and osteoarthritic human cartilage. The Journal of bone and joint surgery. 57(1), pp.76-80.

Mao, X., Chu, C.L., Mao, Z. & Wang, J.J. 2005, The development and identification of constructing tissue engineered bone by seeding osteoblasts from differentiated rat marrow stromal stem cells onto three-dimensional porous nano-hydroxylapatite bone matrix in vitro, Tissue & cell, 37, (5), pp. 349-357.

Marlovits, S., Zeller, P., Singer, P., Resinger, C. & Vécsei, V. 2006, "Cartilage repair: generations of autologous chondrocyte transplantation", European Journal of Radiology, vol. 57, no. 1, pp. 24-31.

Maroudas, A., Bullough, P.E.T.E.R., Swanson, S.A.V. and Freeman, M.A.R., 1968. The permeability of articular cartilage. The Journal of bone and joint surgery., 50(1), pp.166-177.

Mauck, R.L., Yuan, X. and Tuan, R.S., 2006. Chondrogenic differentiation and functional maturation of bovine mesenchymal stem cells in long-term agarose culture. *Osteoarthritis and cartilage*, *14*(2), pp.179-189.

Mayne, R. 1989, Cartilage collagens. What is their function, and are they involved in articular disease?, Arthritis & Rheumatism, 32(3), pp. 241-246.

McDevitt, C.A., Marcelino, J. and Tucker, L., 1991. Interaction of intact type VI collagen with hyaluronan. FEBS letters, 294(3), pp.167-170.

McIlwraith, C.W., 2013. Oral joint supplements in the management of osteoarthritis. In Equine Applied and Clinical Nutrition (pp. 549-557).

Melero-Martin, J. & Al-Rubeai, M. 2007, In vitro expansion of chondrocytes, Topics in tissue engineering, 3, pp. 1-37.

`

Meretoja, V.V., Dahlin, R.L., Kasper, F.K. & Mikos, A.G. 2012, Enhanced chondrogenesis in co-cultures with articular chondrocytes and mesenchymal stem cells, Biomaterials, 33, (27), pp. 6362-6369.

Mikos, A.G. and Temenoff, J.S., 2000. Formation of highly porous biodegradable scaffolds for tissue engineering. Electronic Journal of Biotechnology, 3(2), pp.23-24.

Miller, L.M. and Smith, R.J., 2005. Synchrotrons versus globars, point-detectors versus focal plane arrays: Selecting the best source and detector for specific infrared microspectroscopy and imaging applications. Vibrational spectroscopy, 38(1-2), pp.237-240.

Milner, P.I., Gibson, J.S. & Wilkins, R.J. 2012, Cellular physiology of articular cartilage in health and disease, INTECH Open Access Publisher.

Mistry, H., Connock, M., Pink, J., Shyangdan, D., Clar, C., Royle, P., Court, R., Biant, L.C., Metcalfe, A. and Waugh, N., 2017. Autologous chondrocyte implantation in the knee: systematic review and economic evaluation.

Mirzaei, S., Karkhaneh, A., Soleimani, M., Ardeshirylajimi, A., Seyyed Zonouzi, H. and Hanaee‐Ahvaz, H., 2017. Enhanced chondrogenic differentiation of stem cells using an optimized electrospun nanofibrous PLLA/PEG scaffolds loaded with glucosamine. Journal of Biomedical Materials Research Part A, 105(9), pp.2461-2474.

Mok, S.S., Masuda, K., Häuselmann, H.J., Aydelotte, M.B. and Thonar, E.J., 1994. Aggrecan synthesized by mature bovine chondrocytes suspended in alginate. Identification of two distinct metabolic matrix pools. Journal of Biological Chemistry, 269(52), pp.33021-33027.

Muir, H., 1978. Proteoglycans of cartilage. Journal of Clinical Pathology. Supplement (Royal College of Pathologists)., 12, p.67.

Mujeeb, A. and Ge, Z., 2014. Biomaterials for Cartilage Regeneration. Journal of the American Academy of Orthopaedic Surgeons, 22(10), pp.674-676.

Muschler, G.F., Nakamoto, C. and Griffith, L.G., 2004. Engineering principles of clinical cell-based tissue engineering. JBJS, 86(7), pp.1541-1558.

`

National institute for health and clinical excellence 2017, Autologous chondrocyte implantation for treating symptomatic articular cartilage defects of the knee. Available: https://www.nice.org.uk/guidance/ta477/ [2018, 05/05].

Nehrer, S., Breinan, H., Ramappa, A., Hsu, H., Minas, T., Shortkroff, S., Sledge, C., Yannas, I. & Spector, M. 1998, Chondrocyte-seeded collagen matrices implanted in a chondral defect in a canine model, Biomaterials, 19, (24), pp. 2313-2328.

Nejadnik, H., Hui, J.H., Feng Choong, E.P., Tai, B.C. and Lee, E.H., 2010. Autologous bone marrow–derived mesenchymal stem cells versus autologous chondrocyte implantation: an observational cohort study. The American journal of sports medicine, 38(6), pp.1110-1116.

Ng, K.W., Wang, C.C., Mauck, R.L., Kelly, T.N., Chahine, N.O., Costa, K.D., Ateshian, G.A. & Hung, C.T. 2005, A layered agarose approach to fabricate depth-dependent inhomogeneity in chondrocyte-seeded constructs, Journal of Orthopaedic Research, 23, (1), pp. 134-141.

Nguyen, B.V., Wang, Q.G., Kuiper, N.J., El Haj, A.J., Thomas, C.R. and Zhang, Z., 2010. Biomechanical properties of single chondrocytes and chondrons determined by micromanipulation and finite-element modelling. Journal of the Royal Society Interface, *7*(53), pp.1723-1733.

Nigg, B.M., Herzog, W. and Herzog, W., 1999. Biomechanics of the musculo-skeletal system (Vol. 2). New York: Wiley.

Nikpou, P., Nejad, D.M., Shafaei, H., Roshangar, L., Samadi, N., Navali, A.M., Sadegpour, A.R., Shanehbandi, D. & Rad, J.S. 2016, Study of chondrogenic potential of stem cells in co-culture with chondrons, Iranian Journal of Basic Medical Sciences, 19, (6), pp. 638.

Nuernberger, S., Cyran, N., Albrecht, C., Redl, H., Vécsei, V. and Marlovits, S., 2011. The influence of scaffold architecture on chondrocyte distribution and behavior in matrix-associated chondrocyte transplantation grafts. Biomaterials, 32(4), pp.1032-1040.

Ondarcuhu, T. and Joachim, C., 1998. Drawing a single nanofibre over hundreds of microns. EPL (Europhysics Letters), 42(2), p.215.

Petit, B., Masuda, K., D'souza, A.L., Otten, L., Pietryla, D., Hartmann, D.J., Morris, N.P., Uebelhart, D., Schmid, T.M. and Thonar, E.M., 1996. Characterization of crosslinked collagens synthesized by mature articular chondrocytes cultured in alginate beads: comparison of two distinct matrix compartments. Experimental cell research, 225(1), pp.151-161.

Pham, Q.P., Sharma, U. and Mikos, A.G., 2006. Electrospinning of polymeric nanofibers for tissue engineering applications: a review. Tissue engineering, 12(5), pp.1197-1211.

Pittenger MF, Mackay AM, Beck SC, Jaiswal RK, Douglas R, Mosca JD, Moorman MA, Simonetti DW, Craig S and Marshak DR. Multilineage Potential of Adult Human Mesenchymal Stem Cells. Science 1999;284(5411):143-147.

Polur, I., Lee, P.L., Servais, J.M., Xu, L. & Li, Y. 2010, Role of HTRA1, a serine protease, in the progression of articular cartilage degeneration, Histology and histopathology, 25, (5), pp. 599-608.

Poole, A.R., Kojima, T., Yasuda, T., Mwale, F., Kobayashi, M. & Laverty, S. 2001, Composition and structure of articular cartilage: a template for tissue repair. Clinical orthopaedics and related research, 391 (2), pp. S26-S33.

Poole, C.A. 1997, Review. Articular cartilage chondrons: form, function and failure, Journal of anatomy, 191, (1), pp. 1-13.

Poole, C.A., 1992. Chondrons: the chondrocyte and its pericellular microenvironment. Articular cartilage and osteoarthritis, pp.201-220.

Poole, C.A., Flint, M.H. & Beaumont, B.W. 1984, Morphological and functional interrelationships of articular cartilage matrices, Journal of anatomy138, (1), pp. 113-138.

Poole, C.A., Flint, M.H. and Beaumont, B.W., 1987. Chondrons in cartilage: ultrastructural analysis of the pericellular microenvironment in adult human articular cartilages. Journal of orthopaedic research, 5(4), pp.509-522.

`

Poole, C.A., Flint, M.H. and Beaumont, B.W., 1988. Chondrons extracted from canine tibial cartilage: preliminary report on their isolation and structure. Journal of Orthopaedic Research, 6(3), pp.408-419.

Potter, K., Kidder, L.H., Levin, I.W., Lewis, E.N. and Spencer, R.G., 2001. Imaging of collagen and proteoglycan in cartilage sections using Fourier transform infrared spectral imaging. Arthritis & Rheumatology, 44(4), pp.846-855.

Qing, C., Wei-ding, C. and Wei-min, F., 2011. Co-culture of chondrocytes and bone marrow mesenchymal stem cells in vitro enhances the expression of cartilaginous extracellular matrix components. Brazilian Journal of Medical and Biological Research, 44(4), pp.303-310.

Rahfoth, B., Weisser, J., Sternkopf, F., Aigner, T., Von Der Mark, K. and Bräuer, R., 1998. Transplantation of allograft chondrocytes embedded in agarose gel into cartilage defects of rabbits. Osteoarthritis and cartilage, 6(1), pp.50-65.

Ramakrishna, S., Fujihara, K., Teo, W.E., Lim, T.C. and Ma, Z., An introduction to electrospinning and nanofibers. 2005. Singapura: World Scientific Publishing Company.

Redman, S.N., Oldfield, S.F. & Archer, C.W. 2005, Current strategies for articular cartilage repair, European cells & materials, 9 (2), pp. 23-32; discussion 23-32.

Richardson, J.B., Caterson, B., Evans, E.H., Ashton, B.A. and Roberts, S., 1999. Repair of human articular cartilage after implantation of autologous chondrocytes. J Bone Joint Surg Br, 81(6), pp.1064-1068.

Roughley, P.J., 2001. Articular cartilage and changes in arthritis: noncollagenous proteins and proteoglycans in the extracellular matrix of cartilage. Arthritis Research & Therapy, 3(6), p.342.

Saha, S., Kirkham, J., Wood, D., Curran, S. and Yang, X.B., 2011. Adult stem cells for articular cartilage tissue engineering. Stem cell and tissue engineering. World Scientific, Singapore, pp.211-230.

Salter, D.M., Hughes, D.E., Simpson, R. and Gardner, D.L., 1992. Integrin expression by human articular chondrocytes. Rheumatology, 31(4), pp.231-234.

Schmid, T.M. and Linsenmayer, T.F., 1985. Immunohistochemical localization of short chain cartilage collagen (type X) in avian tissues. The Journal of cell biology, 100(2), pp.598-605.

Schurman, D.J. and Smith, R.L., 2004. Osteoarthritis: current treatment and future prospects for surgical, medical, and biologic intervention. Clinical orthopaedics and related research, 427, pp.S183-S189.

Shafaei, H., Bagernezhad, H. and Bagernajad, H., 2017. Importance of Floating Chondrons in Cartilage Tissue Engineering. World journal of plastic surgery, 6(1), p.62.

Smith, L.A. and Ma, P.X., 2004. Nano-fibrous scaffolds for tissue engineering. Colloids and surfaces B: biointerfaces, 39(3), pp.125-131.

Solchaga, L.A., Gao, J., Dennis, J.E., Awadallah, A., Lundberg, M., Caplan, A.I. and Goldberg, V.M., 2002. Treatment of osteochondral defects with autologous bone marrow in a hyaluronan-based delivery vehicle. Tissue engineering, 8(2), pp.333-347.

Solchaga, L.A., Goldberg, V.M. and Caplan, A.I., 2001. Cartilage regeneration using principles of tissue engineering. Clinical Orthopaedics and Related Research, 391, pp.S161-S170.

Song, L., Baksh, D. and Tuan, R.S., 2004. Mesenchymal stem cell-based cartilage tissue engineering: cells, scaffold and biology. Cytotherapy, 6(6), pp.596-601.

Sonomoto, K., Yamaoka, K., Kaneko, H., Yamagata, K., Sakata, K., Zhang, X., Kondo, M., Zenke, Y., Sabanai, K., Nakayamada, S. and Sakai, A., 2016. Spontaneous differentiation of human mesenchymal stem cells on poly-lactic-co-glycolic acid nano-fiber scaffold. PloS one, 11(4), p.e0153231.

Sophia Fox, A.J., Bedi, A. and Rodeo, S.A., 2009. The basic science of articular cartilage: structure, composition, and function. Sports health, 1(6), pp.461-468.

`

Steele, J., McCullen, S., Callanan, A., Autefage, H., Accardi, M., Dini, D. & Stevens, M. 2014, Combinatorial scaffold morphologies for zonal articular cartilage engineering, Acta biomaterialia, 10(5), pp. 2065-2075.

Steward, A.J., Liu, Y. and Wagner, D.R., 2011. Engineering cell attachments to scaffolds in cartilage tissue engineering. JOM, 63(4), pp.74-82.

Stewart, M.C., Saunders, K.M., Burton-Wurster, N. & Macleod, J.N. 2000, Phenotypic stability of articular chondrocytes in vitro: the effects of culture models, bone morphogenetic protein 2, and serum supplementation, Journal of bone and mineral research, 15(1), pp. 166-174.

Stockwell, R.A., 1979. Biology of cartilage cells (Vol. 7). CUP Archive.

Svoboda, K.K., 1998. Chondrocyte-matrix attachment complexes mediate survival and differentiation. Microscopy research and technique, 43(2), pp.111-122.

Szirmai, J.A., 1974. The concept of the chondron as a biomechanical unit. In Biopolymere und Biomechanik von Bindegewebssystemen (pp. 87-91). Springer, Berlin, Heidelberg.

Tan, H. and Marra, K.G., 2010. Injectable, biodegradable hydrogels for tissue engineering applications. Materials, 3(3), pp.1746-1767.

Temenoff, J.S. & Mikos, A.G. 2000, Review: tissue engineering for regeneration of articular cartilage, Biomaterials, 21, (5), pp. 431-440.

Teo, W.E. and Ramakrishna, S., 2006. A review on electrospinning design and nanofibre assemblies. Nanotechnology, 17(14), p.R89.

Tijore, A., Irvine, S.A., Sarig, U., Mhaisalkar, P., Baisane, V. and Venkatraman, S., 2018. Contact guidance for cardiac tissue engineering using 3D bioprinted gelatin patterned hydrogel. Biofabrication, 10(2), p.025003.

Treppo, S., Koepp, H., Quan, E.C., Cole, A.A., Kuettner, K.E. and Grodzinsky, A.J., 2000. Comparison of biomechanical and biochemical properties of cartilage from human knee and ankle pairs. Journal of Orthopaedic Research, 18(5), pp.739-748.

Tsuchiya, K., Chen, G., Ushida, T., Matsuno, T. and Tateishi, T., 2004. The effect of coculture of chondrocytes with mesenchymal stem cells on their cartilaginous phenotype in vitro. Materials science and engineering: C, 24(3), pp.391-396.

Tsuchiya, A., Yano, M., Tocharus, J., Kojima, H., Fukumoto, M., Kawaichi, M. and Oka, C., 2005. Expression of mouse HtrA1 serine protease in normal bone and cartilage and its upregulation in joint cartilage damaged by experimental arthritis. Bone, 37(3), pp.323-336.

Van de Witte, P., Dijkstra, P.J., Van den Berg, J.W.A. and Feijen, J., 1996. Phase separation processes in polymer solutions in relation to membrane formation. Journal of Membrane Science, 117(1-2), pp.1-31.

Van Osch, G.J., Brittberg, M., Dennis, J.E., Bastiaansen-Jenniskens, Y.M., Erben, R.G., Konttinen, Y.T. and Luyten, F.P., 2009. Cartilage repair: past and future–lessons for regenerative medicine. Journal of cellular and molecular medicine, 13(5), pp.792-810.

Van Pham, P., 2016. Mesenchymal Stem Cells in Clinical Applications. In *Stem Cell Processing* (pp. 37-69). Springer International Publishing.

Varghese, S. and Elisseeff, J.H., 2006. Hydrogels for musculoskeletal tissue engineering. In Polymers for regenerative medicine (pp. 95-144). Springer Berlin Heidelberg.

Vega, S.L., Kwon, M.Y. and Burdick, J.A., 2017. Recent advances in hydrogels for cartilage tissue engineering. European cells & materials, 33, p.59.

Vijayan, S., Bentley, G., Briggs, T.W.R., Skinner, J.A., Carrington, R.W.J., Pollock, R. and Flanagan, A.M., 2010. Cartilage repair: A review of Stanmore experience in the treatment of osteochondral defects in the knee with various surgical techniques. Indian journal of orthopaedics, 44(3), p.238.

Vinatier, C., Bouffi, C., Merceron, C., Gordeladze, J., Brondello, J.M., Jorgensen, C., Weiss, P., Guicheux, J. & Noel, D. 2009, Cartilage tissue engineering: towards a biomaterial assisted mesenchymal stem cell therapy, Current stem cell research & therapy, 4, (4), pp. 318-329.

`

Vonk, L.A., de Windt, T., Kragten, A., Beekhuizen, M., Mastbergen, S., Dhert, W., Lafeber, F., Creemers, L. & Saris, D. 2014, Enhanced cell-induced articular cartilage regeneration by chondrons; the influence of joint damage and harvest site, Osteoarthritis and Cartilage, 22 (11), pp. 1910-1917.

Vonk, L.A., Doulabi, B.Z., Huang, C., Helder, M.N., Everts, V. & Bank, R.A. 2010, Preservation of the chondrocyte's pericellular matrix improves cell-induced cartilage formation, Journal of cellular biochemistry, 110, (1), pp. 260-271.

Vrana, E., Builles, N., Hindie, M., Damour, O., Aydinli, A. and Hasirci, V., 2008. Contact guidance enhances the quality of a tissue engineered corneal stroma. Journal of Biomedical Materials Research Part A, 84(2), pp.454-463.

Wakitani, S., Goto, T., Pineda, S.J., Young, R.G., Mansour, J.M., Caplan, A.I. and Goldberg, V.M., 1994. Mesenchymal cell-based repair of large, full-thickness defects of articular cartilage. JBJS, 76(4), pp.579-592.

Waldman, S.D., Grynpas, M.D., Pilliar, R.M. & Kandel, R.A. 2003, The use of specific chondrocyte populations to modulate the properties of tissue-engineered cartilage, Journal of orthopaedic research, 21, (1), pp. 132-138.

Walenda, T., Bork, S., Horn, P., Wein, F., Saffrich, R., Diehlmann, A., Eckstein, V., Ho, A.D. and Wagner, W., 2010. Co-culture with mesenchymal stromal cells increases proliferation and maintenance of haematopoietic progenitor cells. Journal of cellular and molecular medicine, 14(1-2), pp.337-350.

Wang, Q., Hughes, N., Cartmell, S. & Kuiper, N. 2010,. The composition of hydrogels for cartilage tissue engineering can influence glycosaminoglycan profile, Eur Cell Mater, 19 (2). 86-95, pp. b93.

Wang, Q.G., El Haj, A.J. & Kuiper, N.J. 2008, Glycosaminoglycans in the pericellular matrix of chondrons and chondrocytes, Journal of anatomy, 213, (3), pp. 266-273.

Wang, Q.G., Magnay, J.L., Nguyen, B., Thomas, C.R., Zhang, Z., El Haj, A.J. & Kuiper, N.J. 2009, Gene expression profiles of dynamically compressed single chondrocytes and chondrons, Biochemical and biophysical research communications379 (3), pp. 738-742.

Weiss, C., Rosenberg, L. and Helfet, A.J., 1968. An ultrastructural study of normal young adult human articular cartilage. The Journal of Bone & Joint Surgery, 50(4), pp.663-674.

Wilson, S.L., Wimpenny, I., Ahearne, M., Rauz, S., El Haj, A.J. & Yang, Y. 2012, Chemical and topographical effects on cell differentiation and matrix elasticity in a corneal stromal layer model, Advanced Functional Materials, 22 (17), pp. 3641-3649.

Wimpenny, I., Ashammakhi, N. and Yang, Y., 2012. Chondrogenic potential of electrospun nanofibres for cartilage tissue engineering. Journal of tissue engineering and regenerative medicine, 6(7), pp.536-549.

Wise, J.K., Cho, M., Zussman, E., Yarin, A., Megaridis, C. & Cho, M. 2014, Electrospinning techniques to control deposition and structural alignment of nanofibrous scaffolds for cellular orientation and cytosceletal reorganization, Nanotechnology and Tissue Engineering, ed. CT Laurencin and LS Nair, Nanotechnology and Tissue Engineering, , pp. 285-303.

Woo, K.M., Jun, J.H., Chen, V.J., Seo, J., Baek, J.H., Ryoo, H.M., Kim, G.S., Somerman, M.J. and Ma, P.X., 2007. Nano-fibrous scaffolding promotes osteoblast differentiation and biomineralization. Biomaterials, 28(2), pp.335-343.

Woodruff, M.A. and Hutmacher, D.W., 2010. The return of a forgotten polymer—polycaprolactone in the 21st century. Progress in polymer science, 35(10), pp.1217-1256.

Wu, L., Prins, H., Helder, M.N., van Blitterswijk, C.A. & Karperien, M. 2012, Trophic effects of mesenchymal stem cells in chondrocyte co-cultures are independent of culture conditions and cell sources, Tissue Engineering Part A, 18(15), pp. 1542-1551.

Wu, L., Prins, H.J., Helder, M.N., van Blitterswijk, C.A. and Karperien, M., 2012. Trophic effects of mesenchymal stem cells in chondrocyte co-cultures are independent of culture conditions and cell sources. Tissue Engineering Part A, 18(15-16), pp.1542-1551.

`

Yang, R., Tan, L., Cen, L. & Zhang, Z. 2016, An injectable scaffold based on crosslinked hyaluronic acid gel for tissue regeneration, RSC Advances, 6, (20), pp. 16838-16850.

Yang, Y., Wimpenny, I. & Ahearne, M. 2011, Portable nanofiber meshes dictate cell orientation throughout three-dimensional hydrogels, Nanomedicine: Nanotechnology, Biology and Medicine7(2), pp. 131-136.

Yang, Y., Wimpenny, I. and Ahearne, M., 2011. Portable nanofiber meshes dictate cell orientation throughout three-dimensional hydrogels. Nanomedicine: Nanotechnology, Biology and Medicine, 7(2), pp.131-136.

Yoo, H.S., Lee, E.A., Yoon, J.J. and Park, T.G., 2005. Hyaluronic acid modified biodegradable scaffolds for cartilage tissue engineering. Biomaterials, 26(14), pp.1925-1933.

Yu, F., Cao, X., Li, Y., Zeng, L., Yuan, B. and Chen, X., 2013. An injectable hyaluronic acid/PEG hydrogel for cartilage tissue engineering formed by integrating enzymatic crosslinking and Diels–Alder "click chemistry". Polymer Chemistry, 5(3), pp.1082-1090.

Yuan, T., Zhang, L., Li, K., Fan, H., Fan, Y., Liang, J. and Zhang, X., 2014. Collagen hydrogel as an immunomodulatory scaffold in cartilage tissue engineering. Journal of Biomedical Materials Research Part B: Applied Biomaterials, 102(2), pp.337-344.

Zarrintaj, P., Manouchehri, S., Ahmadi, Z., Saeb, M.R., Urbanska, A.M., Kaplan, D.L. and Mozafari, M., 2018. Agarose-based biomaterials for tissue engineering. Carbohydrate polymers.

Zhang, L., Hu, J. & Athanasiou, K.A. 2009, The role of tissue engineering in articular cartilage repair and regeneration, Critical Reviews in Biomedical Engineering, 37(1), pp. 1-57.

Zhang, M., Zhou, Q., Liang, Q.Q., Li, C.G., Holz, J.D., Tang, D., Sheu, T.J., Li, T.F., Shi, Q. & Wang, Y.J. 2009, IGF-1 regulation of type II collagen and MMP-13 expression in rat endplate chondrocytes via distinct signaling pathways, Osteoarthritis and cartilage, 17 (1), pp. 100-106.

Zhang, Z., 2014. Chondrons and the pericellular matrix of chondrocytes. Tissue Engineering Part B: Reviews, 21(3), pp.267-277.

`

Zhang, Y., Guo, W., Wang, M., Hao, C., Lu, L., Gao, S., Zhang, X., Li, X., Chen, M., Li, P. and Jiang, P., 2018. Co-culture systems-based strategies for articular cartilage tissue engineering. Journal of cellular physiology, 233(3), pp.1940-1951.

Zhao, J., Han, W., Chen, H., Tu, M., Zeng, R., Shi, Y., Cha, Z. and Zhou, C., 2011. Preparation, structure and crystallinity of chitosan nano-fibers by a solid–liquid phase separation technique. Carbohydrate polymers, 83(4), pp.1541-1546.

Zhu, N. and Chen, X., 2013. Biofabrication of tissue scaffolds. In Advances in biomaterials science and biomedical applications. InTech.

`

Appendix

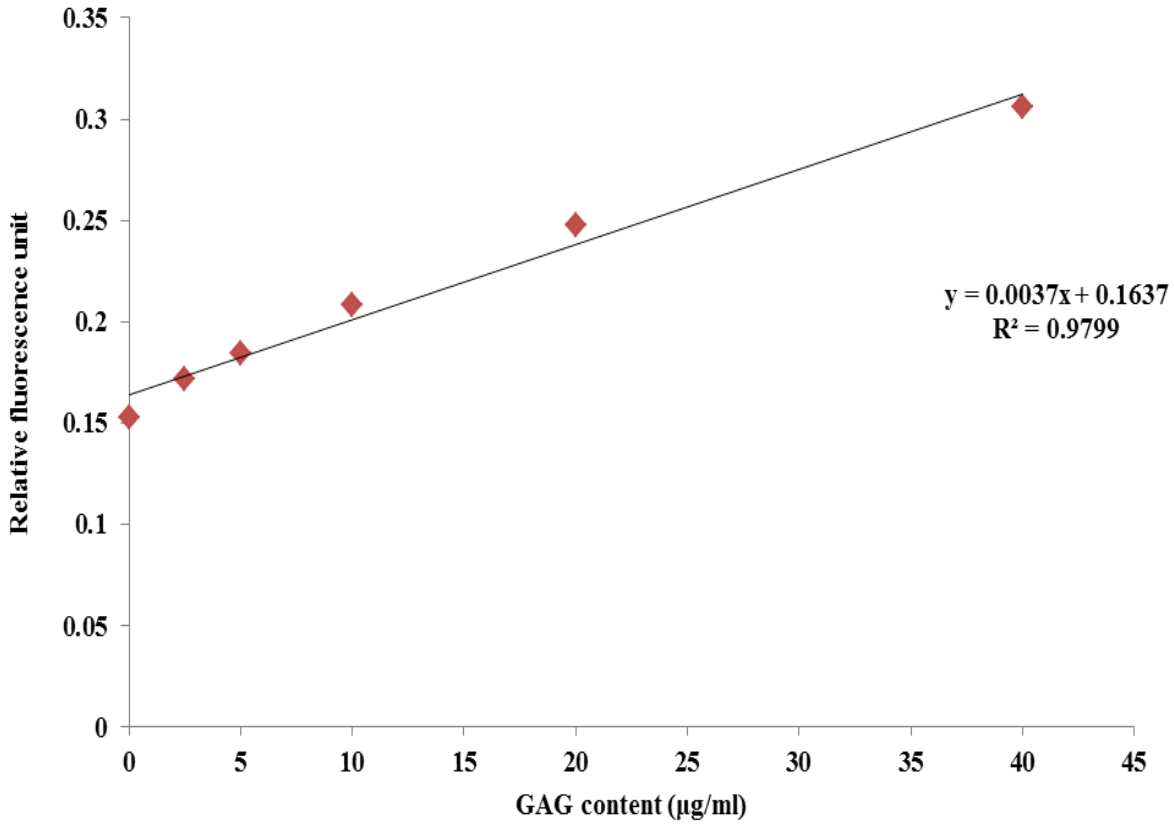

Figure 1: Typical standard curve performed for DMMB assay using serial dilutions of GAG ranging from 0 to 40 µg/ml

`

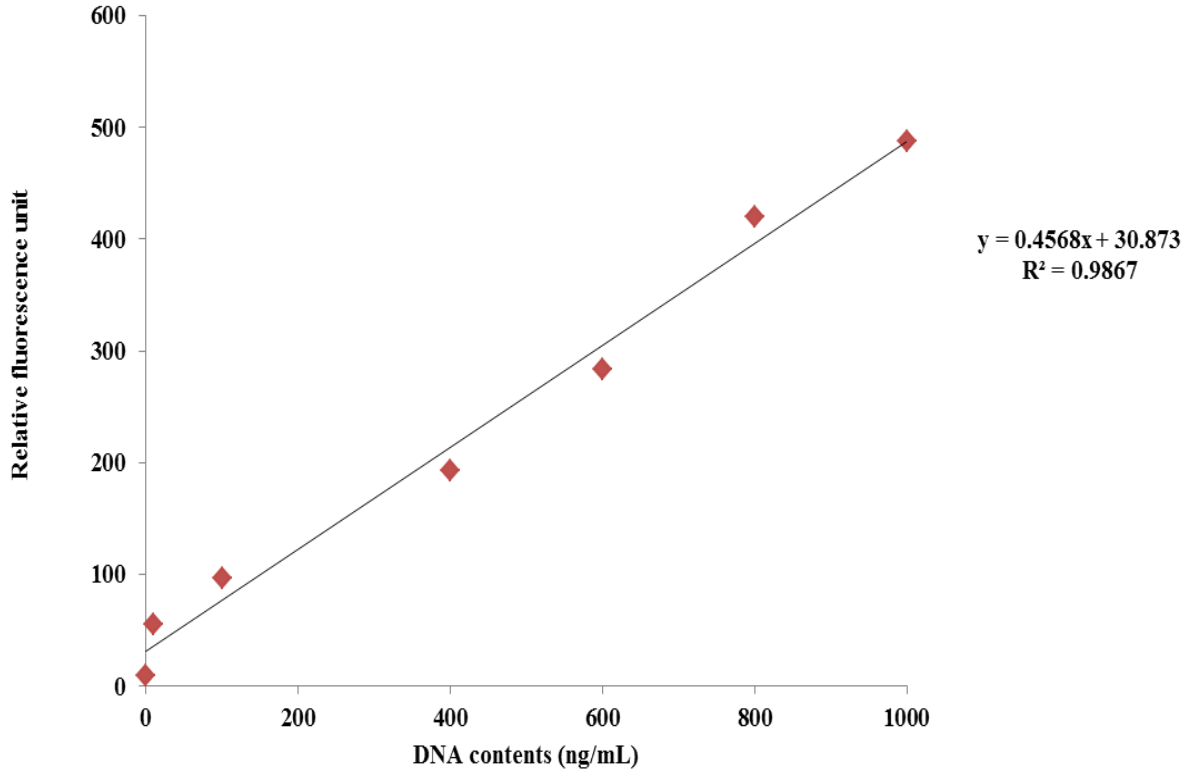

Figure 2: Typical standard curve performed for PicoGreen assay using serial dilutions of DNA ranging from 0 to 1000 ng/ml

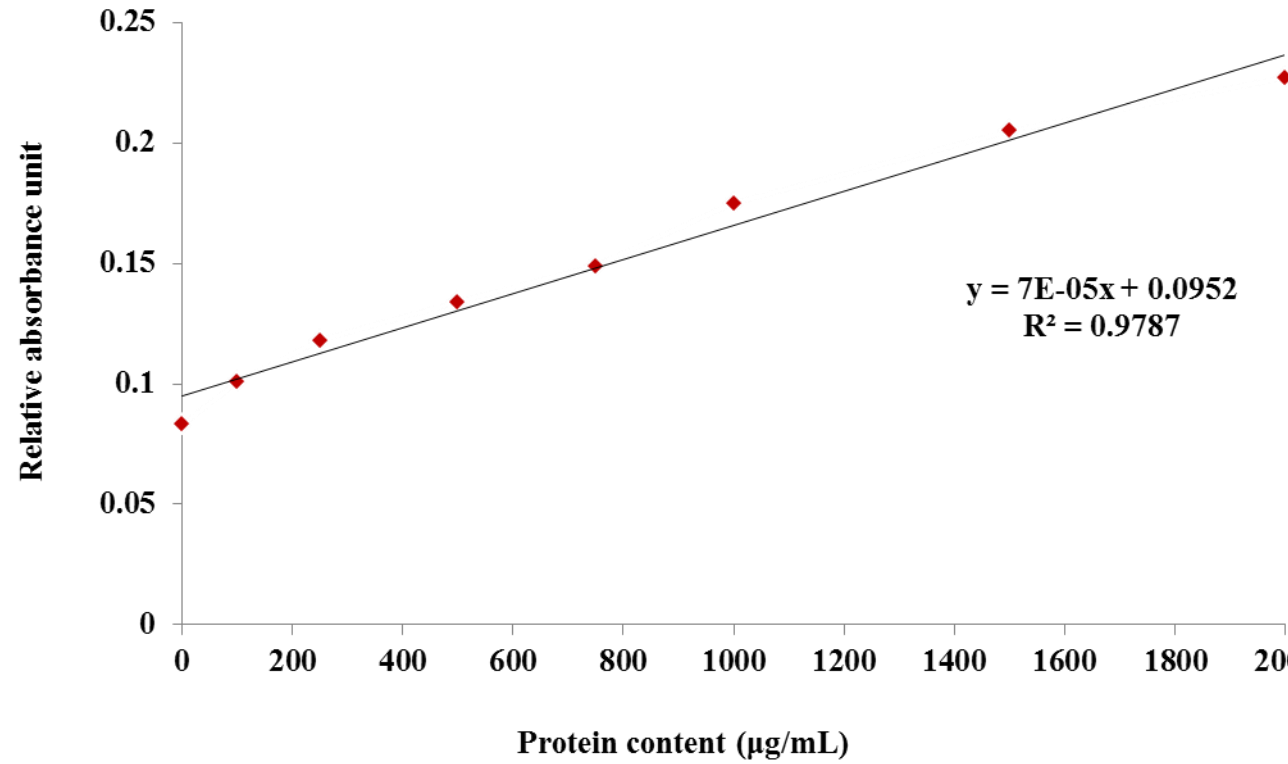

Figure 3: Typical standard curve performed for BCA assay using serial dilutions of protein ranging from 0 to 2000 µg/ml

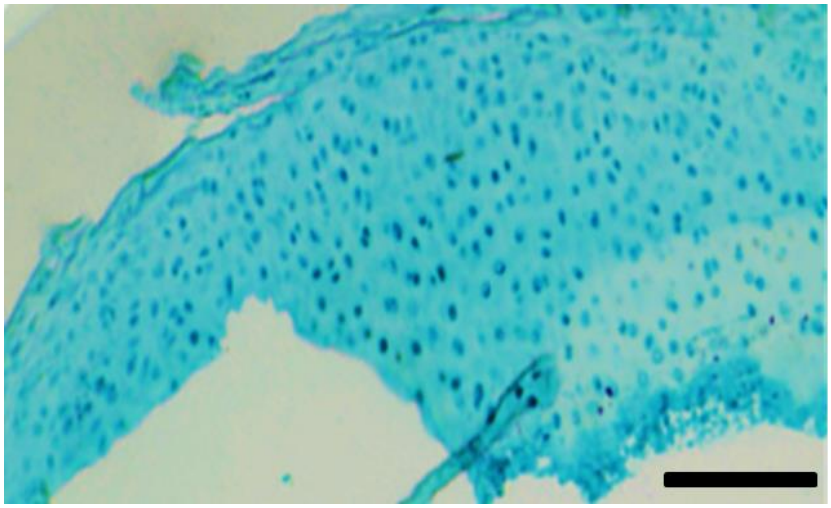

Figure 4: Illustration of freshly dissected bovine cartilage stained by alcian blue. Scale bars represent 150 µm.

`

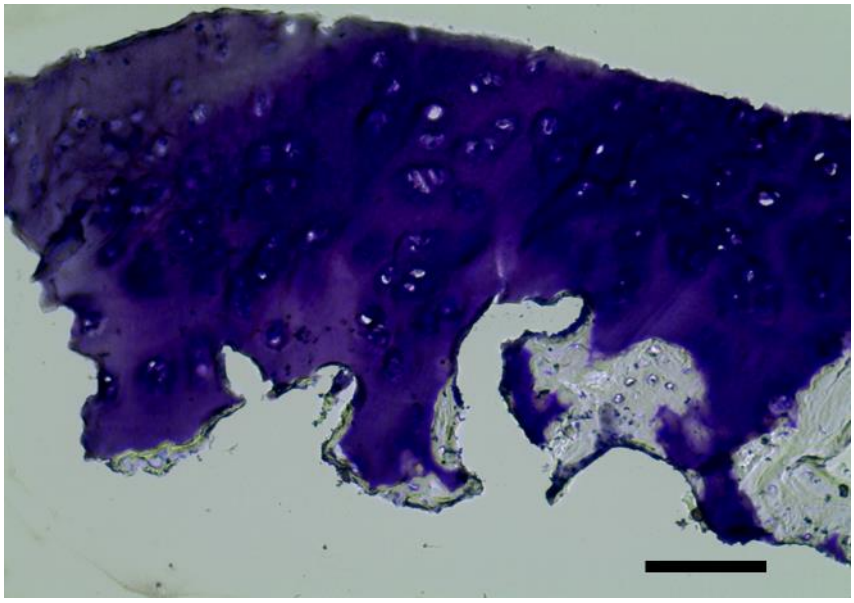

Figure 5: Illustration of freshly dissected bovine cartilage stained by toluidine blue. Scale bars represent 150 μm.